STRUCTURE AND FUNCTION STUDIES OF THE NUCLEUS

BY

MICHAEL PAUL CZUBRYT

A Thesis
Submitted to the Faculty of Graduate Studies
in Partial Fulfillment of the Requirements
for the Degree of

DOCTOR OF PHILOSOPHY

Department of Physiology
Faculty of Medicine
University of Manitoba
and the Division of Stroke and Vascular Disease
St. Boniface General Hospital Research Centre
Winnipeg, Manitoba

THE UNIVERSITY OF MANITOBA

FACULTY OF GRADUATE STUDIES

*****

COPYRIGHT PERMISSION PAGE

Structure and Function Studies of the Nucleus

BY

Michael Paul Czubryt

A Thesis/Practicum submitted to the Faculty of Graduate Studies of The University of Manitoba in partial fulfillment of the requirements of the degree of

Doctor of Philosophy

DEDICATION

I dedicate this thesis to my wife, Irene.

Her support and understanding make difficult times easier.

Her sense of humor keeps me smiling when smiling is the last thing I want to do.

Her dedication to everything she does inspires me to do the best I can.

Her friendship makes life enjoyable.

Her wit and intelligence keep me alert and make me consider other perspectives.

Her love is the most important thing in my life.

And her laugh makes me laugh.

"My most brilliant achievement was ... to persuade my wife to marry me"

– Winston Churchill

TABLE OF CONTENTS

ABSTRACT

Modern studies of the cell nucleus have provided a highly detailed view of its roles and the structures and mechanisms that carry out these roles, but many facets of nuclear physiology remain unclear. The present thesis focuses on three main areas of nuclear research. **First**, several calcium binding proteins in pig cardiac and rat liver nuclei were isolated and identified using high salt extraction followed by Stains-All staining and $^{45}Ca^{2+}$ overlays of western blots. These proteins, including calsequestrin and calnexin, exhibited distinct partitioning between the nucleoplasm and nuclear envelope. These findings will aid in understanding the function of the nuclear calcium pool. **Second**, we investigated nuclear nucleoside triphosphatase (NTPase), an enzyme bound to the nuclear envelope that provides energy for the export of poly A(+) mRNA from the nucleus. Using a novel corpulent rat model, we examined how alterations in nuclear envelope composition affected NTPase activity. Corpulent rats had greatly increased NTPase activity, and this correlated well with an increase in nuclear membrane [cholesterol]. Corpulent rat nuclei also exhibited greater fragility in a novel nuclear membrane integrity assay we developed using salt-induced lysis. Alteration of nuclear envelope composition thus has both structural (nuclear fragility) and functional (NTPase activity) consequences. **Third**, nuclear localization signal-mediated import of proteins to the nucleus through the nuclear pore complex was examined. Many studies have identified cytosolic factors required for nuclear import, however, few have examined import regulation. Using a nuclear protein import assay in permeablized aortic smooth muscle cells, we found that H_2O_2 inhibited import in a time- and dose-dependent manner by acting on a cytosolic factor. H_2O_2 activated the MAP kinase ERK2. Activated ERK2, in turn, mimicked

H_2O_2's effect on nuclear import. ERK2, therefore, mediates nuclear protein import inhibition caused by H_2O_2. Immunocytochemistry revealed that the cytosolic level of Ran, a key import factor, increased specifically in response to H_2O_2 treatment, which may reflect an alteration in the nucleocytoplasmic cycling of Ran. Altered Ran cycling is known to inhibit import, thus the downstream target of ERK2 may be Ran or one of its accessory proteins. This study was the first to link the MAP kinase pathway with import.

ACKNOWLEDGMENTS

I would not have been able to complete this work without the help of many people:

Dr. Grant Pierce – my friend and mentor. I could fill a thesis describing the impact he has had on my life. It is he who first encouraged me to enter grad school. Any success I attain is a testament to the model he has been and will continue to be for me, as both a scientist and teacher. Words cannot adequately describe the gratitude I have for him.

The members of my advisory committee – **Drs. Elissavet Kardami, Larry Hryshko, James Gilchrist and Ian Dixon.** They have been steadfast in their support of me, as instructors, as advisors and as friends. Thank you.

My friends and colleagues in the Pierce Lab. There have been so many of you over the past nine years. I thank you for your friendship and help, which made my experiences in the lab so happy and fulfilling. I wish each of you the greatest success in the future.

My family. I thank my father for instilling in me a curiosity and love for science. I thank my mother for her tireless support, love and encouragement. I thank both my parents for the values that they have instilled in me. I thank my brothers and sister for their love and friendship. I would also like to thank my in-laws for their support, especially as I worked to complete this thesis.

I would like to thank my new son, **Thomas**, for the lifetime of joy he has already brought me. Most importantly, I thank **God** for the many blessings I have in my life.

LIST OF FIGURES

LIST OF TABLES

A. REVIEW OF LITERATURE

I. Structure and Function of the Nucleus

1. Role of the Nucleus in Cell Function

Eukaryotic cells are distinguished from those of prokaryotes primarily by the presence of the largest of the cellular organelles, the nucleus. The evolution of the nucleus was a critical step in the genesis of multicellular organisms. Indeed, prokaryotes are virtually all single-celled and represent the most ancient forms of life on earth. The development of the nucleus provided eukaryotes with very important advantages by fulfilling a number of crucial roles for the proper functioning of the cell.

The most obvious role of the nucleus is enhanced protection of the cell's genetic material. DNA has a fragile structure, prone to cuts or cleavage, nicks in the sugar-phosphate backbone and loss or mutation of nucleotides. This damage may occur by exposure of DNA to endonucleases, UV radiation, oxidizing agents, free radicals, osmotic changes or even simple physical shock. The nuclear envelope protects DNA, as well as DNA binding proteins and nascent RNAs, by physically buffering the nucleoplasm and contents from the rest of the intracellular environment and by adding a further layer of insulation from the extracellular milieu.

The existence of the nucleus also permits segregation of DNA replication and transcription from the process of translation. The main consequence of the separation of these processes is that the cell has greater control over each of these processes. Proteins such as DNA binding proteins, transcription factors and polymerases required for replication and transcription are synthesized in the cytosol, but fulfill their functions in the nucleus. The cell gains tremendous control over the rates and timing of these

processes by regulating the entry of these factors into the nucleus. For example, the transcription factor NF-κB, a downstream effector of a number of cell signaling cascades, is prevented from entering the nucleus when bound to its inhibitor protein, IκB. Phosphorylation of IκB causes release of NF-κB, exposing a nuclear localization signal and permitting translocation to the nucleus (106). This mechanism provides the cell with finer control over the action of NF-κB by regulating not only the activation of the protein, but also by regulating its appearance in the nucleus. Similarly, mRNAs to be translated to proteins must travel from their synthesis site in the nucleus to the ribosomes in the cytosol; control over the entry of mRNAs into the cytosol may in turn partially determine rates of translation (37).

Another role of the nucleus, in particular the nuclear envelope, is to provide anchoring points for chromatin. Anchoring of chromatin to the nuclear envelope not only provides enhanced structural stability for DNA, it may also provide another level of control for the cell over rates of replication and transcription. Prior to these processes, DNA must be unwound from nucleosomes and the individual DNA strands separated from each other. Recent evidence suggests that replication and translation of DNA is preferentially blocked at points of anchorage of heterochromatin to the nuclear envelope (81, 188). A gene's relative location on a chromosome with regard to anchor points may even affect its transcription rate (81).

Lastly, the nucleus plays a critical role during mitosis and meiosis. During prophase, nuclear envelope breakdown is a necessary initial step to allow alignment of chromatids along the cell midline during metaphase, followed by segregation of parent-daughter DNA strands during anaphase. During the initial portion of telophase in mitosis, new

nuclear envelopes quickly self-assemble around the putative nuclei of the two daughter cells, preventing further mixing of DNA and ensuring proper allocation of individual copies of the genome to each daughter cell. In meiosis, however, nuclear envelope reassembly is blocked at this point to allow for a second round of "mitosis," during which DNA strands are again separated to ensure a haploid DNA content in the daughter (germ) cells. It is immediately prior to this second round of division that "crossing over" of genetic material occurs, allowing assortment of genes and creation of non-identical germ cells. This process is critical for evolution by introducing random fluctuations in the genome that may result in useful mutations for the species. Only after this round of division without replication does nuclear envelope reassembly occur in meiosis. Therefore, the proper timing of nuclear envelope reassembly may ensure appropriate control of critical spatiotemporal events in both mitosis and meiosis.

2. *Architecture of the Nucleus*

In keeping with the critical roles of the nucleus in cell physiology, nuclear structure is highly developed and consists of three discrete components: the nuclear envelope, the nuclear pore complex and the nuclear matrix. Chromatin, i.e. the nucleic acid component of nuclei plus interacting proteins, is associated with the nuclear matrix, but a discussion of the highly complex structure of chromatin is beyond the scope of this thesis. The reader is directed to a number of excellent reviews of this topic (81, 125, 207, 228).

a. Nuclear Envelope

The nuclear envelope is a complex spheroid structure consisting of a double set of lipid bilayer membranes surrounding the nuclear core, or *nucleoplasm* (i.e. the nuclear matrix and chromatin; Figure 1). The lipid bilayers are each typically on the order of 5 nm thick, and are separated by an aqueous gap called the perinuclear space, which is generally between 10 and 60 nm thick (108). The exact biochemical composition of the nuclear membrane varies widely depending on tissue type and species. In comparison to other cellular membranes, the nuclear membrane has a very high protein content of approximately 70% by weight, and a relatively low lipid content of approximately 20% by weight (108). Of the lipid content, approximately 10% by weight is cholesterol or related sterols, with the remainder being a mixture of phospholipids, sphingolipids and phosphoinositides (108). It is unclear whether the exact lipid profile of the inner versus the outer nuclear membrane is different.

The outer lipid bilayer is contiguous with the endoplasmic reticulum, and is observed by electron microscopy to be punctuated by attached ribosomes. The inner nuclear membrane lacks ribosomes, but is internally lined by a nuclear lamina (see Section A.I.2.c.i). The inner nuclear membrane is generally considered to be a separate structure from the outer membrane, but has been shown to be contiguous with the outer nuclear membrane at the sites of nuclear pores, where the membrane is termed pore membrane (116). The pore membrane may provide the continuity required to transfer integral membrane proteins between the inner and outer nuclear membranes (352). Despite the continuity of the two membranes, cells are apparently able to specify proteins to localize to one or the other membrane, perhaps by secondary interactions with the lamina,

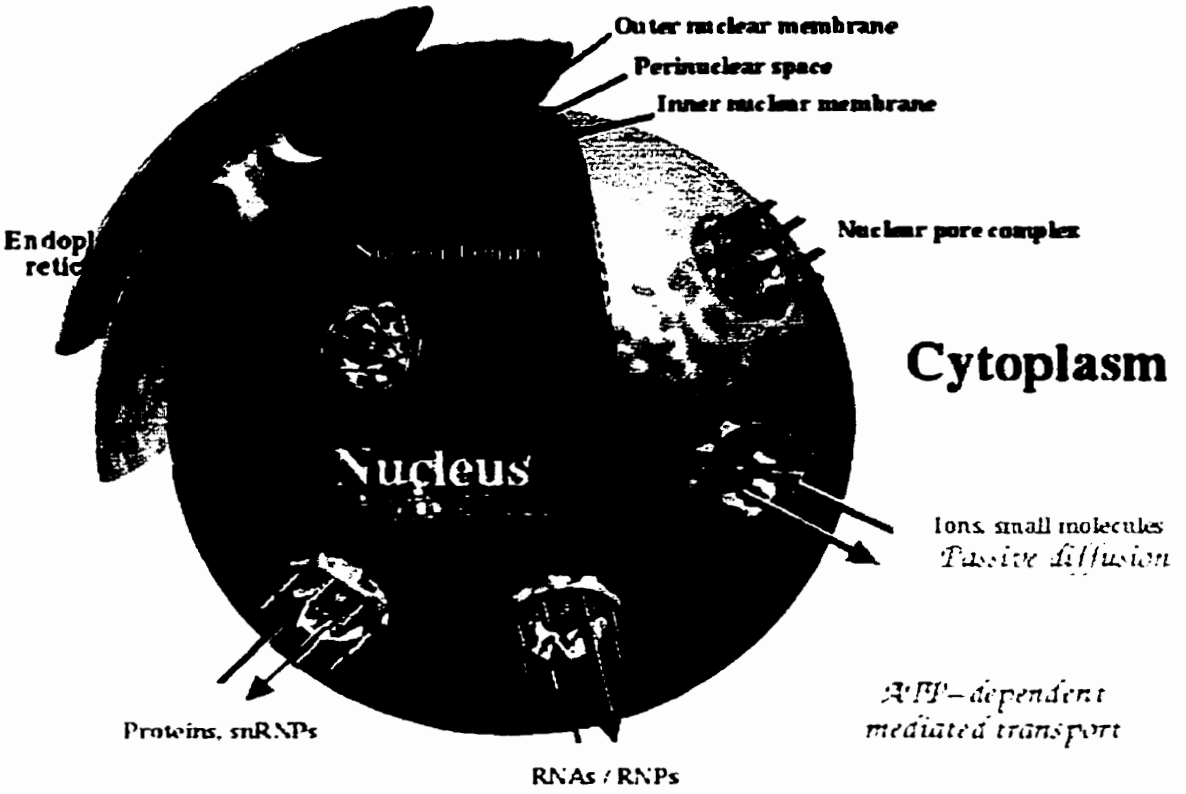

Figure 1. Schematic diagram of the nucleus showing nuclear pores and perinuclear space

This figure originally appeared in Panté and Aebi, 1996 (252).

or to localize in the outer nuclear membrane but not the endoplasmic reticulum (85, 129). The lamin B receptor p58 has been demonstrated to possess a domain that targets it to the inner nuclear membrane (320, 321).

The perinuclear space between the nuclear membranes is contiguous with the lumen of the endoplasmic reticulum (116). Despite this continuity, however, the perinuclear space may behave as a functionally distinct cellular compartment. This possibility is suggested by the presence of numerous calcium channels and pumps that are distinctly localized to the inner or outer nuclear membrane (148), as well as nuclear membrane-associated calcium binding proteins (86, 114). One possibility is that the cell may be able to regulate nuclear [Ca^{2+}] independently of cytoplasmic [Ca^{2+}], perhaps by using the perinuclear space as a calcium sink (see Section A.III). Another possibility is that perinuclear calcium may be involved in gating of the nuclear pore complex (see Section A.I.2.b.iii).

b. Nuclear Pore Complex

Although the role of the nuclear envelope is principally to segregate the nuclear contents from the cytoplasm, some degree of communication between these two compartments is nevertheless critical for the cell to function properly. With the exception of certain free radicals and gases, which to some extent are able to cross the nuclear membrane by dissolution through the phospholipid bilayers, almost all traffic between the nucleus and cytoplasm must travel through the nuclear pore complex (NPC) (Figure 2 and 3).

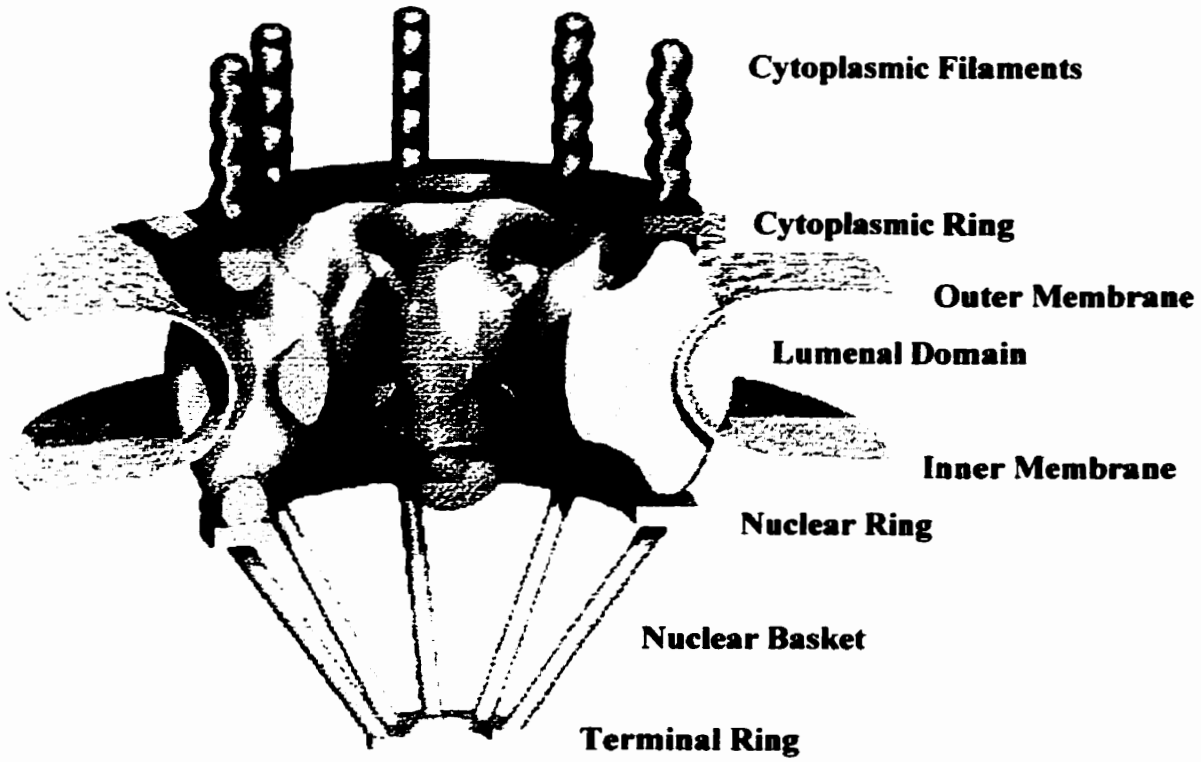

Figure 2. Schematic diagram of the nuclear pore complex
Modified from Panté and Aebi, 1993 (253).

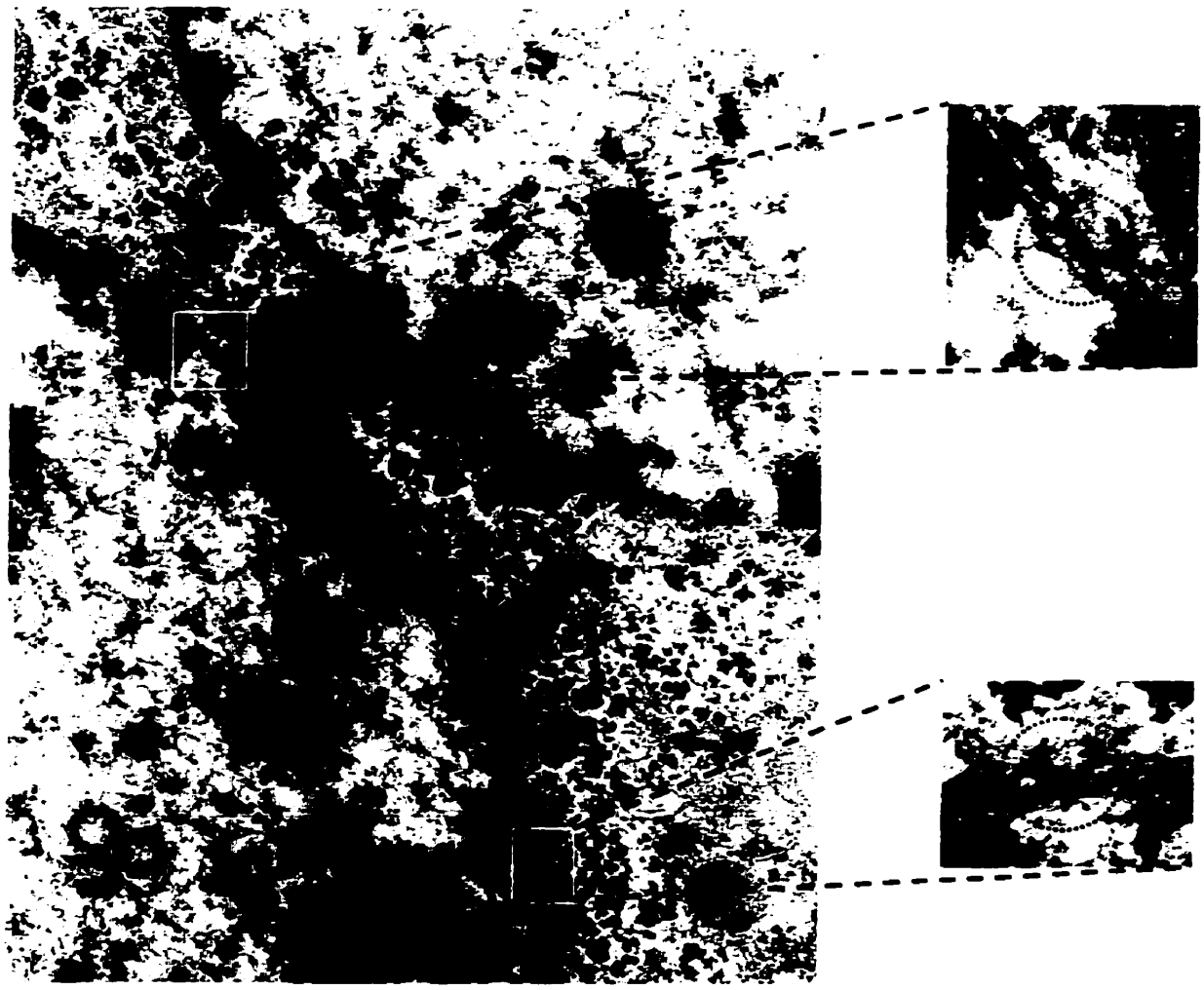

Figure 3. Electron micrograph of liver tissue sample showing NPCs

A sample of rat liver tissue was processed for electron microscopy as detailed in Methods. The boxed areas are contrast-enhanced and detailed in the insets, showing two nuclear pore complexes (circled). Magnification: ~28000x (main image), ~84000x (insets).

The factors that regulate nuclear pore number and density have not yet been determined. However, it has been observed that pore density is generally higher in metabolically active tissues and lower in relatively quiescent tissues, with reported pore densities of <1 pore/μm^2 in avian erythrocytes which are transcriptionally quiescent to nearly 190 pores/μm^2 in *Tetrahymena* macronuclei (225). Pore density may also be linked to the cell cycle, since HeLa cell pore numbers double prior to S phase (216). Pore density does not appear to be linked to the amount of nuclear DNA, the nuclear surface area or volume, or the genome size (215). It is also unclear whether pore distribution in the nuclear envelope is regulated, but there have been reports of non-random pore distribution (108, 204, 214). Furthermore, it has been observed that pore clustering can occur under certain experimental conditions (31, 187).

i. General Structure

The NPC is one of the largest single structures in the cell. While its overall structure appears to be fairly well conserved, the *Xenopus* NPC at 125 MDa is considerably larger than the yeast NPC at 60 MDa (326). The complex is typically ~125 nm wide in vertebrates, and ~100 nm wide in yeast. Both types of NPCs contain a central pore which is ~50 nm deep and which can vary in width from approximately 9-25 nm. The pore was originally thought to be composed of over 100 individual proteins in multiple copies, to give a collection of over 1000 proteins making up the pore complex (251). It is now estimated that the vertebrate pore complex is actually composed of only ~50 individual proteins, usually in 8 or 16 copies per pore (95). A recent report by Rout *et al.* purports to have identified **all** of the proteins comprising the yeast nuclear pore

complex, having identified 29 nucleoporins and 11 transport factors isolated from highly purified NPC preparations (290).

The NPC is constructed of three major assemblies: the core spoke complex, the cytoplasmic ring and the nuclear ring. The core spoke complex is built up from eight identical spoke structures that are symmetrically arranged around the central pore, giving the pore complex core eight-fold rotational symmetry. Furthermore, the spokes are vertically symmetrical, giving the complete core an 822 symmetry, with the asymmetric unit having a mass of approximately 3.3 MDa, similar to that of a ribosome (252). Equally spaced around the outer border of the core are eight peripheral channels of approximately 9 nm in diameter. It was originally thought that these channels might be responsible for the diffusion of ions and small molecules through the pore. Advanced three-dimensional electron microscopic techniques have shown, however, that the peripheral channels are embedded deep within the outer region of the core spoke complex, and accessible only from the perinuclear lumen (12, 115). Recent theories suggest that the channels exist to permit bulky cytoplasmic extensions of outer nuclear membrane proteins to traverse the pore's periphery as the proteins migrate along the pore membrane to become inner nuclear membrane proteins (116, 352).

The cytoplasmic ring in vertebrate NPCs has a molecular mass of about 32 MDa, and extends about 15 nm above the outer nuclear membrane, while the nuclear ring is about 21 MDa (116, 252). Together, the two rings may act as grommets to rivet the outer and inner nuclear membrane bilayers, respectively, to the core spoke complex. Null mutation of a protein believed to be a component of the nuclear ring leads to nuclei with unusual invaginations of the inner nuclear envelope and membrane seals over the pore openings.

This suggests that the nuclear ring, at least, may stabilize the nuclear membrane and help route the nuclear membranes around the pore (350). Two nucleoporins, gp210 and Pom121, may provide additional stabilization of the pore complex in the nuclear envelope. The glycoprotein gp210 has a large domain located in the nuclear envelope lumen, a small transmembrane domain, and a short domain located in the NPC. Pom121, on the other hand, has a small domain embedded in the nuclear envelope lumen, a transmembrane domain, and a large NPC embedded domain. Together, these two proteins appear to solidly anchor the pore complex to the nuclear envelope (252, 326). This does not necessarily mean, however, that the pore is prevented from moving within the fluid nuclear envelope, as relatively rapid movements of pore complexes across the nucleus have been observed (49).

A rotationally symmetrical set of eight proteinaceous filaments extend outward into the cytosol from the cytoplasmic ring (252). Similarly, a basket-like structure composed of eight long (up to 100 nm) (286) filaments joined at a ring-like structure has been observed extending from the nuclear ring into the nucleoplasm (252). Initial controversy over whether the nuclear baskets truly existed or were artifacts of the fixing process in preparing samples for electron microscopy has been resolved. It appears that the fragile basket assembly may have been lost during sample preparation in early reports that did not observe this structure. Furthermore, it has been demonstrated that chelation of divalent cations with EGTA causes disappearance of the basket, suggesting that the basket may have open and closed states which may have contributed to the earlier disparate results (252). Recent studies using atomic force microscopy support this idea, showing that the basket structure does assume an open and closed conformation in

response to calcium levels (327). It has been hypothesized that the filaments and basket may play roles in binding molecules prior to transit through the pore (291). This theory is supported by the localization of RanBP2/Nup358 to the distal ends of the cytoplasmic filaments (252, 354). RanBP2 is able to bind Ran, a critical component of the nuclear import complex (see Section A.II.1.b.iv), and is therefore a likely candidate for the initial cytoplasmic docking site for cargoes bound to the nucleus (354).

The NPC appears to contain a translumenal plug or barrel-like structure residing inside the pore itself. The existence of this structure has also been a source of controversy, with some labs observing it while others deny its existence (252). This structure may play a role in gating of the nuclear pore (see Section A.I.2.b.iii).

ii. Nucleoporins

The vast majority of proteins that comprise the nuclear pore complex are collectively referred to as *nucleoporins*. These proteins fulfill two major functions: they provide the physical structure of the pore complex, and many of them contribute to transport processes. To date, nearly 30 nucleoporins have been identified in yeast (290), with another ~20 identified in vertebrates (326). The exact definition of a nucleoporin has been somewhat controversial. Including all nuclear pore associated proteins would necessarily entail redefining many import/export factors as nucleoporins. Including only proteins with stable attachments to the NPC would exclude proteins such as human Nup153 and Nup98, which are structurally related to other nucleoporins but which have also been demonstrated to be mobile elements (243, 363). With regard to nomenclature, nucleoporins have been divided into Nups, which are integral nucleoporins that are

associated with the nuclear membrane, and Poms, which are peripheral membrane proteins not anchored to the nuclear membrane (252).

Nucleoporins vary widely in size, with many being in the 40-100 kDa range but with some as large as 358 kDa (290, 296). Nucleoporin structure also varies widely, even between genetic homologues from different species. The homology between vertebrate and yeast nucleoporins is generally less than 30% identical (296). Furthermore, yeast and vertebrate nucleoporins are generally unable to substitute for one another in complementation studies, although there are several important exceptions (9, 169, 328, 347).

Approximately half of all identified nucleoporins contain as many as 45 xFxFG, GLFG or FG structure repeats (291, 296). These repeats do not seem to be required for targeting of nucleoporins to the NPC, and deletion of these FG-containing regions in individual nucleoporins generally does not result in lethality or transport abnormalities (99, 326). Due to the large number of nucleoporins containing these repeats, it has been hypothesized that these repeats may fulfill a role in binding import or export factors during transit through the pore (326). Indeed, many nucleoporins containing these repeats bind a variety of importin/karyopherin transport factors, including importin α2, importin-β1 and Ran (23, 66, 107, 238, 281, 296). Two models of the nuclear transport process, the older solid-state model (8) and the recent Brownian affinity gating model (see Section A.I.2.b.iii) (290), depend on transient interactions between proteins of the pore complex and the transported molecules. The Brownian model specifically implicates the FG repeats as being instrumental in this process. The finding that a number of the repeats can be deleted without affecting import suggests that there may be a large degree of overlap

in the function of the various nucleoporins *in vivo* (326). The nucleoporins lacking the repeat sequences have been hypothesized to be strictly structural and not contribute to nucleocytoplasmic trafficking (95).

Many nucleoporins are post-transcriptionally modified by the addition of large sugar-rich residues like *O*-linked *N*-acetylglucosamine (225, 291). Wheat germ agglutinin or mushroom lectin are able to inhibit import, likely due to interaction with these glycosyl residues (4, 359). In fact, in testing novel *in vitro* import assays, it is customary to prove import through the pore by using wheat germ agglutinin to block import (4). It is unclear, however, exactly what purpose these moieties serve in the intact NPC, since removal or modification of the glycosyl groups did not affect nuclear import or pore assembly (226).

The importance of individual nucleoporins has been assessed in a number of deletion studies in yeast. For example disruption of the genes coding for the nucleoporins Nup84p, Nup85p or Nup120p leads to defects in poly (A)+ RNA export, nuclear envelope structure and nuclear pore complex organization (315). A variety of other mutant or null-expressed nucleoporins exhibit numerous defects in NPC clustering, nuclear envelope defects including seals over the NPCs, and nuclear or nucleolar organization changes (95). Defects in nucleolar organization are not surprising, since a number of nucleoporins contain zinc-finger or leucine-zipper DNA binding motifs, and thus may play a role in organization of chromatin (326).

Several nucleoporin genes have even been identified as proto-oncogenes. The *CAN* gene codes for the human nucleoporin Nup214, the loss of which in embryonic mice causes cell cycle arrest in G_2, as well as inhibition of nuclear protein import and mRNA export (340). In humans, acute myeloid leukemia and myelodysplastic syndrome arises as

a result of a chromosomal translocation that fuses the DNA-binding protein DEK to the COOH terminal two-thirds of CAN (39). This region of CAN contains a number of FG repeats and interacts with several other nucleoporins, including Nup84 (28), and hCRM1, a human importin-β homologue (107). Overexpression of CAN/Nup214 interferes with nucleocytoplasmic transport, and also causes growth arrest in G_0 and apoptosis (39). Another nucleoporin implicated in myeloid cancers is Nup98, a GLFG-containing nucleoporin required in several RNA export pathways (268). Similar to the situation with CAN, gene fusions of Nup98 with other genes is responsible for its oncogenicity (15, 168, 279). Finally, the human *TPR* gene has been implicated in human papillary thyroid carcinomas via fusion of Tpr with the *TRK* gene product (124). Cloning and characterization of Tpr have revealed that it, too, is a nucleoporin (25, 57). The similar genesis of these cancers, via fusion of a nucleoporin with other genes, indicates the importance of proper placement and functioning of nucleoporins in the normal functioning of the cell.

iii. Gating of the Pore

As mentioned earlier, the nuclear pore appears variously to contain a central, translumenal plug or barrel-like structure with an apparent mass of ~14 MDa (252). Some groups have suggested that this structure may actually be proteins or RNAs caught in the act of traveling through the pore, since it was seen only occasionally (252). More recent analyses using powerful electron and atomic force microscope techniques provide strong evidence, however, that this structure is real, and is an actual part of the import complex.

In these studies, the pore has a high incidence of lumenal occupancy, which can be reproduced in multiple preparations (252).

One possibility is that the plug is part of a gating mechanism for the pore, allowing the NPC to regulate the size of the pore lumen to accommodate varying sizes of traffic, or perhaps even open and close completely to regulate import and export rates (100). Evidence to support these ideas comes from reports that depletion of perinuclear calcium results in appearance of the translumenal plug (259, 346). At the same time, depletion of perinuclear calcium also causes attenuation or blockade of nuclear protein import, or the diffusion of small molecules into the nucleus (123, 259, 324). The importance of perinuclear calcium in the appearance of the lumenal plug may explain the earlier confusion over its existence, since the various preparations used may have compromised the nuclear envelope lumen or otherwise resulted in calcium loss.

Two recent studies, however, have reported that lumenal calcium does not, in fact play a role in regulating nuclear protein import (206, 330). In both studies, the authors suggested that earlier data showing an effect by lumenal calcium depletion might have actually represented an ER depletion of calcium, leading to an unspecified ER stress response that may have affected import. Another possibility advanced was that differences in species, cell type or experimental conditions may explain the disparate data, but ultimately the reasons for the disagreements are not currently known.

Two more recent reports may shed some light on these findings. Bustamante *et al.* reported that the gating of the nuclear pore is actually regulated by both calcium and ATP (56). This agrees with the other report, which shows that NPCs in cardiomyocytes also exhibit gating dependent on both calcium and ATP/GTP (258). In this study, the authors

propose that the NPC has three conformations: an open state, in which small molecules (~10 kDa) and large imported molecules (histone H1) freely pass through the pore; a closed or non-selective block state in which the depletion of lumenal calcium closes the pore, blocking transit of both types of molecules; and a selective block state, caused by depletion of ATP/GTP, in which the pore diameter reduces at one end, but opens at the other end due to relaxation of the NPC, allowing small molecules to pass freely through but blocking passage of large molecules. This model may explain the earlier disagreements, since in those studies, calcium was regulated but ATP/GTP were not. On a side note, it has also been demonstrated that opening and closing of the pore, with concomitant changes in movement of molecules through the pore, can be regulated by aldosterone (105).

The model advanced by Perez-Terzic *et al.* for the cardiomyocyte NPC suggests that the lumenal transporter or plug structure actually consists of a double iris system, with the NPC able to selectively open or close each iris (258). This suggestion agrees with earlier models that had also proposed a double iris system for the NPC (10, 11).

The elucidation of the complete yeast NPC composition and overall architecture led Rout *et al.* to propose a novel mechanism for nuclear transport called the Brownian affinity gating model (290). In this model, simple Brownian diffusion is used to explain the transit of molecules through the pore complex. The pore is visualized as being quite narrow, making it extremely difficult for most large molecules to pass through the lumen. Molecules (i.e. transporters or importins/exportins) that interact with nucleoporin FG repeats, however, increase their mean residence time in the pore, and therefore increase their likelihood of being further attracted to other FG nucleoporins deeper in the pore.

This effect, combined with asymmetrical distribution of various nucleoporins through the pore and asymmetrical distribution of transport factors to the cytoplasm and nucleus, leads to vectorial, directed motion through the pore. Proteins that bind the FG nucleoporins "see" a larger apparent diffusion channel than proteins that do not, since they easily interact with the pore proteins and thus more easily enter the lumen. This concept leads to the idea of a virtual gate, which discriminates between transported (i.e. nucleoporin-binding) and excluded (non-binding) molecules, but which requires no moving parts. Furthermore, energy expenditure in the form of hydrolysis of nucleotide triphosphates is not required for actual transport, except to maintain gradients of import factors across the nuclear envelope by recycling of the Ran GTPase (see Sections A.II.1.b.iv and A.II.1.b.vii).

Although this model is an attractive one that appears to model many aspects of nuclear transport, there are a number of caveats to keep in mind. First, this study localized individual nucleoporins to discrete regions of the nuclear pore complex. However, there is little information on how these various nucleoporins interact with one another or what their **precise** location is. Further information, perhaps in the form of high-resolution x-ray crystallographic studies, is required to understand how these many proteins interact. Second, no explanation is given for the changes in appearance of the NPC observed by atomic force and electron microscopy on closure of the pore, as no information is provided on steric changes in the pore structure, and no explanation is offered for the role of calcium in pore gating. Finally, this model does not seem able to reconcile the observation of three gating states observed in the cardiomyocyte NPCs, although this may be due to species-specific differences. Therefore the model may be an

excellent starting point for a clearer understanding of the import process, but further clarification of interactions and movements of nucleoporins in the NPC is required.

c. Nuclear Matrix

The nuclear matrix, or nucleoskeleton, can be identified as the large proteinaceous network that remains after the nucleus has been treated to remove nucleic acids and lipids (143). The matrix itself can be subdivided into several constituent components: the nuclear lamina, the core filaments, the diffuse skeleton and the nucleoli.

i. Nuclear Lamina

The nuclear lamina is a 20-50 nm thick proteinaceous layer found immediately interior to the inner nuclear membrane. It consists chiefly of intermediate filament-related proteins called lamins, which in humans fall into three classes: lamins A, B1 and B2. Up to six distinct lamins may be found in the cell by differential splicing of the lamin genes, including a fourth common class, lamin C, which is a splicing product of lamin A (111, 356). Lamins A and B contain a CaaX box to allow isoprenylation and carboxymethylation, which permits direct anchoring in the nuclear membrane. The lamina may also be anchored to the inner nuclear membrane by binding to "lamin receptors" which recognize lamin B (111), or via lamina-associated proteins found in the inner nuclear envelope (289). Lamins also appear to be able to bind to chromatin (356). Lamins typically contain a rod domain connecting a head and tail region. They also possess a nuclear localization signal in the tail domain, and a nearby cdc2 and/or protein

kinase C phosphorylation site which, when phosphorylated, appears to block the NLS and prevent nuclear entry of the lamin (111, 129, 135, 141).

The nuclear lamina stabilizes the inner nuclear envelope and appears to be critical for proper nuclear structure and function. Conversely, lamin proteolysis facilitates apoptosis, apparently by promoting nuclear envelope breakdown (278). Nuclear structure abnormalities resulting from lamin defects appear to play a role in a number of pathologies. For example, *Drosophila* with an insertional mutation of nuclear lamin Dm_0 exhibit delayed development, reduced viability, an impairment of locomotion and are sterile. On further examination, the flies were found to have incomplete nuclear envelopes with clustering of nuclear pore complexes and an accumulation of annulate lamellae (187). These findings suggest that the nuclear lamina may normally play a role in orchestrating the clustering of pore complexes, and are in agreement with evidence that lamins play a critical role in the restructuring of the nuclear envelope following mitosis (111).

Lamins are able to bind to both DNA and histones (356). The interaction of chromatin (specifically heterochromatin, i.e. repressed or silent chromatin) with the lamina suggests a possible role for the lamina in regulating gene expression (81, 188). Knockout mice for lamin A/C exhibit abnormal nuclei, with herniation of the nuclear envelope away from chromatin (356). These mice suffer from a severe form of muscular dystrophy. In humans, an autosomal dominant form of Emery-Dreifuss muscular dystrophy which is hallmarked by muscle wasting is caused by a mutation in the gene that encodes lamin A/C (43). A second mutation in the lamin A/C gene results in Dunnigan-type familial partial lipodystrophy, in which adipose tissue is lost (62). A

possible mechanism whereby lamin mutations can cause such widely divergent diseases is that heterochromatin may not bind properly to the nuclear lamina, resulting in inappropriate expression of unidentified genes. Both muscle and adipose tissue derive from mesenchymal precursors, and a nuclear lamina defect in these precursors may lead to the diseases described, and perhaps others (356). Another possible route for lamins to influence gene expression is by binding transcription factors, as has been demonstrated for the tumor-suppressor Rb, which is concentrated at the nuclear periphery and binds to lamin A/C *in vitro* (202).

A major protein component associated with the nuclear lamina and the inner nuclear membrane is a 46 kDa nuclear nucleoside triphosphatase, or NTPase (E.C. 3.6.1.15) (76). The NTPase is a cleavage product of lamins A and C (79, 335), and provides energy to the nuclear pore complex for export of poly (A)+ mRNA from the nucleus through the pore (5-8, 77, 78). NTPase activity is stimulated by poly (A)+ mRNA (33, 304), and phosphorylation of the NTPase results in an increased affinity for mRNA and alterations in NTPase activity and translocation of mRNA out of the nucleus (219, 305).

ii. Core Filaments

The core filaments are an assortment of 10 nm diameter protein filaments that connect the nucleoli with the nuclear lamina, and that also interconnect with each other. The exact composition of these filaments is unclear, although antibodies against conserved sequences in intermediate filaments bind to the core filaments (143). Recent work has identified the yeast myosin-like proteins Mlp1p and Mlp2p, which form long nuclear filaments connecting nuclear pore complexes with distal regions of the

nucleoplasm, as homologues of the vertebrate Tpr protein, which also forms 300 nm long nuclear filaments as well as cytoplasmic filaments attached to the NPC (329). Other studies have identified nuclear filaments constructed of lamins (144, 298). Finally, a set of intranuclear filaments which react with an antibody to the NPC nucleoporin Nup 153 has been observed, and which may correspond to the nuclear envelope lattice, a repeating protein structure sometimes associated with the nuclear baskets of the NPC (84, 291). Ultimately, however, it is unknown whether these various filaments truly correspond to the "core filaments" or whether other types of filaments remain to be identified.

iii. Diffuse Skeleton

The "diffuse skeleton" refers to a diffuse material seem by electron microscopy to attach or associate with the core filaments. Its identity and fine structure are unknown, but it has been shown to react with antibodies against actin, the nuclear matrix protein NuMa, or lamin A, or with antibodies against conserved sequences in intermediate filaments (143). Recent reports provide evidence that the intranuclear lattice may be composed of oligomers of NuMa (127, 131).

iv. Nucleoli

Nucleoli are the site of rRNA polymerization and ribosome synthesis for the cell. They are composed of fibrillar centers embedded in a dense fibrillar component. The core filaments (see Section A.I.2.c.ii) are present in the nucleoli in higher density than elsewhere in the nucleoplasm, thus comprising the dense fibrillar component. The fibrillar centers appear to be storage sites for proteins involved in transcription of DNA,

such as polymerases and topoisomerases, and are located in nodes in the network of core filaments (143).

II. Nucleocytoplasmic Trafficking

Proper control of nuclear functions requires the existence of control mechanisms to regulate the movement of cargo (e.g. proteins, nucleic acids and ribonucleoproteins) across the nuclear envelope via the nuclear pore. Recently, much progress has been made in identifying and characterizing the pathways controlling this trafficking.

1. Import to the Nucleus

a. Diffusion

As indicated earlier, gases and certain activated oxygen species, for example hydrogen peroxide and NO, are able to cross the nuclear envelope simply by diffusing through the phospholipid bilayers. Water may also cross the envelope when dynamic movements of phospholipids and/or cholesterol create transient aqueous pores, but a far faster and likely more relevant method for water to enter or leave the nucleus is by traveling through the NPC.

The central pore of the NPC is large enough to permit free diffusion of molecules smaller than approximately 40-60 kDa, but it is important to note two caveats. First, while individual ions are small enough to be expected to transit freely through the pore, there is evidence of ion currents operating through the pore complex which affect ion transfer. This is discussed in detail in Sections A.II.2 and A.III.2.a. Furthermore, a number of proteins smaller than 40 kDa, although small enough to freely diffuse through

the pore, show compartmentalization between the nucleus and the cytoplasm (17). The second caveat is that as molecular mass increases, the time required for transit through the pore increases. Molecules greater in size than 40-60 kDa enter the nucleus very slowly by diffusion, taking up to 24 hours to equilibrate with the nucleus, and molecules greater in size than ~70 kDa do not diffuse into the nucleus at all (361). In order for large molecules to enter the nucleus at physiologically useful rates, they must be actively transported, i.e. energy must be expended to facilitate the import of these molecules.

It is obviously not efficient to import molecules that are not required for nuclear function, or to import molecules that are not yet needed but which may be needed later. To solve this problem, a number of import systems have evolved to ensure that only required molecules are imported to the nucleus. These systems not only maximize efficiency, they also allow a great degree of control by the cell over **which** molecules may enter the nucleus, as well as **when** they may enter. The most common mechanism employed by the cell is the use of *nuclear localization signals* (NLSs), which are sequences of amino acids usually found in the protein to be imported, and which confer nuclear targeting on the protein. To date, two main import mechanisms have been identified, each depending on different types of NLSs, as well as a number of specialized systems for import of particular types of nuclear proteins or nucleic acids. The two major mechanisms utilize either the importin-mediated pathway, or the transportin-mediated pathway.

b. Importin-Mediated Import

i. Nuclear Localization Signals

Early studies revealed the existence of specific protein sequences that caused nuclear localization of their parent molecules (92, 165, 166). Mutation of these sequences interfered with import (165, 183). Based on this early work, artificial nuclear localization signals based on the Simian Virus 40 large T antigen were created that were able to cause the nuclear uptake of normally non-nuclear proteins such as human serum albumin (117, 184). Since that time, a relatively large number of NLSs have been identified, some of which use non-classical import pathways (Table 1). Although there is no consensus sequence for a classical NLS, the general construction is a peptide approximately 7-9 amino acids long, consisting primarily of basic amino acids (121). A variation on this construction is the so-called *bipartite* class of NLS (160, 287). This NLS consists of two stretches of basic amino acids separated by a spacer region. For example, the nucleoplasmin bipartite NLS has two basic residues separated by ten residues from another span of four basic residues (287). The identity of the spacer region is apparently unimportant for import, but the length of the spacer does seem to modulate the efficiency of import.

Despite the differences in structure of the two classes of NLS, they appear to share a common mechanism for regulating import. It has been demonstrated that both the SV40 NLS and the bipartite nucleoplasmin NLS use the same import receptor (121, 122). In general, it appears that NLSs are readily swappable between proteins with only minor effects on import rate. However, the context of the NLS with respect to the protein it occurs in does appear to be important, possibly due to masking effects or steric hindrance

Table 1. Selection of identified nuclear localization signals

Protein	Sequence (Length)	Transporter
SV40 Large T Antigen	PKKKRKV (7)	Importin-α1
Nucleoplasmin	KRPAAIKKAGQAKKKK (16)	Importin-α1
Human Interleukin-5	KKYIDRQKEKCGEERRRTRQ (20)	Importin-α1
c-myc	PAAKRVKLD (9)	Importin-α1
c-jun, v-jun	RKRKL (5)	Importin-α1
Yeast SWI5	KKYENVVIKRSPRKRGRPRK (20)	Importin-α1
HRNPA1 M9	NQSSNFGPMKGGNFGGRSSGPYG GGGQYFAKPRNQGGY (38)	Importin-β2
HIV-1 Rev	RQARRNRRRRWR (12)	Importin-β1
U snRNA	m3G cap	Snurportin

References: (121, 160, 162, 186, 242, 333)

of the NLS by other regions of the protein (288). The reason for the diversity of NLSs *in vivo* is currently unknown, but one possibility is that the different NLSs may permit more precise control of the import of individual substrates into the nucleus relative to one another. This is supported by the finding that different domains of import receptors may have differential affinity for different NLSs (see Section A.II.1.b.ii) (137, 307).

Most NLS-containing proteins have only one or two NLSs, but it has been demonstrated that artificially increasing the number of NLSs per imported molecule results in greater uptake of the molecule into the nucleus (97). This apparent dose dependency of import suggested that an NLS receptor might exist. The demonstration that the rate of import was saturable made this possibility a near certainty (117).

ii. Importin-α, the NLS "Receptor"

Initial efforts to identify the NLS receptor focused on the nuclear pore complex itself, since it was assumed that such a large structure must surely contain the receptor (267). No NPC components, however, were observed to directly bind NLS-containing proteins. At the same time, cytosol fractionation experiments revealed that nuclear protein import required at least two soluble cytosolic factors (233). It was soon demonstrated that one of these factors, a ~60 kDa protein later dubbed importin-α, was the sought after NLS "receptor" (122, 272).

The role of importin-α is to recognize and bind to the classical (i.e. SV40 T antigen-type) NLS on cytoplasmic proteins bound for the nucleus, then bind to the pore-docking protein (see Section A.II.1.b.iii) (3). Importin-α is therefore not so much a receptor as it is an *adaptor* molecule, acting as a go-between for the nucleus-bound cargo and the pore-

docking protein. This step does not require the expenditure of energy and is temperature-independent.

Görlich originally cloned importin-α from *Xenopus laevis* oocytes, reporting six closely related forms of a 528 amino acid protein (122). Examination of the structure of importin-α reveals several interesting features: the NH_2 terminal contains a basic stretch of 40 highly conserved amino acid residues comprising the importin-β binding (IBB) domain, the central region contains eight (ten in yeast) degenerate *armadillo* repeats, and the COOH terminal contains an acidic domain (119, 137, 349). The IBB domain is required for binding of importin-α by the pore-docking protein, importin-β (119, 236, 349). The *armadillo* repeat region appears to contain two individual binding sites for NLSs (82, 137). Competition experiments with two different types of NLS have led to the theory that individual importin-α molecules may preferentially recognize more than one NLS, and that the degeneracy of the *armadillo* repeats across different importin-α homologues may allow for the recognition of particular NLSs by particular homologues (137). Evidence to support this theory was reported by Sekimoto *et al.*, who demonstrated that importin-α1-mediated import of Stat1 cannot be competed with the SV40 large T antigen NLS, which also binds to importin-α1 (307). The acidic region in the COOH terminal contains a binding site for the protein CAS, a factor required for export of importin-α out of the nucleus after a round of import (see Section A.II.1.b.vii) (137).

Other groups have identified both a nuclear localization signal in the NH_2 terminal (236) and a putative nuclear export signal in the central region (38). The role of the NLS is unclear, since it is overlapped by the IBB domain, thus preventing autologous importin-α binding during import when importin-β is bound to this domain (236). The

role of the nuclear export signal is also unclear, since it appears to be neither necessary nor sufficient for export of importin-α from the nucleus (137), in contrast to earlier data that first identified the nuclear export signal (38). It is possible that both these regions may interact with as-yet-unidentified cofactors to fine-tune import and export of importin-α.

Importin-α homologues have been independently identified in a wide variety of organisms, and sometimes independently in the same organism, leading to confusion over nomenclature. In *Saccharomyces cerevisiae*, importin-α is also called karyopherin-α, srp1p and KAP60, and is coded by the gene *SRP1* (257). Three homologues in humans have been denoted hSRP1, hSRP1α and hSRP1γ (240), importin-α1, α2 and α4, respectively (137), or karyopherin-α1 and α2 for hSRP1 and hSRP1α (257). Recently, novel homologues have been identified in plants (146, 163), humans (174, 175) and mice (167). There are currently well over a dozen homologues, and it is likely that many more remain to be found.

One of the reasons that a standardized nomenclature has not yet been established is the rapid pace of discovery of novel forms of importin-α, many having been discovered in just the last two years. Another reason is the degree of homology between homologues. Based on sequence similarity, importin-α proteins can be grouped into three subfamilies, in which intrafamily sequence identity is about 80%, and in which interfamily sequence identity is about 50% (175). The current theory for the large numbers of importin-α homologues is that different forms may recognize different NLSs, or may exhibit differential tissue and/or species expression. Recent data tends to support this theory, as

five mouse importin-α proteins classified into three subfamilies have been identified, each with unique tissue expression patterns (167).

iii. Importin-β1

Soon after the discovery of importin-α, a 97 kDa import factor dubbed importin-β or karyopherin-β, was identified in bovine erythrocytes and *Xenopus laevis* oocytes (2, 70, 272). Importin-β was found to bind to both importin-α and to several xFxFG nucleoporins, revealing its role in docking the basic import complex (i.e. the NLS-bearing protein and importin-α) to a docking site on the nuclear pore complex in an energy- and temperature-independent process (70, 272).

Importin-β has now been renamed importin-β1 or karyopherin-β1, since it has been found to actually be the first member of a large superfamily of importin-β homologues, with 14 members in yeast alone (3, 257). The hallmarks of this superfamily include an NH_2 terminal Ran binding region and a nucleoporin binding region (118). Only importin-β1 is involved in the "classical" NLS-mediated nuclear import pathway, although one importin-β homologue called CAS is involved in export of importin-α to the cytosol (see Section A.II.1.b.vii) (181). Another member of the superfamily, transportin or karyopherin-β2, is discussed in further detail later in this thesis. The other importin-β homologues act to import or export a variety of specific protein classes (3). The importance of importin-β1 is shown by the fact that the null mutation is lethal in yeast (357).

As mentioned earlier, importin-β1 binds to three major types of proteins. The Ran binding domain is found in the NH_2 terminal region, but binding of RanGTP and RanGDP (which only binds in the presence of a Ran binding protein, RanBP1) is mediated by two separate regions (69). The nucleoporin binding region maps to the COOH terminal 60% of the protein, but more specific information on exactly where the nucleoporins bind has not yet been reported (72). The region of importin-β1 that binds the IBB domain of importin-α consists of 19 tandemly repeated HEAT motifs, which have a helix-turn-helix structure (73). The tight binding of importin-β1 to importin-α resembles the binding of importin-α to an NLS (73). An interesting observation is that the RanGTP binding site of importin-β1 overlaps the importin-α binding site. The binding of RanGTP therefore destabilizes the formation of the import complex, since RanGTP binds to importin-β1 with greater affinity than importin-α does (237). This effect becomes important for the proper cycling of Ran between the nucleus and cytoplasm, which in turn regulates protein import (see Section A.II.1.b.iv). Importin-β1 also possesses a nuclear export signal (151).

Two recent observations suggest that the role of importin-β1 may be even more complex than previously thought. First, the protein Rev, the U small nuclear ribonucleoproteins, and a number of ribosomal proteins have been reported to be imported by importin-β1 in the absence of importin-α (134, 157, 249), suggesting that importin-β1 may be able to recognize NLSs on its own. Second, the import of histone H1 is mediated by an importin-β/importin 7 heterodimer, which behaves as a nuclear import receptor (156). Together, these data suggest that importin-β1 may be able to act as its own NLS receptor. This would not be unexpected, since virtually all of the other

importin-β homologues do not use or require adaptor proteins (3). It has also been shown that importin-β1 appears to be able to enter the nucleus on its own (180).

iv. Ran and the RanGTP/RanGDP Cycle

Ran, or Ran/TC4, has long been acknowledged to be a key player in nuclear protein transport processes, but the understanding of Ran's role and mode of action has changed dramatically over time. Ran was initially identified as a 25 kDa homologous relative of the small GTPase Ras, a key component of various intracellular signaling pathways (96). Moore and Blobel soon identified Ran as one of two required components for nuclear protein import in a cytosol fractionation study (230). It is an abundant protein, comprising ~0.4% of total cellular protein, and is predominantly localized to the nucleus (280). Since nuclear import was energy-dependent, and since Ran was required for import, early models of import suggested that the energy requirements of import may be met by GTP hydrolysis by Ran (121). This appeared to be borne out by experiments in which nuclear protein import using a mutated Ran, which was only able to hydrolyze xanthosine 5'-triphosphate (XTP) instead of GTP, became dependent on XTP alone (348). Import in the absence of XTP could not be rescued by GTP or ATP, suggesting that nucleotide hydrolysis by Ran was the only energy source required for import. It soon became apparent, however, that this model of Ran's role was too simplistic, as Ran's interactions with other proteins were discovered and analyzed.

Like many GTPases, the hydrolytic activity of Ran is normally very low (44). It requires the action of a GTPase activating protein, which has been identified as the cytoplasmic protein RanGAP1. RanGAP1 increases Ran's rate of GTP hydrolysis by

100 000-fold (30, 34, 172). Ran also exchanges GDP for GTP very slowly, and so requires a guanine nucleotide exchange factor (GEF). The RanGEF has been identified as the chromatin-associated nuclear protein RCC1, which increases the rate of GTP/GDP exchange by 100 000-fold (172). Due to the localization of the Ran accessory proteins, virtually all GTP hydrolysis by Ran must occur in the cytosol, and virtually all exchange of GDP for GTP must occur in the nucleus. As a corollary to this, there must be a gradient of high [RanGTP] in the nucleus and high [RanGDP] (or low [RanGTP]) in the cytosol.

At the time these phenomena were being described, a seemingly incongruous effect of RanGTP was reported by Schlenstedt *et al.* (302). Using a yeast mutant of Ran that stabilized the GTP-bound form, they showed that the yeast homologue of Ran blocked nuclear protein import and poly (A)+ RNA export when bound to GTP. A subsequent study showed that another Ran accessory protein, Ran binding protein 1 (RanBP1) which further accelerates RanGAP1-mediated GTP hydrolysis by an order of magnitude (35), stabilized the binding of RanGDP, but not RanGTP, to importin-β1 bound to NLS-bearing proteins (71). At the same time, RanGTP dissociates the importin-α1/importin-β1 complex (237), as described in the last section. Together, these data show that in order for import to occur, RanGDP must be present in the cytoplasm, but RanGTP in the cytoplasm interferes with import.

It has now been shown that the export of importins from the nucleus, a process that also requires Ran, is inhibited by RanGDP in the cytosol due to destabilization of the export complex, but stabilized by RanGTP in the nucleus (211, 235). It appears, then, that the asymmetrical distribution of RCC1 and RanGAP1 leads to the establishment of a

RanGTP gradient that supports import complex formation in the cytosol (low [RanGTP]) and disassociation in the nucleus (high [RanGTP]). In effect, the gradient establishes vectorial movement of imported molecules. Conversely, when importins are recycled back to the cytoplasm, the formation of the export complex is stabilized in the nucleus and destabilized in the cytoplasm, again resulting in vectorial movement (17). An example of importin recycling is the export of importin-α1 by its export factor, CAS (181). A schematic showing the Ran cycle is depicted in Figure 4.

Several recent experiments have provided some very interesting and somewhat surprising data. In models of export and import, GTP hydrolysis of Ran was apparently not necessary for transport to occur (98, 282, 306). This could be explained, however, by the fact that this held true only for single transport events, i.e. only one round of transport. To continue transport processes, GTP had to be added. These findings demonstrate that the hydrolysis does not appear to be required for the transport process itself, but is instead required only to reset import and export factors to their correct locations for subsequent transport events (3).

The Ran gradient is clearly critical for nucleocytoplasmic trafficking to occur. Experimental collapse of the gradient inhibits nuclear import, as well as a number of export pathways (153). Furthermore, it is possible to reverse the direction of nuclear transport by artificially reversing the RanGTP gradient (241). Since there is a strong outward gradient of Ran from the nucleus, and since Ran is small enough to diffuse freely through the pore, Ran may equilibrate over time with the cytosol. To prevent this from happening, a factor called NTF2 is employed by the cell.

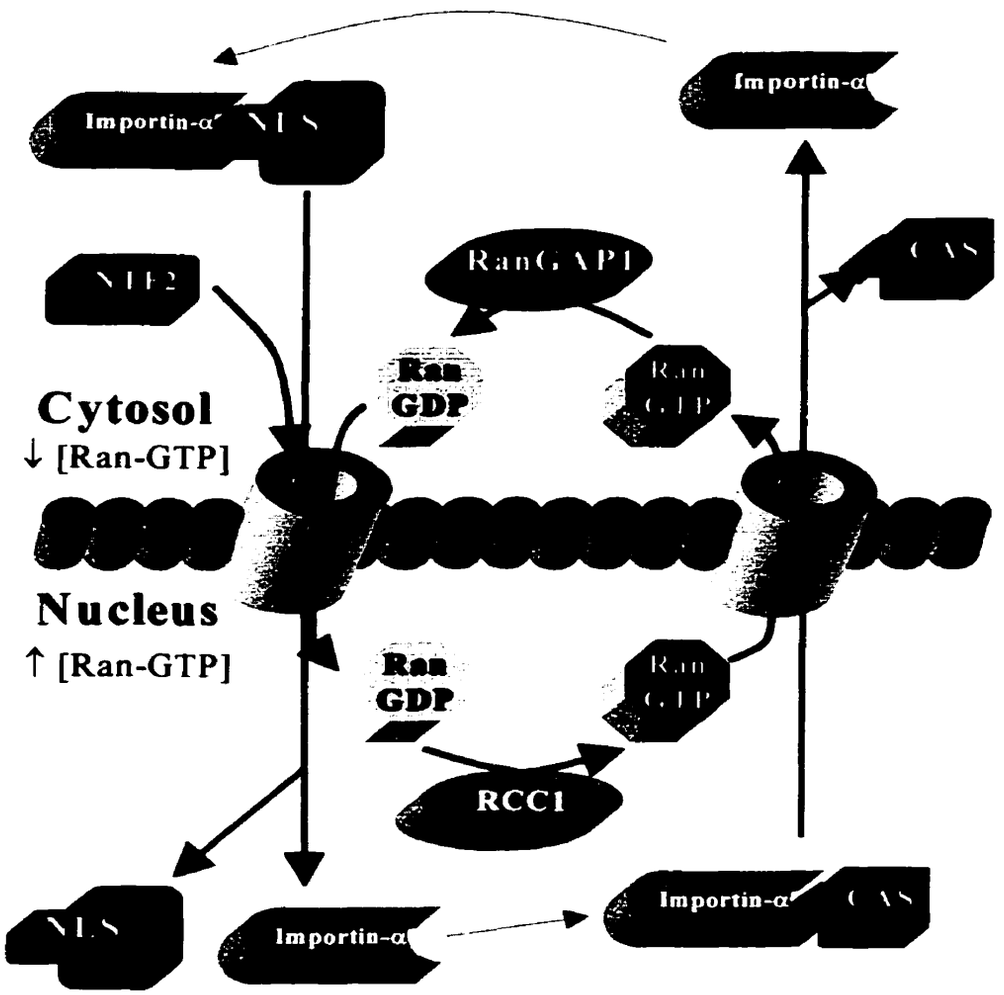

Figure 4. Schematic diagram of nuclear protein import and Ran cycling

RanGDP in the cytosol, in conjunction with NTF2, causes cycling of NLS-bearing proteins bound to an importin-α/importin-β complex (for clarity, importin-β and RanBP1 have been omitted). In the nucleus, RanGDP is converted to RanGTP by RCC1. The high [RanGTP] in the nucleus destabilizes the import complex. Importin-α is recycled back to the cytosol by formation of an export complex with CAS, which is stabilized by high [RanGTP]. In the cytosol, Ran hydrolyzes GTP to GDP with the aid of RanGAP1 and RanBP1. The low [RanGTP] in the cytosol destabilizes the export complex, freeing importin-α for another round of import. CAS and NTF2 are recycled back to their compartments (not pictured).

v. NTF2

Nuclear transport factor 2, or NTF2, was initially discovered by two independent groups working with *Xenopus laevis* oocytes and HeLa cells as a protein that supported nuclear protein import (231, 256). It was found to be homologous to human placental protein 15 (pp15), a previously identified protein of unknown function (41). The structure of NTF2 is highly conserved in nature and is coded for by the *NTF2* gene in *Saccharomyces cerevisiae* (83). The resulting protein has a mass of ~14 kDa, but is normally found as a homodimer of ~30 kDa (231, 256). NTF2 has a conical shape with a hydrophobic cavity to which Ran binds (50).

The function of NTF2 was unclear when it was first discovered, but it was observed that import failed when NTF2 was removed from cytosol in import assays by binding to the nucleoporin p62 (256). It was also found that NTF2 bound to the import factor Ran (231), but only when Ran was in a GDP-bound state (255, 325). Moore and Blobel suggested that the role of NTF2 might be to act as a Ran-GDP dissociation inhibitor (RanGDI), similar to RabGDI, which is involved in targeting GDP-Rab to vesicular membranes (231). This was a very astute hypothesis, as it has now been confirmed that NTF2 is, indeed, a Ran-GDP dissociation inhibitor (358). NTF2 inhibits the dissociation of GDP from Ran when bound to RanGDP. It also inhibits the binding of GTP to Ran. In this way, Ran can be kept in a GDP-bound form in the cytosol, allowing formation of import complexes that are otherwise destabilized by RanGTP (see Section A.II.1.b.iv). In support of this model, it has been demonstrated that nuclear protein import is inhibited by NTF2 mutants that do not bind RanGDP (74). NTF2 has also been reported to transport

Ran into the nucleus, thereby preventing the depletion of nuclear Ran levels due to diffusion down its gradient into the cytosol (283, 318).

NTF2 possesses a binding site for xFxFG regions of nucleoporins, in particular p62, which is separate from its Ran binding site (75). Recent experiments in which the xFxFG binding site is mutated to inhibit binding of NTF2 to nucleoporins, but in which the Ran binding site is unaffected, have shown inhibition of the import of RanGDP (29). Furthermore, antibodies against NTF2 block nuclear import of Ran, which in turn blocks nuclear protein import (323). Together, these data suggest that NTF2 functions not only as a RanGDI, but also as a Ran nuclear import factor, specifically regulating movement of Ran into the nucleus by binding to both Ran and to nucleoporins in the pore complex.

vi. Other Soluble Import Factors

An early study reported that hsp70/hsc70, a heat shock protein or its cytosolic cognate, were required for import in permeablized nuclear protein import assays (312). The significance of this finding, however, is unclear, since nuclear protein import can be reconstituted *in vitro* using recombinant forms of importin-α, importin-β, Ran and NTF2 alone (339).

It is likely that many more import factors remain to be discovered – factors that, while not **required** for import, would possibly fine-tune the rate or selectivity of import, for example. Furthermore, there are likely to be many more tissue and species specific isoforms and homologues of the currently identified import factors, as well as import factors for import pathways that are yet to be identified (see Sections A.II.1.c and A.II.1.d).

vii. Putting It All Together: A Mechanistic Model of Import through the Pore

From the preceding discussions of the Brownian affinity gating model and the Ran GTP/GDP cycle, it is possible to envision an overall model of classical NLS-mediated import through the nuclear pore complex. The whole process starts with an NLS-bearing protein binding to the *armadillo* repeats of importin-α1. This complex then binds to the HEAT motifs of importin-β1 via the IBB domain of importin-α1. RanGDP, likely complexed to NTF2, also binds to importin-β1, although it is uncertain at exactly which time NTF2 binds the import complex. This pentameric complex diffuses to an open nuclear pore complex (open due to the presence of perinuclear calcium and ATP), and interacts with nucleoporins of the cytoplasmic filaments, most likely RanBP2 (91), via the nucleoporin-binding domains of importin-β1 and NTF2, and the FG repeats of the nucleoporin.

This interaction increases the residence time of the import complex at the pore, prompting further interactions between the import complex and other nucleoporins deeper in the pore complex. The concentration gradient of the import factors (which are predominantly cytoplasmic), in conjunction with asymmetrical distribution of nucleoporins through the pore which tend to "pull" the complex along, drives the import process, resulting in entry of the import complex to the nucleus.

Inside the nucleus, RCC1 exchanges GTP for the GDP bound to the Ran molecule, causing destabilization and separation of the import complex component proteins, thus delivering the NLS-bearing cargo. RanGTP binds to CAS (the importin-α1 exporter), which binds importin-α1, and together this export complex travels back through the pore.

This process again likely exploits a CAS gradient out of the nucleus and asymmetrical arrangement of nucleoporins (possibly different from those mediating import). Upon entry into the cytoplasm, RanGAP1 and RanBP1 facilitate the hydrolysis of GTP to GDP, and the export complex destabilizes, releasing the cargo (importin-α1) back into the cytosol. Importin-β1 is also recycled back to the cytosol, but appears to possess its own nuclear export signal and thus does not require a CAS homologue (151). RanGDP is now available for another round of import, as are the importins. This model of import is presented schematically in Figure 4.

This scheme appears to be the best current fit to the available data. However, several questions remain unanswered. It is unclear whether NTF2 actually enters the nucleus with the import complex, and if so, how it re-enters the cytoplasm. It is also unclear exactly how the import and export complexes move through the pore and if this truly does not require energy in the form of nucleotide triphosphate hydrolysis, or how CAS recycles back to the nucleus. With the current pace of research in this area, it is likely that these questions and more will be answered very soon.

viii. Regulation of Import

The critical role of the nuclear protein import process in normal cell functioning demands that the cell tightly control import. Indeed, as mentioned earlier, mutation of a number of nucleoporin genes results in myeloid leukemias, while blockade of import results in lethality, cell cycle blockade and apoptosis. It has been suggested that it may be possible to develop pharmacological methods of modulating import to treat diseases characterized by transcription factor dysregulation (109). To date, several methods of

regulating import of proteins to the nucleus have been identified, of varying degrees of complexity.

The simplest method of regulating import is by encoding an NLS in the primary sequence of a given protein – proteins without NLSs are not directly imported, as discussed above. A variation on this theme is the possibility of alternative splicing of mRNAs to include or exclude coding regions for NLSs. For example, the transcription factor E2F can be differentially spliced to include or exclude a bipartite NLS, thus regulating the appearance of E2F in the nucleus (89). Similar examples of NLS splicing include nuclear mitotic apparatus protein (NuMa) (334), CaM kinase (322) and deoxynucleotidyl transferase (32). Regulation of alternative splicing itself, however, is often highly complex and the precise mechanism varies from protein to protein.

Another method of controlling import is by masking and unmasking of an endogenous NLS. An example of this method, as described earlier, is NF-κB, which in non-stimulated cells is bound to its inhibitor, IκB. The binding of IκB to NF-κB covers the NLS of NFκB, preventing its entry into the nucleus. Phosphorylation of IκB in response to a variety of stimuli (e.g. TNFα) results in release of NF-κB, unmasking of its NLS and efficient translocation to the nucleus (106). A similar mechanism is used by c-fos and the PKA C-subunit (158). The binding factors that prevent nuclear localization are sometimes referred to as cytoplasmic retention factors or anchors (161). A variation of this theme occurs in PKC-α, which is normally cytoplasmic. Phorbol ester binding to PKC-α results in a conformational change which unmasks an NLS and allows localization to the nuclear envelope (158). In this way, PKC-α has a built-in anchoring mechanism.

A novel import mechanism called piggybacking is employed by the two subunits of the mouse DNA primase (229). The 54 kDa subunit possesses an NLS which directs its movement into the nucleus. The 46 kDa subunit, in contrast, lacks an NLS, and when expressed alone in COS-1 cells, remains in the cytoplasm. Transfection of these cells with both subunits, however, results in translocation of both subunits to the nucleus: the 46 kDa subunit piggybacks into the nucleus with the 54 kDa subunit.

One of the most widely used methods of regulating import of individual substrates, however, is phosphorylation. Even before the identification of the SV40 NLS, phosphorylation sites just upstream of the NLS were documented (300). It was later shown that including this upstream sequence in import assays, as opposed to simply using the minimal residues comprising the SV40 NLS, resulted in faster uptake of import substrates to the nucleus (285). It was subsequently demonstrated that this upstream region contained a casein kinase II (CKII) phosphorylation site at S^{111}/S^{112}. Phosphorylation of either of these residues increased the rate of nuclear accumulation of import substrate (284), apparently by enhancing recognition of the NLS by importin-α1 (147). Soon afterward, it was also shown that the upstream region of the SV40 NLS contained a $p34^{cdc2}$ (cyclin-dependent kinase, or cdk) phosphorylation site at T^{124}, and that phosphorylation of this residue resulted in a reduced maximal accumulation of import substrate in the nucleus (159). The overall **rate** of import, however, was unaffected. This combination of these two phosphorylation sites was designated a "CcN" motif, which represents the CKII, cdk and NLS signals present (158). This single motif, therefore, can both up-regulate and maximally limit nuclear protein import.

A number of proteins have now been demonstrated to possess partial or complete CcN sites, including p53, c-myc, lamin A/C and B-myb (158). Phosphorylation sites for other protein kinases have also been identified which regulate nuclear import, including a cAMP-dependent protein kinase site in the *Drosophila* transcription factor Dorsal (46). The reverse of this scenario has also been demonstrated: dephosphorylation of S^{238} in v-Jun results in nuclear accumulation of v-Jun (333), while dephosphorylation of a serine residue in Ca^{2+}/calmodulin-dependent protein kinase II results in its nuclear targeting (133). Phosphorylation can be used by the cell to afford great control over temporal events. The yeast transcription factor SWI5, for example, is targeted to the nucleus at only certain stages of the cell cycle, and this translocation is regulated by the phosphorylation of sites within the NLS by the cyclin-dependent kinase CDC28 (162).

There are other methods of regulating both import and export that have been found. A novel nuclear export factor for U snRNA called PHAX, for example, appears to be regulated by phosphorylation (246). Formation of the export complex containing PHAX requires phosphorylation of PHAX in the nucleus. In the cytoplasm, PHAX is dephosphorylated, which causes disassembly of the export complex and release of the cargo. Phosphorylation of the NPC itself may be important for regulation of nucleocytoplasmic trafficking. A number of pore complex nucleoporins are phosphorylated in a cell cycle-dependent manner, but it is unclear what consequences this has for transport or pore structure (196). Other modifications besides phosphorylation also play a role in transport. The association of RanGAP1 with the nuclear pore complex is dependent on the modification of RanGAP1 with an ubiquitin-like protein which increases the size of RanGAP1 from 70 kDa to 90 kDa (213). RanGAP1 lacking the

modification remains in the cytosol and does not interact with the NPC. These examples demonstrate that the cell uses many mechanisms to modulate nuclear transport. It is likely that many more remain to be discovered.

c. *Transportin-Mediated Import*

As stated at the start of this section, two major import pathways have been highly characterized to date. The first is the classical NLS importin pathway, and the second is the transportin-mediated pathway. There are a number of parallels as well as differences between these two pathways that have been discovered.

Just as the importin pathway uses a basic NLS to target proteins to the nucleus, the transportin pathway uses a conserved, 38 residue sequence called M9 that bestows nuclear uptake (316). Soon after the discovery that M9 targeted the heterogenous nuclear ribonucleoprotein (hnRNP) A1 to the nucleus, it was also found that M9 could act as an export signal for the same hnRNP A1 protein (222). M9 therefore acts as a nucleocytoplasmic shuttling sequence, able to mediate movement of RNPs into or out of the nucleus (221). It has not been possible with mutation analysis to separate the import-mediating residues from the ones that mediate export (40, 222). Another difference between M9 and the SV40 NLS is that, while the SV40 NLS or similar sequence is found in a wide range of proteins, M9 appears to be fairly specific for ribonucleoproteins (211).

Whereas the SV40 NLS binds to an adaptor protein (importin-α1), and then to the importer (importin-β1), M9 binds directly to its importer, transportin (also known as importin-β2 or karyopherin-β2) (3, 42). However, like importin-mediated import, transportin requires GTP hydrolysis by Ran (42), although single rounds of transport can

occur without hydrolysis (98, 282). Transportin also interacts with nucleoporins in the NPC, which can be competed out with classical importin/SV40 NLS components, suggesting that importin-β1 and transportin bind to common elements in the pore (42).

While transportin is the import protein for M9 bearing ribonucleoproteins, it does not mediate export of these proteins (221). RanGTP is able to disrupt transportin complexes in the nucleus just as it disrupts importin-β1 complexes, therefore it is unlikely that a stable export complex containing transportin could form in the nucleus (153). To date, the transportin exporter has not been identified.

The transportin import pathway appears to be well-conserved in nature. Both transportin itself and the M9 sequence have homologues in humans, *Saccharomyces cerevisiae*, *Drosophila melanogaster*, *Xenopus laevis*, and *Schizosaccharomyces pombe*, most of which can be substituted for one another in import assays (317).

d. Other Import Modalities

The two import mechanisms discussed above are currently the most understood, but a number of other nuclear transporters have been identified. For example, ribosomal proteins are imported by karyopherins β3 and β4, while the yeast Hog1p MAP kinase is imported by a novel importin coded for by the gene *NMD5* (3). A very unusual import signal is that used by the U snRNPs, which consists of the 5'-2,2,7-terminal trimethylguanosine cap structure of the U snRNA portion of the snRNP. Import of these molecules is mediated by a novel import factor called snurportin (145). It has also been demonstrated that ERK2 enters the nucleus using a non-classical import pathway (110,

359). Many other combinations of unique import signals and import factors have recently been identified (242), and others are sure to follow.

2. *Nuclear Ion Transport*

Early characterization studies of the cell nucleus revealed the surprising finding that sodium and potassium ions partitioned between the nucleus and cytosol (63, 361). Indeed, the concentration of sodium in the nucleus was reported to be an order of magnitude higher in the nucleus than in the cytosol. At the same time, microinjection studies revealed that small molecule tracers freely traveled between the nucleus and cytosol (361). It was assumed that ions, being even smaller than the tracers, also freely traveled between the cytosol and nucleus, and the observed concentration differences were due to preferential binding of ions to cytoplasmic or nuclear structures.

It had also been shown, however, that some cells exhibited an electrical potential between the nucleus and cytoplasm (193). This would argue that at least some of the ions must be unbound, and in turn the nuclear envelope must act to some degree as a barrier to free diffusion of ions. Ten years ago, Mazzanti *et al.* (217) provided evidence by patch clamping of mouse pronuclei that K^+ selective channels exist in the nuclear envelope, which resulted in a hyperpolarization of the nucleus relative to the cytosol of approximately –10 mV. It was suggested at the time that these ion movements may serve to balance charge changes that occur with the movement of macromolecules through the NPC, or to balance the very large negative charge of DNA due to its high phosphate composition via the Donnan effect (55). The identity of the K^+ channels was suggested to be the nuclear pore complex, since the number of nuclear pores appeared to correlate

with the number of channels (218). This idea was supported by the finding that the individual channels did not seem to bridge the cytosol with the perinuclear lumen, or the perinuclear lumen with the cytoplasm. Instead, the channels crossed both lipid bilayers, bridging the cytosol directly with the nucleus (150). To explain the ability of the NPC to restrict ion flow, it was suggested that the lumenal plug in the pore might play a role, effectively reducing the lumenal diameter and possibly reducing free diffusion of ions.

These channels were characterized in patch clamping experiments, and are now called large conductance nuclear ion channels (NICs) (54, 55). The major species responsible for current flow through these channels has been confirmed as potassium. The sodium channel blocker tetrodotoxin and the calcium channel blocker diltiazem had no effect on the conductance of the NIC. The potassium channel blockers Cs^+ and TEA were also without effect. This suggests that the NICs are a novel form of potassium channel (55). An interesting finding, however, is that, while GTP had no effect on the conductance of NICs, GTP-γ–S blocked ion flow. This suggests that GTP hydrolysis may be required for the proper functioning of the channel (55).

It has also been found that the nuclear envelope may act as an effective barrier to proton movements. Studies using intracellular pH sensitive fluorescent probes have revealed a pH gradient across the nuclear envelope, resulting in a higher nuclear pH relative to the cytoplasm by 0.3 to 0.5 pH units (308). The significance of nuclear partitioning of protons and potassium ions has not yet been revealed. However, partitioning of calcium between the nucleus and cytosol has been intensively investigated, and roles for nuclear calcium are well established.

III. Nuclear Calcium

For many years, the role of cytosolic calcium in the cell has been under intense investigation. Cytosolic calcium is a critical second messenger, transducing signals in a large number of intracellular communications pathways. Arguably, it is the single most-commonly-used second messenger in the cell. Calcium also plays a key role in excitable tissues, mediating both muscle contraction and nerve conduction (24). However, until relatively recently, it was unclear what role nuclear calcium played in the cell, and whether nuclear calcium could be considered an independent intracellular calcium pool. Although controversy still exists, it appears that nuclear calcium is indeed regulated independently of cytosolic or SR/ER calcium. This unique calcium pool may play a critical role in nuclear physiology.

1. Role of Nuclear Calcium

Calcium in the nucleus has been implicated in regulating or modulating nearly every major nuclear function examined. Calcium has been known to be a regulator of gene expression since its first implication in the regulation of prolactin synthesis (351). Since then, calcium responsive DNA binding elements such as CREB and SRF have been identified. CREB is a binding protein for the cAMP response element (CRE) that binds to the c-fos promoter. CREB is regulated by calcium entering cells by L-type voltage gated calcium channels, causing activation of CRE-containing genes (88, 309-311). Similarly, the serum response factor SRF is also responsive to calcium, which promotes binding of SRF to the serum response element SRE in the c-fos promoter and, again, activation of the gene (21, 227). c-fos is an immediate early gene product which, when coupled to c-

jun forms the AP-1 transcription factor, which binds to and activates a large number of gene promoters. Through the use of other calcium-binding proteins such as calmodulin, calcium is able to regulate other genes as well, such as that of proopiomelanocortin (192). It has even been suggested that, by acting through CREB, nuclear calcium may impact learning and memory (132).

Calcium has also been implicated in the regulation of cell cycling. Calcium spikes are associated with changes in the stage of the cell cycle (265), and with cell cycle-specific events such as nuclear envelope breakdown (314) and entry to mitosis, where cellular calcium transients appear to arise from the nucleus (353). Related to these effects, calcium also appears to be a trigger to induce differentiation (142) and is required for effective replication and repair of DNA (19, 67).

Calcium plays roles in other nuclear events such as modulation of the intranuclear contractile system (20, 270, 301). There is also evidence that there is feedback between cytosolic and nuclear calcium and activity of the apoptosis suppressor bcl-2 (164, 203, 271). Finally, it has been suggested that nuclear calcium may interact with cytoplasmic calcium to positively or negatively affect excitation-contraction coupling in cardiomyocytes (36). An important role specifically for perinuclear calcium, as opposed to nucleoplasmic calcium, is regulation of the permeability of the nuclear pore complex (see Section A.I.2.b.iii).

Obviously calcium is a major determinant of nuclear function, and precise regulation of nuclear calcium is required by the cell. The molecular basis for this regulation is the subject of the following section.

2. *Regulation of Nuclear Calcium*

a. Nuclear Calcium Pumps and Channels

As discussed earlier, it was originally thought that small ions like calcium could readily diffuse across the nuclear envelope through the NPC. Nicotera *et al.*, however, demonstrated that an ATPase activity existed in isolated nuclei that permitted them to take up and sequester $^{45}Ca^{2+}$ (244), and that this calcium could be released by stimulation by inositol 1,4,5-trisphosphate (IP_3) (201, 245). There may be two calcium ATPases, one on the inner nuclear membrane and one on the outer membrane. The outer membrane pump has been characterized and is identical to that of the endoplasmic reticulum (185), while the inner membrane pump has not been characterized (197).

Many groups have demonstrated differential calcium levels in the nucleus and cytoplasm, and nuclear calcium transients in a variety of cell types (14, 51, 103, 138, 139, 178, 195, 269). The direction and magnitude of the gradient, however, seems to vary by cell type. Although some reports have failed to show differential regulation of nuclear and cytosolic calcium (13), this phenomenon is now widely accepted (22, 260).

The question that remains is how nucleocytoplasmic calcium gradients are maintained. It does not seem credulous that **no** diffusion of calcium through the pore occurs, even if the lumenal plug reduces trafficking. The current model of nuclear calcium regulation suggests that inositol phosphates are partially responsible (197). As previously mentioned, IP_3 receptors exist in the nucleus, and calcium currents flowing through these receptors have been characterized (200). It has now been shown that inositol 1,3,4,5-tetrakisphosphate (IP_4) also regulates nuclear calcium signaling via two classes of nuclear IP_4 receptors (152, 179). The IP_3 receptors are localized to the inner

nuclear membrane, while high affinity IP_4 receptors are localized to the outer nuclear membrane (148) and low affinity IP_4 receptors are localized to the inner membrane (152). Together with the nuclear envelope calcium ATPase, these inositol phosphate-sensitive calcium channels actually regulate two distinct pools of nuclear calcium: one in the nucleoplasm, and one in the perinuclear space.

Binding of IP_3 to the IP_3 receptor results in movement of calcium from the perinuclear space into the nucleoplasm. The activity of the IP_3 receptor can be accelerated by phosphorylation by PKC (212), which is interesting in light of the fact that PKC-α localizes to the nucleus after stimulation (158). Binding of IP_4 to the high affinity, outer nuclear membrane IP_4 receptor results in movement of calcium from the cytoplasm into the perinuclear space. This mode of nuclear uptake is favored when cytosolic $[Ca^{2+}]$ exceeds 0.8 μM, indicating calcium-induced calcium uptake (197). Together, these two receptors can drive calcium from the cytosol into the nucleoplasm via the perinuclear space, which would tend to counteract any loss of calcium through the nuclear pore. The role of the low affinity IP_4 receptor is currently unknown, but it may function to move calcium out of the nucleus and into the perinuclear space. The role of the outer nuclear membrane calcium ATPase seems to be regulation of uptake of calcium by the nucleus when cytosolic calcium is below 0.8 μM, and may play the role of a safety mechanism in times of cellular distress (148, 197). It is reported that this ATPase directs calcium from the cytosol into the perinuclear space (112).

b. Nuclear Calcium Binding Proteins

In order for calcium to carry out its functions in the nucleus, it must interact with calcium binding proteins (CaBPs). The wide variety of nuclear CaBPs are too numerous to list here, but several important examples of nuclear CaBPs are discussed.

One of the most important CaBPs in the nucleus, and indeed the cell, is calmodulin. Calmodulin can be envisioned as the effector for many of calcium's roles in the nucleus, including gene expression (192), cell cycling (64, 65) and DNA replication (19). Calmodulin exerts its myriad effects by interacting with a variety of nuclear calmodulin-binding proteins, including myosin light chain kinase and calmodulin kinase II, which in turn have multiple downstream targets (19). Nuclear protein kinase II (88, 311) and the phosphatase, calcineurin (270) are activated by calmodulin and in turn may activate or deactivate other nuclear proteins, such as the cAMP response element binding protein CREB (88, 311).

Another important nuclear calcium binding protein is the calcium activated neutral cysteine protease, calpain. As opposed to many other proteases which act to breakdown unnecessary or potential dangerous proteins, calpain seems to cleave specifically between active domains of proteins, often resulting in the generation of new, functional protein products (113, 247). For example, nuclear nucleoside triphosphatase is generated by the cleavage of lamins A/C by calpain (76, 335). Calpain is also responsible for mediating breakdown of the transcription factors c-fos and c-jun (140), and may play a role in nuclear envelope breakdown (113).

The protein calreticulin has also been described to have important nuclear effects. Calreticulin was originally thought to be simply an endoplasmic reticulum lumenal

calcium sink protein. It contains many calcium binding sites and is therefore able to bind large amounts of calcium and sequester it (224). This permits very high levels of calcium to be kept within the endoplasmic reticulum without precipitation of calcium compounds like calcium phosphate. Recently, however, calreticulin has been shown to also localize to the nucleus and possess other functions. Calreticulin is able to bind to sequences in the genes of the superfamily of nuclear hormone receptors (52, 90), suggesting a role for calreticulin in the modulation of expression of these genes. Calreticulin also modulates glucocorticoid-sensitive gene expression, possibly through a similar mechanism (223). But the most interesting finding has been that calreticulin gene expression is critical for cardiac development (220). Knockout mice for calreticulin exhibit dramatic cardiac abnormalities. Calreticulin is highly expressed throughout the developing heart, but is only a minor component of the mature heart.

These proteins represent only a small number of the currently identified nuclear calcium binding proteins, however, they clearly have a dramatic effect on normal cell physiology. It is also highly likely that many more nuclear calcium binding proteins remain to be found.

B. HYPOTHESIS

The present thesis tests three distinct hypotheses with regard to nuclear structure and function:

1. Unidentified calcium-binding proteins exist within the nucleus that may play roles in regulation of nuclear calcium pools. The objectives of this study are:
    a. To survey which calcium-binding proteins are present in both an excitable (cardiomyocyte) and non-excitable (hepatocyte) tissue.
    b. To positively identify one or more of these calcium-binding proteins.
2. Alterations in lipid metabolism will result in alteration of nuclear envelope composition. In turn, alterations in the composition of the nuclear membrane lipid bilayers will affect the activity of enzymes associated with the nuclear envelope, and the structural integrity of the nucleus. The objectives of this study are:
    a. To examine a genetic animal model of hyperlipidemia and determine whether nuclear envelope composition is altered.
    b. To examine the effects of altered nuclear envelope composition on the activity of an envelope-associated enzyme, the nuclear nucleoside triphosphatase.
    c. To examine the effects of altered nuclear envelope composition on nuclear integrity.
3. Hydrogen peroxide will inhibit nuclear protein import via a simple oxidative mechanism, in a time- and dose-dependent manner. The objectives of this study are:
    a. To examine and characterize the effect of H_2O_2 on nuclear protein import.
    b. To determine the mechanism by which H_2O_2 exerts its effects.

C. MATERIALS

I. General Chemicals and Supplies

Product	Source
^{32}P as orthophosphoric acid	NEN/Mandel (Guelph, ON)
$^{45}Ca^{2+}$ as calcium chloride	NEN/Mandel (Guelph, ON)
Acetone	Mallinckrodt Inc. (St. Louis, MO)
Acrylamide	Gibco/BRL (Burlington, ON)
Activated ERK2	Calbiochem-Novabiochem (La Jolla, CA)
Ammonium formate	Sigma-Aldrich Canada Ltd. (Oakville, ON)
Ammonium molybdate	Mallinckrodt Inc. (St. Louis, MO)
Ammonium persulfate	Sigma-Aldrich Canada Ltd. (Oakville, ON)
ANS (1-amino 2-naphthal 4-sulfonic acid)	Sigma-Aldrich Canada Ltd. (Oakville, ON)
Aprotinin	Sigma-Aldrich Canada Ltd. (Oakville, ON)
Araldite 502	Sigma-Aldrich Canada Ltd. (Oakville, ON)
Ascorbate	Mallinckrodt Inc. (St. Louis, MO)
ATP	Sigma-Aldrich Canada Ltd. (Oakville, ON)
Benzamidine	Sigma-Aldrich Canada Ltd. (Oakville, ON)
Bis-acrylamide	BioRad Laboratories (Canada) Ltd. (Mississauga, ON)
BODIPY FL-conjugated BSA	Molecular Probes Inc. (Eugene, OR)
Bovine Serum Albumin (BSA)	Sigma-Aldrich Canada Ltd. (Oakville, ON)
Bromophenol Blue	BioRad Laboratories (Canada) Ltd. (Mississauga, ON)
Catalase	Sigma-Aldrich Canada Ltd. (Oakville, ON)
Chloroform	Mallinckrodt Inc. (St. Louis, MO)
Cholesterol esterase	Sigma-Aldrich Canada Ltd. (Oakville, ON)
Cholesterol oxidase	Sigma-Aldrich Canada Ltd. (Oakville, ON)
Cholesteryl oleate	Sigma-Aldrich Canada Ltd. (Oakville, ON)
Coomassie Brilliant Blue R-250	LKB Bromma (Sweden)

Product	Source
Creatine phosphate	Sigma-Aldrich Canada Ltd. (Oakville, ON)
Creatine phosphokinase	Sigma-Aldrich Canada Ltd. (Oakville, ON)
D-19 Developer	Eastman Kodak (Rochester, NY)
Daidzein	Sigma-Aldrich Canada Ltd. (Oakville, ON)
o-Dianisidine	Sigma-Aldrich Canada Ltd. (Oakville, ON)
Digitonin	Sigma-Aldrich Canada Ltd. (Oakville, ON)
Dithiothreitol (DTT)	Sigma-Aldrich Canada Ltd. (Oakville, ON)
DMEM	Gibco/BRL (Burlington, ON)
Dimethylsulfoxide	Sigma-Aldrich Canada Ltd. (Oakville, ON)
DNase I	Worthington Biochemicals (Freehold, NJ)
(2-Dodecen-1-yl)succinic anhydride	Sigma-Aldrich Canada Ltd. (Oakville, ON)
ECL Immunoenzyme Detection Kit	Amersham Canada Ltd. (Oakville, ON)
EDTA	Sigma-Aldrich Canada Ltd. (Oakville, ON)
Edwal Superflat	Falcon Safety Products (Somerville, NJ)
EGTA	Sigma-Aldrich Canada Ltd. (Oakville, ON)
Ektamatic SC Print Paper	Eastman Kodak (Rochester, NY)
Electron Microscopy Copper Grids	Electron Microscopy Sciences (Fort Washington, PA)
Ethanol	Fisher Scientific (Nepean, ON)
Ethyl acetate	Fisher Scientific (Nepean, ON)
Excellulose Columns	Pierce (Rockford, IL)
FBS	Gibco/BRL (Burlington, ON)
Fixer	Eastman Kodak (Rochester, NY)
Formaldehyde	Sigma-Aldrich Canada Ltd. (Oakville, ON)
Fungizone	Gibco/BRL (Burlington, ON)
GDP	Sigma-Aldrich Canada Ltd. (Oakville, ON)
Genistein	Sigma-Aldrich Canada Ltd. (Oakville, ON)
Glutaraldehyde	Sigma-Aldrich Canada Ltd. (Oakville, ON)
Glycerol	Fisher Scientific (Nepean, ON)

Product	Source
Glycine	Gibco/BRL (Burlington, ON)
GTP	Sigma-Aldrich Canada Ltd. (Oakville, ON)
HEPES	Sigma-Aldrich Canada Ltd. (Oakville, ON)
Hoechst 33258	Sigma-Aldrich Canada Ltd. (Oakville, ON)
Hydrochloric acid	Fisher Scientific (Nepean, ON)
Hydrogen peroxide	Sigma-Aldrich Canada Ltd. (Oakville, ON)
Imidazole	Sigma-Aldrich Canada Ltd. (Oakville, ON)
Insulin	Sigma-Aldrich Canada Ltd. (Oakville, ON)
p-Iodonitrotetrazolium violet (INT)	Sigma-Aldrich Canada Ltd. (Oakville, ON)
Iron sulfate	Sigma-Aldrich Canada Ltd. (Oakville, ON)
KCl	Sigma-Aldrich Canada Ltd. (Oakville, ON)
Lead citrate	Sigma-Aldrich Canada Ltd. (Oakville, ON)
Leupeptin	Sigma-Aldrich Canada Ltd. (Oakville, ON)
Magnesium acetate	Sigma-Aldrich Canada Ltd. (Oakville, ON)
Magnesium chloride	Sigma-Aldrich Canada Ltd. (Oakville, ON)
Mannose 6-phosphate	Sigma-Aldrich Canada Ltd. (Oakville, ON)
β-Mercaptoethanol	Sigma-Aldrich Canada Ltd. (Oakville, ON)
MES	Sigma-Aldrich Canada Ltd. (Oakville, ON)
Methanol	Mallinckrodt Inc. (St. Louis, MO)
MOPS	Sigma-Aldrich Canada Ltd. (Oakville, ON)
Nitrocellulose Membranes	Gibco/BRL (Burlington, ON)
p-Nitrophenol	Sigma-Aldrich Canada Ltd. (Oakville, ON)
p-Nitrophenolphosphate	Sigma-Aldrich Canada Ltd. (Oakville, ON)
Non-activated ERK2	Calbiochem-Novabiochem (La Jolla, CA)
Osmium tetroxide	Electron Microscopy Sciences (Fort Washington, PA)
Paraformaldehyde	TAAB Labs. Equip. Ltd. (Reading, UK)
PD98059	Calbiochem-Novabiochem (La Jolla, CA)
PEI-Cellulose TLC Plates	Scientific Adsorbents Inc. (Atlanta, GA)

Product	Source
Pepstatin A	Sigma-Aldrich Canada Ltd. (Oakville, ON)
Perchloric acid	Anachemia Science (Winnipeg, MB)
Peroxidase	Sigma-Aldrich Canada Ltd. (Oakville, ON)
Phosphate-free DMEM	Gibco/BRL (Burlington, ON)
Photo-Flo	Eastman Kodak (Rochester, NY)
Potassium acetate	Sigma-Aldrich Canada Ltd. (Oakville, ON)
Potassium chloride	Mallinckrodt Inc. (St. Louis, MO)
Potassium phosphate dibasic	Sigma-Aldrich Canada Ltd. (Oakville, ON)
Potassium phosphate monobasic	Sigma-Aldrich Canada Ltd. (Oakville, ON)
Propylene oxide	Sigma-Aldrich Canada Ltd. (Oakville, ON)
Protein-A agarose	Calbiochem-Novabiochem (La Jolla, CA)
RNase A	Worthington Biochemicals (Freehold, NJ)
Serum Cholesterol Assay Kit	Sigma-Aldrich Canada Ltd. (Oakville, ON)
Serum Glucose Assay Kit	Sigma-Aldrich Canada Ltd. (Oakville, ON)
Serum Triglyceride Assay Kit	Stanbio Laboratory Inc. (San Antonio, TX)
Skim Milk Powder	Carnation/Nestle Foods (USA)
Sodium acetate	Sigma-Aldrich Canada Ltd. (Oakville, ON)
Sodium azide	Sigma-Aldrich Canada Ltd. (Oakville, ON)
Sodium bisulfite	Sigma-Aldrich Canada Ltd. (Oakville, ON)
Sodium chloride	Sigma-Aldrich Canada Ltd. (Oakville, ON)
Sodium cholate	Sigma-Aldrich Canada Ltd. (Oakville, ON)
Sodium dodecyl sulfate (SDS)	BioRad Laboratories (Canada) Ltd. (Mississauga, ON)
Sodium hydroxide	Sigma-Aldrich Canada Ltd. (Oakville, ON)
Sodium phosphate dibasic	Sigma-Aldrich Canada Ltd. (Oakville, ON)
Sodium pyruvate	Sigma-Aldrich Canada Ltd. (Oakville, ON)
Sodium selenite	Sigma-Aldrich Canada Ltd. (Oakville, ON)
Sodium succinate	Sigma-Aldrich Canada Ltd. (Oakville, ON)
Sodium sulfite	Sigma-Aldrich Canada Ltd. (Oakville, ON)

Product	Source
Soybean trypsin inhibitor	Sigma-Aldrich Canada Ltd. (Oakville, ON)
SpectraPor Dialysis Membranes	Spectrum (Laguna Hills, CA)
Stains-All	Sigma-Aldrich Canada Ltd. (Oakville, ON)
Sucrose	Sigma-Aldrich Canada Ltd. (Oakville, ON)
Sulfosuccinimidyl 4-[*N*-maleimidomethyl] cyclohexane-1-carboxylate	Pierce (Rockford, IL)
Sulfuric acid	Fisher Scientific (Nepean, ON)
SuperSignal Western Blotting Kit	Pierce (Rockford, IL)
TEMED	Sigma-Aldrich Canada Ltd. (Oakville, ON)
Toluidine Blue	Sigma-Aldrich Canada Ltd. (Oakville, ON)
Transferrin, Holo-	Sigma-Aldrich Canada Ltd. (Oakville, ON)
Trichloroacetic acid	Sigma-Aldrich Canada Ltd. (Oakville, ON)
2,4,6-Tris[dimethylaminomethyl]phenol	Sigma-Aldrich Canada Ltd. (Oakville, ON)
Tris-(2-carboxyethyl) phosphine HCl	Calbiochem-Novabiochem (La Jolla, CA)
Tris-HCl	Sigma-Aldrich Canada Ltd. (Oakville, ON)
Tris-OH	Sigma-Aldrich Canada Ltd. (Oakville, ON)
Triton X-100	Fisher Scientific (Nepean, ON)
Trypsin/EDTA	Gibco/BRL (Burlington, ON)
Tween-20	Sigma-Aldrich Canada Ltd. (Oakville, ON)
Uranyl acetate	Electron Microscopy Sciences (Fort Washington, PA)
Vectashield	Vector Laboratories, Inc (Burlingame, CA)
Xanthine	Sigma-Aldrich Canada Ltd. (Oakville, ON)
Xanthine oxidase	Sigma-Aldrich Canada Ltd. (Oakville, ON)
X-OMAT AR Film	Eastman Kodak (Rochester, NY)

II. Antibodies

Primary Antibody	Type	Host	Source
Active MAP kinase	Monoclonal	Rabbit	Promega (Madison, WI)
Cardiac calsequestrin	Monoclonal	Rabbit	SWant (Bellinzona, Switzerland)
DNA	Monoclonal	Mouse	Pierce (Rockford, IL)
Ran	Monoclonal	Mouse	Transduction Labs (Lexington, KY)

Secondary Antibody	Type	Host	Conjugate	Source
Anti-mouse IgG	Monoclonal	Goat	HRP	BioRad Laboratories (Canada) Ltd. (Mississauga, ON)
Anti-mouse IgG	Monoclonal	Sheep	FITC	Amersham Canada Ltd. (Oakville, ON)
Anti-rabbit IgG	Monoclonal	Goat	$Alexa_{488}$	Molecular Probes Inc. (Eugene, OR)
Anti-rabbit IgG	Monoclonal	Goat	HRP	BioRad Laboratories (Canada) Ltd. (Mississauga, ON)

III. Confocal Filter Blocks

Filter Set	Excitation Filter	Dichroic Mirror	Emission Filter
UBHS	None	488 + UV reflector	515
VHS	None†	510 LP	515
IN2	None	440 LP	Em1:405±35 Em2:460 LP

†VHS 488DF10 excitation filter removed

Abbreviations: LP – Longpass filter; Em1, Em2 – emission filters 1 and 2

D. METHODS

I. Animal Protocols

1. Sprague-Dawley Rats

Male Sprague-Dawley rats (250-350 g) were maintained in the St. Boniface General Hospital Research Centre animal care unit with food and water *ad libitum*. Care and treatment of the animals was in conformity with the Guidelines of the Canadian Council on Animal Care, and subject to prior review by animal care committees. These guidelines were adhered to for all other animals used in the studies listed below. Animals were given an intraperitoneal overdose of a cocktail of ketamine (60 mg/kg) and xylazine (10 mg/kg) and then sacrificed by decapitation. Excised tissues (i.e. livers and hearts) were used immediately or quick frozen in liquid nitrogen and stored at –80°C as necessary.

2. JCR:LA-cp Rats

Male and female JCR:LA-*cp* rats were bred in the established breeding colony at the University of Alberta using a standardized breeding protocol (295). The study included corpulent *cp/cp* animals, as well as lean *+/?* animals, so designated because they consist of both +/+ and *+/cp* animals in the ratio of 1:2 as a result of crossing *+/cp* animals. Access to water and standard rat chow was unrestricted. Male and female animals of either genotype were sacrificed at 3, 6 or 9 months of age as described for Sprague-Dawley rats. Body, heart and liver weight measurements were determined at time of sacrifice.

3. Rabbits

Male albino New Zealand white rabbits were given free access to food and water in the St. Boniface General Hospital Research Centre animal care unit. Anaesthesia was induced by administration of 5% halothane in 2L/min oxygen, followed by 3% halothane in 2 L/min oxygen by face mask. Sacrifice was performed by cardiac excision, at which time the aorta was removed.

II. Tissue Isolation

1. Isolation of Rat Hepatic Nuclei

Normal rat hepatic nuclei were isolated from male Sprague-Dawley rats (250-350 g) according to Gilchrist *et al.* (113). Briefly, rats were sacrificed after ketamine/xylazine overdose by decapitation and the livers excised into STM buffer (250 mM sucrose, 50 mM Tris-OH, 5 mM $MgCl_2$, pH 7.4) containing protease inhibitors (1 mM dithiothreitol, 1mM phenylmethylsulfonylfluoride, 1 μM leupeptin). All subsequent STM solutions also contained these protease inhibitors. Usually fifteen or thirty livers were used at a time (total mass ~200 or 400 g, respectively). The livers were scissor-minced, washed three times and homogenized in five volumes of STM in a Potter-Elvehjem glass tube with a loose fitting Teflon pestle (Wheaton Instruments, 10 strokes at setting three). The homogenate was filtered through 4-ply gauze, then pelleted at 1400x*g* for 10 minutes. The supernatants were discarded and the pellets rehomogenized in 5 volumes of STM. The suspension was centrifuged again as above, the supernatant discarded and the pellet resuspended in one volume of STM. This was diluted with 2 volumes of STM containing 2.3 M sucrose, and the final suspension layered onto 2.3 M sucrose STM cushions. The

nuclei were pelleted through the cushions by ultracentrifugation at 35000x*g* for 40 minutes (Beckman SW28 rotor), and the pellet collected in STM. The final protein concentration of the nuclei was typically between 60-80 mg/ml. Nuclei were quickly frozen in liquid nitrogen and stored at -85°C. All solutions were kept on ice throughout the entire procedure.

Nuclei from male or female JCR:LA-*cp* corpulent (*cp/cp*) or lean (+/?) rat livers were isolated using the same procedure.

2. *Isolation of Pig Cardiac Nuclei*

Pig cardiac nuclei were isolated from fresh pig hearts using a method based on that of Jackowski and Liew (154). The atria were trimmed away and only the ventricles used. The mass of starting material was usually 150-160 g. The endo- and epicardia were removed and the tissue scissor-minced in STM with several washings. The tissue was then homogenized in five volumes of STM as per the liver tissue above. The homogenate was filtered through 6-ply gauze and pelleted at 1400x*g* for 10 minutes. The supernatant was discarded and the pellet rehomogenized in five volumes of STM. The suspension was filtered through a 200 mesh steel filter and then centrifuged as above. The supernatant was discarded and the pellet resuspended in a small volume of STM, then quickly frozen in liquid nitrogen. The frozen slurry was slowly thawed back to 4°C and diluted with five volumes of STM. The suspension was centrifuged again as above, the supernatant discarded and the pellet resuspended in 2.2 M sucrose STM. This suspension was then layered onto discontinuous sucrose/STM gradients consisting of a bottom layer of 2.7 M sucrose STM and an upper layer of 2.3 M sucrose STM. The gradients were

then ultracentrifuged in a Beckman SW28 rotor at 90000x*g* for 70 minutes. The cardiac nuclei were concentrated and collected by pipette at the 2.3/2.7 interface. The nuclei were diluted with ten volumes of STM and pelleted at 1400x*g* for 10 minutes to collect the nuclei. The nuclear pellet was suspended in STM with a typical protein concentration of 4-6 mg/ml. Nuclei were frozen in liquid nitrogen and stored at -85°C. All solutions were kept on ice throughout the procedure.

3. Isolation of Nuclear Envelopes

The procedure for isolation of nuclear envelopes from both rat hepatic and pig cardiac nuclei is the same, and is a modification of the procedure of Kaufmann *et al.* (170). Nuclei were diluted in STM to a concentration of 5 mg/ml and treated with 250 µg/ml DNase I and 250 µg/ml RNase A, then incubated on ice for 60 minutes with constant stirring. The solution was then centrifuged at 12000x*g* for 10 minutes. The pellets were diluted in half the original volume of STM and stirred; a half volume of 2 M NaCl in STM was then slowly added, and the whole solution incubated on ice for 30 minutes with constant stirring. The suspension was centrifuged as above and the supernatant saved ("high salt fraction"). This fraction represented the nucleoplasmic contents. The pellet was resuspended in STM buffer to a final concentration of 5-10 mg/ml (cardiac samples) or 10-15 mg/ml (hepatic samples). Any samples not used immediately were frozen in liquid nitrogen and stored at -85°C.

4. Smooth Muscle Cell Culture from Rabbit Aorta

Vascular smooth muscle cells were obtained from aortic explants of New Zealand white rabbits as described (299). The aorta was removed from the animal, washed clean of red blood cells, and the adventitia removed. The aorta was cut into rings ~3 mm in length, and the rings placed into Dulbecco's Modified Eagle's Medium (DMEM) supplemented with 20% fetal bovine serum (FBS) plus 10% fungizone. The rings were incubated at 37°C in an atmosphere of 95%:5% O_2:CO_2 for 10-12 days to allow migration of fibroblasts and endothelial cells. After seven days the rings were removed into fresh FBS/DMEM and incubated as above for another seven days to allow migration of smooth muscle cells. The rings were removed and the cells grown to confluence in 10% FBS/DMEM plus 1% fungizone. The cells were then passaged with 0.05% trypsin, 0.53 mM EDTA onto glass coverslips in fresh medium. Cells were either maintained in 10% FBS/DMEM or Starvation Medium (STV) (DMEM plus 5 μg/ml holo-transferrin, 1 nM sodium selenite, 200 μM ascorbate, 10 nM insulin, 2.5 μM sodium pyruvate), plus 1% fungizone. Cells were fed with 10% FBS/DMEM + 1% fungizone 24 to 48 hours prior to use. Cells used were always of the first passage.

5. Isolation of Rat Liver Cytosol

A male Sprague-Dawley rat (~250 g) was sacrificed as described in Section C.I.1 above and the liver quickly removed into ice-cold STM buffer. The liver was scissor-minced and washed several times with STM buffer, then homogenized. The homogenate was centrifuged in a Beckman JA-20 rotor at 1400x*g* for 10 minutes at 4°C. The supernatant was removed and centrifuged at 3300x*g* for 15 minutes at 4°C. This

supernatant was then centrifuged in a Beckman SW28 rotor at 100 000x*g* for one hour at 4°C. The final supernatant was removed as "cytosol." Cytosol was dialyzed overnight through Spectrapor 1 dialysis tubing against multiple changes of Import Buffer (20 mM HEPES, 110 mM potassium acetate, 5 mM sodium acetate, 2 mM magnesium acetate, 0.5 mM EGTA, pH 7.3) including 1 mM DTT and 1 μg/ml each of leupeptin, pepstatin A, and aprotinin.

III. Characterization of Isolated Nuclei

1. Visualization of Isolated Nuclei

Aliquots of rat hepatic and pig cardiac nuclei were treated with equivolume 0.05% Toluidine Blue and air-dried on coverslips, then photographed at 40x magnification with phase contrast. Aliquots of rat hepatic and pig cardiac nuclei were also incubated with the DNA-specific stain Hoechst 33258 at a final concentration of 2 μg/ml for ten minutes and visualized by UV confocal scanning laser microscopy using a Bio-Rad MRC600 system equipped with a UV argon ion laser in normal scanning mode. The dye was excited with the 351 nm laser line at 10% power, and the filter blocks used were the UBHS (ultra-violet/blue, high selectivity) block with the OG515 filter removed in position #1, and the IN2 block in position #2, with data collected from the first photomultiplier. The microscope objectives used were a Nikon Fluor 100x/1.3 N.A. oil immersion lens for the hepatic nuclei (with zoom factor 2.0) and a Nikon Fluor 40x/1.3 N.A. oil immersion lens for the cardiac nuclei (with zoom factor 5.0).

2. *Subcellular Marker Enzyme Assays*

a. Na^+/K^+ ATPase

The presence of Na^+/K^+ ATPase in sarcolemma or plasmalemma allows the determination of contamination of nuclear fractions by these membranes by assaying for this enzyme (264). Duplicate tubes were prepared containing 200 µl ATPase cocktail (250 mM Tris-OH, 600 mM NaCl, 17.5 mM $MgCl_2$, 5 mM EGTA, 25 mM NaN_3, pH 7.0 at 37°C), 300 µl 48% sucrose, 250 µl H_2O and 50 µl sample, plus either 100 µl 200 mM KCl or H_2O. To each tube was added 100 µl ATP. Tubes were vortexed, then placed in a water bath at 37°C for ~12 minutes (time was recorded). Following incubation, the tubes were placed into an ice bath for 30 seconds. To each tube was added 1.5 ml F+S Reagent (3.5 mM ammonium molybdate, 0.9 N H_2SO_4) and 100 µl ANS Reagent (4 mM 1-amino 2-naphthal 4-sulfonic acid, 50 mM $NaHSO_3$, 23 mM Na_2SO_3). Tubes were mixed, dried and warmed to room temperature. Absorbance was read at 690 nm. Blanks received water instead of sample, and standards were prepared by adding 100 µl 1 mM KH_2PO_4 to 900 µl H_2O, then treating as for the other samples. ATPase activity was then calculated using previously derived equations (264). Purified sarcolemma samples were obtained (264) and assayed for comparative purposes.

b. K^+-p-Nitrophenolphosphatase

This enzyme is also found in sarcolemma and plasmalemma (264), and therefore may also serve as a marker for contamination of nuclear fractions. Duplicate tubes were prepared containing 200 µl pNPPase cocktail (250 mM sucrose, 25 mM $MgCl_2$, 5 mM

EGTA, pH 7.8 at 37°C), 550 µl H_2O and 50 µl sample, plus either 100 µl 200 mM KCl or H_2O. To each tube was added 100 µl 50 mM *p*-nitrophenolphosphate. After vortexing, the tubes were placed in a water bath at 37°C for ~6 minutes (time was recorded). Tubes were then placed in an ice bath for 30 seconds. Exactly two milliliters 1.0 N NaOH was added to each tube to stop the reaction. Tubes were mixed, warmed to room temperature, dried and the absorbance read at 490 nm. Blanks contained H_2O instead of sample, and standards contained 5 µl 10 mM *p*-nitrophenol plus 995 µl H_2O. pNPPase activity was calculated using standard equations (264). As in the Na^+/K^+ ATPase assay, purified sarcolemmal samples were assayed and used for comparison.

c. Mannose-6-Phosphatase

Contamination of nuclear samples by sarco/endoplasmic reticulum fragments can be assessed by measuring levels of mannose-6-phosphatase (114). To plastic test tubes was added 240 µl 50 mM MES (pH 6.5) plus 20 µl crude nuclei, or 250 µl 50 mM MES (pH 6.5) plus 10 µl sarco/endoplasmic reticulum or nuclear envelopes (blanks received 260 µl 50 mM MES (pH 6.5) alone). Next were added 40 µl 100 mg/ml BSA in 50 mM MES (pH 6.5) and 100 µl 10 mM mannose-6-phosphate. The tubes were incubated at 30°C for 30 minutes, then the reaction was quenched by the addition of 200 µl 10% SDS. This assay generates inorganic phosphate as the final product. To correct for non-specific phosphate production, identical tubes were prepared and treated as above, but the SDS was added first to inactivate any phosphatases.

Inorganic phosphate produced was measured using the method of Raess and Vincenzi (273). To each of the above tubes was added 200 µl 0.9% ascorbate plus 200 µl 1.25%

ammonium molybdate in 6.5% H_2SO_4, with a 30 second delay between tubes. Tubes were incubated at room temperature for 30 minutes, centrifuged at low speed for 5 minutes to remove particulates, and the absorbance read at 660 nm, with each tube being read 30 seconds apart in the order they were first given molybdate. Concentrations of inorganic phosphate were calculated using a standard curve, with KH_2PO_4 as the standard (114). Purified samples of isolated endoplasmic reticulum (114) were used for comparison to samples.

d. Succinic Dehydrogenase

Succinic dehydrogenase is an enzyme highly enriched in mitochondria, and is therefore used as a marker assay for mitochondrial contamination (263). On ice, 0.5 mg/ml *p*-iodonitrotetrazolium violet (INT) (~1 mM) was dissolved in SDH cocktail (50 mM K_2HPO_4, 50 mM sodium succinate, 50 mM sucrose, pH 7.4). Exactly fifty microliters of sample or water was added to test tubes, which were placed on ice and to each of which was added 1 ml of the INT/SDH cocktail. The rack of tubes was then placed into a water bath at 37°C and a timer started. When suitable color had developed, the rack was transferred back to the ice bath and the time recorded. After ~1 minute, 0.3 ml 20% trichloroacetic acid was added, followed by 3.0 ml ethyl acetate. Tubes were vortexed vigorously to extract color into the organic layer. Tubes were centrifuged at low speed in the cold room for ten minutes, and then warmed to room temperature. The top layer was read at 490 nm and the activity of succinic dehydrogenase calculated according to published equations using $\varepsilon_{INT}=1.85x10^4$ (263). Succinic dehydrogenase activity in purified mitochondrial fractions (263) were used for comparative purposes.

e. K^+-EDTA Myosin ATPase

This assay measures contamination arising from myofibrils (208). To individual assay tubes was added 0.7 ml ATPase mix (0.5 M KCl, 10 mM imidazole, pH 7.0) plus 0.1 ml EDTA solution (100 mM EDTA buffered with KOH, pH 7.0). Immediately prior to incubation 0.1 ml 50 mM Tris-ATP (pH 7.0) was added. The reaction was started by the addition of 0.1 ml sample (~500 µg). The samples, including a standard (100 µM KH_2PO_4) were incubated at 37°C for 15 min, and the reaction terminated with the addition of 1 ml 10% trichloroacetic acid. To each tube was added 1.5 ml F+S Reagent and 0.1 ml ANS Reagent, and then the tubes were incubated at room temperature for ten minutes, followed by five minutes low speed centrifugation. Absorbance of the samples was determined at 690 nm, using a blank treated as above, except with the sample protein being added after the addition of trichloroacetic acid. The activity of samples was calculated based on that of the standard (263). Myofibrils were isolated (263) and assayed for K^+-EDTA myosin ATPase activity for comparative purposes.

3. Nuclear Nucleoside Triphosphatase Assay

Assays were completed in plastic tubes in 350 µl Reaction Buffer (250 mM sucrose, 20 mM MOPS, pH 7.4) containing EDTA (1 mM), $MgCl_2$ (1 mM or as required), and GTP or ATP (5 mM or as required). The reaction was started by the addition of 50 µl isolated nuclei (protein concentration ~3-10 mg/ml) and carried out for 20 minutes (or as required) at 37°C. The reaction was stopped by the addition of 200 µl 10% sodium dodecyl sulfate (SDS). Inorganic phosphate generated in the reaction was measured as

described in the mannose-6-phosphatase assay above. Identical assays were run as blanks, in which the SDS had been added prior to the reaction. NTPase dependence on time, [GTP], [ATP] and [Mg^{2+}] was determined for nuclei derived from lean and corpulent JCR:LA-*cp* rats, and Hanes K_M and V_{max} values determined. Free concentrations of ligands were determined from total concentrations using the Maxchelator program (© C. Patton, 1994).

4. Nuclear Cholesterol and Phospholipid Content

Cholesterol and phospholipids were extracted from 100 µl isolated nuclei (0.3 - 1.0 mg total protein content) by first diluting with 600 µl water, then by adding 3 ml 2:1 chloroform:methanol and vortexing for 15 seconds. One milliliter water was added and the tubes vortexed for 15 seconds; then, one milliliter chloroform was added and the tubes again vortexed for 15 seconds. Samples were left to extract in the dark at 4°C overnight. The samples were then centrifuged in a tabletop centrifuge for 10 minutes at low speed (750x*g*). Following centrifugation, the upper, non-aqueous layer was removed by pasteur pipette to a separate test tube and the solvent evaporated off under a stream of nitrogen gas. The dry samples were resuspended in ethanol and assayed for cholesterol (248) and phospholipid content (182).

For the cholesterol assay, resuspended samples in 200 µl ethanol were combined with 800 µl Reagent 2 (0.5% Triton X-100, 3 mM sodium cholate, 0.1 M Tris-HCl, 0.25 u/ml cholesterol oxidase, 0.1 mg/ml *o*-dianisidine, 0.01 mg/ml peroxidase, pH 6.6), then incubated at 37°C for 20 minutes. Samples were read at this point at 450 nm to measure free cholesterol. To each tube was then added 1 ml of Reagent 3 (0.5% Triton X-100, 3

mM sodium cholate, 0.1 M Tris-HCl, 1 u/ml cholesterol esterase, pH 6.6), followed by incubation at 37°C for 30 minutes. Samples were again read at 450 nm to measure total cholesterol. Esterified cholesterol could be calculated by subtracting free cholesterol from total cholesterol. A standard stock solution (0.5 mg/ml cholesterol and 0.5 mg/ml cholesteryl oleate in 1:1 ethanol:acetone) was used to generate a standard curve.

To measure phospholipid content, each tube of dried sample from above was treated with 0.7 ml perchloric acid and heated at 150°C in a dry block for 2 hours. Once tubes had cooled, 4 ml H_2O was added to each tube, followed by 0.2 ml fresh 5% ammonium molybdate and 0.2 ml fresh ANSA Solution (10 mM 1-amino 2-naphthal 4-sulfonic acid, 1.0 M $NaHSO_3$, 50 mM Na_2SO_3). Tubes were placed in boiling water for 20 minutes, then centrifuged at 1000x*g* for 5 to 10 minutes. Supernatants were decanted and absorbance read at 660 nm. Final concentration of phospholipid was calculated using a standard containing 25 μM KH_2PO_4 that was treated as the other samples had been.

IV. Identification and Localization of Nuclear Calcium-Binding Proteins

1. Sodium Dodecyl Sulfate-Polyacrylamide Gel Electrophoresis (SDS-PAGE) of Nuclear Proteins

Aliquots of rat hepatic and pig cardiac nuclei, high salt supernatants and nuclear envelopes were diluted to a concentration of 2 mg/ml with STM buffer, then diluted again with equivolume 2x SDS-PAGE Sample Buffer (375 mM Tris-OH, 4% SDS, 20% glycerol, 10% β-mercaptoethanol, 0.04% bromophenol blue, pH 8.8). Samples of 100 μl each were then resolved by 3-13% linear gradient SDS-PAGE (Bio-Rad Protean II system; 18 mA constant current overnight). Gels were subsequently stained with either

Coomassie Brilliant Blue R-250 or with Stains-All (114), or else were immediately used for western blotting.

2. Western Blotting and $^{45}Ca^{2+}$ Overlays of Nuclear Proteins

Following electrophoresis, gels were incubated in Towbin's Buffer (25 mM Tris-OH, 192 mM glycine, 20% methanol, pH 8.3) (338) for 30 minutes, then electroblotted onto 0.45 μm nitrocellulose membranes using the Bio-Rad Transblot system and Towbin's Buffer. Blotting was carried out at 10°C and 400 mA constant current for 60 minutes. Following completion of transfer, blots were washed in three changes of Overlay Buffer (60 mM KCl, 10 mM imidazole, 5 mM $MgCl_2$, pH 6.8) (209) for 20 minutes each, then incubated in Overlay Buffer containing 1 μCi/ml $^{45}Ca^{2+}$ for 10 minutes. Blots were then washed in two changes of double-distilled, deionized water for 5 minutes each, dried between pieces of filter paper, and placed into autoradiograph cassettes with Kodak X-OMAT AR film and intensifying screens for 7 days at -85°C.

3. Immunoblotting of Nuclear Proteins with Calsequestrin Antibodies

Eight percent acrylamide mini gels were prepared and aliquots of the pig cardiac high salt nucleoplasmic fraction (3 mg/ml final concentration) and purified dog cardiac calsequestrin (0.5 mg/ml final concentration) in SDS-PAGE sample buffer were run on the gels (50 mA constant current for one hour). The gels were then electroblotted onto nitrocellulose using a mini-blot system similar to the larger system described above (250 mA constant current for one hour). Blots were then washed in Blotto A (5% skim milk in TBST (10 mM Tris-OH, 0.05% Tween-20, 150 mM NaCl, pH 8.8)) for 30 minutes with

constant rocking. Blots were incubated with a 1:1000 dilution of rabbit anti-dog cardiac calsequestrin antibodies in Blotto A for 45 minutes, then washed twice for 7 minutes each with TBST. Following this step, blots were incubated with a 1:10 000 dilution of goat anti-rabbit IgG antibodies conjugated to horseradish peroxidase in 1:1 Blotto A:TBST for 60 minutes. Blots were given four 5 minute washes with TBST, then treated with an ECL immunoenzyme detection kit according to manufacturer's directions. The blots were exposed to Kodak X-OMAT AR film for 60 seconds, and the film was developed.

V. Nuclear Membrane Integrity Assay

This assay was carried out as described previously (87). One milligram liver nuclei from lean or corpulent rats was treated with STM buffer containing varying [NaCl] (from 0 to 1000 mM) for 30 minutes on ice, then centrifuged at 7500x*g* in a microfuge. Supernatants were removed and nuclear nucleotide release into the supernatant quantified by absorbance readings in a spectrophotometer at 260 nm, with non-protein containing salt solutions as blanks. Data were normalized to the maximal absorbance values observed. The accuracy of the assay was confirmed by salt-induced lysis of control rat liver nuclei as described above. Lysates were then treated with 2 μg/ml Hoechst 33258 and fluorescence of both pellets and supernatants measured in a Spex Flurolog spectrofluorometer (λ_{ex}=346 nm; λ_{em}=460nm) to accurately quantify release of DNA from lysed nuclei (87). Throughout the assay, all solutions contained 1 mM phenylmethylsulfonylfluoride, 1 mM dithiothreitol, and 1 μM leupeptin to prevent proteolysis of nuclei which would confound the salt-induced lysis values.

VI. Nuclear Import Assay

1. Generation of Import Substrate

The import substrate used was BODIPY-BSA conjugated to the SV40 large T antigen nuclear localization signal (PKKKRKV – see Table 1). The NLS was custom synthesized with an NH_2 terminal CGGG spacer/conjugation point and a COOH terminal ED moiety to protect the sequence during synthesis, to give a final sequence of CGGGPKKKRKVED. To create the conjugate, 4 mg of BODIPY-BSA was suspended in 500 µl PBS (137 mM NaCl, 2.7 mM KCl, 10 mM Na_2HPO_4, 1.8 mM KH_2PO_4, pH 7.4) to which was added 1 mg sulfosuccinimidyl 4-[*N*-maleimidomethyl]cyclohexane-1-carboxylate, a cross-linking agent. The solution was incubated at 37°C for 30 minutes, then desalted on a 5 ml Excellulose column that had been equilibrated with 5 column volumes of PBS. Eight fractions of 500 µl each were collected with PBS as the eluant. The fractions of interest (3-5) were identified by their orange color due to the BODIPY fluorophore. Two milligrams of NLS was suspended in 500 µl Coupling Buffer (50 mM MES, 0.4 mM tris-(2-carboxyethyl) phosphine HCl, pH 5.0) and incubated at 37°C for 30 minutes, after which the solution was combined with the previously isolated BODIPY-BSA fractions. This mixture was placed in a dark-colored bottle and allowed to conjugate overnight at 4°C with constant stirring in the dark. The conjugates were passed through another 5 ml Excellulose column that had been previously equilibrated with 10 mM HEPES (pH 7.3) plus 110 mM potassium acetate. Eight 500 µl fractions were collected using 10 mM HEPES (pH 7.3) plus 110 mM potassium acetate as eluant (Note: this separation step was carried out twice, once each on half of the total conjugation mixture, to prevent overloading of the column). Fractions of interest (2-5) were identified by their

orange color and pooled together. An aliquot of the final conjugate solution was run on a 9% mini-SDS-PAGE gel at 30 mA for 45 minutes, next to an aliquot of the original BODIPY-BSA. The gel was stained with Coomassie Brilliant Blue R-250 and the number of NLSs conjugated per BODIPY-BSA molecule estimated from the gel shift of the final conjugate, using a molecular mass of 1.5 kDa per NLS. In multiple preparations of conjugate, approximately 10-15 NLS moieties were bound to each BODIPY-BSA molecule. The final conjugate was aliquoted as required and stored at –85°C.

2. Import Assay Protocol

Assays were carried out using the procedure of Adam *et al.* (4) with minor modifications. Rabbit aortic vascular smooth muscle cells growing on glass coverslips were rinsed three times with Import Buffer, then permeablized by 5 minute treatment with 40 μg/ml digitonin in Import Buffer. Cells were rinsed four times with Import Buffer, then the coverslips were inverted over 50 μl Import Cocktail (Import Buffer plus 50% rat liver cytosol, 1 mM ATP, 5 mM creatine phosphate, 20 units/ml creatine phosphokinase, and 1 μg/ml each of leupeptin, pepstatin A, and aprotinin) plus 5 μl import substrate on parafilm in a humidified plastic box. Import assays were typically carried out for 30 minutes at 37°C. Cells were then lifted off the parafilm by pipetting small amounts of Import Buffer beneath the coverslips, and the coverslips removed and washed once with Import Buffer. Cells were fixed in 3.7% formaldehyde in Import Buffer for 10 minutes. Coverslips were then placed into a Leiden dish for imaging. Import assay results were measured on a BioRad MRC600UV confocal system connected to a Nikon Diaphot 300 epifluorescence microscope and using a Nikon Fluor 40X/N.A.

1.3 oil immersion objective lens. The 488 nm laser line was used at 10% power in conjunction with a VHS (violet, high selectivity) filter block. Three images were collected of each field of cells and Kalman filtered to reduce random noise in the photomultiplier. Images were then analyzed using Molecular Dynamics ImageSpace 3.2.1 software. Some images were processed using Confocal Assistant 4.02 (© T.C. Brelje, 1994-1996). Multiple fields of cells were visualized per experiment and averaged, so that each data point represents results for approximately 60-180 cells measured in 3-4 experiments.

3. Verification of Nuclear Integrity Following Digitonin Treatment

Rabbit aortic vascular smooth muscle cells growing on coverslips were treated with 40, 80 or 800 μg/ml digitonin for five minutes as described for the import assay above. Cells were washed four times with PBS, then the backs of the coverslips were dried and each coverslip covered with 200 μl 1% BSA + 0.02% NaN_3 in PBS and 4 μl of a 1:50 dilution of mouse anti-DNA antibodies. Coverslips were incubated with antibodies overnight at 4°C, then washed ten times with PBS, including several five minute incubations. Each coverslip was then covered with 200 μl 1% BSA + 0.02% NaN_3 in PBS and 4 μl of a 1:50 dilution of fluorescein isothiocyanate-conjugated sheep anti-mouse IgG antibodies. Coverslips were incubated at 4°C for 1.5 hours, then washed three times with PBS. Cells were visualized by confocal microscopy as described for the import assay above.

4. Treatment of Import Cocktail or Permeablized Cells

For some experiments, import cocktail was treated with 0.1, 0.5 or 1.0 mM H_2O_2 for 30, 60 or 120 minutes at 37°C, with or without 0.3 mg/ml catalase. Alternately, import cocktail was treated with 2 mM xanthine plus 0.03 U/ml xanthine oxidase, or with 0.1 mM H_2O_2 plus 0.1 mM $FeSO_4$, or with 40 ng/ml activated ERK2. Some aliquots of import cocktail were also pretreated for 45 minutes prior to H_2O_2 treatment with 75 μM genistein or daidzein, or 20 μM PD98059 at 37°C. Controls received import buffer alone. The nuclear import assay or western blotting was then carried out. For treatment of permeablized cells, aortic vascular smooth muscle cells were permeablized with 40 μg/ml digitonin for 5 minutes, then treated with 1.0 mM H_2O_2 for 30 minutes, with 2 mM xanthine plus 0.03 U/ml xanthine oxidase for 10 minutes or with 0.1 mM H_2O_2 plus 0.1 mM $FeSO_4$ for 60 minutes. Cells were then rinsed briefly with import buffer and nuclear import assays carried out.

VII. Western Blotting of Nuclear Import Cocktail

Import cocktail was treated as described the last section, then dissolved in 2x SDS-PAGE Sample Buffer and run on 10% acrylamide SDS-PAGE gels (10 mA overnight). Gels were transferred onto nitrocellulose (400 mA for one hour), and the blots blocked overnight in 10% skim milk in PBS, with constant shaking. Blots were briefly washed in Blocking Buffer (1% skim milk plus 0.05% Tween-20 in PBS), then probed with anti-ACTIVE MAPK primary antibodies (1:10 000 dilution) in Blocking Buffer for one hour at room temperature. Blots were washed twice for ten minutes each in Blocking Buffer, then once for five minutes in PBS. Blots were then probed with horseradish peroxidase-

conjugated secondary antibodies (1:10 000 dilution) in Blocking Buffer for one hour at room temperature. Blots were washed twice for ten minutes each in Blocking Buffer, then twice more for five minutes each in PBS. Immunoreactive bands were visualized using a SuperSignal Kit and exposed to Kodak X-OMAT AR film. Films were scanned on a Umax Powerlook II scanner and intensity measured using Un-Scan-It Gel software, version 5.1 (Silk Scientific, Orem, UT).

VIII. Immunocytochemistry of Aortic Smooth Muscle Cells

Rabbit aortic smooth muscle cells grown on glass coverslips were treated with 1.0 mM H_2O_2 with or without either 0.3 mg/ml catalase or 20 μM PD98059 as described above. Cells were then washed five times with PBS and fixed in 1% paraformaldehyde in PBS for 15 minutes at 4°C. Cells were washed again, then permeablized in 0.1% Triton X-100 in PBS for 15 minutes at 4°C. Cells were washed repeatedly in PBS and incubated with anti-Ran antibodies (1:250 dilution) in PBS containing 1% BSA and 0.02% sodium azide overnight at 4°C. Cells were washed 12 times with PBS, then incubated with $Alexa_{488}$-conjugated secondary antibodies (1:1000 dilution) in PBS plus 1% BSA and 0.02% sodium azide for 90 minutes at 4°C. After washing 3 times, cells were mounted onto glass slides with Vectashield as mountant and observed by confocal microscopy. Cytoplasmic fluorescence was measured as described for nuclear fluorescence in section C.VI.2.

IX. Immunoprecipitation of Ran from Aortic Smooth Muscle Cells

This protocol was adapted from an existing procedure (277). Three plates of rabbit aortic vascular smooth muscle cells were grown to confluence in 100 mm plastic petri dishes. The cells were washed briefly in PBS, then washed again in phosphate-free DMEM. Cells were incubated in 10 ml per plate phosphate-free DMEM plus 500 μCi ^{32}P-orthophosphate for three hours fifteen minutes at 37°C. At this point, one plate was treated with 100 μl 20 mM PD98059 in dimethylsulfoxide while the other two received 100 μl dimethylsulfoxide alone, with 45 minute incubation at 37°C. Plates then received either 100 μl 100 mM H_2O_2 (treated plates) or 100 μl H_2O (control plate) and were incubated at 37°C for one hour. Cells were washed twice with ice-cold TBS (137 mM NaCl, 2.7 mM KCl, 25 mM Tris-OH, pH 7.4), then lysed in one milliliter per plate Lysis Buffer (50 mM HEPES, 1% Triton X-100, 100 mM NaCl, 5 mM $MgCl_2$, 10 mM benzamidine, 1 mg/ml BSA, 10 μg/ml aprotinin, 10 μg/ml leupeptin, 10 μg/ml soybean trypsin inhibitor, pH 7.4) on ice for 20 minutes. Cells were then scraped down and pipetted repeatedly to further break them up. Lysates were cleared by centrifugation in eppendorf tubes at 12000x*g* at 4°C for 30 minutes. One milliliter lysate supernatant was removed from each tube into fresh tubes, and 2 μl anti-Ran antibody added to each. Solutions were incubated on ice for 2 hours with occasional tumbling, then 7.5 μl protein A-agarose was added to each tube and the tubes rotated at 4°C for one hour. Samples were briefly centrifuged to pellet them and the pellets washed with 1 ml Wash Buffer (50 mM HEPES, 500 mM NaCl, 5 mM $MgCl_2$, 0.1% Triton X-100, 0.005% SDS, pH 7.4). The pellets were washed a total of six times, then resuspended in 20 μl per tube Elution Buffer (2 mM EDTA, 2 mM DTT, 0.2% SDS, 0.5 mM GTP, 0.5 mM GDP) and

incubated at 68°C for 20 minutes. Solutions were briefly centrifuged and the supernatants collected as "eluate." Eluates were spotted on to PEI-cellulose TLC plates one centimeter from the bottom of the plate, then run in a TLC tank using TLC Buffer (1.2 M ammonium formate, 0.8 M HCl) as the running solvent for ~90 minutes. Plates were air-dried, then exposed to Kodak X-OMAT AR film for ~24 hours. Radiolabeled spots on the TLC plate corresponding to GTP and GDP were scraped off and counted in an LS6500 liquid scintillation counter (Beckman). GTP-bound Ran was expressed as a percentage of total Ran (GTP- plus GDP-bound) then normalized to controls.

X. Determination of Serum Cholesterol, Glucose and Triglycerides

Blood samples from lean and corpulent JCR:LA-*cp* rats were centrifuged at low speed (750x*g*) for ten minutes and serum levels of cholesterol, glucose and triglycerides were spectrophotometrically determined using commercial kits according to manufacturers' suggestions (see Materials section).

XI. Transmission Electron Microscopy of Liver Tissue Samples

1. Tissue Preparation

A six month old corpulent female JCR:LA rat was sacrificed by an injection of ketamine and xylazine as described in Section C.I.1, and the liver excised. Several small pieces of liver tissue were diced up with a new razor blade, then fixed for three hours in a large excess of 5% glutaraldehyde in 0.1 M Sorensen's Buffer (0.08 mM Na_2HPO_4, 0.02 mM KH_2PO_4, pH 7.3). The tissue was then diced into ~1 mm pieces and washed in 5%

sucrose in 0.1 M Sorensen's Buffer overnight. The tissue was post-fixed with 1% OsO_4 in 0.1 M Sorensen's Buffer for two hours.

Tissue was dehydrated by successive washes in 30 (10 min), 50 (10 min), 70 (10 min), 90 (10 min x2) and 100 (10 min x3) percent ethanol, followed by a 20 minute wash in 100% methanol. The tissue was then treated with 100% methanol:propylene oxide (1:1) for 10 minutes, followed by treatment with 100% propylene oxide for 10 minutes. For tissue embedding, araldite resin (88.2 g araldite 502, 69 g (2-dodecen-1-yl)succinic anhydride, 3 ml 2,4,6-tris[dimethylaminomethyl]phenol) was mixed and used. The tissue was embedded with progressively higher ratios of araldite resin:propylene oxide according to the following schedule: 75% propylene oxide:25% araldite (1 hour); 50% propylene oxide:50% araldite (2 hours); 25% propylene oxide:75% araldite (2 hours). At this point, the tissue pieces were placed individually into Beem capsules, covered with 100% araldite resin and incubated at room temperature for 2 hours. The plastic was then allowed to harden at 60°C for 48 hours.

Araldite-embedded tissue blocks were removed from the Beem capsules and trimmed in a pyramitome (LKB) using glass knives, resulting in a flat trapezoidal block surface. Thin sections (~50-70 nm thickness, as determined by optical interference color) were prepared on an ultramicrotome (LKB) and removed onto copper EM grids.

Sections were stained with uranyl acetate (5-7%) and commercial lead citrate (2 mg/ml, pH~12 with NaOH). Both solutions were centrifuged prior to use to remove any undissolved material. Grids were placed section side down onto single drops of uranyl acetate solution for 30 minutes, then rinsed three times in distilled water and dried. Grids were treated briefly with 0.01 N NaOH, followed by treatment with lead citrate for four

minutes and three brief rinses with 0.01 N NaOH. Grids were then washed three times in distilled water and dried.

2. Transmission Electron Microscopy and Photography

Sample grids were visualized on a Philips EM201 transmission electron microscope at various magnifications as required. Photographs were taken at a power reading of "80," with a one-half second exposure. Completed rolls of film were developed in Kodak D-19 developer for two minutes. The film was quickly placed into stop bath for 10 seconds, then fixed in Kodak Fixer for two minutes, and finally washed for ~30 minutes in running water. Processing was finished by immersing the film in Kodak Photo-Flo for 20 seconds, and the film dried on an air dryer for ~15 minutes.

For printing, Kodak 8x10 Ektamatic SC paper was used. The paper was exposed for five seconds, using Kodak Polycontrast filter "3." The paper was developed with a Kodak Ektamatic Processor using Activator (S2A) and Stabilizer (S30). Prints were allowed to air-dry and pressed flat until fixed. The micrographs were fixed in used half-strength Kodak fixer for ten minutes, then washed in running 20°C water for one hour. Prints were then gloss-coated by immersing in Edwal Superflat for four minutes, and dried in a photographic print dryer at 250°C.

XII. Protein Assay

Protein content was determined with the method of Lowry *et al.* (194), or with Markwell's variation of Lowry's method to prevent interference from membrane lipids where significant lipid concentration was encountered (205).

XIII. Statistical Analysis

Values were calculated with standard errors of the mean (SEM). Variation between means was determined by two-tailed Student's t-test, or by one-way analysis of variance with Student-Neuman-Keuls post-hoc test. $p<0.05$ was considered statistically significant. K_M and V_{max} values were calculated with the Hyper program (© J.S. Easterby, 1992), using Hanes plots. Nuclear and cytoplasmic fluorescence values, and nuclear membrane integrity assay values, are reported as percentage of control values.

E. RESULTS

I. Identification and Localization of Calcium-Binding Proteins in the Nucleus

In view of the important roles for calcium in the nucleus (see Review of Literature, Section A.III.1), it seems likely that a pool of nuclear calcium should exist that can be precisely controlled by the cell. Fluorescence studies using calcium sensitive indicators have revealed that calcium levels in the nucleus do, in fact, change independently of cytoplasmic levels (136, 139, 269, 355). Other studies have demonstrated that isolated nuclei are capable of ATP dependent Ca^{2+} uptake (244) and 1,4,5-inositol triphosphate inducible Ca^{2+} release (212, 245). It is therefore possible that an independently controlled nuclear calcium pool does exist.

The questions of how this nuclear calcium pool would be regulated and altered largely remain to be answered, and it was to this end that this study was undertaken. It is very possible that the nucleus may contain currently unidentified Ca^{2+} binding proteins that may regulate intranuclear Ca^{2+} and alter nuclear function. Our study was initiated, therefore, to identify the presence of Ca^{2+} binding proteins in nuclei from the heart and the liver. Cardiac and hepatic tissues were chosen because they are very different in terms of excitability and nuclei isolation procedures have been well established for both tissues (114, 154). The localization of these proteins within the nucleus was also determined in the hope that it may provide preliminary information on the function of these proteins.

1. Isolation of Purified Nuclei

For the purposes of this study, a supply of intact, purified nuclei was required. Rat liver and pig heart provide abundant supplies of intact nuclei when processed using a

gradient ultracentrifugation technique (see Methods). Purified nuclei from rat hepatic cells were of smooth, round shape and upon staining with the DNA-specific stain Toluidine Blue showed several distinct nucleoli per nucleus (Figure 5*A*). Subsequently isolated nuclear envelopes retained their round shape, but the nucleoli disappeared (not shown). Purified nuclei from pig cardiac cells were elongated in shape and also showed a number of nucleoli upon staining with Toluidine Blue (Figure 5*B*). Nuclear envelopes derived from these nuclei lost their nucleoli, but retained their elongated shape (not shown). Figures 6*A* and 6*B* depict nuclei from rat hepatic and pig cardiac tissue, respectively, stained with Hoechst 33258 and visualized by UV confocal laser scanning microscopy, demonstrating the classic nuclear structure of each tissue type. These observations agree with those reported previously for hepatic (114) and cardiac (154) nuclei, although it is unknown why the structures of the two types of nuclei differ. Nuclei of most cell types resemble those of hepatocytes, i.e. spherical. The cardiac nuclei may be elongated due to the dense packing of muscle fibres in the cardiomyocytes, which would tend to stretch the nuclei in the direction of the long axis of the cell.

Gradient ultracentrifugation, however, does not exclude the possibility of contamination of a fraction of interest with other cellular components. It is therefore necessary to assay the purified nuclei for marker enzymes that would indicate the presence of contaminating fractions. Several marker assays were used to ensure nuclear purity: Na^+/K^+ ATPase and K^+-*p*-nitrophenolphosphatase for plasmalemma/sarcolemma contamination; mannose-6-phosphatase for endo-/sarcoplasmic reticulum contamination; succinic dehydrogenase for mitochondria contamination; and K^+-EDTA myosin ATPase for myofibril contamination (assayed in cardiac nuclei only). The results of these assays

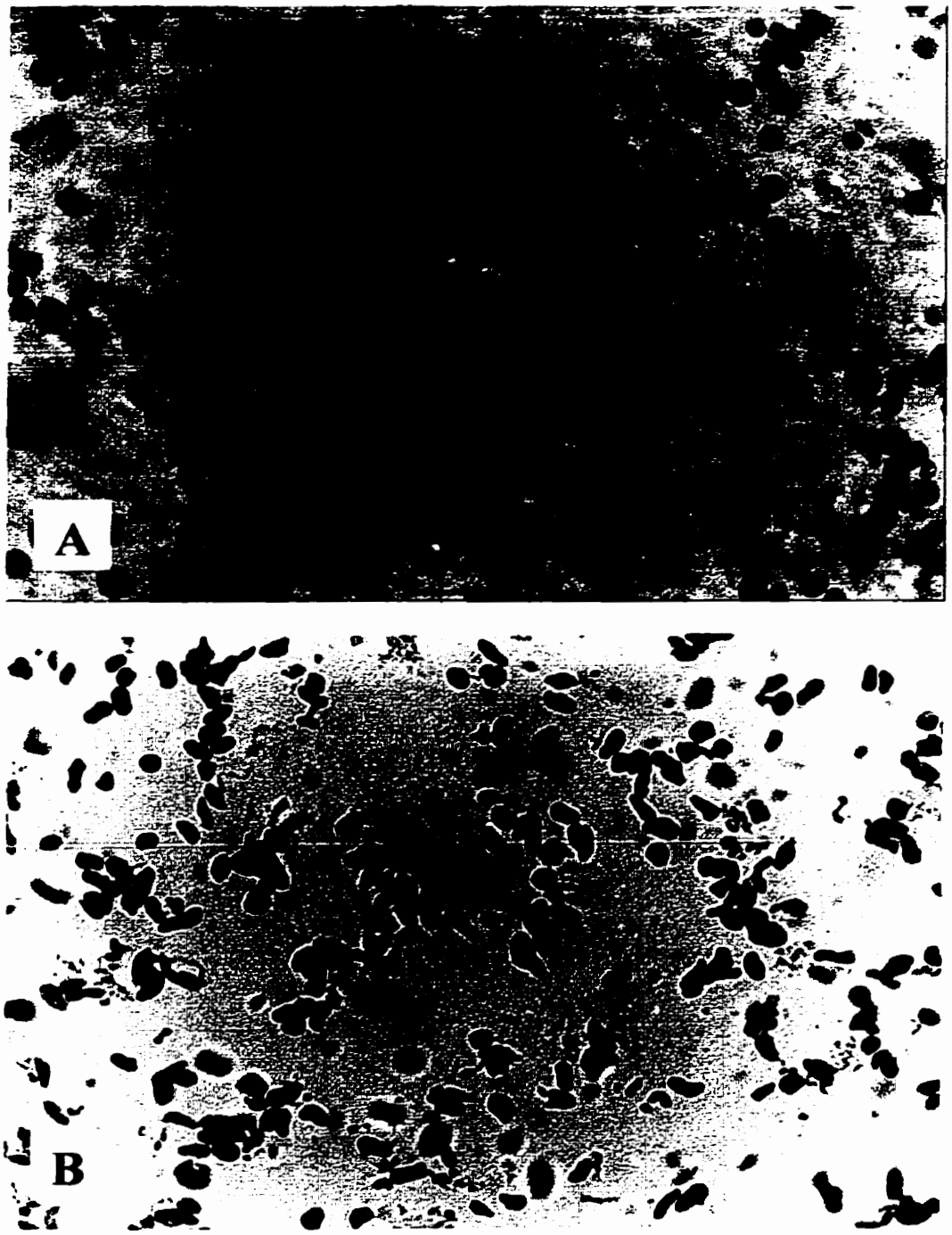

Figure 5. Photomicrographs of hepatic and cardiac nuclei

Isolated rat hepatic (*A*) and pig cardiac nuclei (*B*) were treated with 0.05% Toluidine Blue, smeared on cover slips and air-dried. The nuclei were photographed under phase contrast at 40x magnification.

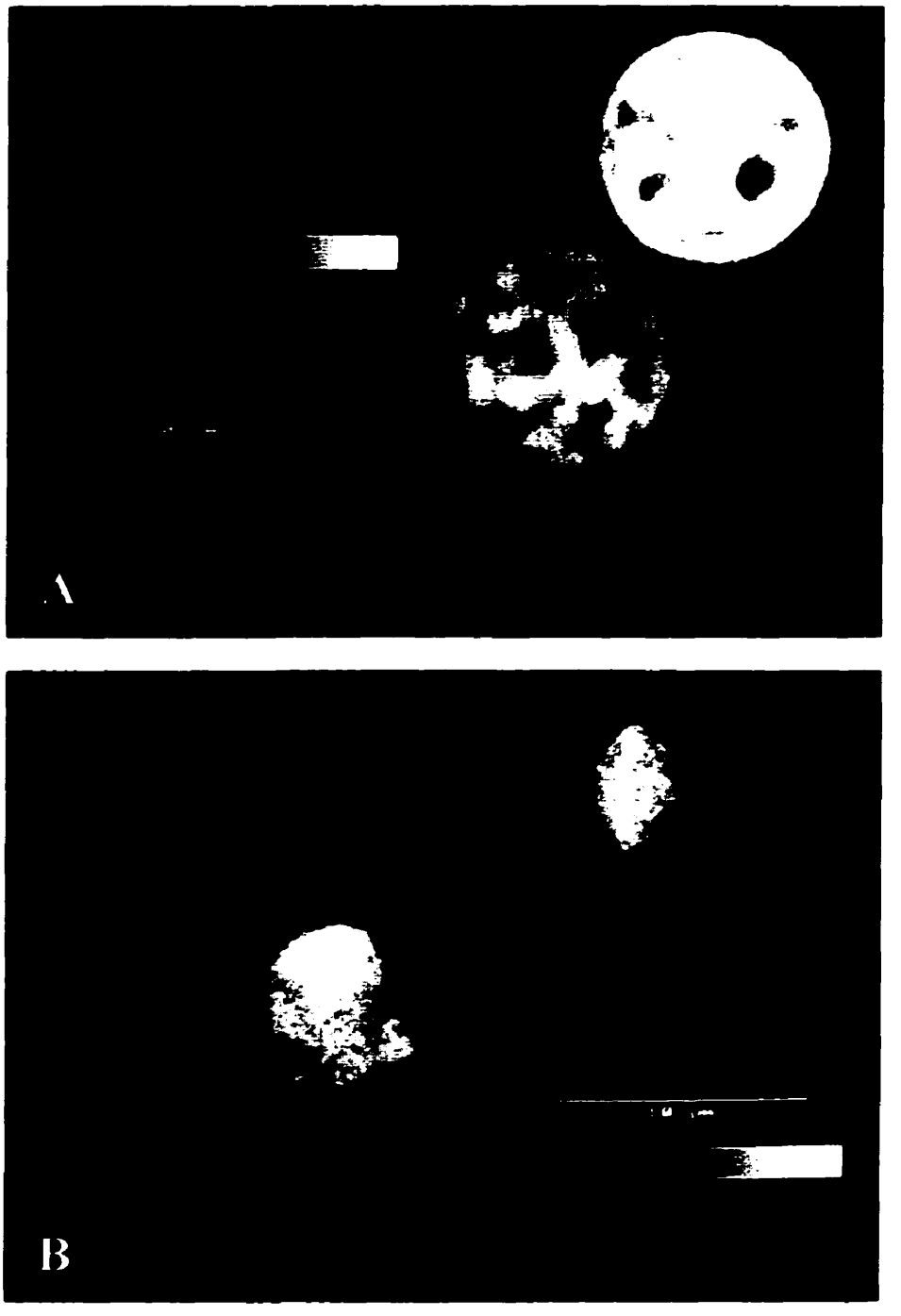

Figure 6. Visualization of hepatic and cardiac nuclei by confocal microscopy

Rat hepatic (*A*) and pig cardiac nuclei (*B*) were treated with the DNA-specific stain Hoechst 33258 and visualized by confocal scanning laser microscopy. A gray-scale was used to reveal areas with relatively low staining with Hoechst 33258 (black) and areas with relatively high staining (white). The scale bar is 10 μm.

are shown in Table 2. The activities of these marker enzymes were very low, and in most cases barely detectable. To insure that our assays were indeed working properly and gain perspective on enzyme activities in other purified fractions, the appropriate enzyme activities were also determined in purified sarcolemma, mitochondria, endoplasmic reticulum and myofibrils. The values obtained revealed that the assays were functioning appropriately, and the data reinforce the contention that both the hepatic and cardiac nuclei preparations contained negligible contamination. The use of gradient ultracentrifugation therefore serves as an excellent method for producing large amounts of highly purified, intact nuclei, although a large quantity of starting material is required for these purposes.

2. Localization of Ca^{2+} Binding Proteins

SDS-PAGE of hepatic nuclear fractions followed by staining with the dye Stains-All produced the electrophoretic profiles shown in Figure 7. Stains-All is a cationic carbocyanine dye which stains neutral and basic proteins red, while staining acidic proteins blue (59). Since calcium binding proteins often have regions of acidic residues which confer the ability to bind calcium, they often stain blue with Stains-All. A number of calcium binding proteins have been found to stain blue with Stains-All in the past (58, 59, 114, 224). The prominent blue staining bands in Figure 7 have been denoted with arrows. They include a 93 kDa band in the nuclear envelope fraction (lane 3), and 120 and 110 kDa bands in the nucleoplasmic fraction (lane 2). Not shown in the figure is a 55 kDa band which stains blue and is only visible with further purification or concentration, but has been observed by this lab on several occasions in both the nucleoplasmic and

Table 2. Activities of selected subcellular marker enzymes

Sample	Mannose-6-phosphatase (nmol/mg/min)	K^+-pNPPase (μmol/mg/hr)	Na^+-K^+ ATPase (μmol/mg/hr)	K^+-EDTA Myosin ATPase (μmol Pi/mg/hr)	Succinic Dehydrogenase (nmol/mg/min/)
Liver Nuclei	40.61±6.62	0.13±0.03	0.16±0.03	n.a.	0.0240±0.0082
Cardiac Nuclei	3.11±1.93	0.28±0.17	0.33±0.08	0.232±0.083	0.0747±0.0355
Endoplasmic Reticulum	253.78	n.a.	n.a.	n.a.	n.a.
Sarcolemma	n.a.	32.93	27.10	n.a.	n.a.
Myofibrils	n.a.	n.a.	n.a.	24.6	n.a.
Mitochondria	n.a.	n.a.	n.a.	n.a.	0.528

n=3 or 4 for liver and cardiac nuclei, respectively; n=1 for other samples
n.a. = not assayed
Values represent means±SEM

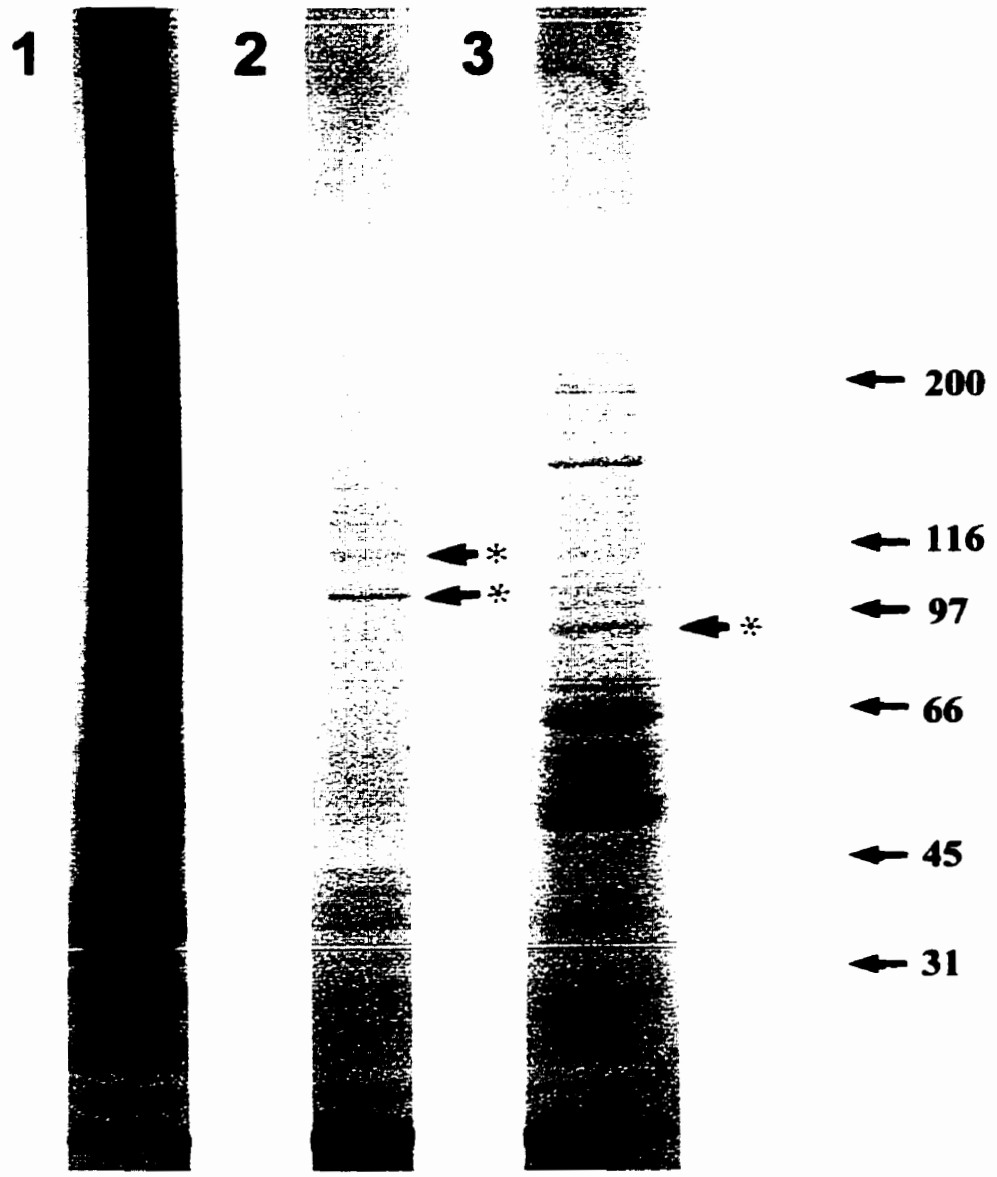

Figure 7. Stains-All staining of hepatic nuclear proteins

Samples of proteins (1 mg/ml) from rat hepatic nuclear fractions were prepared as in the Methods section, digested in SDS-PAGE buffer, and run on a 3-13% gradient slab electrophoresis gel at 18 mA overnight. The gel was then incubated in 25% isopropanol with several changes of solvent for 24 hrs. This was followed by incubation of the gel in Stains-All. *Lane 1* represents purified whole nuclei. *Lane 2* represents the high salt supernatant (nucleoplasmic) fraction. *Lane 3* represents the nuclear envelope fraction. Arrowheads indicate major blue staining proteins. The asterices indicate blue staining bands that were later found to bind $^{45}Ca^{2+}$. The numbers to the right of the figure indicate standard molecular mass markers.

nuclear envelope fractions. Most of these bands are not visible in whole nuclear fractions (lane 1) due to relatively small amounts of these proteins, and only the enrichment which occurs with processing to nuclear envelopes allows these bands to be visualized.

Similar profiles for the cardiac nuclear fractions are shown in Figure 8. As in the hepatic nuclear fractions, the prominent blue staining bands are denoted with arrows. These bands include 120, 110, 93 and 35 kDa bands in the nuclear envelope fraction (lane 3), and a 55 kDa band in the high salt fraction (lane 2). With the exception of the 35 kDa protein, all of these bands are visible in the whole nuclear fraction, unlike the hepatic nuclear fraction.

The Stains-All survey of liver and cardiac nuclear fractions identified several potential calcium-binding proteins, therefore $^{45}Ca^{2+}$ overlays were performed to positively identify which bands corresponded to true calcium-binding proteins. The overlays obtained from hepatic and cardiac nuclear fractions are pictured in Figures 9 and 10, respectively. The hepatic fractions show prominent calcium binding proteins, denoted by large arrows, at 93 kDa in the nuclear envelope fraction (lane 3), and at 120 and 110 kDa in the nucleoplasmic fraction (lane 2). It is interesting to note that the major $^{45}Ca^{2+}$ binding bands on the overlays correspond to the blue staining bands on the Stains-All gel (Figure 7), indicating that the use of Stains-All to quickly identify calcium binding proteins is justified. There are also minor calcium-binding proteins (small arrows) at 28 and 47 kDa in the nucleoplasmic fraction, and at 110 kDa in the nuclear envelope fraction.

The cardiac fractions reveal major calcium binding proteins at 110, 93 and 35 kDa in the nuclear envelope fraction (lane 3), and another major band at 55 kDa in the

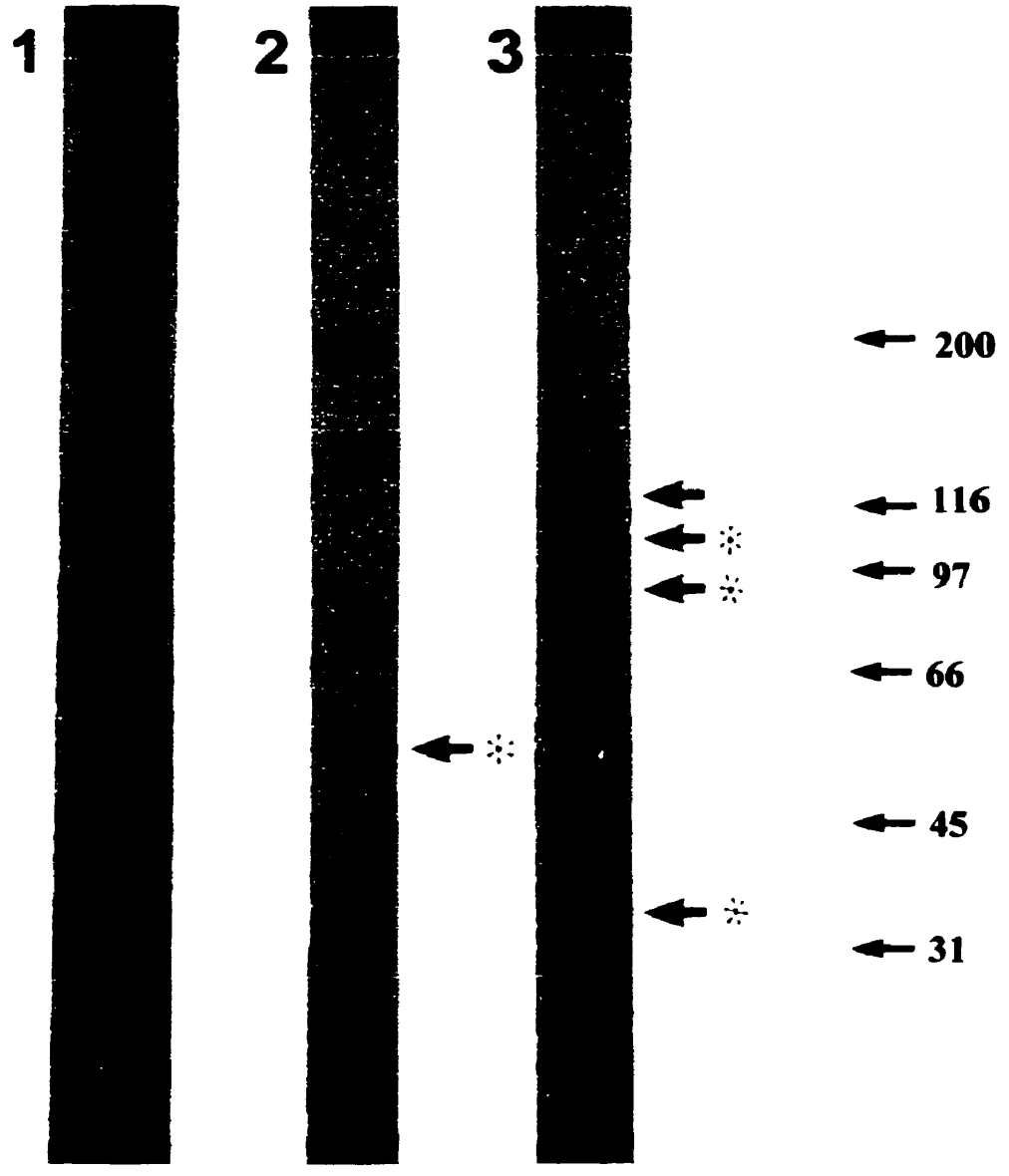

Figure 8. Stains-All staining of cardiac nuclear proteins

Samples of proteins (1 mg/ml) from pig cardiac nuclear fractions were prepared as in the Methods section, digested in SDS-PAGE buffer, and run on a 3-13% gradient slab electrophoresis gel at 18 mA overnight. The gel was then incubated in 25% isopropanol with several changes of solvent for 24 hrs. This was followed by incubation of the gel in Stains-All. *Lane 1* represents purified whole nuclei. *Lane 2* represents the high salt supernatant (nucleoplasmic) fraction. *Lane 3* represents the nuclear envelope fraction. Arrowheads indicate major blue staining proteins. The asterices indicate blue staining bands that were later found to bind $^{45}Ca^{2+}$. The numbers to the right of the figure indicate standard molecular mass markers.

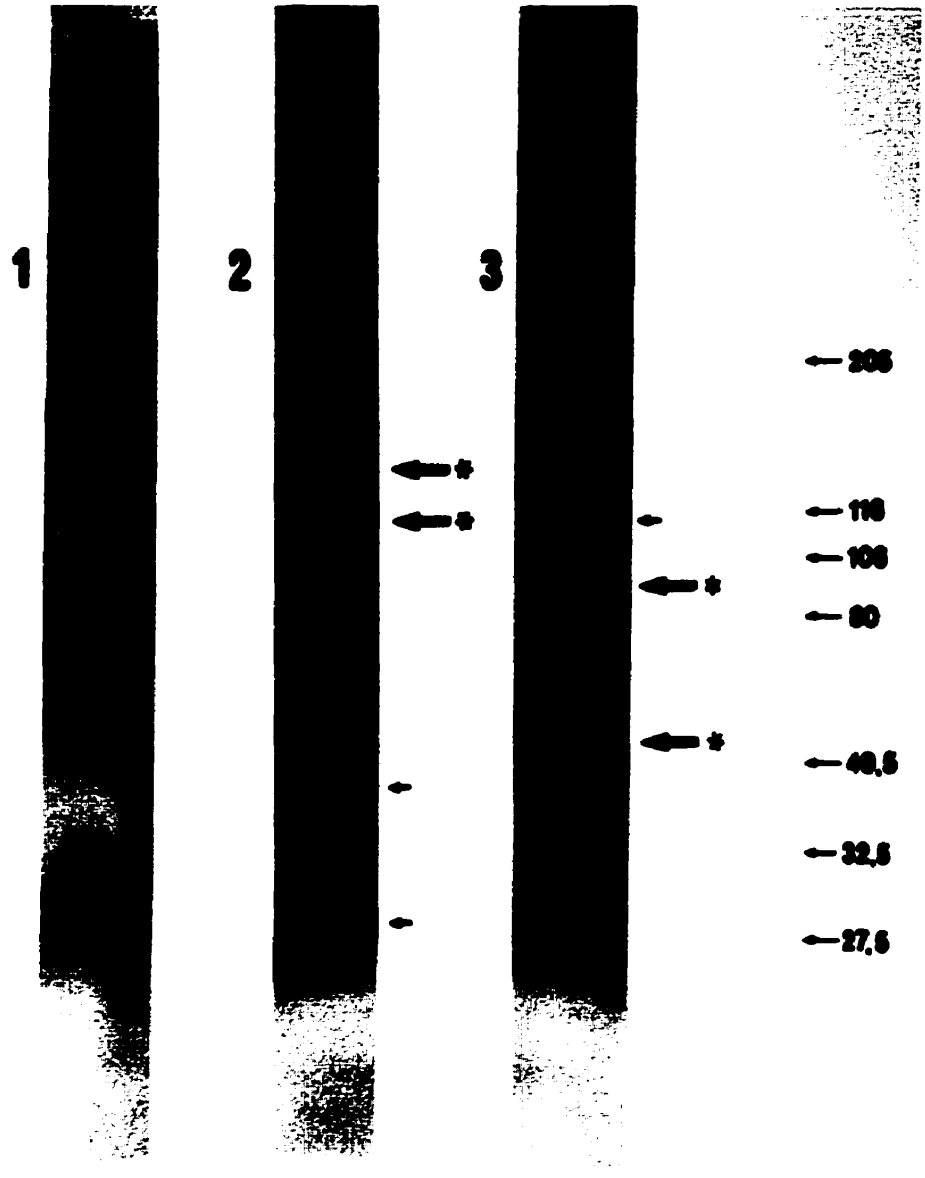

Figure 9. $^{45}Ca^{2+}$ overlays of hepatic nuclear proteins

An identical SDS-PAGE gel was run as in Figure 7. After electrophoresis, the gel was electroblotted onto 0.45 μm nitrocellulose membranes, then incubated with 1 μCi/ml $^{45}Ca^{2+}$, and exposed to Kodak X-OMAT AR film at -85°C for 7 days. *Lane 1* represents purified whole nuclei. *Lane 2* represents the high salt supernatant (nucleoplasmic) fraction. *Lane 3* represents the nuclear envelope fraction. Large arrowheads indicate major $^{45}Ca^{2+}$ binding proteins. Small arrowheads indicate minor $^{45}Ca^{2+}$ binding proteins. Asterices indicate $^{45}Ca^{2+}$ binding bands that also stained blue with Stains-All. The numbers to the right of the figure indicate standard molecular mass markers.

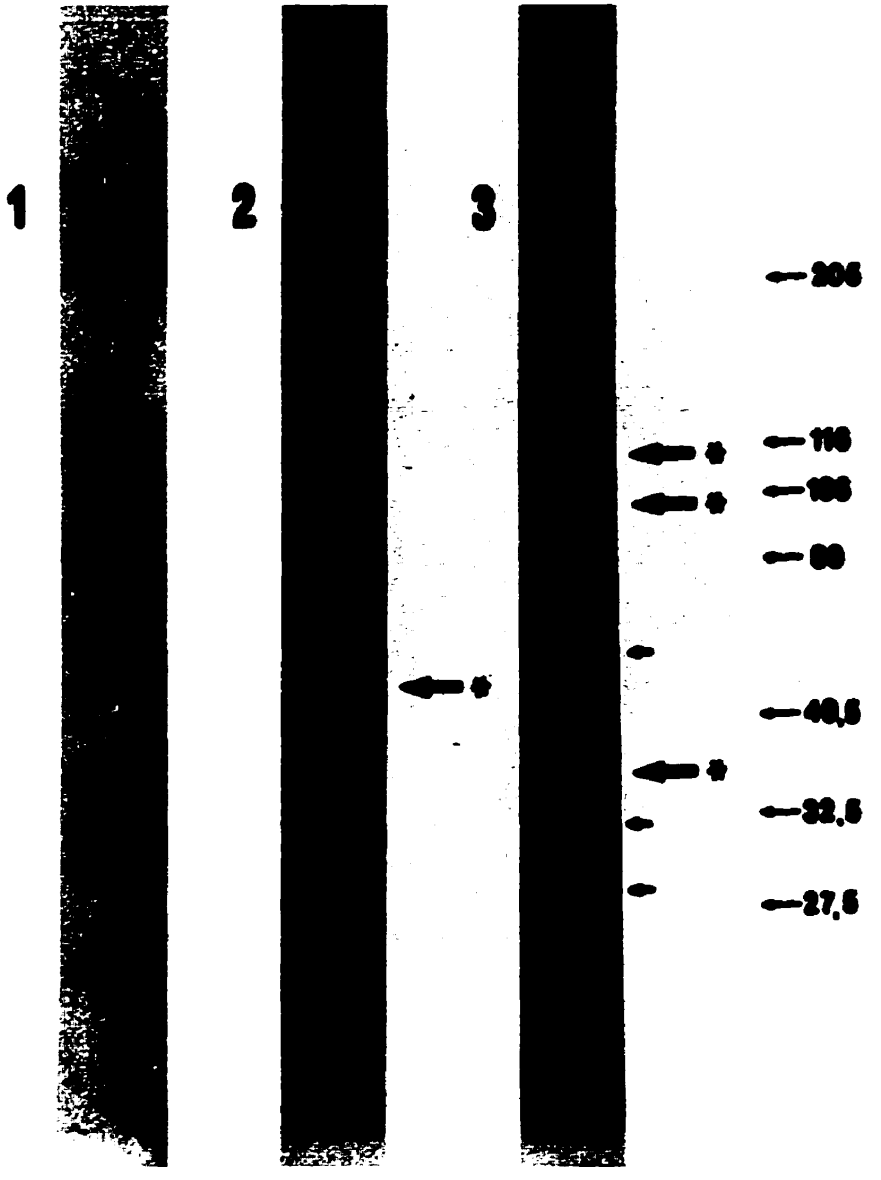

Figure 10. $^{45}Ca^{2+}$ overlays of cardiac nuclear proteins

An identical SDS-PAGE gel was run as in Figure 8. After electrophoresis, the gel was electroblotted onto 0.45 μm nitrocellulose membranes, then incubated with 1 μCi/ml $^{45}Ca^{2+}$, and then exposed to Kodak X-OMAT AR film at -85°C for 7 days. *Lane 1* represents purified whole nuclei. *Lane 2* represents the high salt supernatant (nucleoplasmic) fraction. *Lane 3* represents the nuclear envelope fraction. Large arrowheads indicate major $^{45}Ca^{2+}$ binding proteins. Small arrowheads indicate minor $^{45}Ca^{2+}$ binding proteins. Asterices indicate $^{45}Ca^{2+}$ binding bands that also stained blue with Stains-All. The numbers to the right of the figure indicate standard molecular mass markers.

nucleoplasmic fraction (lane 2). Note that although there was a major blue staining band at 120 kDa in the cardiac nuclear envelope fraction, there was only a weak corresponding calcium binding band. This band may represent a high abundance but low affinity calcium binding protein. Minor calcium binding bands are also seen at approximately 60 and 31 kDa, plus a doublet at 28 kDa in the nuclear envelope fraction.

3. Positive Identification of a Major Cardiac Nuclear Calcium Binding Protein

The single 55 kDa calcium binding band in the cardiac nucleoplasmic fraction was targeted for full identification. A major cellular calcium binding protein with a molecular mass of 55 kDa is calsequestrin, previously localized to the lumen of the ER/SR (58-60). To examine the possibility that calsequestrin also localizes to the cardiac nucleoplasm, immunoblots of the purified cardiac high salt fraction were performed.

The results of immunoblotting the pig cardiac nucleoplasmic 55 kDa protein and purified rabbit cardiac calsequestrin are shown in Figure 11. The cardiac calsequestrin antibody bound specifically to the 55 kDa protein from the pig cardiac high salt fraction (lane A). Lane B shows purified rabbit cardiac calsequestrin as a positive control. The antibody was specific for the cardiac isoform and did not bind to rabbit skeletal calsequestrin (results not shown). These results strongly implicate calsequestrin as the identity of the 55 kDa protein.

Figure 11. Immunoblot of cardiac 55 kDa protein with calsequestrin antibodies

The pig cardiac high salt supernatant fraction (3 mg/ml) was run on an 8% SDS-PAGE mini-gel alongside purified rabbit cardiac calsequestrin (0.5 mg/ml), a positive control (lanes *A* and *B*, respectively). Gels were electroblotted after electrophoresis onto a nitrocellulose membrane, labeled with anti-cardiac calsequestrin antibodies and detected by immunofluorescence as described in Methods. Film exposure time was 60 seconds.

II. Altered Function of the Nuclear Nucleoside Triphosphatase in a Genetically Obese Animal Model

1. The JCR:LA-cp Rat Model

In this study, we were interested in the potential for changes in nuclear envelope composition to affect the function of envelope-associated enzymes. The nuclear nucleoside triphosphatase was of particular interest, since it is both a critical nuclear enzyme and is associated with the inner nuclear membrane (see Review of Literature, Section A.I.2.c.i). An added benefit is the existence of an assay for the rapid determination of NTPase activity (see Methods). The JCR:LA-*cp* corpulent rat offers a valuable model to examine the potential for membrane lipid content in nuclei to change *in vivo* in response to high circulating lipid levels, and to test whether altered nuclear membrane lipid content will alter NTPase activity.

The JCR:LA-*cp* rat is a relatively novel animal model which carries the autosomal recessive *cp* (corpulent) gene first isolated by Koletsky (176, 177). Rats that are homozygous for the *cp* gene (*cp/cp*) are obese, hyperlipidemic (94) and insulin resistant (292, 294). However, the nature of the hyperlipidemia and the degree of insulin resistance exhibits sexual dimorphism. Due to hepatic hypersecretion of VLDL, both sexes are hypercholesterolemic, but females show a more severe hypertriglyceridemia than males (295). Besides showing sexual dimorphism, the serum lipid profiles of the JCR:LA-*cp* corpulent rats have also been reported to change with age (93). For example, serum cholesterol levels in corpulent female animals are elevated versus lean animals at all ages, and increase with age. In comparison, serum cholesterol levels in corpulent male animals have been reported to be elevated versus lean males at all ages, but stay fairly constant

between the ages of 3 and 9 months (295). Animals that are homozygous normal (+/+) or heterozygous (*+/cp*) are lean, with normal insulin and lipid metabolism. These animals therefore serve as an excellent model for our studies, and have the added benefit of a natural "negative control" in the form of the lean animals.

The animals used were divided into groups based on age (3, 6 and 9 months old at time of sacrifice), sex and genotype (lean or corpulent). Body and liver weights recorded at the time of sacrifice of the animals are listed in Table 3. Both the body weight and the liver weight of the corpulent animals were significantly elevated compared to lean controls. For the most part, liver weight to body weight ratios were unchanged in corpulent animals compared to the leans, with the exception of the 3 month old animals of both sexes, in which this ratio was increased. In the 6 month old females, the liver to body weight ratio was decreased in the corpulent animals compared to the leans.

Serum levels of glucose, cholesterol and triglycerides were significantly elevated in the corpulent animals versus the lean animals of both sexes and in all age groups, with the exception of the serum glucose levels of the 9 month old males, in which there was no significant difference between the lean animals and the corpulent ones (Table 4). Of particular note is the more severe hypertriglyceridemia observed in the corpulent female animals. These results from non-fasted rats are consistent with values reported previously for fasted animals (93).

Since the liver is the main site of mammalian lipid metabolism, hepatic nuclei were isolated from animals in each group under study. Visual examination of hepatic nuclei from all groups revealed no observable morphological differences between samples.

Table 3. Body and liver weights of lean and corpulent rats

Age (mon)	Sex	Genotype	Body Mass (g)	Liver Mass (g)	Liver:Body ($x10^3$)
3	Female	*+/?*	205±3	6.3±0.1	30.6±0.5
		cp/cp	376±6‡	12.7±0.2‡	33.8±0.6‡
6	Female	*+/?*	271±16	8.1±0.3	30.4±0.7
		cp/cp	502±8‡	14.0±0.4‡	28.0±0.7*
9	Female	*+/?*	234±4	7.1±0.2	30.3±1.0
		cp/cp	533±17‡	18.3±1.0‡	30.0±1.3
3	Male	*+/?*	336±3	10.1±0.2	30.1±0.4
		cp/cp	518±9‡	18.2±0.6‡	34.9±1.0‡
6	Male	*+/?*	388±3	10.6±0.2	27.2±0.7
		cp/cp	694±16‡	20.1±0.8‡	29.0±1.2
9	Male	*+/?*	439±6	11.3±0.3	25.8±0.7
		cp/cp	803±23‡	21.7±0.6‡	27.0±0.3

Values represent means±SEM. n=10-22
*$p<0.05$ vs. lean animals
‡$p<0.01$ vs. lean animals

Body and organ weights were recorded at time of sacrifice.

Table 4. Serum levels of glucose, cholesterol and triglycerides of non-fasted rats

Age (mon)	Sex	Genotype	[Glucose] (mg/dl)	$[Cholesterol]_{free}$ (mg/dl)	[Triglycerides] (mg/dl)
3	Female	*+/?*	159±4	8.9±2.7	49±3
		cp/cp	239±17‡	35.6±5.8‡	536±31‡
6	Female	*+/?*	131±16	30.2±4.3	43±6
		cp/cp	326±18‡	48.3±6.5*	495±42‡
9	Female	*+/?*	155±7	50.7±1.5	77±4
		cp/cp	299±29‡	126.1±12.4‡	539±69‡
3	Male	*+/?*	163±8	18.6±1.5	58±5
		cp/cp	229±27*	36.7±5.0‡	322±43‡
6	Male	*+/?*	243±43	14.3±5.4	42±5
		cp/cp	378±34*	60.3±2.3‡	247±32‡
9	Male	*+/?*	152±6	39.4±3.5	61±2
		cp/cp	224±31	95.9±7.0‡	181±12‡

Values represent means±SEM. n=4-8
*$p<0.05$ vs. lean animals
‡$p<0.01$ vs. lean animals

Blood samples were collected from non-fasted JCR:LA-*cp* rats at time of sacrifice and centrifuged briefly to allow collection of serum. Serum samples were assayed for glucose, cholesterol and triglyceride content as described in Methods.

Isolated nuclei were round, with punctate nucleoli and little or no observable contamination, virtually identical to the nuclei pictured in Figure 5*A*.

2. Alteration of NTPase Activity in Nuclei from Corpulent Animals

NTPase activity was examined as a function of reaction time (Figures 12 and 13). NTPase activity was linear for 20-30 minutes in all assays. NTPase activity was significantly increased in nuclei from corpulent females at all ages versus age-matched lean females (Figure 12). In males, however, NTPase activity was significantly increased in only the 6 month old corpulent animals compared to 6 month old lean animals (Figure 13).

NTPase activity is dependent on the presence of nucleoside triphosphates, usually GTP or ATP, therefore NTPase activity was assayed as a function of GTP concentration. Maximal activity in corpulent female nuclei was again significantly increased at all ages compared to lean females of the same age (Figure 14). In male rats, there was a significant increase in maximal NTPase activity in only the six month corpulent animals versus the six month leans (Figure 15). All nuclei examined in both sexes showed classic saturation kinetics as exemplified by sigmoid curves.

NTPase activity was also studied as a function of ATP concentration. The corpulent females showed significantly higher maximal NTPase activity than age-matched lean females at all ages examined (Figure 16). This contrasted sharply with the situation in the males, in which there were no significant differences between corpulent and age-matched lean animals at any age (Figure 17). Once again, all nuclei showed classic saturation kinetics for both sexes.

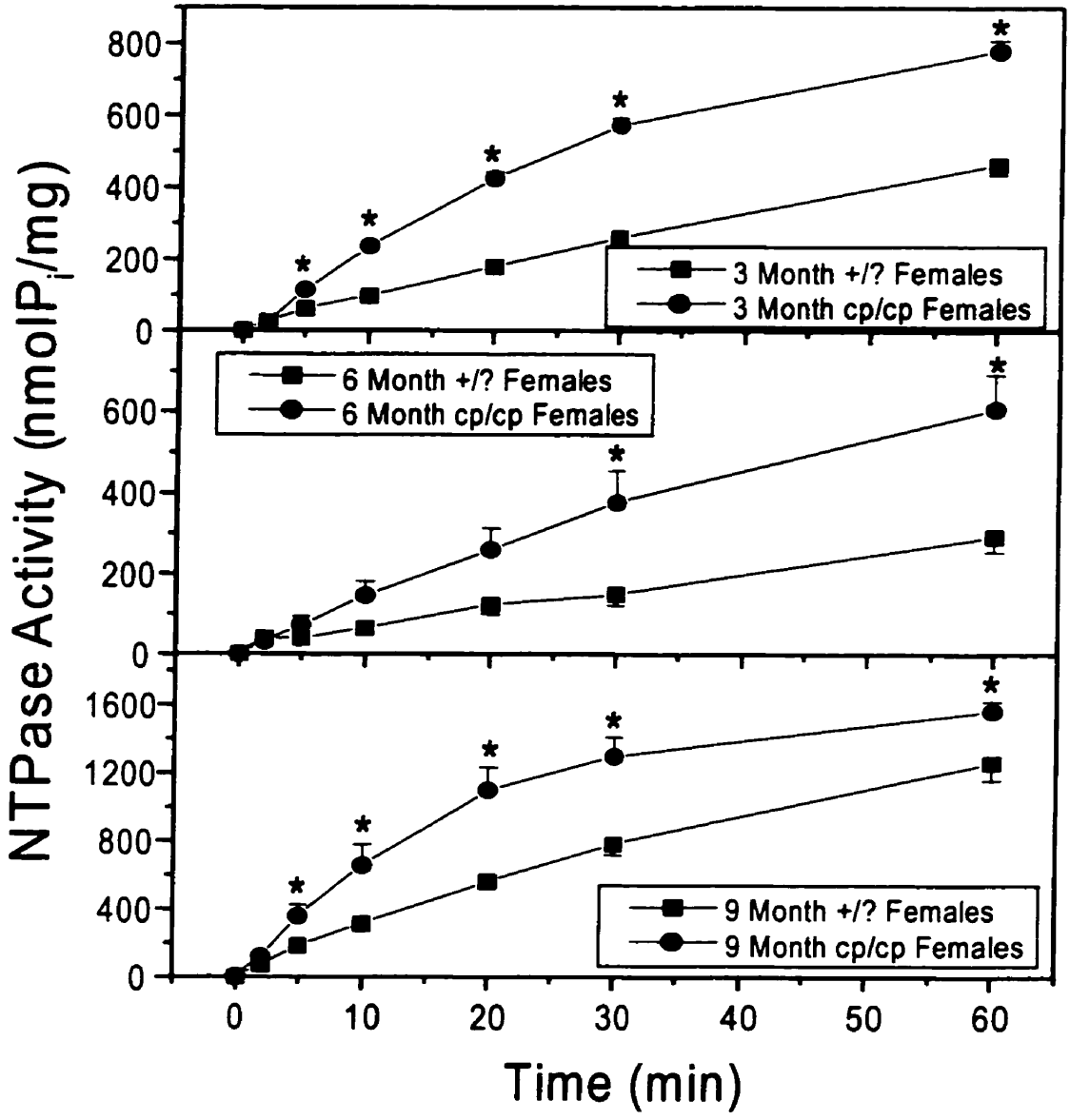

Figure 12. NTPase activity in lean and corpulent 3, 6 and 9 month old female JCR:LA-*cp* rat liver nuclei as a function of reaction time

NTPase activity was assayed as described in Methods, with [GTP]=5 mM, $[Mg^{2+}]_{free}$=1 mM and [EDTA]=1 mM at 37°C. Error bars represent SEM for 3-5 assays. *$p<0.05$ vs. lean animals.

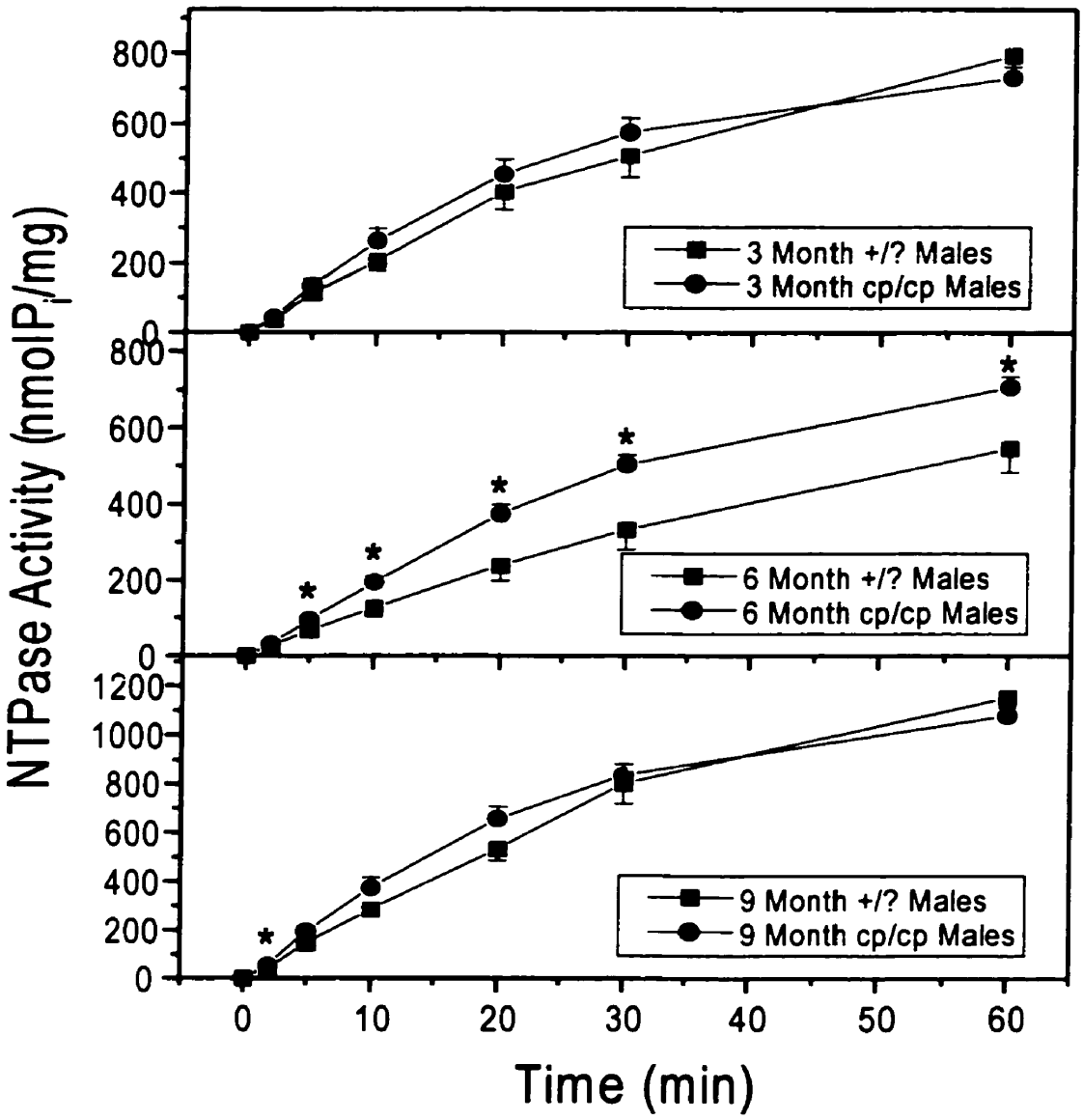

Figure 13. NTPase activity in lean and corpulent 3, 6 and 9 month old male JCR:LA-*cp* rat liver nuclei as a function of reaction time

NTPase activity was assayed as described in Methods, with [GTP]=5 mM, $[Mg^{2+}]_{free}$=1 mM and [EDTA]=1 mM at 37°C. Error bars represent SEM for 3-5 assays. *p<0.05 vs. lean animals.

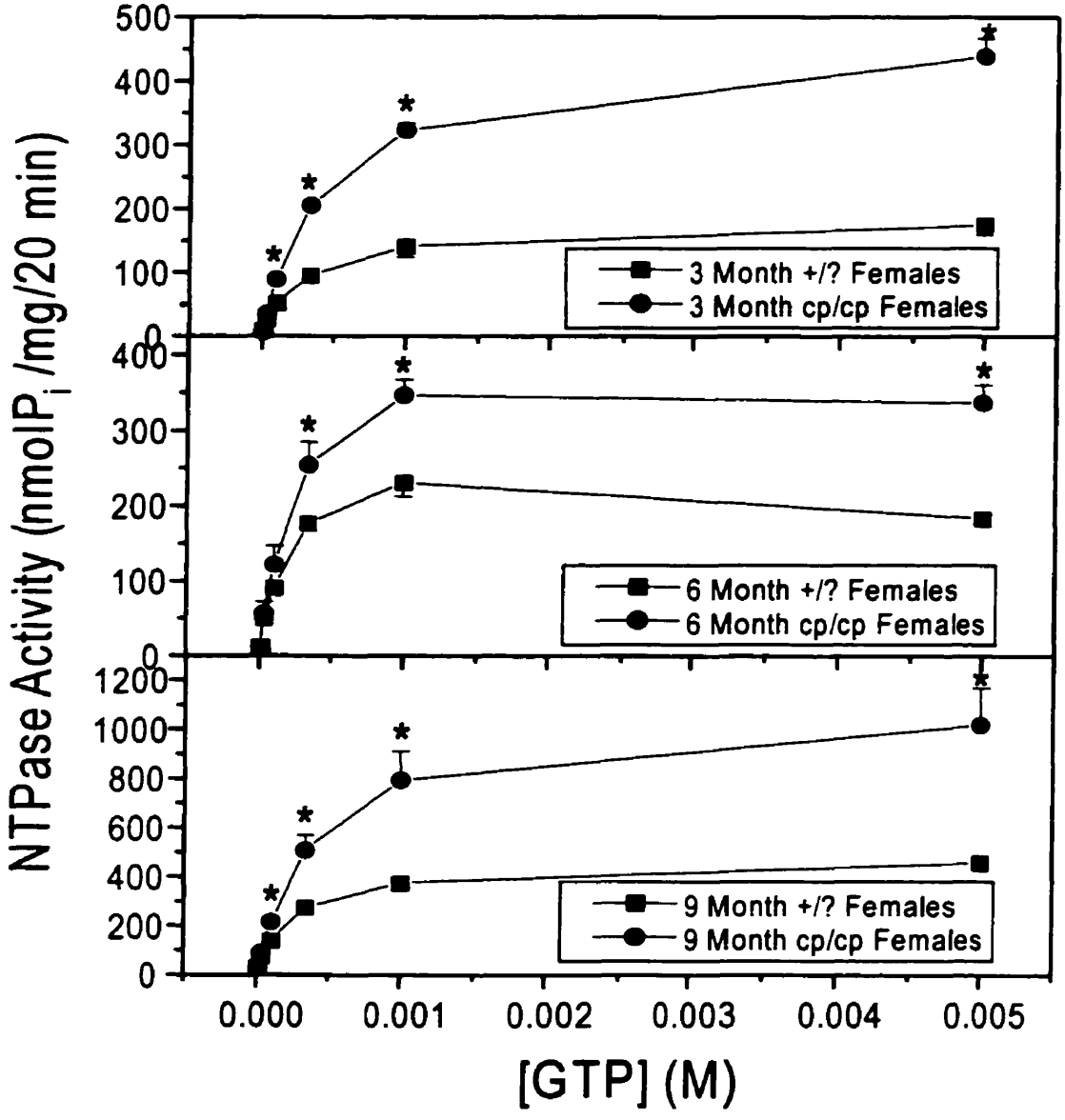

Figure 14. NTPase activity in lean and corpulent 3, 6 and 9 month old female JCR:LA-*cp* rat liver nuclei as a function of [GTP]

NTPase activity was assayed as described in Methods, with $[Mg^{2+}]_{free}$=1 mM, [EDTA]=1 mM and 20 minutes incubation at 37°C. Error bars represent SEM for 3-5 assays. *p<0.05 vs. lean animals.

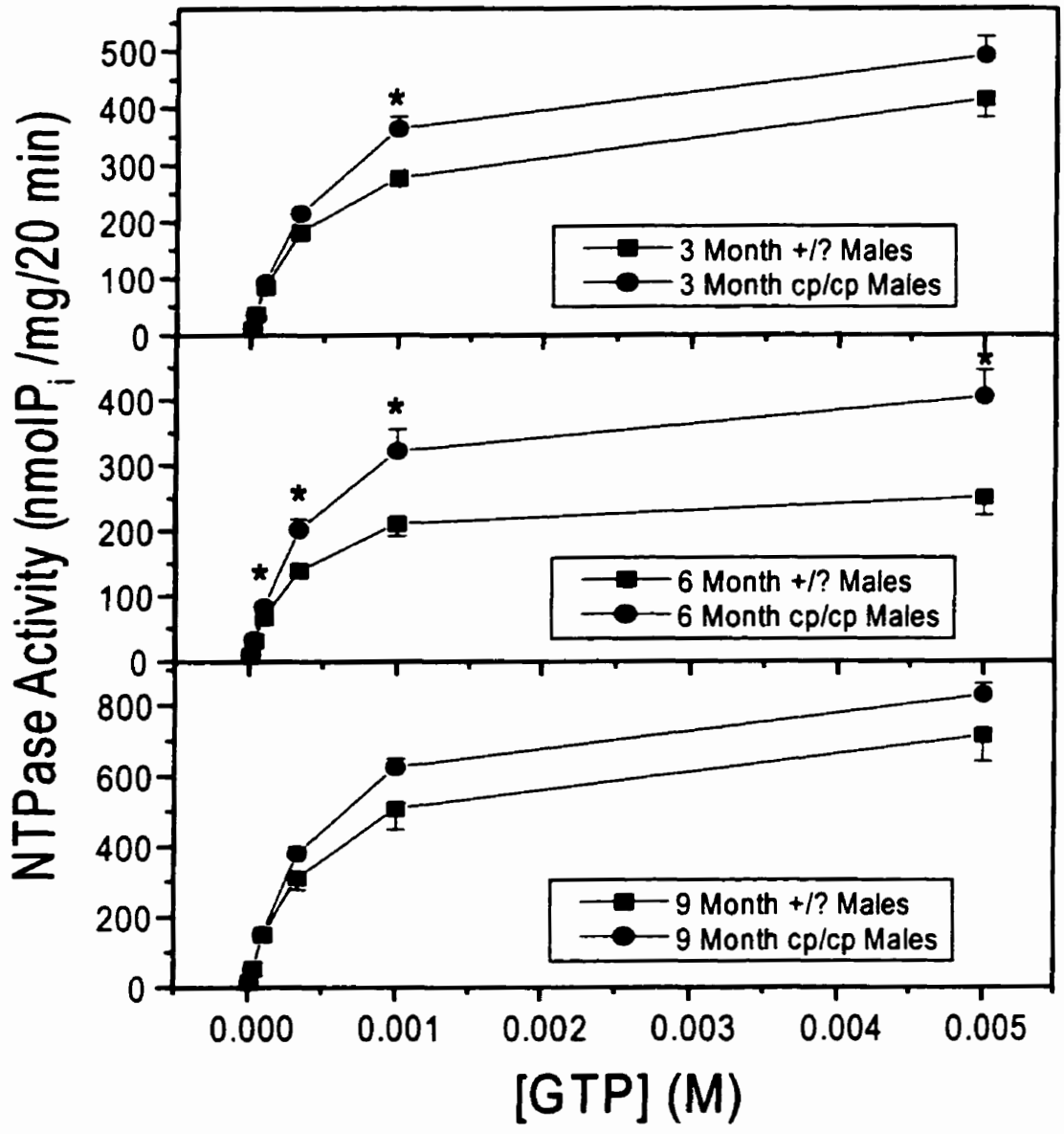

Figure 15. NTPase activity in lean and corpulent 3, 6 and 9 month old male JCR:LA-*cp* rat liver nuclei as a function of [GTP]

NTPase activity was assayed as described in Methods, with $[Mg^{2+}]_{free}$=1 mM, [EDTA]=1 mM and 20 minutes incubation at 37°C. Error bars represent SEM for 3-5 assays. *$p<0.05$ vs. lean animals.

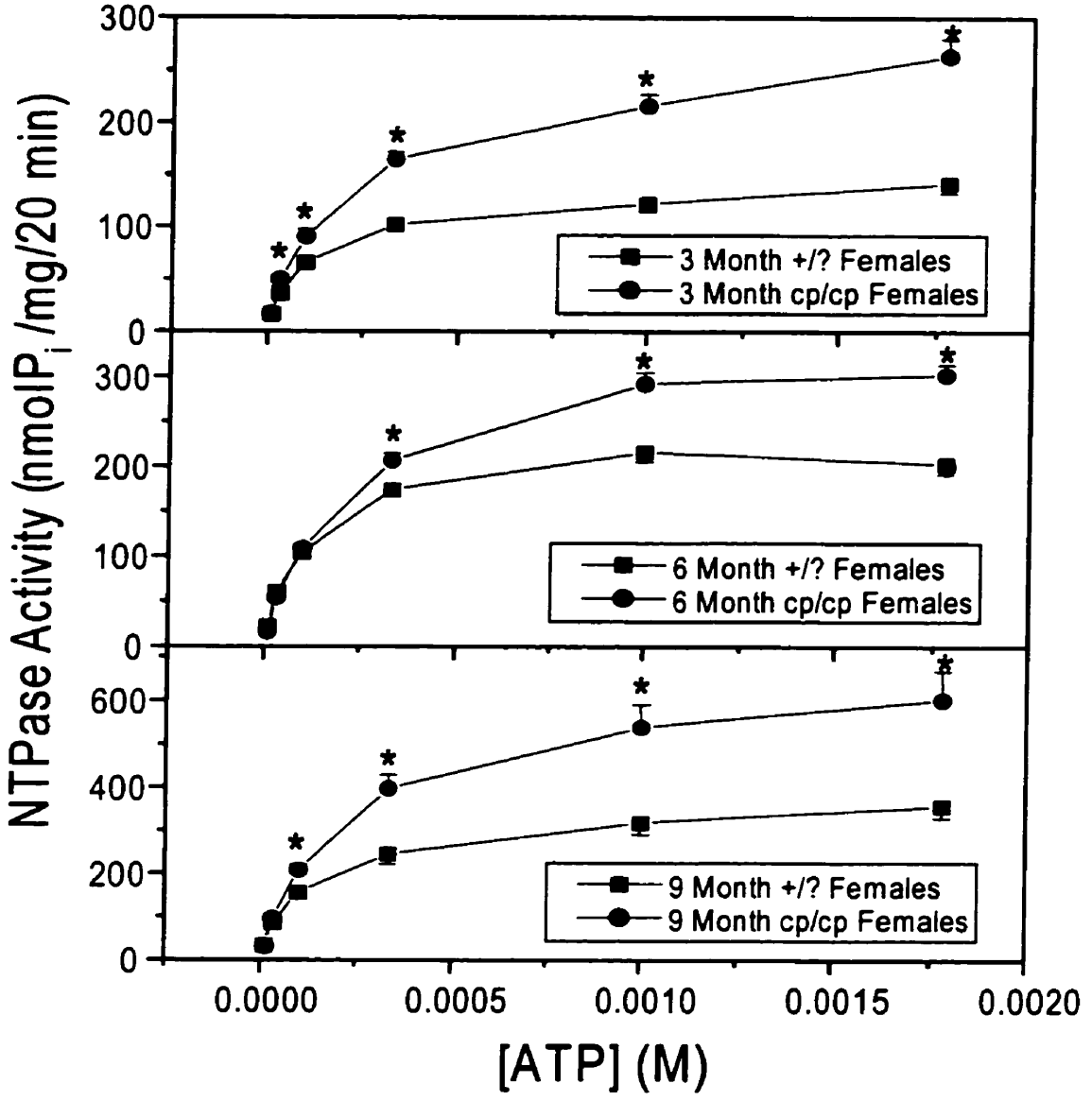

Figure 16. NTPase activity in lean and corpulent 3, 6 and 9 month old female JCR:LA-*cp* rat liver nuclei as a function of [ATP]

NTPase activity was assayed as described in Methods, with $[Mg^{2+}]_{free}$=1 mM, [EDTA]=1 mM and 20 minutes incubation at 37°C. Error bars represent SEM for 3-5 assays. *p<0.05 vs. lean animals.

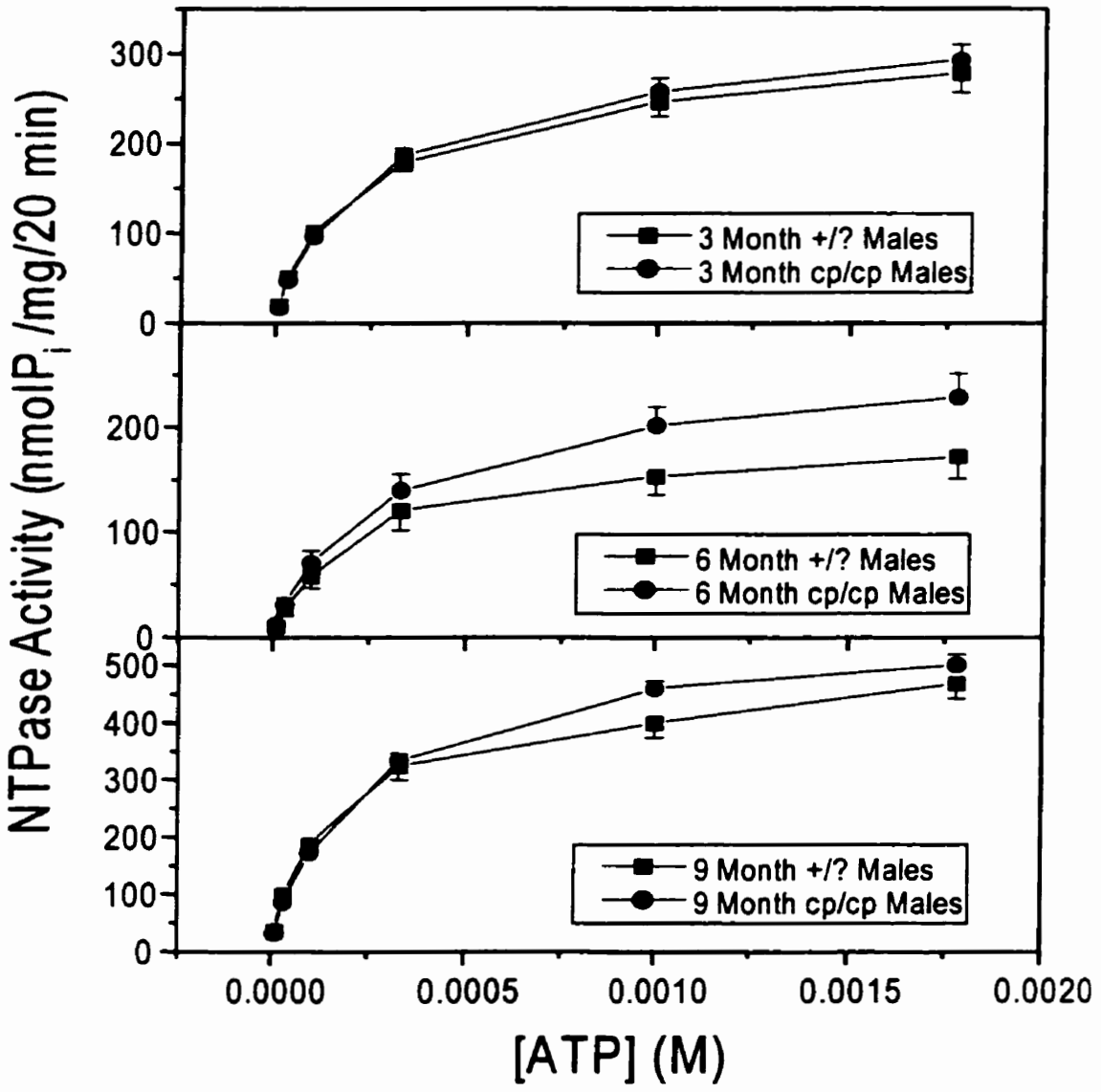

Figure 17. NTPase activity in lean and corpulent 3, 6 and 9 month old male JCR:LA-*cp* rat liver nuclei as a function of [ATP]

NTPase activity was assayed as described in Methods, with $[Mg^{2+}]_{free}$=1 mM, [EDTA]=1 mM and 20 minutes incubation at 37°C. Error bars represent SEM for 3-5 assays. *$p<0.05$ vs. lean animals.

The kinetic parameters V_{max} and K_M were determined for all assays as a function of both [GTP] and [ATP] (Table 5). V_{max} values for NTPase activity of all corpulent females were significantly increased compared to age-matched lean females, regardless of whether GTP or ATP was the substrate. The affinity constant K_M was also increased in the corpulent females at all ages with ATP as the substrate, and in all but the 6 month corpulent females with GTP as the substrate. In contrast, there was no change in either the V_{max} or K_M values in the corpulent males compared with age-matched lean males, with the sole exception of 6 month old corpulent males using GTP as the substrate, in which both values were significantly increased compared to 6 month leans.

NTPase activity was assayed as a function of the required cofactor, free magnesium. NTPase activity was increased in 3 and 9 month old corpulent female nuclei compared to age-matched leans, but only at the 100 μM Mg^{2+} data point in 6 month old corpulent females (Figure 18). In the male animals, NTPase activity was increased in only the 9 month old corpulent animals compared to 9 month old leans (Figure 19).

3. Alterations in Nuclear Structural Characteristics in Corpulent Animals

a. Changes in Nuclear Envelope Composition

To examine whether changes in nuclear envelope composition were responsible for the observed changes in NTPase activity, nuclear content of phospholipids and cholesterol was determined for isolated nuclei from all groups (Table 6). Phospholipid content was significantly increased by approximately 50% in all corpulent female

Table 5. Kinetic parameters of the nuclear NTPase

Age (mon)	Sex	Genotype	*f*[GTP]		*f*[ATP]	
			K_M (μM)	V_{Max} (nmol/mg /20 min)	K_M (μM)	V_{Max} (nmol/mg /20 min)
3	F	*+/?*	270±29	184±16	120±12	147±9
		cp/cp	749±200*	507±32‡	199±15‡	282±18‡
6	F	*+/?*	155±51	222±32	89±19	221±8
		cp/cp	283±41	355±27*	200±18‡	342±13‡
9	F	*+/?*	211±10	474±31	139±14	376±28
		cp/cp	371±36‡	1098±173*	205±18*	667±80*
3	M	*+/?*	443±29	451±37	178±14	301±23
		cp/cp	471±33	540±39	209±10	323±21
6	M	*+/?*	265±32	265±30	223±30	191±20
		cp/cp	388±31*	439±47*	280±43	260±23
9	M	*+/?*	446±22	777±82	162±22	497±30
		cp/cp	477±21	909±34	196±26	553±25

Values represent means±SEM. n=3-6
*$p<0.05$ vs. lean animals
‡$p<0.01$ vs. lean animals

Hanes V_{Max} and K_M values were determined from individual NTPase assays with varying [ATP] and [GTP] as described in Methods. The computer program Hyper v1.01 was used for these calculations.

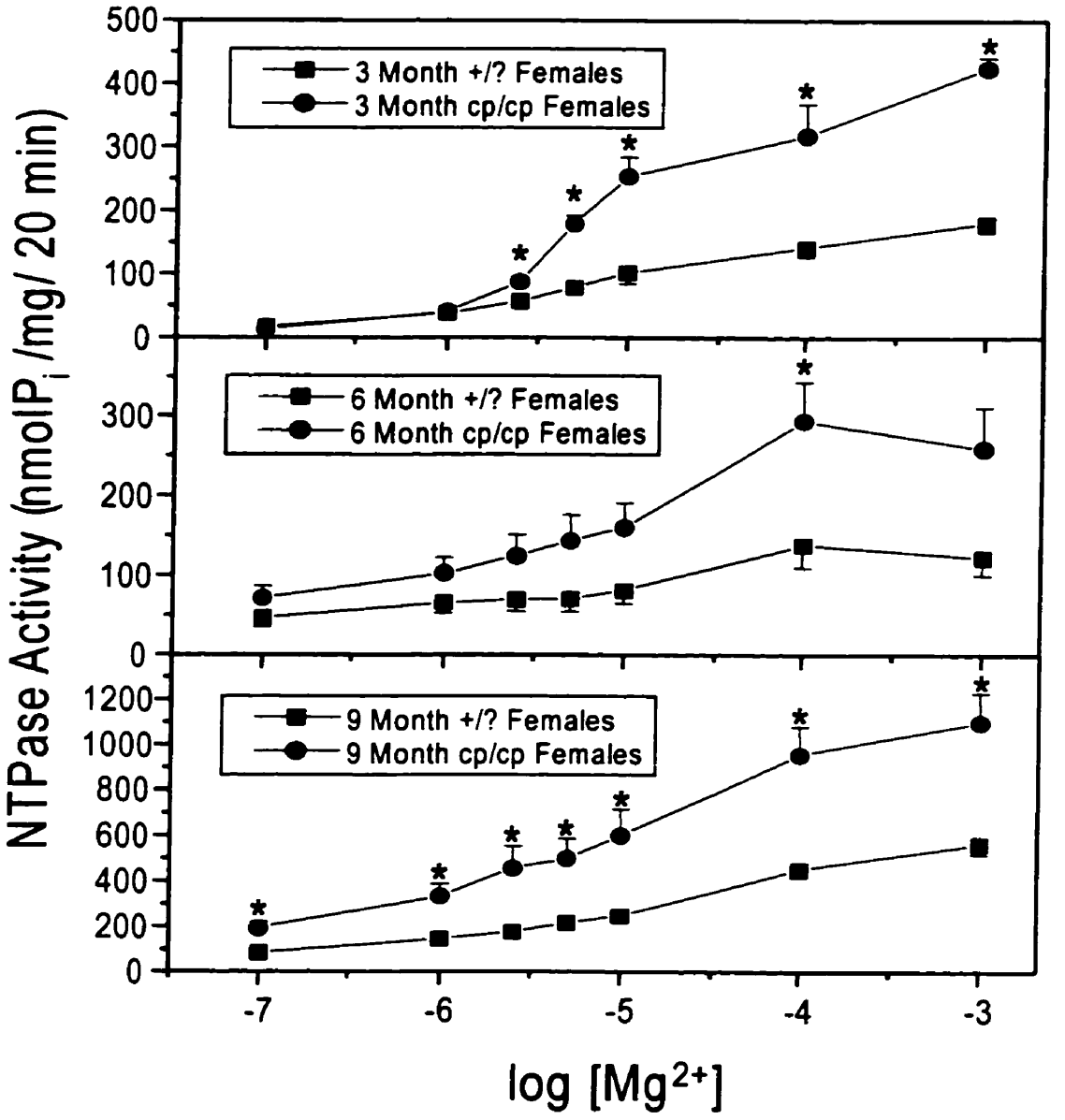

Figure 18. NTPase activity in lean and corpulent 3, 6 and 9 month old female JCR:LA-*cp* rat liver nuclei as a function of $[Mg^{2+}]_{free}$

NTPase activity was assayed as described in Methods, with [GTP]=5 mM, [EDTA]=1 mM and 20 minutes incubation at 37°C. Error bars represent SEM for 3-5 assays. *$p<0.05$ vs. lean animals.

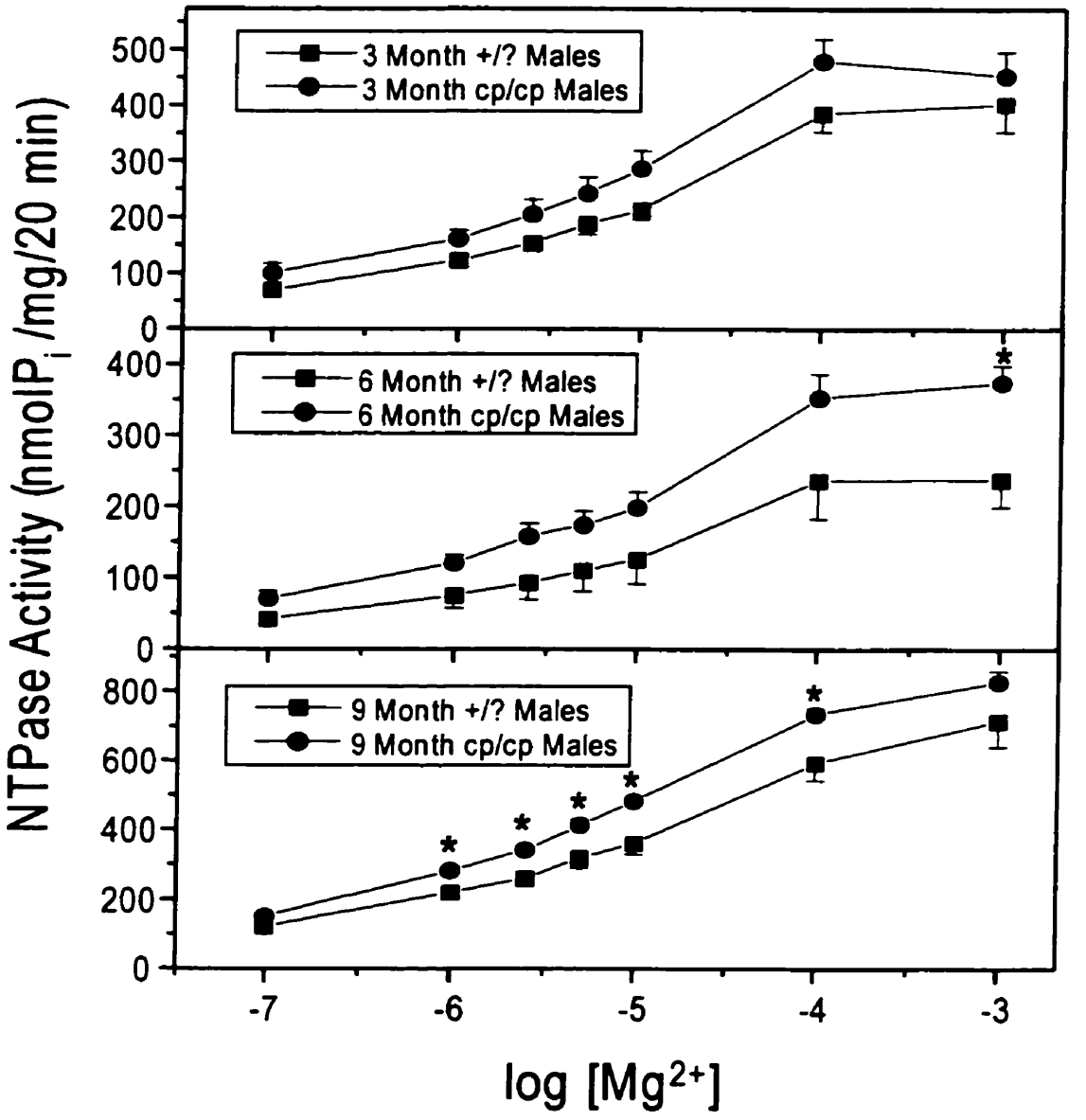

Figure 19. NTPase activity in lean and corpulent 3, 6 and 9 month old male JCR:LA-*cp* rat liver nuclei as a function of $[Mg^{2+}]_{free}$

NTPase activity was assayed as described in Methods, with [GTP]=5 mM, [EDTA]=1 mM and 20 minutes incubation at 37°C. Error bars represent SEM for 3-5 assays. *$p<0.05$ vs. lean animals.

Table 6. Nuclear content of phospholipids and cholesterol

Age (mon)	Sex	Genotype	[Phospholipids] (nmol/mg protein)	% of lean animals	[Cholesterol] (nmol/mg protein)	% of lean animals
3	Female	*+/?*	12.2±0.6	--	1.96±0.20	--
		cp/cp	18.9±0.7‡	155	2.75±0.18*	140
6	Female	*+/?*	13.6±2.4	--	1.29±0.49	--
		cp/cp	20.8±1.8*	153	3.13±0.32*	243
9	Female	*+/?*	31.7±1.9	--	1.54±0.69	--
		cp/cp	48.0±3.1‡	151	5.64±1.15*	366
3	Male	*+/?*	19.9±0.9	--	3.12±0.17	--
		cp/cp	20.5±1.9	103	2.46±0.28	79
6	Male	*+/?*	25.7±3.3	--	2.84±0.66	--
		cp/cp	32.5±5.4	126	2.79±0.38	98
9	Male	*+/?*	55.8±11.4	--	3.30±0.78	--
		cp/cp	54.9±9.9	98	3.53±0.35	107

Values represent means±SEM. n=3-7
*$p<0.05$ vs. lean animals
‡$p<0.01$ vs. lean animals

Nuclear content of cholesterol and phospholipids was determined for isolated rat liver nuclei from the groups indicated, as described in Methods.

samples compared to age-matched lean females. In contrast, there was no significant change in phospholipid content of nuclei isolated from corpulent male animals versus age-matched lean males. There was also no significant change in cholesterol content in the corpulent male nuclei compared to nuclei from lean males. Nuclei isolated from the corpulent females, however, showed a significant increase in cholesterol content versus age-matched lean animals. Furthermore, the magnitude of this increase rose linearly with age ($r=0.999$, $p<0.05$), from 140% of leans at three months to 366% at nine months. These changes in nuclear envelope composition are particularly interesting in light of the findings that the corpulent females exhibited alterations in both NTPase activity and membrane composition in virtually all groups/assay conditions, whereas males had relatively few alterations in NTPase activity, and no significant changes in membrane composition.

b. Changes in Nuclear Envelope Integrity

i. The Nuclear Membrane Integrity Assay

The composition of a cell membrane is responsive to its environment. For example, the lipid composition of many membranes in the heart can be altered in various pathologies like diabetes mellitus (261, 262), ischemia (266) and heart failure (250). Membrane composition can also be modified in vitro in order to obtain mechanistic insight into membrane function. The incubation of cholesterol-enriched liposomes with cardiac sarcolemma (182) or sarcoplasmic reticulum (199) results in the incorporation of cholesterol into these membranes. This allows for the study of the effects of cholesterol on the activities of specific membrane-embedded transport proteins (182, 199). Another

effect that cholesterol has upon membranes is on membrane ordering (190, 313). Cholesterol can condense and rigidify the membrane in a general or local fashion (190, 313). A change in the cholesterol content of the membrane may also alter membrane integrity. This is often measured as a change in osmotic fragility in cells like erythrocytes (48, 239).

The nuclear membrane may also be responsive to the lipid environment. In light of the dramatic alterations in nuclear envelope lipids in the corpulent female JCR:LA-*cp* rat, it is important to evaluate nuclear membrane integrity in these animals. Changes in nuclear integrity may provide further evidence that the altered composition of the nuclear envelope can contribute to the observed alterations in NTPase activity.

The nuclear membrane integrity assay is a simple, rapid technique that can provide semi-quantitative data on the strength and integrity of the nuclear membrane in isolated nuclei. Traditionally it has been necessary to perform technology-intensive or time-consuming protocols (e.g. electron paramagnetic resonance of membrane probes) to obtain such information. This assay, while unable but also unintended to replace such techniques, is capable of informing the researcher if nuclear membrane integrity has been disturbed by manipulations of membrane composition. High concentrations of salt are used to extract proteins from the nuclear membrane. DNA and other nuclear material can then leak from the nucleus during this disruption of the membrane. DNA release may then be quantitatively monitored via absorbance spectrophotometry (Figure 20). The release of nucleotides from the nucleus, therefore, is employed as an effective end point to measure nuclear integrity. This assay is unable to directly measure membrane fluidity, but may serve as an indirect measure of this important characteristic.

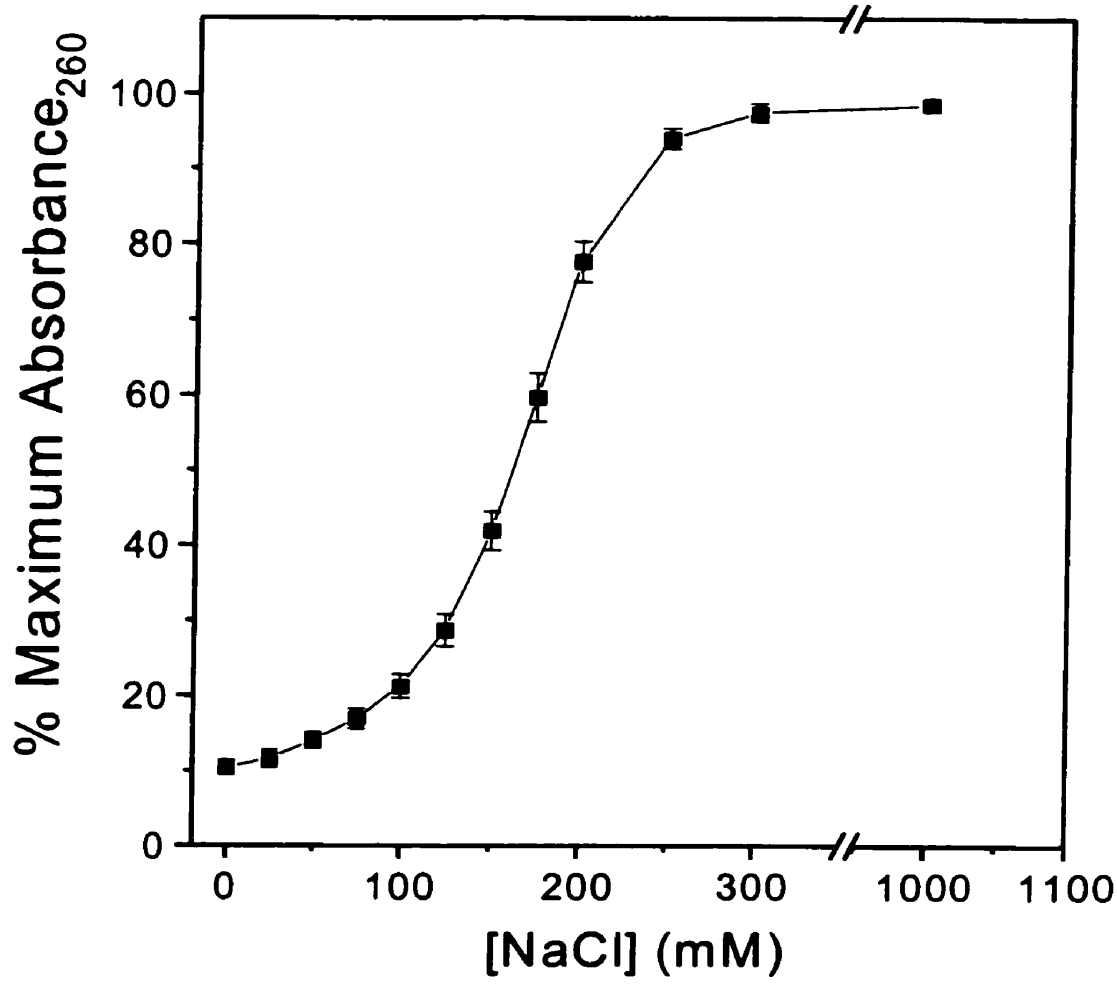

Figure 20. Normalized absorbance$_{260}$ curve for supernatants from isolated rat liver nuclei following nuclear membrane integrity assay

Isolated rat liver nuclei from Sprague-Dawley rats were subjected to nuclear membrane integrity assay as described in the Methods section. Error bars represent the SEM for 31 separate samples.

The integrity assay is performed as described in Methods. Results for nuclei from normal Sprague-Dawley rat liver typically show a sigmoidal release of nucleotides (Figure 20). The measurement of absorbance at 260 nm, however, may not accurately reflect the release of nucleotides, since significant interference from proteins or other molecules may occur. To ensure that this is not the case, DNA released from lysed nuclei and DNA remaining in the leaky nuclear "ghosts" were stained with the intercalating dye Hoechst 33258 and actual DNA concentrations measured by spectrofluorometry (Figure 21). The curve of DNA release closely parallels that of the absorbance curve, and when the curves from Figures 20 and 21 are correlated, a very high coefficient of correlation is obtained ($r=0.97$, $p<0.001$) (Figure 22). The simple nuclear integrity assay, therefore, is a reliable measure of DNA release from isolated nuclei, and provides a relatively easy method to gauge nuclear membrane integrity.

ii. Nuclear Envelope Integrity Alterations *In Vivo* and *In Vitro*

Nuclear membrane integrity was found to be significantly decreased in nuclei from corpulent female rats compared with nuclei from lean females at all ages (Figure 23). This is in contrast to corpulent male nuclei, in which membrane integrity was generally similar in the corpulent animals versus the age-matched leans (Figure 24). These data are summarized in Table 7 with the measurement of RC_{50} values, which is the concentration of salt required to cause release of 50% of the nuclear nucleotide contents. This value enables quick comparison of relative integrity between samples and the determination of statistical significance. The RC_{50} values for corpulent female nuclei are significantly decreased at all ages compared to the age-matched lean nuclei, showing that nuclear

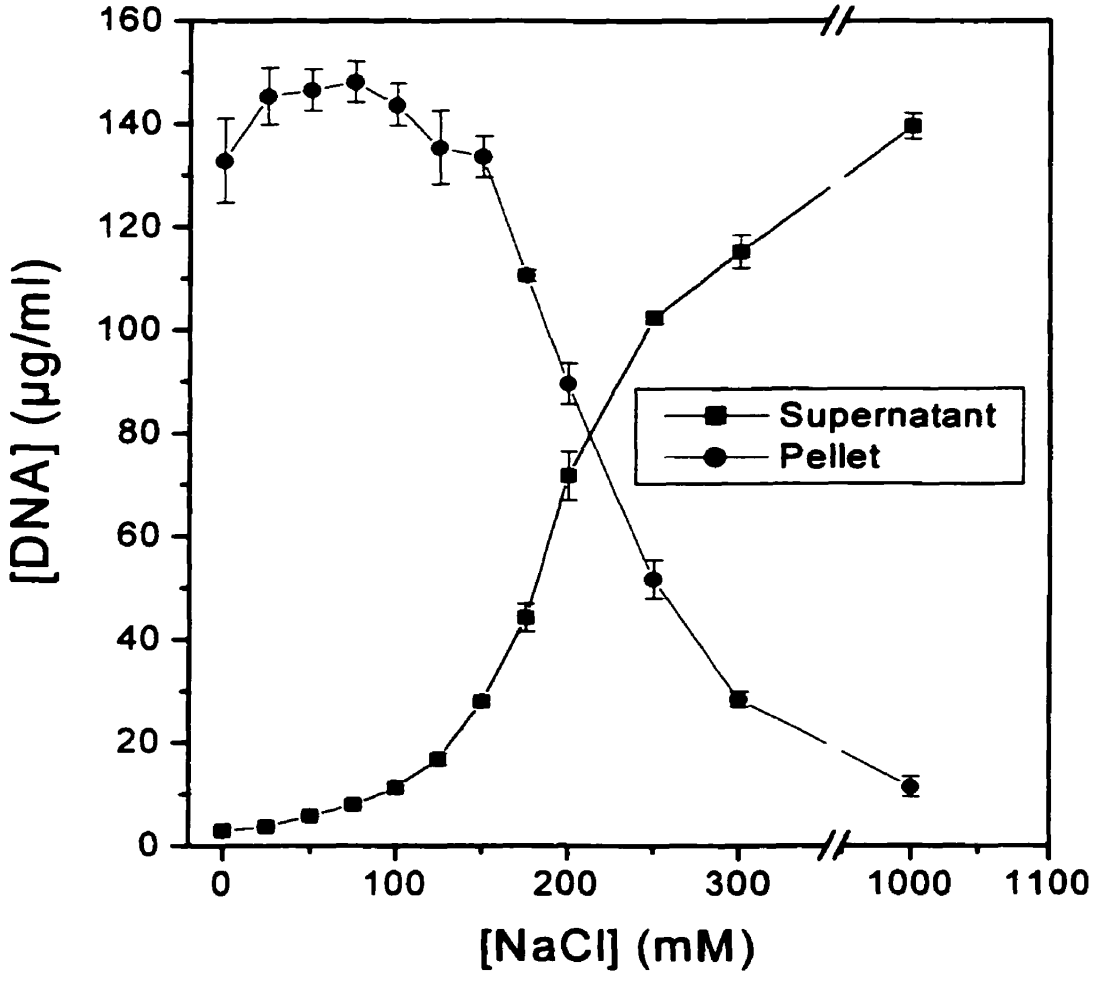

Figure 21. DNA concentration in the supernatant and pellet fractions from the nuclear membrane integrity assay

Supernatant DNA was labeled with 2 µg/ml Hoechst 33258 and the concentration determined by spectrofluorometry as outlined in Methods. DNA remaining in the nuclear pellets was released by treatment with 1 M NaCl and was quantified as per the supernatant. Error bars represent SEM for 3 separate experiments.

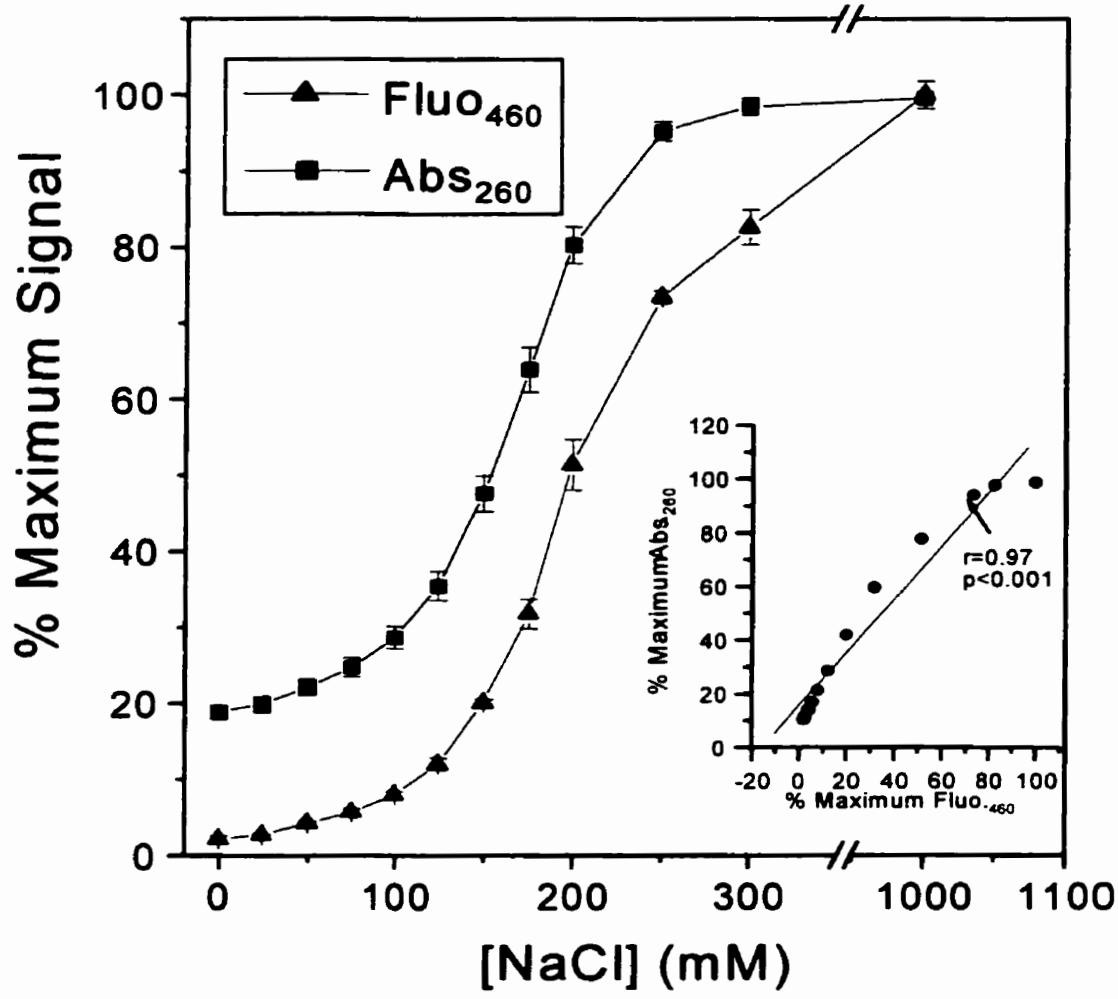

Figure 22. Normalized signals from fluorescence$_{460}$ and absorbance$_{260}$ of the supernatants after nuclear membrane integrity assay

Curves are taken from Figures 20 and 21. Inset: Linear relationship between fluorescence$_{460}$ and absorbance$_{260}$ signals (circles), and the corresponding linear regression (red line). The calculated correlation coefficient value was r=0.97 ($p<0.001$)

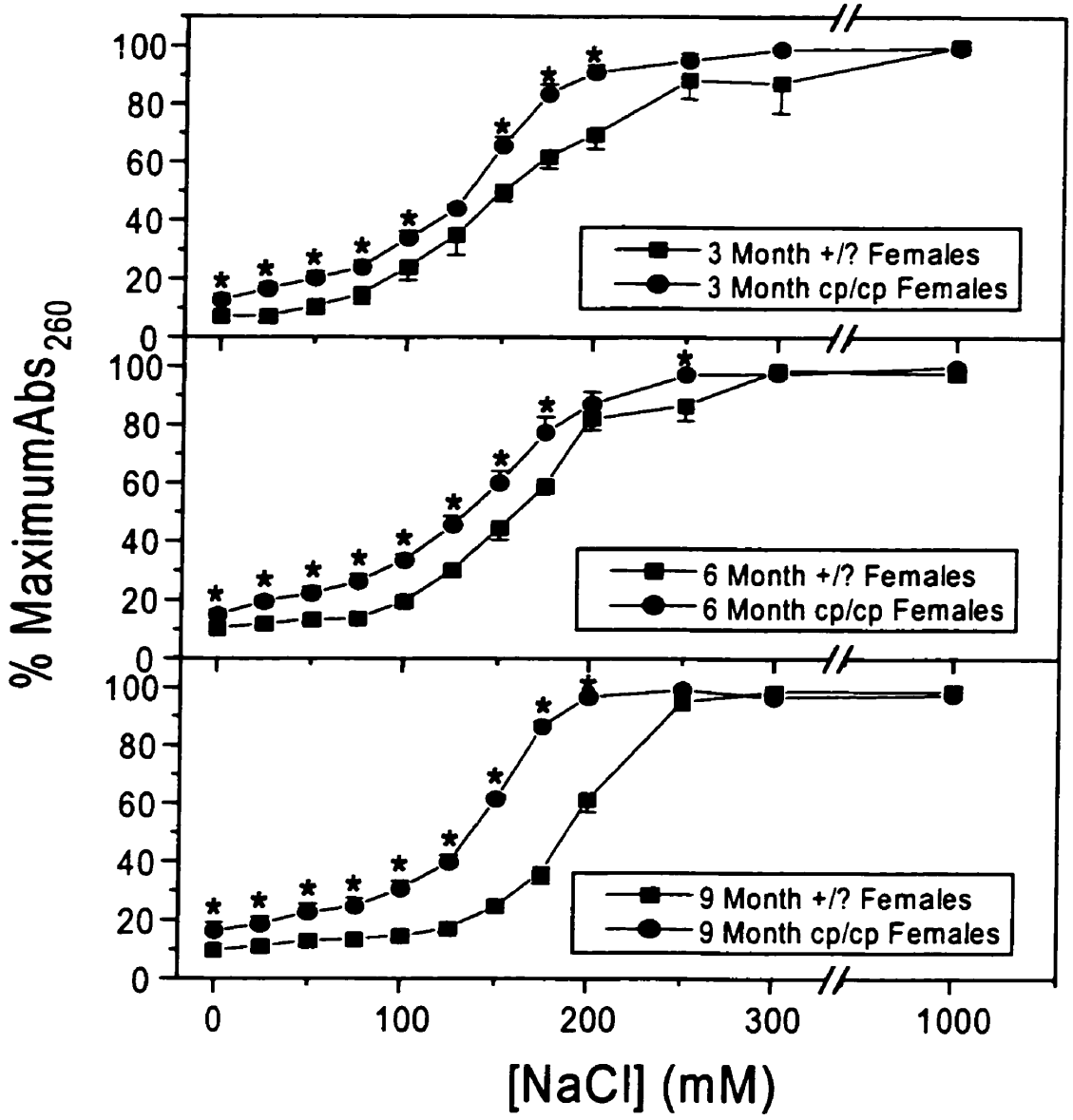

Figure 23. Assay of membrane integrity in nuclei from 3, 6 and 9 month old lean and corpulent female JCR:LA-*cp* rats

Aliquots of nuclei isolated from lean or corpulent rat livers were assayed for nuclear membrane integrity as described in Methods. Error bars represent SEM for 4-5 assays. *$p<0.05$ vs. lean animals.

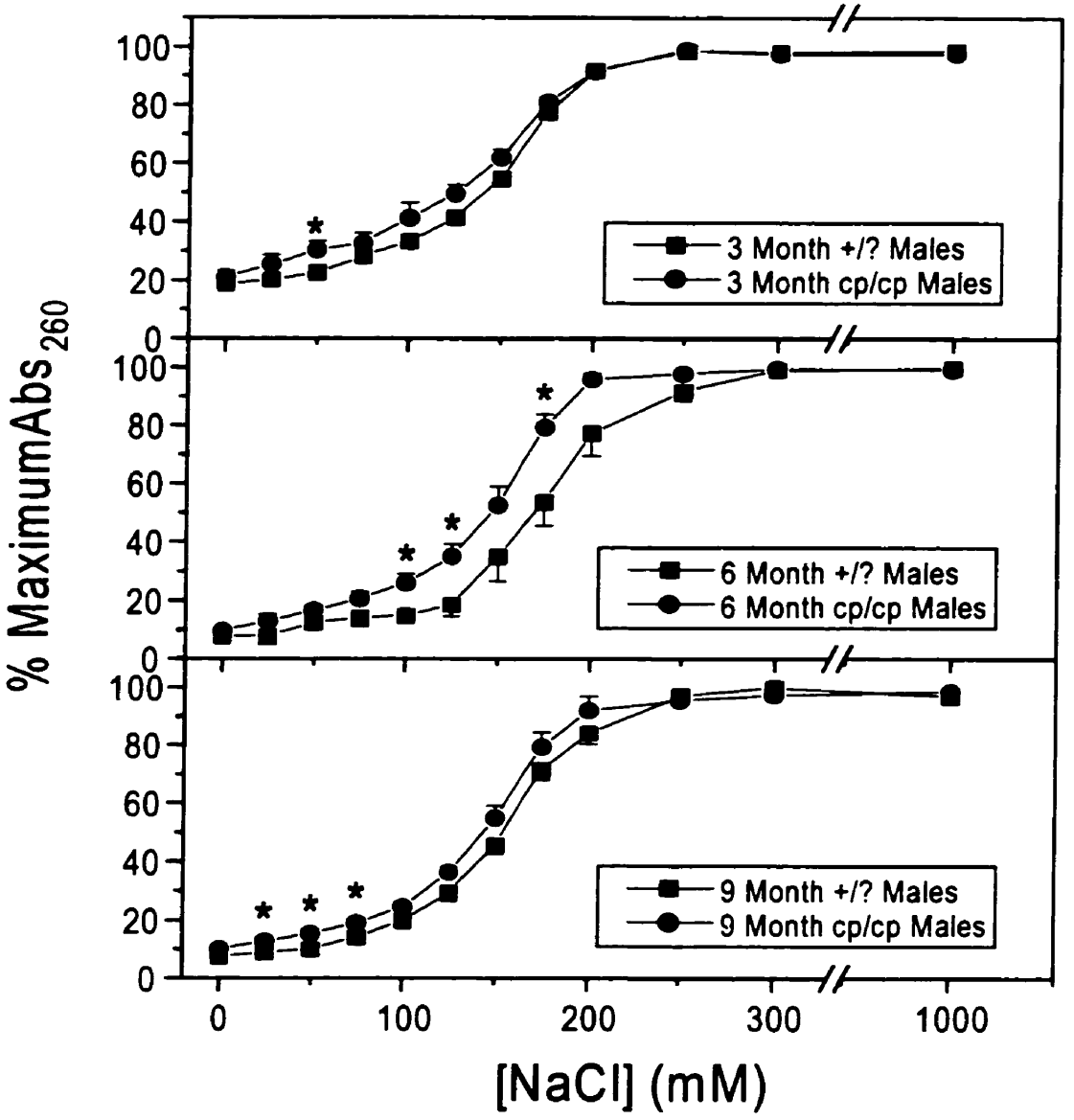

Figure 24. Assay of membrane integrity in nuclei from 3, 6 and 9 month old lean and corpulent male JCR:LA-*cp* rats

Aliquots of nuclei isolated from lean or corpulent rat livers were assayed for nuclear membrane integrity as described in Methods. Error bars represent SEM for 4-5 assays. *$p<0.05$ vs. lean animals.

Table 7. RC_{50} of isolated hepatic nuclei

Age (mon)	Sex	Genotype	RC_{50} (mM NaCl)
3	Female	*+/?*	153±5
		cp/cp	133±2‡
6	Female	*+/?*	158±4
		cp/cp	135±7*
9	Female	*+/?*	190±4
		cp/cp	137±2‡
3	Male	*+/?*	143±2
		cp/cp	124±9
6	Male	*+/?*	172±11
		cp/cp	147±6
9	Male	*+/?*	154±4
		cp/cp	146±4

Values represent means±SEM. n=4-6
*$p<0.05$ vs. lean animals
‡$p<0.01$ vs. lean animals

RC_{50} values represent the concentration (in mM) of NaCl required to cause release of 50% of nucleotide content via salt-induced lysis. The lysis technique is described in Methods.

membrane integrity had been compromised in these animals. Less salt was required to induce the same degree of lysis in the corpulent females than in the leans. Nuclei derived from male animals, however, showed no significant differences in integrity between corpulent and lean animals at any age. Once again, these findings follow the same trend as both the general NTPase assay results and the nuclear envelope composition data.

Since both the phospholipid and the cholesterol content of the corpulent female animals is altered with respect to lean rats, it is unclear whether either one or both of these factors may be responsible for the observed changes in nuclear membrane integrity. To shed further light on this area, isolated nuclei from Sprague-Dawley rat livers were treated with cholesterol-enriched phosphatidylcholine vesicles, or with phosphatidylcholine vesicles alone (275). The cholesterol-treated nuclei were found to have 275% of the content of cholesterol found in either the control or phosphatidylcholine treated nuclei. The phospholipid content was unchanged in any of the samples. When these nuclei were assayed for membrane integrity, the RC_{50} of the nuclei decreased significantly from 143 mM in the controls to 104 mM in the cholesterol-treated nuclei, with no significant change in the phosphatidylcholine treated nuclei (138 mM) (Figure 25).

c. Changes in Nuclear Morphology

The striking differences between nuclei from lean and corpulent animals discussed in the preceding sections begs the question: are there morphological differences in the

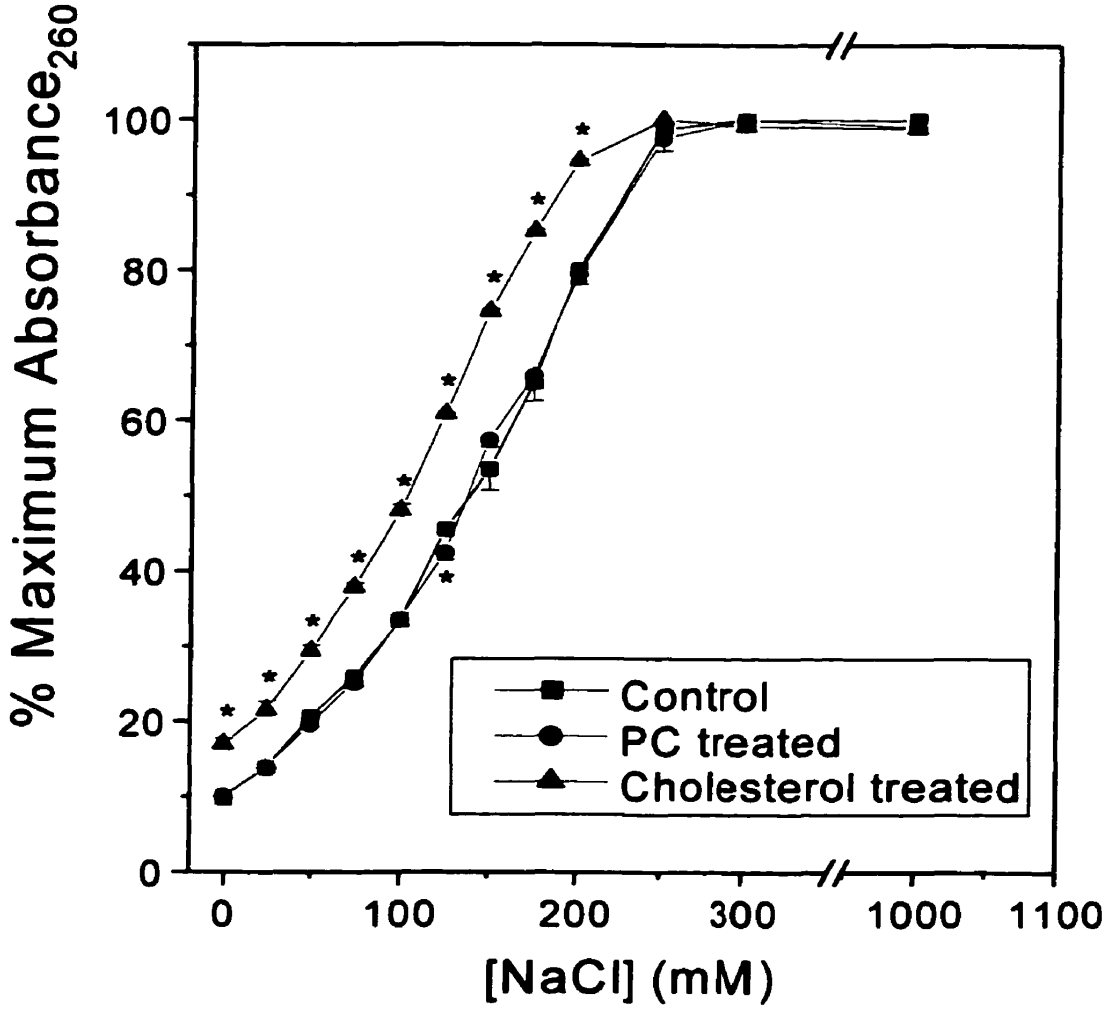

Figure 25. Effect of nuclear membrane cholesterol enrichment on nuclear integrity

Isolated Sprague-Dawley rat liver nuclei were treated with cholesterol-enriched phosphatidylcholine (PC) vesicles, or with PC vesicles alone, and subjected to nuclear membrane integrity assay as described (275). Error bars represent SEM for three separate experiments. *$p<0.05$ vs. control.

nuclei derived from these animals, especially in light of the nuclear membrane integrity data? As stated earlier, there were no obvious differences between nuclei from the various groups when they were examined visually under the light microscope. To further examine the nuclei, samples of 3 and 9 month lean and corpulent female JCR:LA-*cp* rat liver nuclei were stained with Hoechst 33258 and examined by confocal microscopy. As shown in Figure 26, once again no obvious differences were noted between the various samples of nuclei.

To get higher resolution structural data, samples of liver tissue from 6 month old female JCR:LA-*cp* rats were prepared for electron microscopy as described in Methods. The most striking feature of these samples is the presence of many lipid-rich bodies throughout the hepatocytes (Figure 27). (Note: the wavelet structure apparent in the lipid bodies is an artifact of sample section cutting). Upon closer examination, however, it can be seen that these lipid bodies are even found as inclusions in the hepatic nuclei (Figure 28). This pathology appears to be unique to these animals. We found no lipid deposition in nuclei from control tissues. It is again interesting to note that these samples correspond to animals that had major alterations in nuclear lipid composition.

III. Studies of Nuclear Protein Import in Vascular Smooth Muscle Cells

1. Characterization of the Permeablized-Cell Nuclear Protein Import Assay

The import assay used in this study is based on an existing, well-characterized assay (4). This assay, however, has never been carried out in smooth muscle cells. It was therefore necessary to carefully determine optimal conditions for the rabbit aortic vascular smooth muscle cells used in our experiments. We were interested in smooth

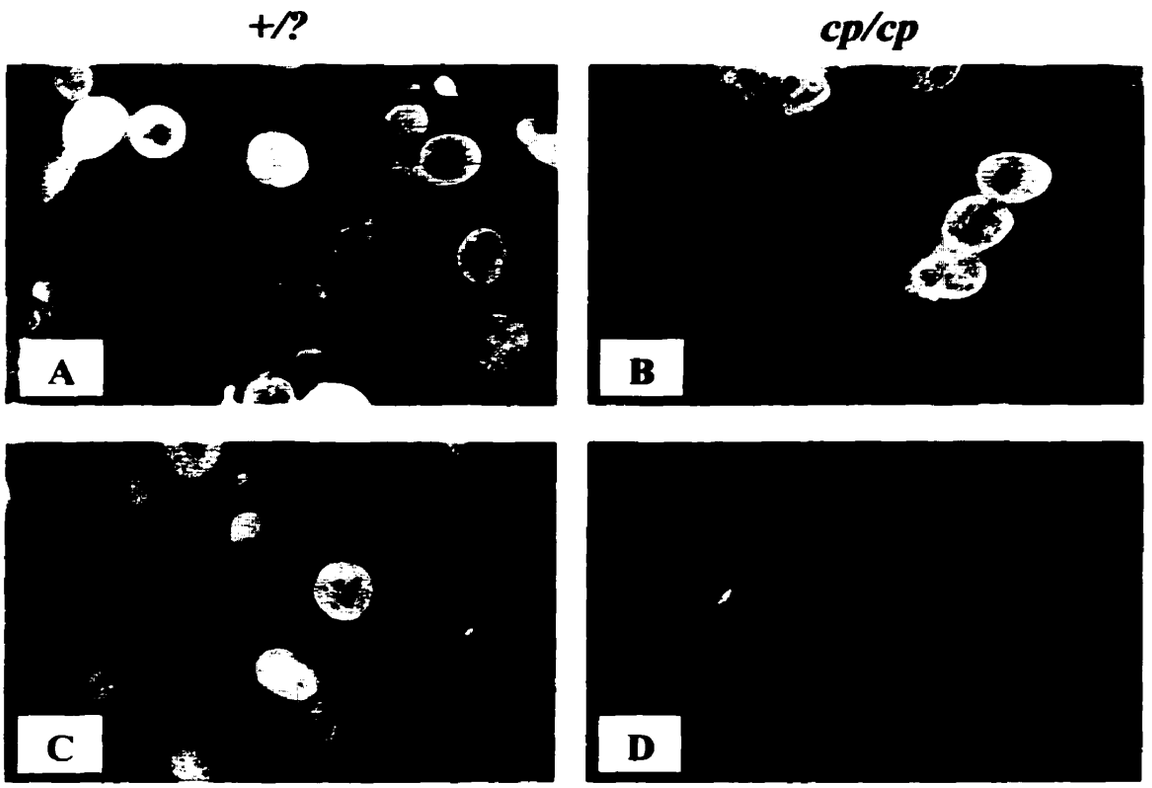

Figure 26. Visualization of liver nuclei from lean and corpulent JCR:LA-*cp* rats

Liver nuclei isolated from lean (*A,C*) or corpulent (*B,D*) three month old (*A,B*) or nine month old (*C,D*) female JCR:LA-*cp* rats were stained with Hoechst 33258 and examined by confocal microscopy as described for rat liver and pig cardiac nuclei in Methods.

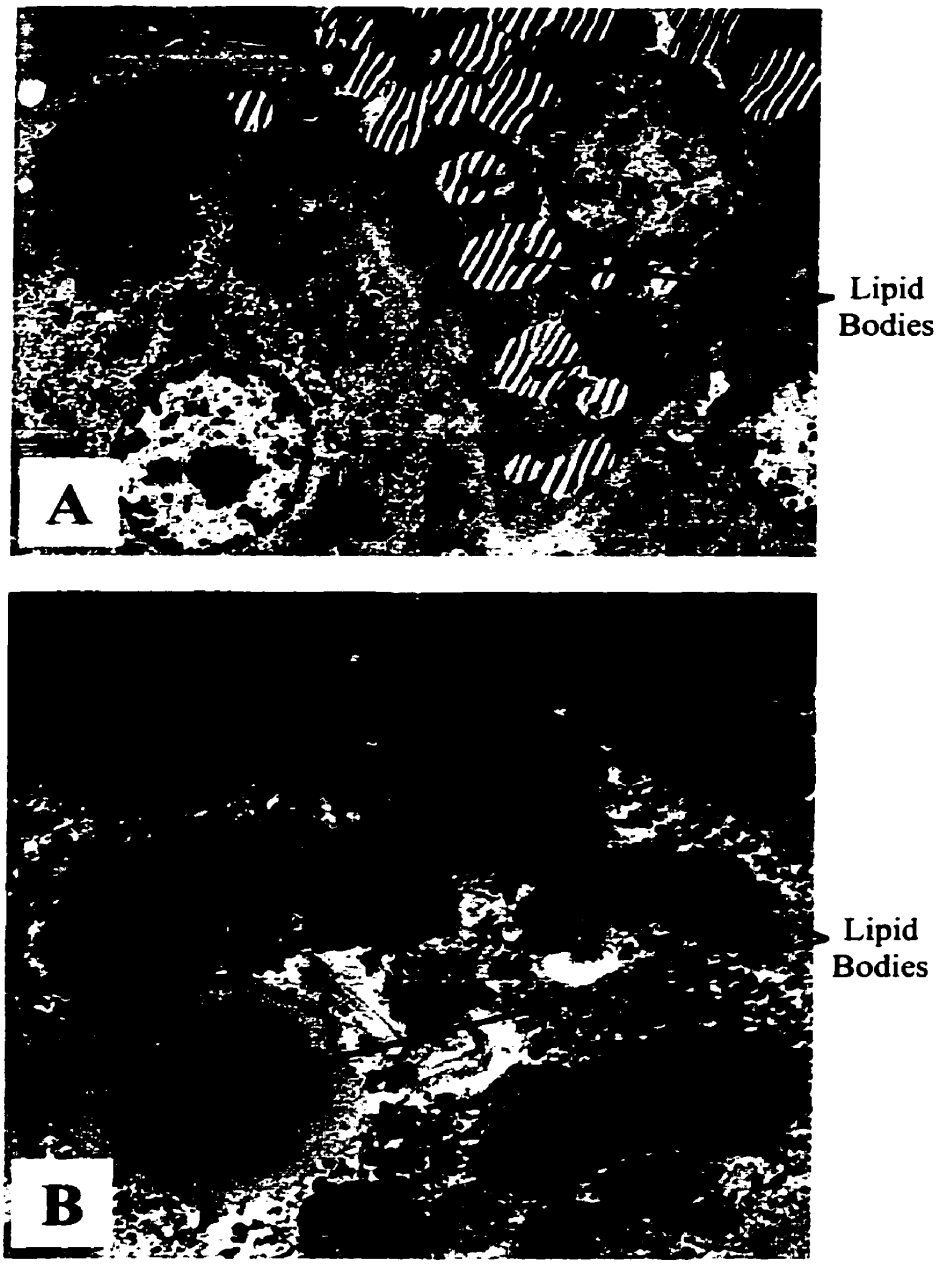

Figure 27. Electron micrographs of lipid bodies in JCR:LA-*cp* liver tissue

Liver tissue samples from a 6 month old corpulent female JCR:LA-*cp* rat were prepared for electron microscopy as described in Methods. Numerous large lipid-laden bodies are visible throughout the cells. Panel *A*, magnification ~3300x. Panel *B*, magnification ~19000x. n, Nucleus; m, Mitochondria.

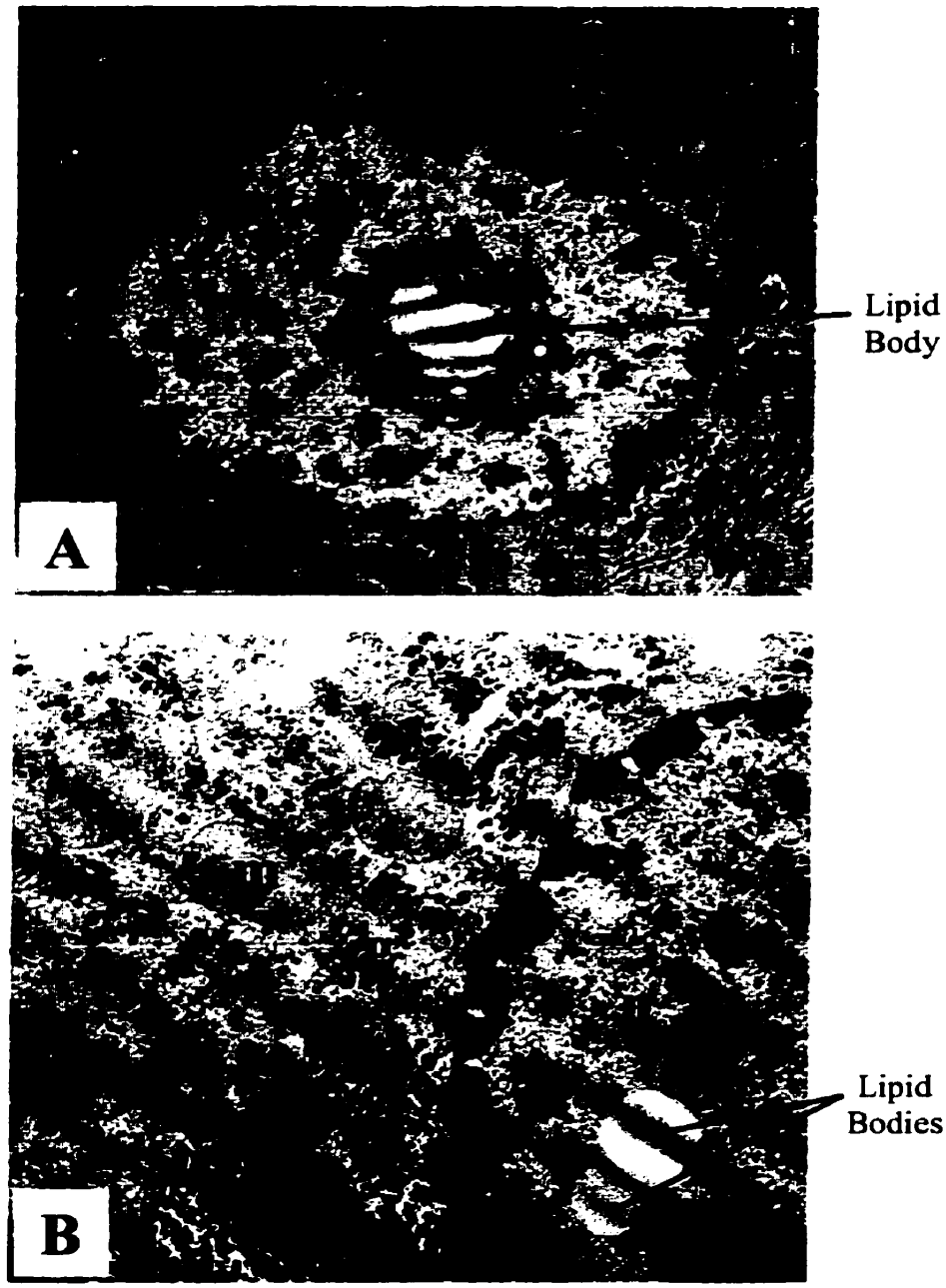

Figure 28. Electron micrographs of lipid body inclusions in the nuclei of JCR:LA-*cp* liver tissue samples

Samples of liver tissue from a 6 month old corpulent female JCR:LA-*cp* rat were prepared for electron microscopy as described in Methods. Panel *A* is a hepatocyte detail revealing a large nuclear inclusion containing a lipid body (magnification ~7700x). Panel *B* details another hepatocyte exhibiting multiple lipid bodies in the nucleus (magnification ~18500x). e, Endoplasmic Reticulum; m, Mitochondria; n, Nucleus; g, Glycogen Deposits.

muscle because these cells exhibit both a quiescent and a proliferating phenotype, and our initial question was whether the phenotype switch in these cells influenced import. For these experiments, smooth muscle cells were harvested from explanted aortic rings and used during the first passage (see Methods). By placing the cells in either a Starvation Medium or an FBS-supplemented medium, the cells could be kept in either a quiescent or a proliferative phenotype, respectively. Unlike many existing culture lines of smooth muscle cells, these cells maintained classic smooth muscle morphology and continued to express smooth muscle cell markers such as α-actin, SM-myosin and caldesmon (299). These cells also responded appropriately to agonists such as norepinephrine, ATP, histamine, endothelin-1, vasopressin, BayK 8644, methoxamine and ouabain (210).

The import assay used in our studies is summarized in Figure 29. Briefly, smooth muscle cells are first permeablized by brief exposure to digitonin. This step opens up the sarcolemma and permits access to the nucleus and the nuclear pore complex. The concentration of digitonin used must be selected so as to prevent permeablization of the nucleus, since the assay depends on nuclear retention of a fluorescent signal molecule. To ensure selective permeablization of the sarcolemma and not the nucleus, anti-DNA antibodies can be employed. Permeablization of the nucleus would permit binding of the antibodies to the now-exposed DNA and could be visualized by confocal microscopy using fluorescent secondary antibodies. Using this approach, we found that treatment of smooth muscle cells for five minutes with concentrations of 80 μg/ml digitonin or higher resulted in permeablization of the nucleus, as shown by fluorescence of the nucleus (Figure 30, panels *B* and *C*). Conversely, treatment with 40 μg/ml digitonin for five minutes permeablized the sarcolemma (as shown by successful import assays – see

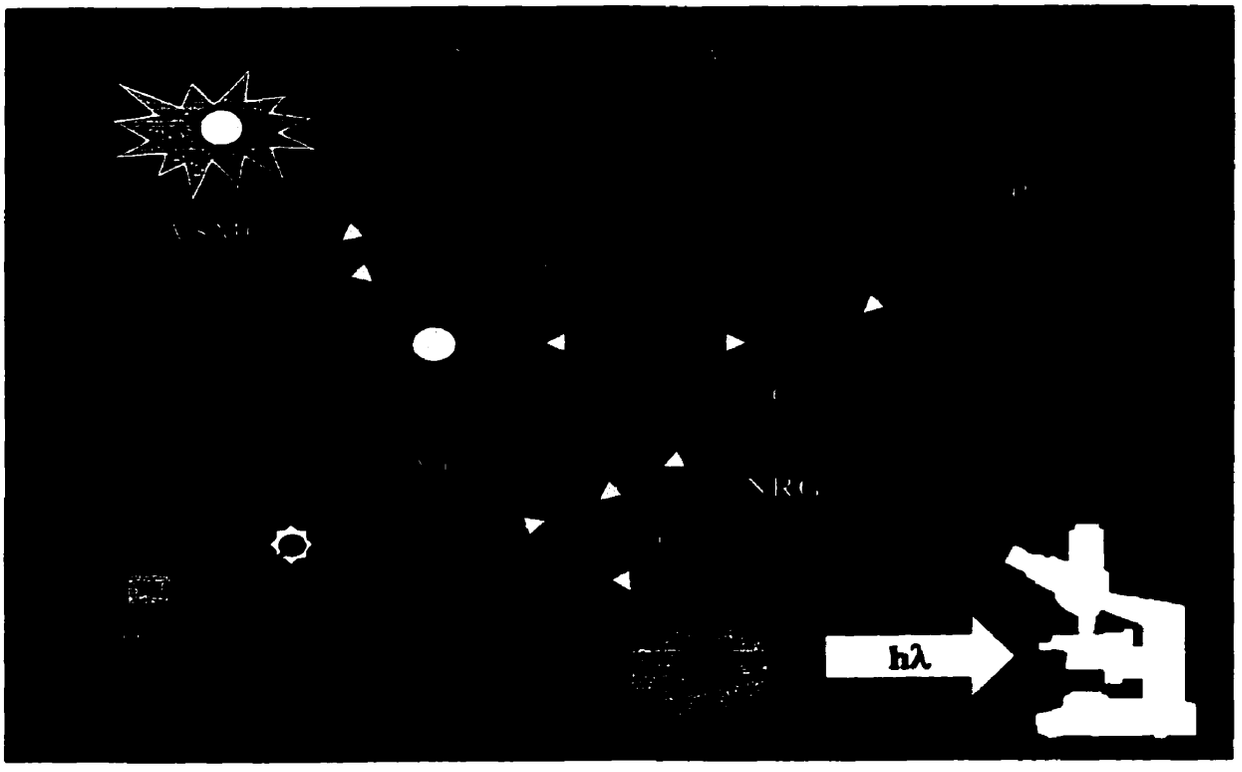

Figure 29. Simplified diagram of the permeablized-cell nuclear protein import assay

Abbreviations: BSA, bovine serum albumin; NLS, nuclear localization signal; NRG, energy generation system (1 mM ATP, 1 mM creatine phosphate, 20 units/ml creatine phosphokinase); VSMC, vascular smooth muscle cell. For details of the assay, see Methods.

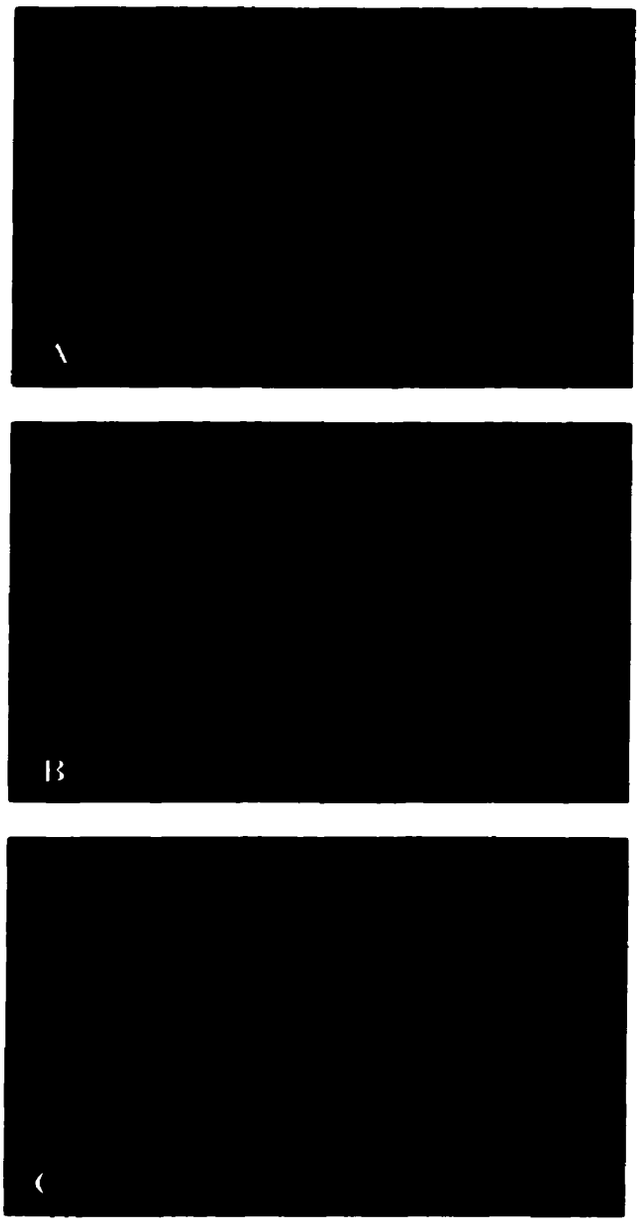

Figure 30. Immunostaining of digitonin-permeablized smooth muscle cells with anti-DNA antibodies

Aortic smooth muscle cells growing on glass coverslips were permeablized for five minutes with 40 (*A*), 80 (*B*) or 800 (*C*) μg/ml digitonin, then immunostained with anti-DNA antibodies as described in Methods. Samples were visualized by confocal microscopy using the VHS filter block.

below), but did not compromise the nucleus (Figure 30, panel *A*).

Permeablization of the cell has the consequence that the cell cytosol (containing critical soluble import factors – see Review of Literature, Section A.II.1.b) is lost during the assay. Exogenous cytosol must therefore be added. Previous studies of import in many different cell systems have used rat liver cytosol, which is easily produced in abundance from single organs and which contains all the necessary import factors (4). Isolation of smooth muscle cytosol in large enough quantities for the present experiments was not possible, due to the very large number of cells necessary to isolate even a small amount of cytosol. We therefore added in exogenous rat liver cytosol, which provides the further benefit that we may now treat either the cytosol (i.e. import factors) or the permeablized cells (i.e. nucleus and nuclear pore complex) with agents or drugs of interest. It was also necessary to add in an energy-generating system to provide a source of ATP to support the import process, so a combination of ATP, creatine phosphate and creatine phosphokinase was added (see Methods).

Although the cytosol is derived from hepatocytes, the resulting data is still applicable to smooth muscle cells. According to the original method for the import assay, a variety of cytosols or cell lysates readily support import (4). Multiple homologues of import factors (e.g. importin-α) have been identified in a variety of tissues (167, 240), but it is unknown whether these homologues exhibit different efficiencies at supporting import. It is therefore unclear whether the use of smooth muscle cytosol in the present studies would alter the results reported here, but there is currently no evidence to suggest that different results would be obtained if the source of cytosol was changed.

A fluorescent and importable protein marker is also required, therefore we conjugated the SV40 large T antigen nuclear localization signal to BODIPY FL-labeled bovine serum albumin. This gives a molecule of approximately 80 kDa, which is too large to diffuse into the nucleus on its own, but which is targeted to the nucleus and must be selectively imported. The accumulation of this marker in the nucleus can then be followed by confocal microscopy with appropriate filters and laser lines to visualize the BODIPY FL fluorophore. Figure 31 demonstrates the results of a typical nuclear import assay carried out at 37°C for 30 minutes, in which the fluorescent reporter molecule was either excluded (Panel *A*) or included (Panel *B*). The appearance of these cells after import assay is similar to that reported by others (4, 120, 232, 332).

2. *Effect of Smooth Muscle Cell Phenotype on Nuclear Protein Import*

Previous studies have suggested that the rate of nuclear protein import may be determined by the cell's current stage in the cell cycle (101, 102). To investigate whether phenotypic modulation in smooth muscle may affect import, serum-starved (i.e. quiescent) or serum-fed (i.e. proliferating) aortic vascular smooth muscle cells were subjected to import assay and the results quantified as a function of time (Figure 32). For the most part, import in the proliferating cells was observed to be significantly higher than in the quiescent cells, in agreement with studies in other tissue types (101, 102).

Import was also examined as a function of assay temperature, since import is an energy dependent process, in both smooth muscle cell phenotypes. At the physiological temperature of 37°C, import was significantly inhibited in the quiescent cells (Figure 33).

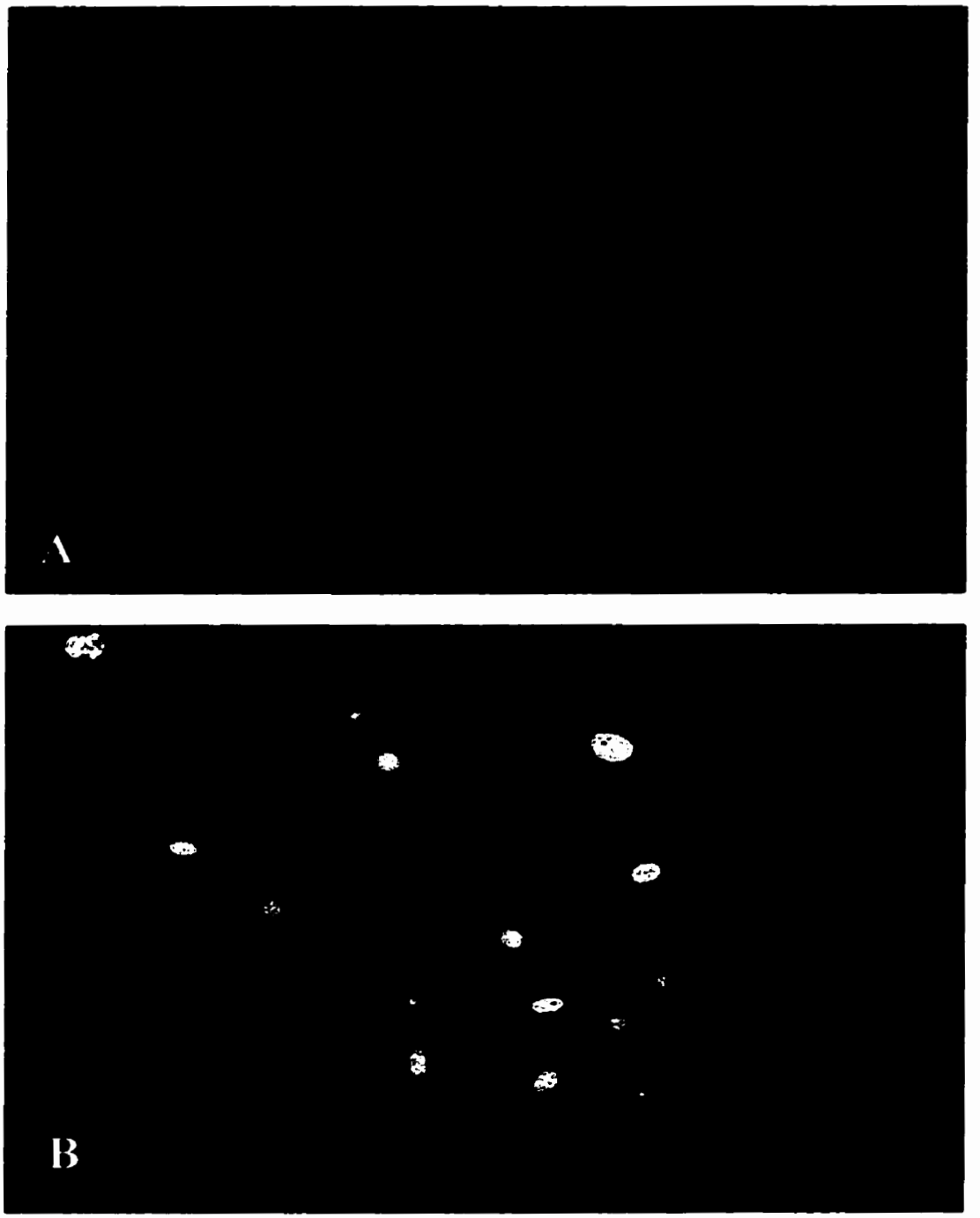

Figure 31. Typical results of nuclear protein import assay

Nuclear import assays were carried out in digitonin-permeablized vascular smooth muscle cells as described in Methods, either without (*A*) or with (*B*) nuclear import substrate (i.e. BODIPY FL-BSA conjugated to SV40 NLS).

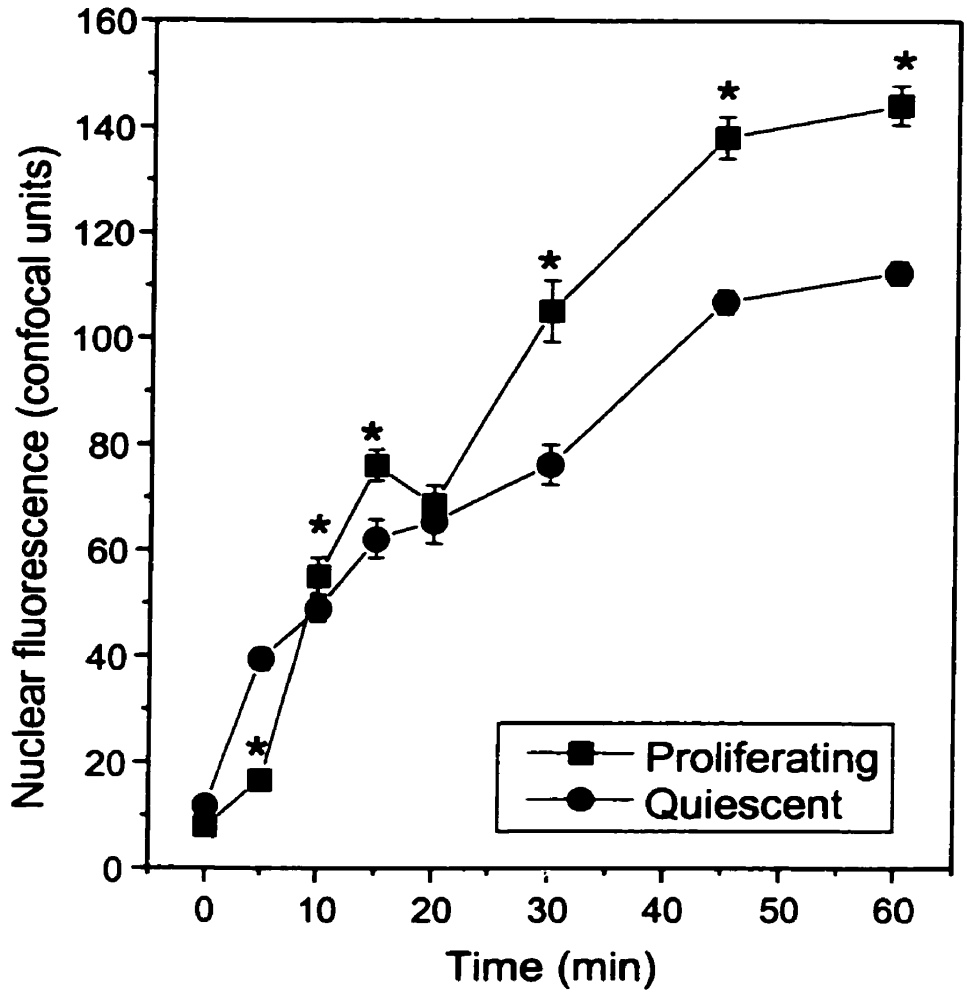

Figure 32. Time dependence of nuclear protein import in proliferating and quiescent vascular smooth muscle cells

Nuclear import assays were carried out as described in Methods at 37°C for various time points in both proliferating (FBS-fed) and quiescent (Starvation Medium-fed) aortic vascular smooth muscle cells. Error bars represent SEM for 9 to 31 cells. *$p<0.05$ vs. quiescent cells.

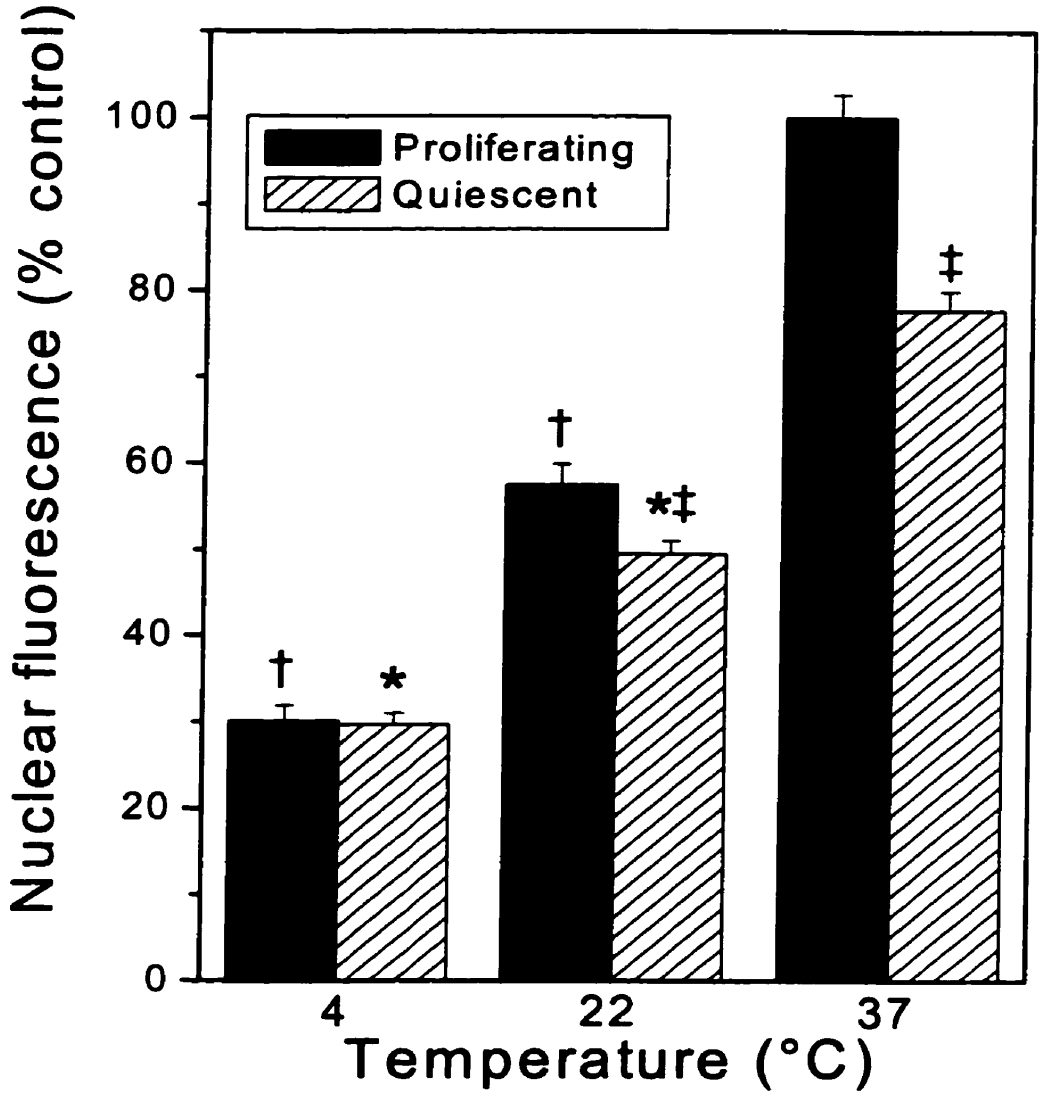

Figure 33. Temperature dependence of nuclear protein import in proliferating and quiescent vascular smooth muscle cells

Nuclear import assays were carried out as described in Methods for 30 minutes at 4, 22 or 37°C in both proliferating (FBS-fed) and quiescent (Starvation Medium-fed) aortic vascular smooth muscle cells. Error bars represent SEM for 66 to 111 cells in three separate experiments. †$p<0.05$ vs. proliferating cells (37°C); *$p<0.05$ vs. quiescent cells (37°C); ‡$p<0.05$ vs. proliferating cells at same temp.

When the temperature was reduced to room temperature (22°C), import was inhibited in both phenotypes, but again, there was a further significant inhibition of import in the quiescent versus the proliferating cells. Upon further reduction of the temperature to 4°C, at which most metabolic processes are dramatically slowed, import was still further inhibited in both cell phenotypes. In contrast to the results found at other temperatures, however, there was no difference in import levels between the two cell phenotypes. One possibility for this is that at this temperature, a common rate-limiting step is dramatically slowed in both cell phenotypes *downstream* of any potential physiologic inhibitor of import found in quiescent cells at higher temperatures. A probable candidate for this rate-limiting step is the energy-dependent translocation of the import complex through the nuclear pore. It is also interesting to note that although import is highly inhibited at this temperature, it is not completely blocked.

3. *Hydrogen Peroxide Inhibition of Import Mediated by ERK2*

a. Hydrogen Peroxide Inhibits Nuclear Protein Import

Hydrogen peroxide is generated by cells in both normal and pathological states. It is a by-product of normal cell aerobic metabolism, and is generated by a variety of cells in processes such as atherogenesis and ischemia (18, 27, 45, 53, 171, 173, 297, 342). H_2O_2 has been implicated in both proliferation and apoptosis of smooth muscle cells (1, 61, 189, 360). In both situations, activation of the mitogen-activated protein kinase ERK2 and stimulation of DNA synthesis has been reported as a result of H_2O_2 exposure (61, 104, 189). In light of these paradoxical findings, it is of interest to determine how H_2O_2 may be exerting its effects on cell functioning. One possibility that has not yet been

examined is the potential for H_2O_2 to affect nuclear protein import, which would have the effect of altering the normal movements of critical proteins such as transcription factors and other DNA-binding proteins into the nucleus. We therefore examined the effect of H_2O_2 on nuclear protein import.

Typical results of the nuclear import assay are shown in Figure 34. The fluorescent import substrate is markedly accumulated in the nucleus after import assay in control cells (Figure 34*A*). When the nuclear import cocktail (rat liver cytosol plus import buffer, an energy production system and protease inhibitors) is pretreated for 60 minutes at 37°C with 1 mM H_2O_2, however, this nuclear fluorescence is substantially reduced (Figure 34*C*). This effect could be attenuated by the inclusion of 0.3 mg/ml catalase, an enzyme that scavenges H_2O_2, during the pretreatment of the cells with H_2O_2 (Figure 34*D*). Treatment of import cocktail with catalase alone had no effect on nuclear protein import (Figure 34*B,E*).

The effect of varying concentrations of H_2O_2 on nuclear import was examined. As shown in Figure 34*E*, pretreatment of import cocktail with concentrations of H_2O_2 as low as 100 μM caused a significant inhibition of nuclear protein import (~90% of control values), and this effect was enhanced as [H_2O_2] was increased. Inclusion of 0.3 mg/ml catalase during pretreatment was able to completely block this effect with 100 and 500 μM H_2O_2. When [H_2O_2] was increased to 1 mM, import was reduced to ~60% of control values. Inclusion of 0.3 mg/ml catalase significantly improved recovery of import, but was unable to completely reverse the effects of the H_2O_2. Increasing the [catalase] to 1.4 mg/ml caused a further significant increase in import recovery, but was still unable to restore import to control values.

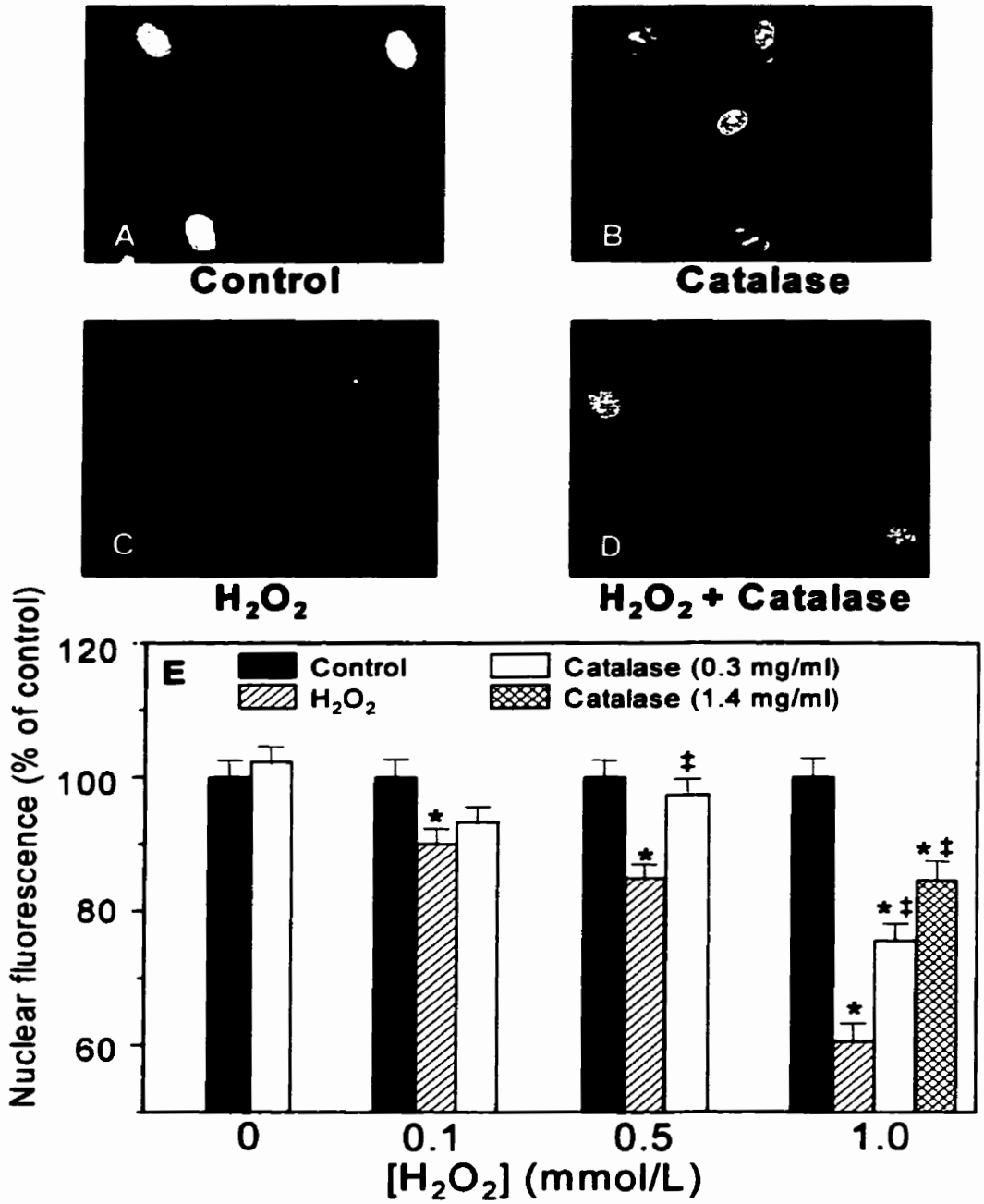

Figure 34. Nuclear protein import is inhibited by treatment with H_2O_2

Import cocktail was untreated (*A*), treated with 0.3 mg/ml catalase (*B*), or treated with 1 mM H_2O_2 without (*C*) or with 0.3 mg/ml catalase (*D*) for 60 minutes at 37°C prior to import assay as described in Methods. Fluorescence was normalized relative to controls and plotted for various [H_2O_2] and [catalase] (*E*). Error bars represent SEM for 61 to 132 cells in 3 or 4 separate assays. *$p<0.05$ vs. control. ‡$p<0.05$ vs. H_2O_2 treated.

Inhibition of import by H_2O_2 also exhibited time dependency, as shown in Figure 35. Increasing the time of treatment of import cocktail with H_2O_2 resulted in a steady decline in import activity. This decline was steeper when 1.0 mM H_2O_2 was used compared to 0.1 mM. Experiments with very long-term exposures to H_2O_2 are difficult, since in aqueous solutions, H_2O_2 eventually breaks down spontaneously to water and oxygen (26). H_2O_2 may also be scavenged by endogenous antioxidants. A blunting of the effect of H_2O_2 on import is eventually observed as a shallowing of the time-dependency curve (Figure 35), most likely due to these phenomena.

In Figure 36, the results of a 30 minute pretreatment regimen with 1 mM H_2O_2 at 37°C are shown. Consistent with the results reported above, pretreatment of the import cocktail significantly reduced the measured nuclear fluorescence in treated versus control cells. However, when the permeablized cells themselves, rather than the import cocktail, were identically pretreated with H_2O_2, there was no effect, despite the higher [H_2O_2] used. Treatment of permeablized cells with 1 mM H_2O_2 for longer time periods than 30 minutes resulted in significant detachment from the coverslips and loss of cells during the import assay, making quantification extremely difficult. The few remaining cells, however, appeared to accumulate import substrate in the nucleus at levels similar to controls (results not shown).

b. Free Radical-Mediated Oxidation: Effects on Nuclear Protein Import

The use of free radical generating systems to pretreat either import cocktail or permeablized cells resulted in different effects than those of H_2O_2 (Figure 36). Superoxide radicals were generated by pretreatment of import cocktail with 2 mM

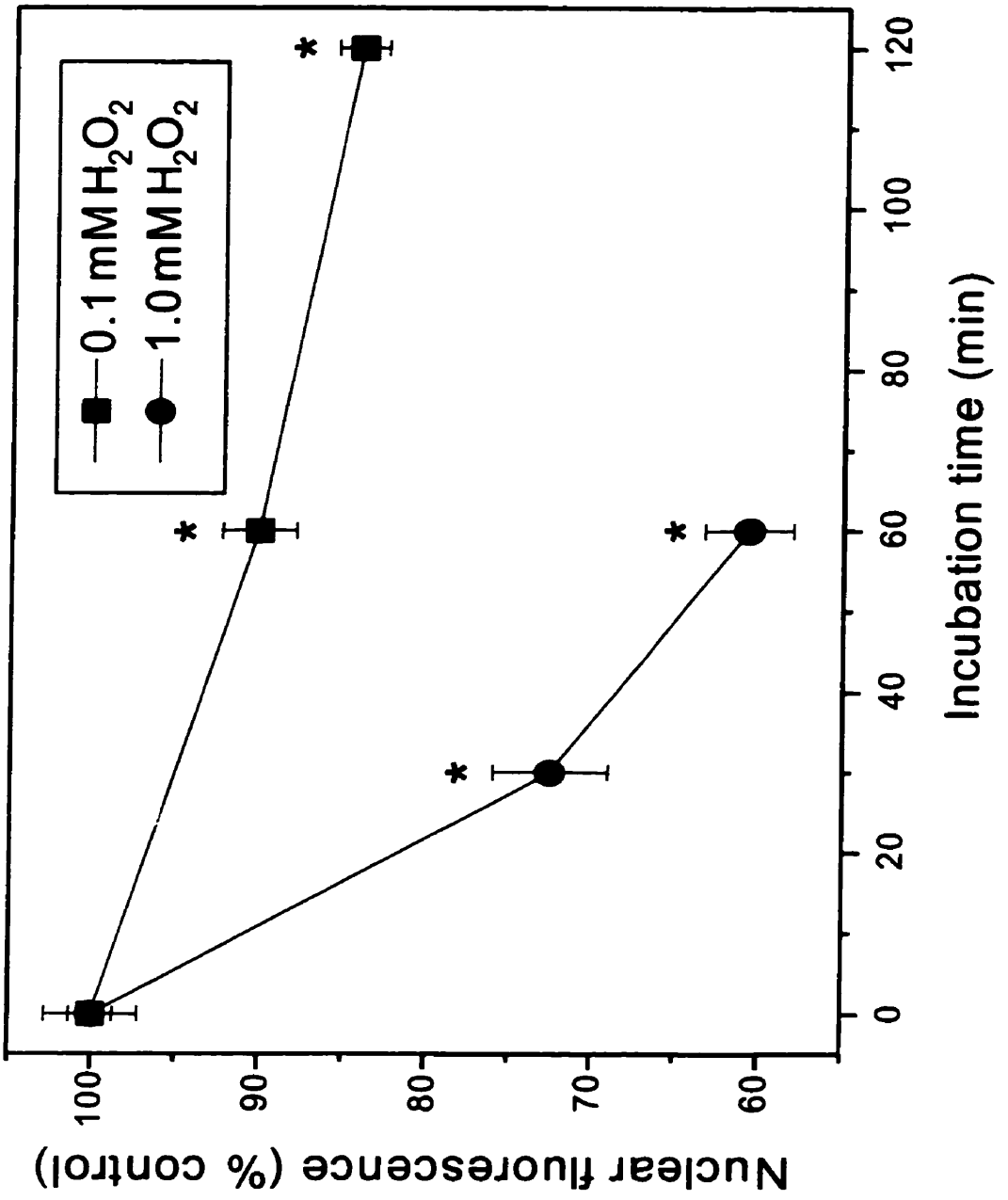

Figure 35. Time-dependency of import inhibition by H_2O_2

Nuclear fluorescence was determined by confocal microscopy following import assay with control or H_2O_2 pretreated import cocktail for various times as described in Methods. Fluorescence was normalized relative to controls. Error bars represent SEM for 61 to 98 cells in 3 separate assays. *$p<0.05$ vs. control.

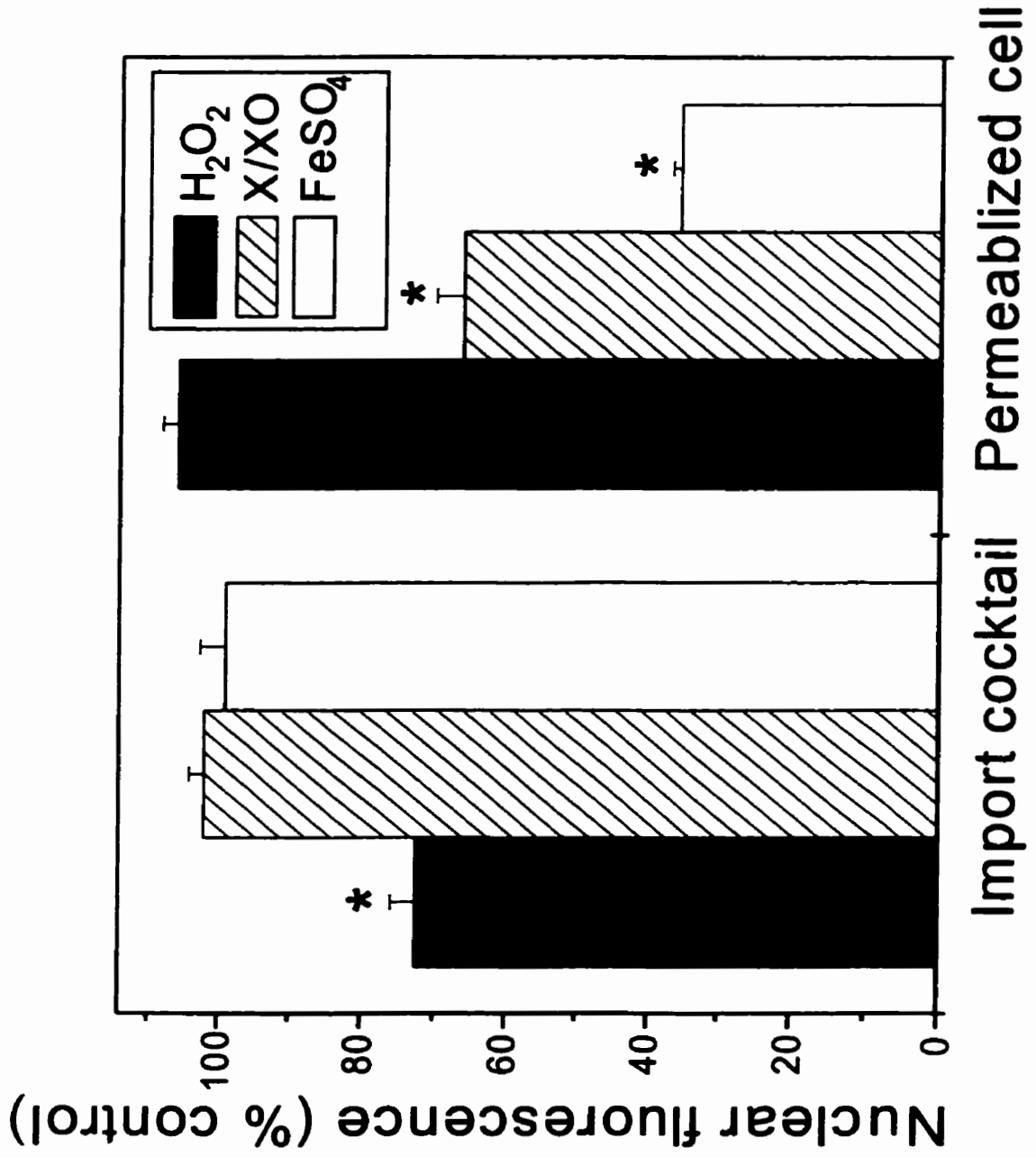

Figure 36. Hydrogen peroxide acts on a cytosolic factor, unlike superoxide or hydroxyl radicals

Import cocktail or permeablized smooth muscle cells were treated with 1.0 mM H_2O_2 for 30 minutes, 2 mM xanthine plus 0.03 U/ml xanthine oxidase for 10 minutes (X/XO), or 0.1 mM H_2O_2 plus 0.1 mM $FeSO_4$ for 60 minutes at 37°C prior to import assay. Error bars represent SEM for 55-172 cells from three or four independent experiments. *$p<0.05$ vs. control.

xanthine plus 0.03 U/ml xanthine oxidase for 10 minutes at 37°C, but had no significant effect on nuclear protein import. Identical treatment of permeablized cells, however, caused a significant inhibition of import (~66% of control). Increasing treatment time of permeablized cells beyond 10 minutes caused significant detachment and loss of cells, making quantification impossible. However, pretreatment of import cocktail with xanthine plus xanthine oxidase for times up to one hour showed no significant differences in import compared to controls (results not shown).

Since Fe^{2+} reacts with peroxide to generate hydroxyl radicals, import cocktail or permeablized cells were treated with 0.1 mM $FeSO_4$ plus 0.1 mM H_2O_2 for 60 minutes at 37°C. Similar results to those obtained with superoxide radicals were observed. Pretreatment of import cocktail caused no significant differences in import compared to controls, but pretreatment of permeablized cells significantly reduced import to ~36% of control values (Figure 36).

c. ERK2 Activation Accompanies Import Inhibition by Hydrogen Peroxide

Hydrogen peroxide has been shown to activate the ERK2 MAP kinase pathway in a number of cell types including smooth muscle (277). We investigated the possibility that H_2O_2 used in our experiments was acting via activation of the ERK2 tyrosine kinase signaling pathway.

The images in Figure 37 show the results of nuclear import assay in control cells (Figure 37*A*) compared to results obtained when the import cocktail was treated for 60 minutes at 37°C with 1 mM H_2O_2 plus 45 minute pretreatment with either 75 μM genistein, a non-specific tyrosine kinase inhibitor (Figure 37*C*), or 75 μM daidzein, its

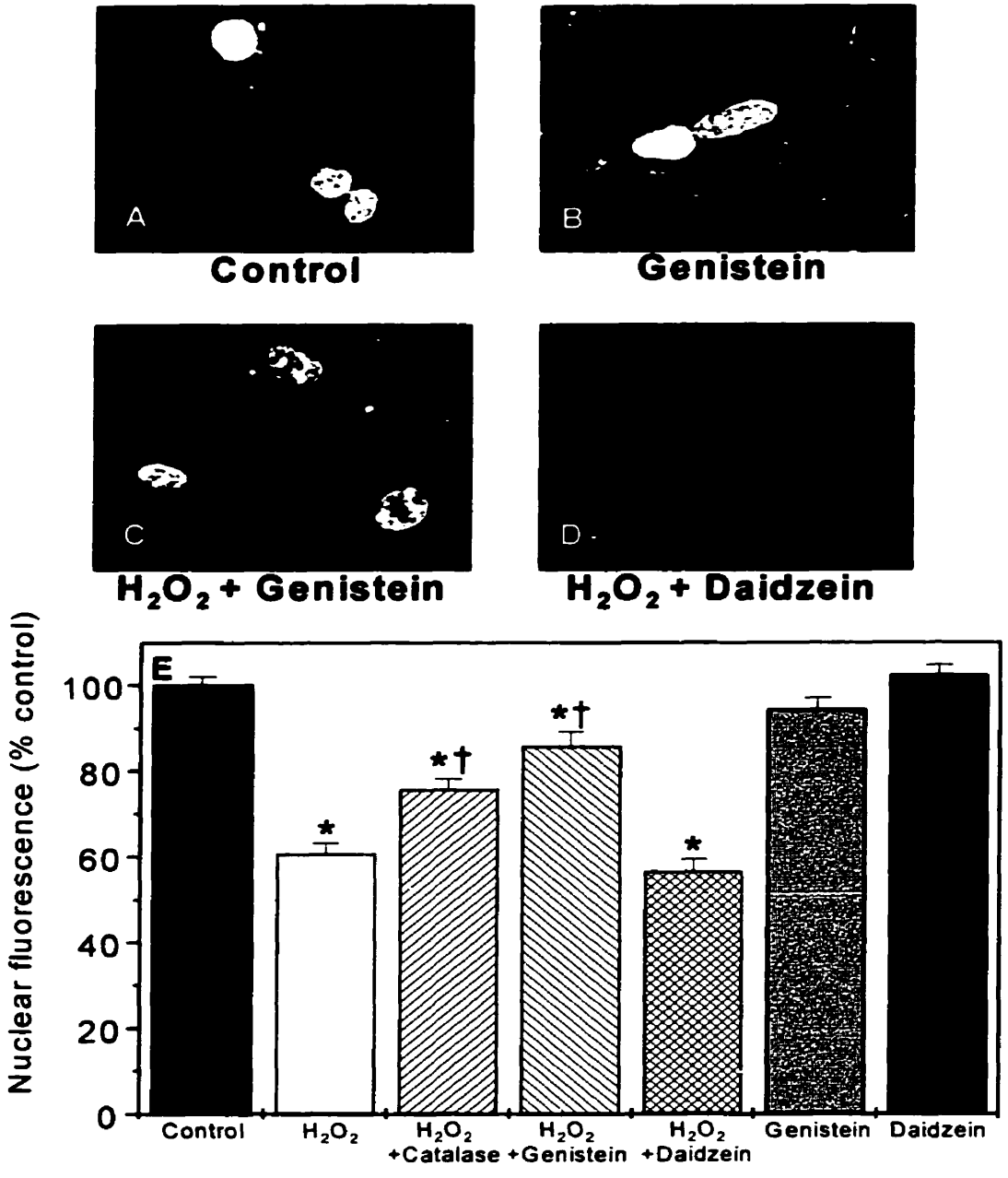

Figure 37. Nuclear import is regulated by MAPK activity

Import cocktail was untreated (*A*), treated with 75 μM genistein (*B*), treated with 1 mM H_2O_2 plus 75 μM genistein (*C*) or with 1 mM H_2O_2 plus 75 μM daidzein (*D*) for 60 minutes at 37°C prior to import assay as described in Methods. Fluorescence was normalized relative to controls and plotted (*E*). Data representing treatment with H_2O_2 or H_2O_2 plus catalase is from Figure 34. Error bars represent SEM for 78 to 112 cells in 3 or 4 separate assays. *$p<0.05$ vs. control. †$p<0.05$ vs. H_2O_2 treated.

inactive analog (Figure 37*D*). Inclusion of 75 μM genistein alone had no effect on import (Figure 37*B*). Import in the cells in which the import cocktail pretreatment had included genistein resembled that in the controls, despite the presence of 1 mM H_2O_2. When the import cocktail contained H_2O_2 plus daidzein instead of genistein, import was significantly reduced to virtually the same degree as H_2O_2 alone.

These data are quantitatively represented in Figure 37*E*. The inclusion of 75 μM genistein in the import cocktail during the pretreatment with H_2O_2 caused a significant recovery of nuclear protein import (~86% of control) compared to pretreatment with H_2O_2 alone. This recovery was even greater than that observed by including 0.3 mg/ml catalase in the pretreatment protocol, and was quantitatively nearly identical to the recovery obtained by including 1.4 mg/ml catalase (Figure 34*E*). Inclusion of 75 μM daidzein failed to block the inhibition of import by 1 mM H_2O_2. Genistein or daidzein alone had no effect on import (Figure 37*E*).

Western blotting of control import cocktail was compared to pretreatment with 1 mM H_2O_2 ± 0.3 mg/ml catalase or 75 μM genistein, and immunostained with an anti-phospho-ERK2 antibody. Figure 38*A* presents a typical immunoblot. The dark band in each lane represents phosphorylated ERK2 (p42), the activated form of ERK2. The band intensity is significantly increased when import cocktail is pretreated with 1 mM H_2O_2 for 60 minutes at 37°C compared to control. Conversely, inclusion of either 0.3 mg/ml catalase or 75 μM genistein during the pretreatment protocol is able to reverse this enhancement. The densitometric band intensity results for three experiments were quantified and are shown in Figure 38*B*.

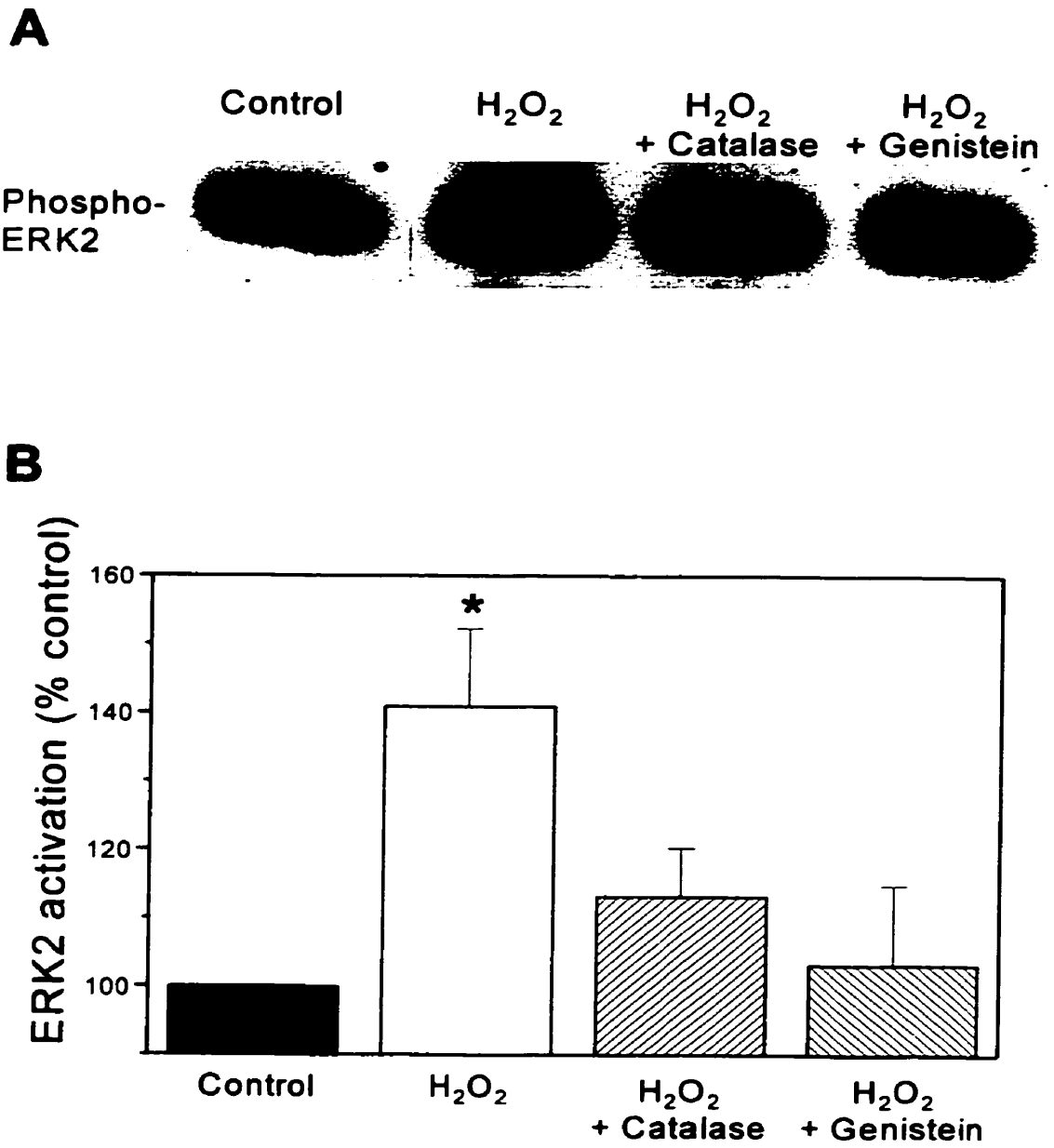

Figure 38. Activation of MAP kinase ERK2 in H_2O_2 treated import cocktail

Import cocktail was treated with 1 mM H_2O_2 for 60 minutes at 37°C, plus either 0.3 mg/ml catalase or 45 minute pretreatment with 75 μM genistein. Panel *A* shows representative bands obtained by western blotting as described in Methods. Panel *B* is the densitometric data obtained from the bands in panel *A*, normalized to controls. Error bars represent SEM for 3 separate experiments. *$p<0.05$ vs. control.

To investigate whether ERK2 activation was coincidental with or causal for the alterations in import observed, import cocktail was pretreated with 20 μM PD98059, a specific inhibitor for the ERK2 activator MEK1, as described in Methods. The inhibition of nuclear protein import by 1 mM H_2O_2 was completely abolished by PD98059 (Figure 39). Treatment of import cocktail with PD98059 alone had no effect on import (Figure 39). Furthermore, treatment of import cocktail with 40 ng/ml activated ERK2 (i.e. phosphorylated ERK2) for 60 minutes at 37°C reduced nuclear import to ~57% of control (Figure 40), similar to levels obtained with 1 mM H_2O_2 (Figure 34*E*). Identical treatment with 40 ng/ml non-activated ERK2, or with 40 ng/ml activated ERK2 that had been inactivated by boiling for 20 minutes, had no effect on import (Figure 40).

d. H_2O_2 Affects Ran Localization and GTP Binding

The GTPase Ran is a required cofactor for nuclear protein import (see Review of Literature, Section A.II.1.b.iv). Interference with GTP hydrolysis by Ran, either by using non-hydrolyzable GTP analogs or by removing the Ran GTPase activating protein RanGAP1, inhibits import (16, 302), although it has been shown that hydrolysis of GTP by Ran is not strictly required for import to occur (306). Rather, Ran appears to be important for proper cycling of import factors between the cytoplasm and nucleus. The cycling of Ran between a GTP and GDP bound state therefore appears to play a permissive role for import to occur. It was important, therefore, to examine the possibility that H_2O_2 and ERK2 activation may affect nucleocytoplasmic cycling of Ran.

Localization of Ran in rabbit aortic smooth muscle cells was examined by staining with anti-Ran antibodies. Control cells exhibited high nuclear staining with low levels in

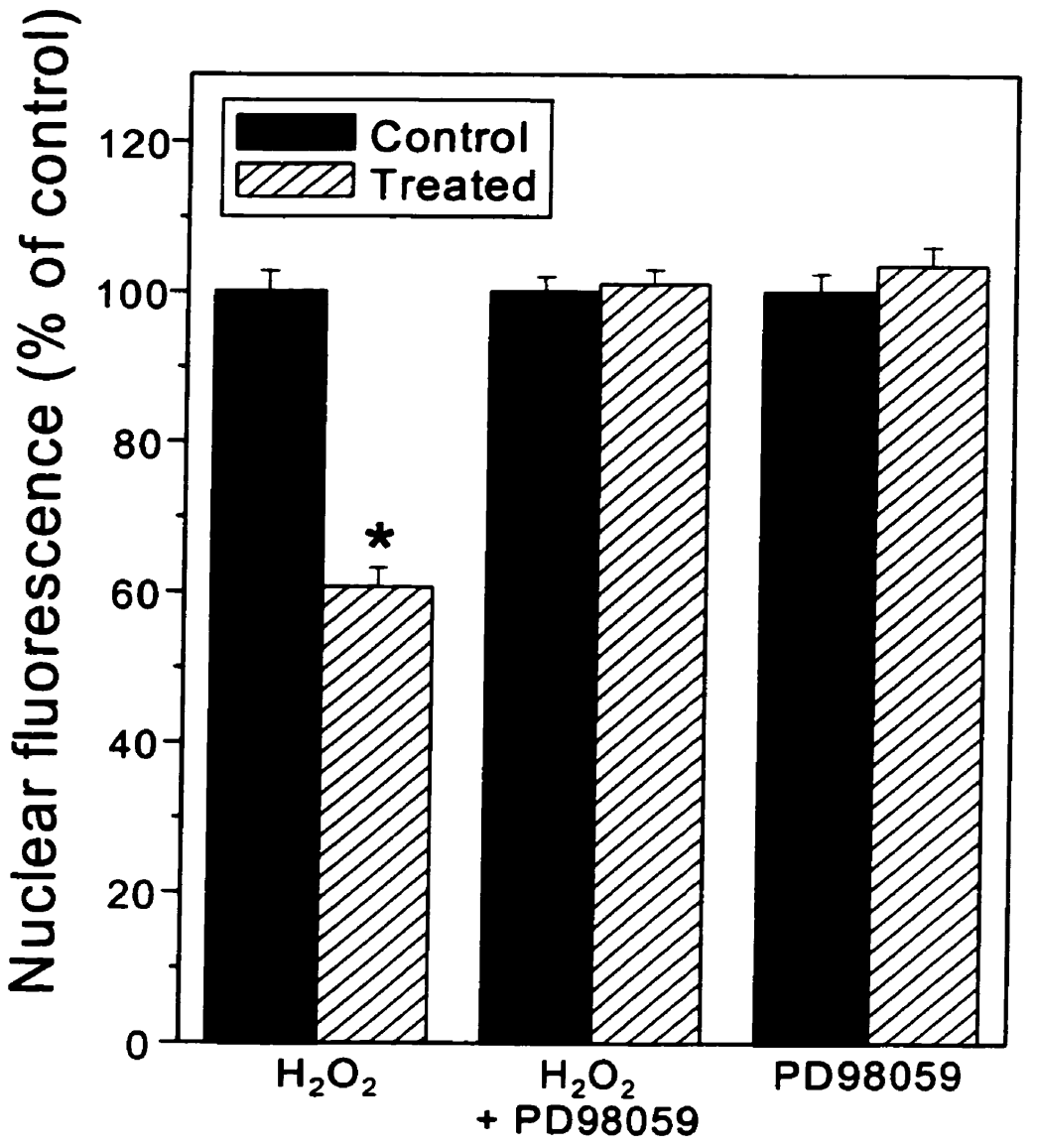

Figure 39. Inhibition of ERK2 activation attenuates the effect of H_2O_2

Import cocktail was untreated (controls), or treated with 1 mM H_2O_2 plus 20 μM PD98059 or 20 μM PD98059 alone for 60 minutes at 37°C prior to import assay. Error bars represent SEM for 61 to 160 cells in 3 or 4 separate assays. *$p<0.05$ vs. control.

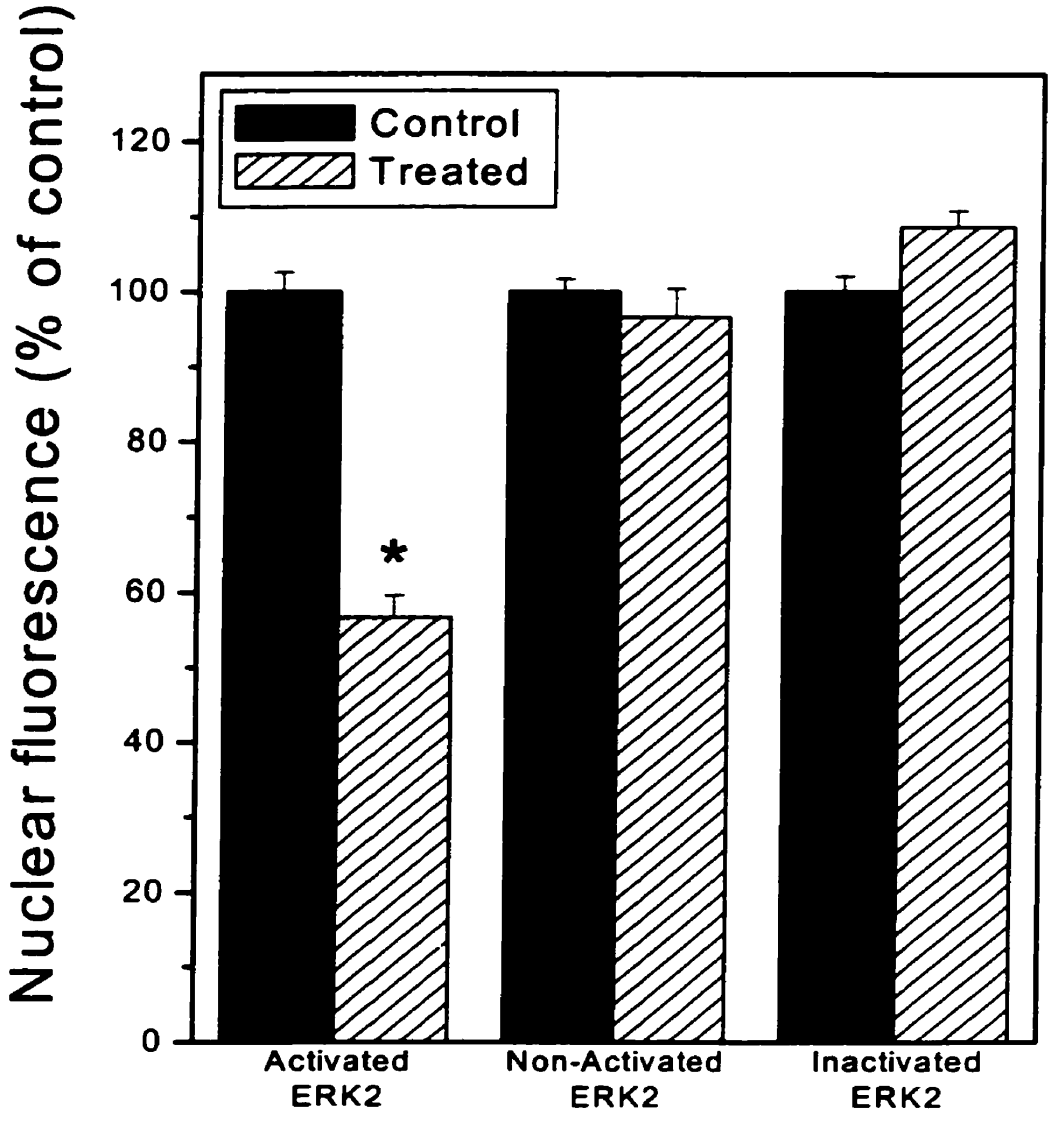

Figure 40. Exogenous activated ERK2 specifically mimics the effect of H_2O_2

Import cocktail was untreated (controls), or treated with 40 ng/ml activated ERK2 for 60 minutes at 37°C prior to import assay. Import cocktail was also treated for 60 minutes at 37°C with 40 ng/ml non-activated ERK2 or 40 ng/ml activated ERK2 that had been boiled for 20 minutes, then used in import assays. Error bars represent SEM for 60 to 109 cells in 3 or 4 separate assays. *$p<0.05$ vs. control.

the cytoplasm (Figure 41*A-C*). Upon treatment with 1 mM H_2O_2 for 60 minutes at 37°C, however, a distinct increase in cytoplasmic fluorescence is observed (Figure 41*D-F*). This rise in cytosolic Ran could be attenuated by either 0.3 mg/ml catalase (Figure 41*G-I*) or 20 μM PD98059 (Figure 41*J-L*). Quantification of fluorescence levels revealed that H_2O_2 treatment nearly doubled the Ran signal in the cytoplasm (Figure 42). While catalase and PD98059 were unable to completely restore control levels of cytoplasmic Ran, they did cause a significant decrease in cytoplasmic Ran compared to H_2O_2 treated cells.

The degree of GTP versus GDP binding to Ran was examined using an immunoprecipitation technique as described in Methods. Treatment of rabbit aortic smooth muscle cells with 1 mM H_2O_2 for 60 minutes caused a greater than five-fold increase compared to control in the amount of GTP bound to Ran relative to the entire pool of Ran (Figure 43). This effect could be attenuated by pretreatment of import cocktail with 20 μM PD98059 for 45 minutes.

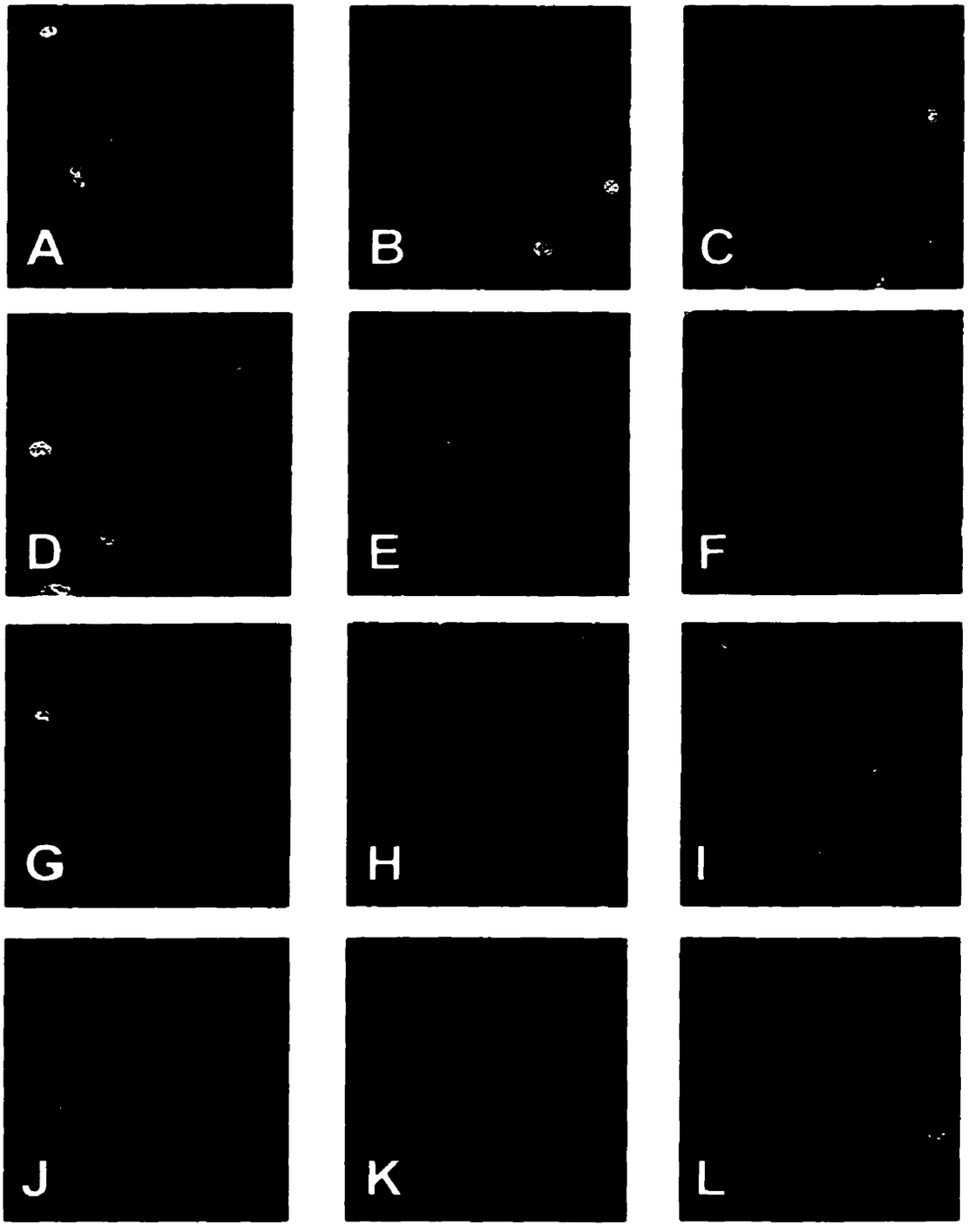

Figure 41. H_2O_2 causes Ran translocation to the cytosol

Rabbit aortic smooth muscle cells were treated with 1 mM H_2O_2 with or without either 0.3 mg/ml catalase or 20 μM PD98059 as described in Methods, then visualized by anti-Ran immunolabeling. Panels *A-C* represent control cells, *D-F* are H_2O_2 treated cells, *G-I* are treated with catalase and H_2O_2, and *J-L* are treated with PD98059 and H_2O_2. These figures are representative of three separate experiments.

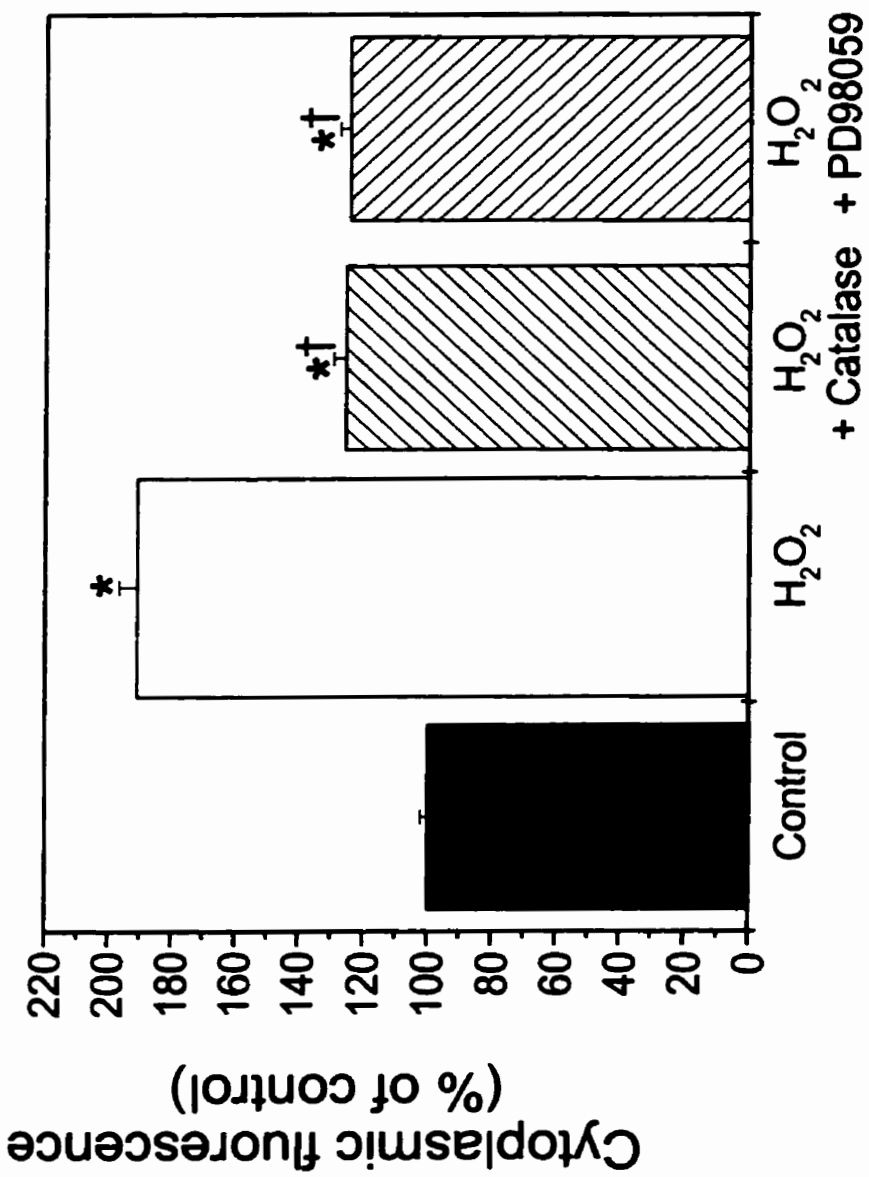

Figure 42. Quantification of cytoplasmic Ran pooling in response to H_2O_2

Quantitative analysis of panels *A-L* in Figure 41. Error bars represent SEM for 3 separate experiments. *p<0.05 vs. control, †p<0.05 vs. H_2O_2-treated.

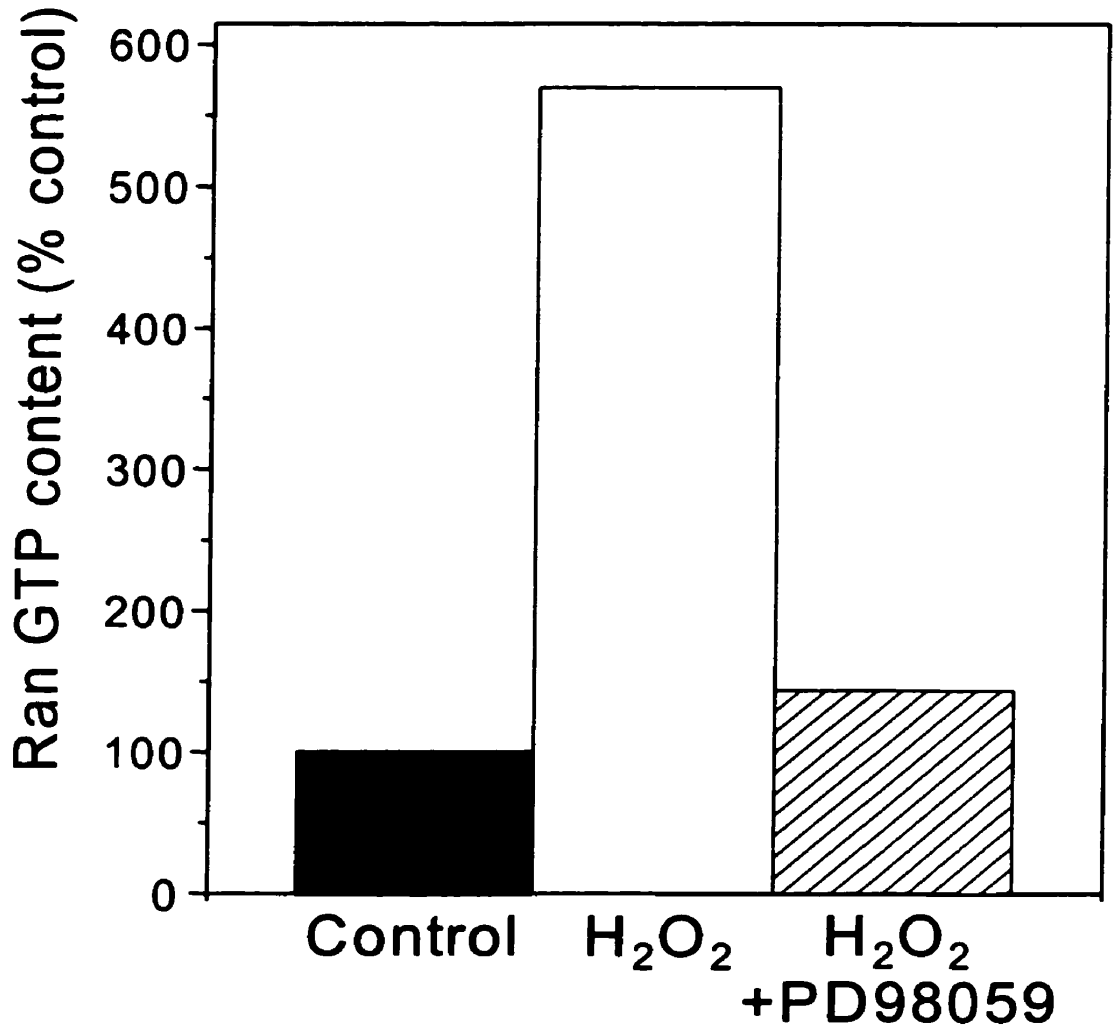

Figure 43. Quantification of GTP binding to Ran in response to H_2O_2

^{32}P-labeled Ran was immunoprecipitated from whole smooth muscle cells that had been treated with H_2O_2 with or without 20 μM PD98059 as described in Methods. GTP and GDP were eluted from the immunoprecipitate, separated by TLC and quantified by liquid scintillation counting. Results were expressed as GTP-bound Ran as a percentage of total Ran and normalized to controls.

F. DISCUSSION

I. Identification and Localization of Calcium-Binding Proteins in the Nucleus

This study putatively identified seven major calcium-binding proteins: three of molecular masses 120, 110 and 93 kDa in rat hepatic nuclei, and four of molecular masses 110, 93, 55 and 35 kDa in pig cardiac nuclei. Several minor calcium-binding proteins were also seen. A number of these proteins are present in small proportion when compared to overall protein content of the nuclei, and thus are not visible in preparations of intact nuclei. It is only with fractionation and processing of the nuclei that some of these proteins become observable due to the relative enrichment of proteins in both nuclear fractions that occurs during the purification procedure (see Figures 7-10).

The present study employed the dye Stains-All to identify calcium-binding proteins. This dye has been used by others for similar purposes (58, 59, 114, 224). Stains-All is not a direct indicator of calcium binding, however blue-staining proteins contain acidic moieties and therefore may contain potential calcium binding sites (59). In the present study, all of the major calcium binding proteins that were observed stained blue except the pig cardiac 93 kDa protein, which was observed to stain variously blue or red. Several minor calcium binding proteins stained red. This is not surprising since the color that a calcium binding protein will stain seems to depend on the relative number of calcium binding sites in the protein. Previous work has shown that troponin C and calmodulin, which each have about one Ca^{2+} binding site per 40 amino acid residues, stain blue with Stains-All (59). In contrast, the $(Ca^{2+}+ Mg^{2+})$-ATPase has only one Ca^{2+} binding site per 500 amino acid residues and stains red with Stains-All (59). Also, not all blue-staining bands bound calcium in our experiments. This is most likely because other acidic proteins

such as phosphoproteins and sialoproteins may stain blue (59). Thus, the use of Stains-All as a preliminary test for the presence of calcium binding proteins was a valuable aid in the initial screening stages of this study, but was used with full knowledge of its limitations. The use of $^{45}Ca^{2+}$ overlays to identify calcium binding proteins has been demonstrated previously (68, 114, 209, 341), and in this study complemented the Stains-All work by positively determining the presence of calcium binding proteins.

A caveat to the use of $^{45}Ca^{2+}$ overlays to identify calcium-binding proteins is that the use of SDS to equalize charges on proteins during electrophoresis also denatures these proteins to various degrees. Partial renaturation may occur during electroblotting, however, it is nonetheless possible that some calcium-binding motifs may be lost. Therefore, it is likely that this technique under-reports the number of calcium-binding proteins in a given sample. Furthermore, the description of calcium-binding proteins as "major" or "minor" must be used with caution, since the true binding capacities of these proteins *in vivo* may be altered by denaturation. True binding capacity should be determined using binding assays on purified proteins. Despite this concern, however, the original paper describing the use of $^{45}Ca^{2+}$ overlays showed that many well-characterized calcium-binding proteins retain the ability to bind calcium following electrophoresis and electroblotting, and may even retain catalytic activity (209). This technique, therefore, is still very useful for surveying calcium-binding proteins, but should be used with full consideration of the potential drawbacks.

The actual identities of the calcium binding proteins reported here remain to be determined. However, candidates do exist. The p93 protein in hepatic nuclei has been previously identified as calnexin (114). It appears likely that the p93 protein in the

cardiac nuclear envelope fraction is also calnexin due to its identical molecular mass, similar affinity for both Stains-All and calcium (see Figures 7-10; also see Gilchrist and Pierce (114)), and the observation that the protein localizes to the same nuclear fraction in both tissues. The p55 protein observed in the cardiac nucleoplasmic fraction appears to be calsequestrin, since this protein has an apparent molecular mass on electrophoresis near 55 kDa (58, 60), both have similar affinities to calcium (68, 341), and both stain blue with Stains-All (58-60). More conclusively, however, antibodies to cardiac calsequestrin were observed to bind specifically to a band of approximately 55 kDa in the cardiac high salt supernatant fraction on immunolabeled western blots (see Figure 11). The identities of the other calcium binding proteins are not yet known, although the possibility that the 110 kDa protein is the Ca^{2+} ATPase seems unlikely, since the ATPase stains bright red with Stains-All (59), but the 110 kDa protein clearly stained blue (Figure 8). The other calcium-binding proteins identified in this study do not appear to correspond to previously identified nuclear calcium-binding proteins, and may in fact be novel proteins whose characteristics remain to be defined.

The roles of these calcium-binding proteins also remain unknown, however it is possible to speculate on the physiological role of at least one of them. Calnexin was previously identified in hepatic nuclei (114). The finding of calnexin in the nuclei of two cell types is particularly interesting in light of its role as a molecular chaperone (155, 274). Calnexin could carry out a similar function for nuclear proteins. This is speculative at this time and will require future investigation. It is important to note that calnexin has a putative nuclear localization sequence (345), reinforcing the concept that calnexin has a role to play in the nucleus as well as the endoplasmic reticulum. Assigning functions at

this time for the other observed calcium binding proteins is not yet possible. However, if p55 is calsequestrin, it may function as a calcium sink for the nucleus in a similar fashion to its role in the sarcoplasmic reticulum, since it is a high-capacity, low-affinity calcium-binding protein (198). In light of the evidence for calcium gradients in the nucleus (136, 139, 269, 355), this would be a logical hypothesis to build upon. The roles of the other proteins (p110, p120 and those in the 28-35 kDa range) remain to be elucidated. Whether these proteins are involved in nuclear calcium homeostasis, or are regulatory proteins themselves regulated by calcium (e.g. calmodulin) are questions that may be answered after further characterization experiments. Furthermore, the precise spatial location of these proteins within the nucleus remains to be determined, which may also shed light on the roles of these proteins.

In summary, this is the first putative identification of the existence of calcium binding proteins in cardiac nuclei. This is also the first description of a full complement of calcium binding proteins in hepatic nuclei. Our work has further characterized for the first time that these calcium-binding proteins are partitioned into distinct nuclear compartments. This is an important preliminary step towards clarifying the function of this entire family of nuclear calcium binding proteins.

II. Altered Function of the Nuclear Nucleoside Triphosphatase in a Genetically Obese Animal Model

The data presented in this study reveal that there are age- and sex-related changes in nuclear NTPase activity in the JCR:LA-*cp* rat. While there are clearly differences in NTPase activity as a function of age in both males and females, lean and corpulent, there

does not appear to be a straightforward pattern to these changes. In contrast, there were striking sex-related differences between lean and corpulent NTPase activity. In general, corpulent females exhibited significantly increased NTPase activity compared with leans under nearly all assay conditions. In contrast, corpulent males showed only isolated differences versus lean animals. These findings are mirrored in the V_{max} values obtained (Table 5), which are significantly increased for all groups of corpulent females, while there are no changes in the V_{max} values obtained for the corpulent males, with the exception of 6 month males using GTP as substrate. Similarly, K_M values were increased for nearly all of the corpulent female groups, but K_M was only increased for the 6 month corpulent males with GTP as substrate. The overall increase in both V_{max} and K_M in corpulent females suggests that while the turnover rate of the NTPase is increased, the affinity of the enzyme for substrate is actually decreased.

In order to gain insight into factors responsible for the changes observed in NTPase activity, we examined the lipid status of these animals. The greater VLDL hyperlipidemia of the female reflects increased numbers of VLDL particles with additional cholesteryl esters and phospholipids over the males (93). Since serum lipid levels were increased in the corpulent animals compared to the lean animals, nuclear lipid content was examined to determine if it had been altered. These data reveal a striking sexual dimorphism (Table 6). Both nuclear membrane phospholipids and cholesterol were significantly increased in corpulent females compared to age-matched leans. In contrast, there were no differences observed between lean and corpulent males for either lipid species. It is interesting to note that nuclear phospholipid content in the corpulent females remained constantly elevated at ~150% of the lean values.

A potential candidate to have modulatory influence on NTPase activity, therefore, is nuclear membrane phospholipid content. It is possible that changes in phospholipid content may have a modulating influence on NTPase activity by altering membrane fluidity, since altered membrane fluidity may affect the activities of embedded enzymes (313). However, alterations in nuclear membrane phospholipid content are not likely to be responsible for the overt changes in NTPase activity observed in the corpulent female rat. It has been shown previously that removal of up to 80% of membrane phospholipids could be carried out without altering NTPase activity (319). The present study did not, however, examine whether changes occurred in the types of phospholipids present in the nuclear membrane, or whether changes were associated with the inner versus the outer nuclear membrane. Previous studies have suggested that changes in the specific phospholipid composition of the nuclear membrane may result in alterations of NTPase activity (343, 344).

Another candidate factor for modulating nuclear NTPase activity is the membrane cholesterol content. The percent increase of nuclear membrane cholesterol content for corpulent females over leans rose linearly with age from ~140% at 3 months to ~366% at 9 months. An increased nuclear membrane NTPase activity was observed in all of these three groups. Conversely, there were only sporadic alterations in NTPase activity in the various male groups, and nuclear cholesterol content was unchanged (Table 6). This presents strong indirect evidence by association that cholesterol may be a causal factor in the increased NTPase activity. When taken together with previous work using cholesterol-enriched liposomes to modulate nuclear membrane cholesterol content and stimulate NTPase activity (275), our data convincingly implicate cholesterol as an

important modulatory factor in NTPase activity, although other factors may have a bearing on the alterations of NTPase activity observed in this study.

The primary difference observed in the present study between the corpulent and lean rats is the sexual dimorphism with respect to the NTPase activity. Thus, it is possible that sex hormones may play a modulatory role in NTPase activity. A precedent does exist for hormonal stimulation of the NTPase. Human chorionic gonadotropin and human luteinizing hormone have both been shown to directly stimulate NTPase in human ovarian nuclear membranes (336). If specific sex hormones are disrupted by the corpulent condition in the female rats, this may explain some of the changes observed. Studies on castrated male and female JCR:LA corpulent rats have revealed that sex hormones play an important role in regulation of lipid metabolism in these animals. Castrated male rats exhibited a doubling of serum triglyceride levels, while castrated females showed approximately halved triglyceride levels (293). Interestingly, however, castration of animals of either sex does not alter the numbers of ischemic lesions observed, suggesting that sex hormones (i.e. testosterone and estrogen) are not determinants of disease in this model (293). In other studies, it has been shown that male and female JCR:LA-*cp* corpulent rats metabolize fatty acids differently (295). Venkatraman and co-workers have demonstrated that altering the intake of various fatty acids by dietary modification can alter NTPase activity (343, 344), therefore this is another possible modulatory influence on NTPase activity.

Another consequence of the altered nuclear membrane lipid environment is a decrease in integrity of the nuclei (Table 7). Only the nuclei from the corpulent female animals show a decrease in membrane integrity, paralleling the changes observed in

nuclear membrane cholesterol content. This data, along with the findings of decreased membrane integrity in cholesterol-enriched nuclei (Figure 25), strongly implicate cholesterol as a major determinant of nuclear membrane integrity (275). This effect may be due to a decrease in membrane fluidity and disorder resulting from increased cholesterol content (313). Conversely, when cholesterol in the nuclear membrane is oxidized by cholesterol oxidase, which would tend to increase membrane fluidity and disorder, the NTPase is inhibited (276).

When examined by transmission electron microscopy, the hepatocytes (including the nucleus) of the 6 month old corpulent female JCR:LA-*cp* rats exhibited bizarre lipid body inclusions (Figures 27 and 28). This finding suggests that there may be pathological morphological alterations in these animals, and together with the NTPase activity results and nuclear integrity data, demonstrates that changes have occurred in the structure and function of the nuclear membrane in the corpulent female animals.

In conclusion, this study has demonstrated the presence of age- and sex-related differences in NTPase activity in the JCR:LA-*cp* corpulent rat model. Our data strongly suggest that these changes arise from alterations in nuclear cholesterol composition, which in turn may arise from differential lipid metabolism and serum lipid profiles in the male and female corpulent versus lean rats. These changes in nuclear cholesterol composition may, in turn, alter nuclear integrity and the functioning of the NTPase. It is intriguing to speculate about the potential effects of modifying nuclear NTPase activity on nucleocytoplasmic trafficking of mRNA (5, 7, 8, 77, 78, 303, 305, 343). Other factors, however, may also play a role in the activity of the NTPase in this animal model. This

study has also broadened our current understanding of factors that influence the structure and function of the nuclear envelope.

III. Inhibition of Nuclear Protein Import by Hydrogen Peroxide

This study is the first characterization of nuclear protein import in aortic vascular smooth muscle cells, and the first report that nuclear protein import is inhibited by hydrogen peroxide in any cell type. Theoretically, H_2O_2 may alter nucleocytoplasmic transport through an effect on a cytoplasmic factor or an action on the nuclear pore complex itself. To determine whether H_2O_2 could exert its effects on import by attacking the nuclear pore complex or nuclear membrane, permeablized smooth muscle cells were pretreated with 1 mM H_2O_2 prior to import assay. No effect was observed when the permeablized cells were treated with H_2O_2 (Figure 36). However, the same concentration of H_2O_2 resulted in a large decrease in import when the import cocktail was treated (Figure 34*E*). These data suggest that H_2O_2 can affect cytosolic factors found in the import cocktail, but not the pore complex itself.

One potential mechanism for the action of H_2O_2 on import is that it may cause oxidation of cytosolic factors required for import (e.g. the NLS receptor or other components of the import complex). To investigate this possibility, two free radical generating systems were used to treat either import cocktail or permeablized cells used in the import assay. Xanthine plus xanthine oxidase produces superoxide radicals, while free iron reacts quickly with H_2O_2 to produce hydroxyl radicals (53, 171, 173). In contrast to the findings with H_2O_2, pretreatment of the import cocktail with either free radical generating system had no effect on import (Figure 36). Increasing the time of

pretreatment with xanthine/xanthine oxidase to one hour still had no effect on import (results not shown). Conversely, when permeablized cells were pretreated with either free radical generating system, import was significantly inhibited (Figure 36). Together these data reveal that H_2O_2 exerts its effect on import using a completely different mechanism than superoxide or hydroxyl radicals, and suggest that oxidation is not involved. They also demonstrate that oxidation of cell structural components including the nuclear pore complex can significantly depress nuclear protein import.

Hydrogen peroxide has been shown to activate the MAP kinase ERK2 in vascular smooth muscle (61, 128, 189, 277) and cardiomyocytes (297). It can also activate other signal transduction pathways, such as the JNK pathway (191). We investigated whether H_2O_2-induced ERK2 activation may play a role in the H_2O_2-induced inhibition of import. When import cocktail was treated prior to H_2O_2 exposure with genistein, an inhibitor of tyrosine kinase-mediated phosphorylation, import was attenuated to levels similar to those obtained with catalase treatment (Figure 37). Daidzein, the inactive analog of genistein, exhibited no effect. Genistein or daidzein alone had no effect on import. H_2O_2 activated ERK2 as shown by western blotting, an effect which could be reversed by catalase or genistein (Figure 38). Together, these data implicate ERK2 as a mediator of nuclear protein import inhibition by H_2O_2. These results also explain why treatment of permeablized cells with H_2O_2 did not affect import, since the H_2O_2 would have been washed away before the import cocktail was applied to complete the assay, and therefore would be unavailable to affect ERK2.

To further investigate the role of ERK2 in inhibition of import, import cocktail was also pretreated with 20 μM PD98059 prior to H_2O_2 treatment. This compound blocks

MEK1, a protein kinase immediately upstream to ERK2 in the MAP kinase signal cascade and a direct activator of ERK2. Like genistein, PD98059 was able to reverse the effects of H_2O_2 on import. However, unlike genistein, PD98059 completely normalized import to control values (Figure 39). It therefore appears that, while ERK2 does mediate the effect of H_2O_2 in inhibiting import, H_2O_2 exerts its primary effect further up the signal cascade. If H_2O_2 activated ERK2 directly, PD98059 would not be expected to have an effect on reversing H_2O_2-induced inhibition of import. Rao has shown that H_2O_2 treatment of intact vascular smooth muscle cells induces SHC-Grb2-SOS complex formation with EGF receptor tyrosine kinase (277). This process leads to activation of Ras, which presumably would lead to activation of the entire MAP kinase cascade leading to ERK2, which was also observed to be activated in Rao's study. It is likely that in our experiments, a similar process is occurring. However, since the import cocktail is devoid of plasma membrane, the involvement of receptor tyrosine kinases is unlikely. H_2O_2 must be exerting its effect, therefore, on another stage of the MAP kinase signaling cascade or on cytosolic tyrosine kinases, although the exact primary target remains unidentified. Clerk *et al.* have suggested the possibility that H_2O_2 may inactivate a phosphatase higher up in the ERK2 signaling pathway, resulting in activation of MAP kinases (80).

Additional evidence to support the role of ERK2 is shown in Figure 40. Treating import cocktail with an activated form of ERK2 alone results in a significant inhibition of nuclear protein import. This effect is similar in magnitude to the inhibition of import observed by treatment with the highest concentrations of H_2O_2 used in this study. Non-activated ERK2, or activated ERK2 that has been inactivated by boiling, do not inhibit

import (Figure 40). Combined with the results discussed above, it appears that the level of activation of ERK2 determines inhibition of nuclear protein import.

The ultimate downstream target of ERK2 activation that affects nuclear protein import is unclear. Phosphorylation of the import substrate is not responsible, since the custom NLS used in this study lacks upstream phosphorylation sites. The nuclear pore complex is also not responsible, since H_2O_2 treatment of permeablized cells had no effect on import (Figure 36). One possibility is suggested by the homology between the signal-transducing GTPase Ras and Ran, the Ras-related GTPase required for protein import (96). Rao's study of the effect of H_2O_2 on the MAPK cascade reported that after exposure to H_2O_2, Ras shifted to a predominantly GTP-bound conformation in response to upstream signals (277). At the same time, it has been reported that extranuclear Ran may exert inhibitory effects on nuclear protein import when its GTP-bound conformation is favored, by disrupting the complex formed between NLS-containing proteins and the importin complex (16, 237, 302, 306).

Since antibodies are not available that differentiate between GTP- and GDP-bound Ran, we first examined total Ran localization by immunocytochemistry. H_2O_2 treatment caused an increase in cytosolic Ran, an effect largely reversible by catalase or PD98059 (Figures 41 and 42). The amount of GTP compared to GDP bound to Ran was then determined. In control cells, the vast majority of Ran is bound to GDP. A large increase in GTP binding occurs when the cells are treated with H_2O_2 (Figure 43), an effect reversible by PD98059. This increase in GTP-bound Ran, taken together with the observed increase in cytosolic Ran, suggests that GTP-bound Ran in the cytosol is stabilized after H_2O_2 treatment. Alternatively, GTP-bound Ran may move out of the

nucleus in response to H_2O_2 treatment and be retained in the cytoplasm. A third possibility is that H_2O_2 interferes with the action of RanGAP1, the cytosolic GTPase activating protein that catalyzes GTP hydrolysis by Ran. A diagram of the potential mechanism of interaction between the ERK2 signaling pathway and nuclear protein import following this third scenario is pictured in Figure 44. Although GTP hydrolysis by Ran appears to be unnecessary for import to occur (306), it does appear to be critical for proper cycling of import factors out of the nucleus. The increase we observed in cytosolic Ran in response to H_2O_2 may be indicative of altered cycling. In any of these scenarios, GTP-bound Ran would then disrupt the formation of the import complex and lead to inhibition of import as described above. It is unlikely that RanGEF (RCC1) is the eventual target of H_2O_2 treatment or ERK2 activation since RanGEF is found predominantly in the nucleus, while our experiments used isolated cell cytosol in the import cocktail.

In both physiological and pathological situations, there may be constant, long-term generation of H_2O_2. Our results demonstrate that even low concentrations of H_2O_2 acting over longer periods of time can progressively inhibit import (Figure 35). This finding is of particular importance in the atherogenic vascular intima, in which infiltrating macrophages and monocytes may be a constant source of H_2O_2 production (254). Since H_2O_2 readily crosses cell membranes (130), it is free to move throughout the intima and affect cells distal to the site of H_2O_2 production. The half-life of H_2O_2 in complex aqueous solutions can be quite short (on the order of minutes (26, 149)) due to spontaneous break-down and endogenous scavenging. Both are relevant under our experimental conditions. We used higher doses of H_2O_2 (1 mM) over the course of one

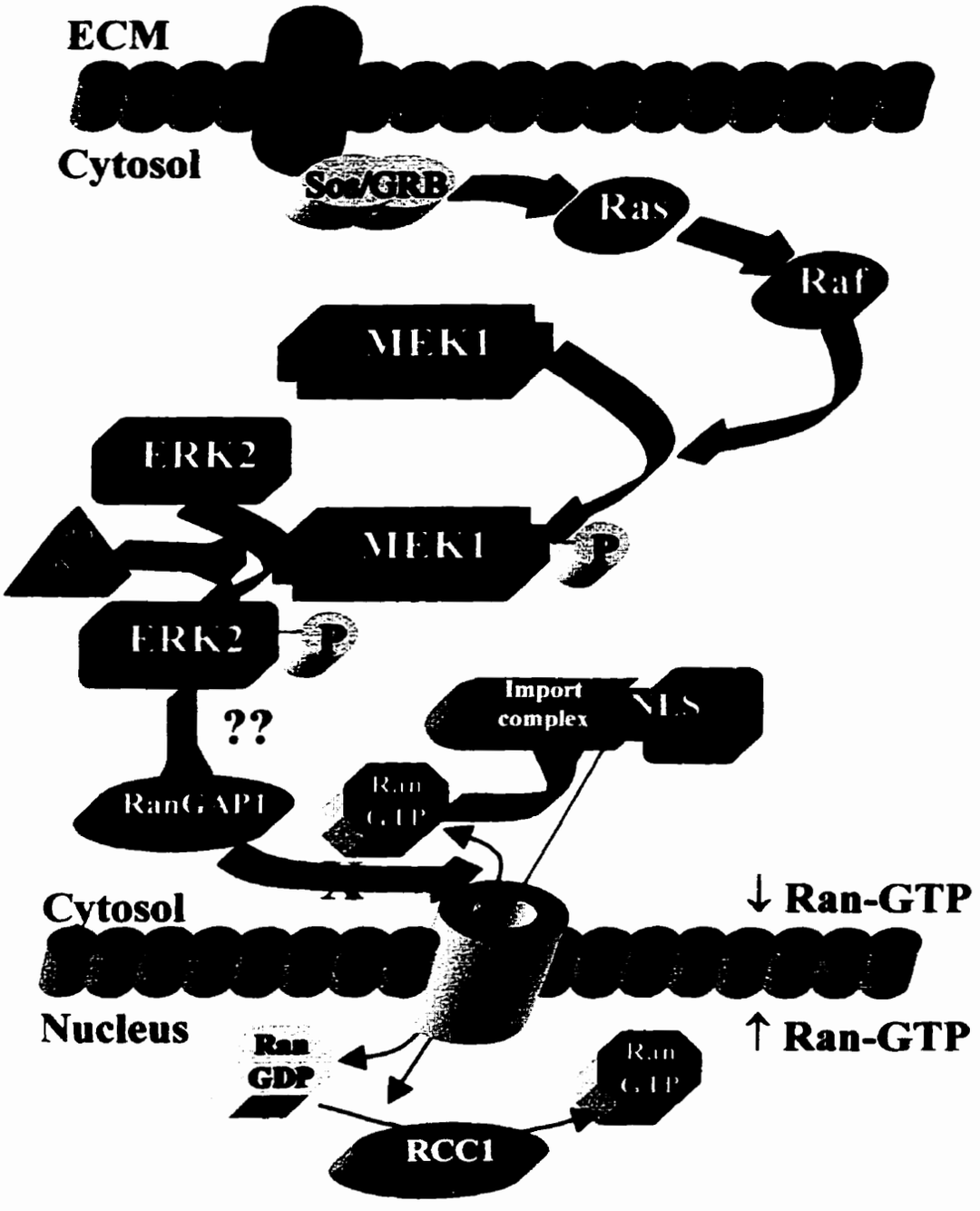

Figure 44. Potential scheme of interaction between the ERK2 pathway and import

Question marks denote possible site of interaction between ERK2 pathway and nuclear protein import mechanism, at RanGAP1. Red inverse arrows indicate inhibitory interactions. Green arrows indicate stimulatory interactions. Red "X" denotes inhibition of the effect of RanGAP1 on RanGTP hydrolysis.

hour exposures for some of the experiments. This approach appears justified, since exogenously added ERK2 closely mimicked the highest concentration of H_2O_2 used in this study with regard to import inhibition (Figure 40). The LD_{50} for H_2O_2 in PC12 cells is reported to be 350 μM, and at 750 μM H_2O_2 there is still significant cell survival (128). These levels are similar to those used in our study. Moreover, since permeablized cells or cell cytosol was used throughout the study, toxicity was not an issue.

Our results have important physiological and pathological significance. Physiologically, it has been suggested that H_2O_2 is required for signal transduction in response to PDGF or angiotensin II in vascular smooth muscle (331, 360). To mimic the effects of PDGF, 0.1 to 1.0 mM exogenous H_2O_2 was required, the same range as that used in this study (331). It has also been suggested recently that H_2O_2 may itself be a second messenger, similar to the role played by nitric oxide (126). This role would be entirely consistent with the findings reported in the present study. The respiratory burst of monocytes and macrophages during microbial killing releases significant amounts of activated oxygen species, including H_2O_2 (18). Activated oxygen species are also produced as the result of the normal leakage of electrons out of mitochondrial electron transport chains (45).

Pathologically, H_2O_2 is generated in cells during ischemia (27, 53, 171, 173, 342). Hyslop *et al.* have reported striatal [H_2O_2] well above 150 μM during global forebrain ischemia in the rat (149). Activated oxygen species including H_2O_2 also play a significant role in atherogenesis by stimulating oxidation of lipoproteins and proliferation of smooth muscle cells. These species are produced by macrophages and monocytes infiltrating the vascular intima, as well as by endothelial and smooth muscle cells themselves (234, 254).

The actual effects of H_2O_2 on smooth muscle are somewhat controversial. H_2O_2 has been demonstrated to cause both smooth muscle proliferation and apoptosis (1, 61, 189, 360), and in both situations is associated with DNA synthesis and ERK2 activation (61, 104, 189). Recent evidence supports the hypothesis that H_2O_2 may be a key modulator of smooth muscle cell survival and proliferation (47). The critical event which determines whether the cell proliferates or dies after H_2O_2 exposure is unknown, but may depend on whether exposure is acute or tonic, since DNA synthesis has been hypothesized to depend on how long ERK2 remains activated (337). ERK2, on activation, translocates to the nucleus via an NLS-independent pathway (110, 359). In the nucleus, ERK2 activates mRNA transcription of a number of transcription factors, including c-*fos*, c-*jun* and *fra-1* (128, 189, 362). Our data show that ERK2 inhibits NLS-dependent nuclear protein import. This may explain how smooth muscle becomes apoptotic concomitant with activation of ERK2: critical growth signals may be prevented from entering the nucleus due to import inhibition, while ERK2 is still able to gain entry to the nucleus via the alternate pathway. This hypothesis is also consistent with previous findings that reduction of nuclear import is associated with cell quiescence (101, 102), which are confirmed by our data showing inhibition of import in quiescent versus proliferating smooth muscle cells (Figures 32 and 33). Our data are not consistent with the pro-growth effects of H_2O_2, although we cannot rule out the possibility that import inhibition prevents growth repressors from entering the nucleus and inhibiting transcription of critical genes. Further work in these areas is necessary.

In summary, this is the first demonstration that activated ERK2 is able to inhibit NLS-dependent nuclear protein import, thus connecting intracellular signaling pathways

with the process of nuclear protein import. H_2O_2 inhibits nuclear protein import in a dose- and time-dependent manner by activation of ERK2. Similar exposure of intact cells to H_2O_2 alters the distribution of Ran between the nucleus and cytosol. Superoxide and hydroxyl radicals are able to inhibit nuclear import by interaction with nuclear structures, but do not mimic the effects of H_2O_2. The data are particularly significant in situations where H_2O_2 is produced at high levels or over long periods of time, such as during ischemia or atherogenesis. It is unclear whether these findings apply only to SV40 NLS-mediated import, or to import in general. However, this study does demonstrate proof of concept and indicates that further studies in this area are warranted. The finding that ERK2 activation affects nuclear protein import has implications for studies of cell proliferation, angiogenesis, hypertrophy, and diseases such as cancer and diabetes.

G. REFERENCES

1. **Abe, M.K., T.-S.O. Chao, J. Solway, M.R. Rosner, and M.B. Hershenson.** Hydrogen peroxide stimulates mitogen-activated protein kinase in bovine tracheal myocytes: implications for human airway disease. *Am J Respir Cell Mol Biol* **11:** 577-585, 1994.

2. **Adam, E.J.H., and S.A. Adam.** Identification of cytosolic factors required for nuclear location sequence-mediated binding to the nuclear envelope. *J Cell Biol* **125:** 547-555, 1994.

3. **Adam, S.A.** Transport pathways of macromolecules between the nucleus and the cytoplasm. *Curr Opin Cell Biol* **11:** 402-406, 1999.

4. **Adam, S.A., R. Sterne-Marr, and L. Gerace.** *In vitro* nuclear protein import using permeablized mammalian cells. *Meth Cell Biol* **35:** 469-482, 1991.

5. **Agutter, P.S.** Influence of nucleotides, cations and nucleoside triphosphatase inhibitors on the release of ribonucleic acid from isolated rat liver nuclei. *Biochem J* **188:** 91-97, 1980.

6. **Agutter, P.S., H.J. McArdle, and B. McCaldin.** Evidence for involvement of nuclear envelope nucleoside triphosphatase in nucleocytoplasmic translocation of ribonucleoprotein. *Nature* **263:** 165-167, 1976.

7. **Agutter, P.S., B. McCaldin, and H.J. McArdle.** Importance of mammalian nuclear-envelope nucleoside triphosphatase in nucleo-cytoplasmic transport of ribonucleoproteins. *Biochem J* **182:** 811-819, 1979.

8. **Agutter, P.S., and D. Prochnow.** Nucleocytoplasmic transport. *Biochem J* **300:** 609-618, 1994.

9. **Aitchison, J.D., M.P. Rout, M. Marelli, G. Blobel, and R.W. Wozniak.** Two novel related yeast nucleoporins Nup170p and Nup157p - complementation with the vertebrate homologue Nup155p and functional interactions with the yeast nuclear pore-membrane protein Pom152p. *J Cell Biol* **131:** 1133-1148, 1995.

10. **Akey, C.W.** Interactions and structure of the nuclear pore complex revealed by cryo-electron microscopy. *J Cell Biol* **109:** 955-970, 1989.

11. **Akey, C.W.** Visualization of transport-related configurations of the nuclear pore transporter. *Biophys J* **58:** 341-355, 1990.

12. **Akey, C.W., and M. Radermacher.** Architecture of the *Xenopus* nuclear pore complex revealed by three-dimensional cryo-electron microscopy. *J Cell Biol* **122:** 1-19, 1993.

13. **Allbritton, N.L., E. Oancea, M.A. Kuhn, and T. Meyer.** Source of nuclear calcium signals. *Proc Natl Acad Sci USA* **91:** 12458-12462, 1994.

14. **Al-Mohanna, F.A., K.W.T. Caddy, and S.R. Bolsover.** The nucleus is insulated from large cytosolic calcium ion changes. *Nature* **367:** 745-750, 1994.

15. **Arai, Y., F. Hosoda, H. Kobayashi, K. Arai, Y. Hayashi, K. Nanao, Y. Kaneko, and M. Ohki.** The inv(11)(p15q22) chromosome translocation of *de novo* and therapy-related myeloid malignancies results in fusion of the nucleoporin gene NUP98, with the putative RNA helicase gene, DDX10. *Blood* **89:** 3936-3944, 1997.

16. **Avis, J.M., and P.R. Clarke.** Ran, a GTPase involved in nuclear processes: its regulators and effectors. *J Cell Sci* **109:** 2423-2427, 1996.

17. **Azuma, Y., and M. Dasso.** The role of Ran in nuclear function. *Curr Opin Cell Biol* **12:** 302-307, 2000.

18. **Babior, B.M.** Oxygen-dependent microbial killing by phagocytes. *N Engl J Med* **298:** 659-668, 1978.

19. **Bachs, O., N. Agell, and E. Carafoli.** Calcium and calmodulin function in the cell nucleus. *Biochim Biophys Acta* **1113:** 259-270, 1992.

20. **Bachs, O., L. Lanini, J. Serratosa, M.J. Coll, R. Bastos, R. Aligué, E. Rius, and E. Carafoli.** Calmodulin-binding proteins in the nuclei of quiescent and proliferatively activated rat liver cells. *J Biol Chem* **265:** 18595-18600, 1990.

21. **Bading, H., D.D. Ginty, and M.E. Greenberg.** Regulation of gene expression in hippocampal neurons by distinct calcium signaling pathways. *Science* **260:** 181-186, 1993.

22. **Badminton, M.N., J.M. Kendall, C.M. Rembold, and A.K. Campbell.** Current evidence suggests independent regulation of nuclear calcium. *Cell Calcium* **23:** 79-86, 1998.

23. **Bailer, S.M., S. Siniossoglou, A. Podtelejnikov, A. Hellwig, M. Mann, and E. Hurt.** Nup116p and Nup100p are interchangeable through a conserved motif which constitutes a docking site for the mRNA transport factor Gle2p. *EMBO J* **17:** 1107-1119, 1998.

24. **Balke, C.W., and M.R. Gold.** Calcium channels in the heart: An overview. *Heart Dis Stroke* **1:** 398-403, 1992.

25. **Bangs, P.L., C.A. Sparks, P.R. Odgren, and E.G. Fey.** Product of the oncogene-activating gene *Tpr* is a phosphorylated protein of the nuclear pore complex. *J Cell Biochem* **61:** 48-60, 1996.

26. **Barnard, M.L., and S. Matalon.** Mechanisms of extracellular reactive oxygen species injury to the pulmonary microvasculature. *J Appl Physiol* **72:** 1724-1729, 1992.

27. **Bast, A., G.R.M.M. Haenen, and C.J.A. Doelman.** Oxidants and antioxidants: State of the art. *Am J Med* **91:** 2S-13S, 1991.

28. **Bastos, R., L. Ribas de Pouplana, M. Enarson, K. Bodoor, and B. Burke.** Nup84, a novel nucleoporin that is associated with CAN/Nup214 on the cytoplasmic face of the nuclear pore complex. *J Cell Biol* **137:** 989-1000, 1997.

29. **Bayliss, R., K. Ribbeck, D. Akin, H.M. Kent, C.M. Feldherr, D. Görlich, and M. Stewart.** Interaction between NTF2 and xFxFG-containing nucleoporins is required to mediate nuclear import of RanGDP. *J Mol Biol* **293:** 579-593, 1999.

30. **Becker, J., F. Melchior, V. Gerke, F.R. Bischoff, H. Ponstingl, and A. Wittinghofer.** RNA1 encodes a GTPase-activating protein specific for Gsp1p, the Ran/TC4 homologue of *Saccharomyces cerevisiae*. *J Biol Chem* **270:** 11860-11865, 1995.

31. **Belgareh, N., and V. Doye.** Dynamics of nuclear pore distribution in nucleoporin mutant yeast cells. *J Cell Biol* **136:** 747-759, 1997.

32. **Bentolila, L.A., M.F. d'Andon, Q.T. Nguyen, O. Martinez, F. Rougeon, and N. Doyen.** The two isoforms of mouse terminal deoxynucleotidyl transferase differ in both the ability to add N regions and subcellular localization. *EMBO J* **14:** 4221-4229, 1995.

33. **Bernd, A., H.C. Schroder, R.K. Zahn, and W.E. Muller.** Nuclear-envelope nucleoside triphosphatase: stimulation by poly(A) (+)mRNA and modulation by microtubule protein. *Aktuelle Gerontol* **13:** 119-121, 1983.

34. **Bischoff, F.R., H. Krebber, T. Kempf, I. Hermes, and H. Ponstingl.** Human RanGTPase-activating protein RanGAP1 is a homologue of yeast Rna1p involved in mRNA processing and transport. *Proc Natl Acad Sci USA* **92:** 1749-1753, 1995.

35. **Bischoff, F.R., H. Krebber, E. Smirnova, W. Dong, and H. Ponstingl.** Co-activation of RanGTPase and inhibition of GTP dissociation by Ran-GTP binding protein RanBP1. *EMBO J* **14:** 705-715, 1995.

36. **Bkaily, G., N. Gros-Louis, R. Naik, D. Jaalouk, and P. Pothier.** Implication of the nucleus in excitation-contraction coupling of heart cells. *Mol Cell Biochem* **154:** 113-121, 1996.

37. **Blobel, G.** Gene gating: a hypothesis. *Proc Natl Acad Sci USA* **82:** 8527-8529, 1985.

38. **Boche, I., and E. Fanning.** Nucleocytoplasmic recycling of the nuclear localization signal receptor α subunit in vivo is dependent of a nuclear export signal, energy, and RCC1. *J Cell Biol* **139:** 313-325, 1997.

39. **Boer, J., J. Bonten-Surtel, and G. Grosveld.** Overexpression of the nucleoporin CAN/NUP214 induces growth arrest, nucleocytoplasmic transport defects, and apoptosis. *Mol Cell Biol* **18:** 1236-1247, 1998.

40. **Bogerd, H.P., R.E. Benson, R. Truant, A. Herold, M. Phingbodhipakkiya, and B.R. Cullen.** Definition of a consensus transportin-specific nucleocytoplasmic transport signal. *J Biol Chem* **274:** 9771-9777, 1999.

41. **Bohn, H., R. Johannsen, and W. Kraus.** New placental protein (pp15) with immunosuppresive properties. *Arch Gynecol* **230:** 167-172, 1980.

42. **Bonifaci, N., J. Moroianu, A. Radu, and G. Blobel.** Karyopherin β2 mediates nuclear import of a mRNA binding protein. *Proc Natl Acad Sci USA* **94:** 5055-5060, 1997.

43. **Bonne, G., M.R. DiBarletta, S. Varnous, H.M. Becane, E.H. Hammouda, L. Merlini, F. Muntoni, C.R. Greenberg, F. Gary, J.A. Urtizberea, D. Duboc, M. Fardeau, D. Toniolo, and K. Schwartz.** Mutations in the gene encoding lamin A/C cause autosomal dominant Emery-Dreifuss muscular dystrophy. *Nat Genet* **21:** 285-288, 1999.

44. **Bourne, H.R., D.A. Sanders, and F. McCormick.** The GTPase superfamily: a conserved switch for diverse cell functions. *Nature* **348:** 125-132, 1990.

45. **Boveris, A.** Mitochondrial production of superoxide radical and hydrogen peroxide. *Adv Exp Med Biol* **78:** 67-82, 1977.

46. **Briggs, L.J., D. Stein, J. Goltz, V.C. Corrigan, A. Efthymiadis, S. Hübner, and D.A. Jans.** The cAMP-dependent protein kinase site (ser^{312}) enhances Dorsal nuclear import through facilitating nuclear localization sequence/importin interaction. *J Biol Chem* **273:** 22745-22752, 1998.

47. **Brown, M.R., F.J.J. Miller, W.-G. Li, A.N. Ellingson, J.D. Mozena, P. Chatterjee, J.F. Engelhardt, R.M. Zwacka, L.W. Oberley, X. Fang, A.A. Spector, and N.L. Weintraub.** Overexpression of human catalase inhibits proliferation and promotes apoptosis in vascular smooth muscle cells. *Circ Res* **85:** 524-533, 1999.

48. **Bruckdorfer, K.R., R.A. Demel, J. De Gier, and L.L.M. Van Deenen.** The effect of partial replacements of membrane cholesterol by other steroids on the osmotic fragility and glycerol permeability of erythrocytes. *Biochim Biophys Acta* **183:** 334-345, 1969.

49. **Bucci, M., and S. Wente.** *In vivo* dynamics of nuclear pore complexes in yeast. *J Cell Biol* **136:** 1185-1199, 1997.

50. **Bullock, T.L., W.D. Clarkson, H.M. Kent, and M. Stewart.** The 1.6 angstroms resolution crystal structure of nuclear transport factor 2 (NTF2). *J Mol Biol* **260:** 422-431, 1996.

51. **Burnier, M., G. Centeno, E. Burki, and H.R. Brunner.** Confocal microscopy to analyze cytosolic and nuclear calcium in cultured vascular cells. *Am J Physiol* **266:** C1118-C1127, 1994.

52. **Burns, K., B. Duggan, E.A. Atkinson, K.S. Famulski, M. Nemer, R.C. Bleackley, and M. Michalak.** Modulation of gene expression by calreticulin binding to the glucocorticoid receptor. *Nature* **367:** 476-480, 1994.

53. **Burton, K.P., J.M. McCord, and G. Ghai.** Myocardial alterations due to free-radical generation. *Am J Physiol* **246:** H776-H783, 1984.

54. **Bustamante, J.O.** Open states of nuclear envelope ion channels in cardiac myocytes. *J Membr Biol* **138:** 77-89, 1994.

55. **Bustamante, J.O.** Restricted ion flow at the nuclear envelope of cardiac myocytes. *Biophys J* **64:** 1735-1749, 1993.

56. **Bustamante, J.O., E.R.F. Michelette, J.P. Geibel, D.A. Dean, J.A. Hanover, and T.J. McDonnell.** Calcium, ATP and nuclear pore channel gating. *Pflügers Arch* **439:** 433-444, 2000.

57. **Byrd, D.A., D.A. Sweet, N. Panté, K.N. Konstantinov, T. Guan, A.C.S. Saphire, P.J. Mitchell, C.S. Cooper, U. Aebi, and L. Gerace.** Tpr, a large coiled coil protein whose amino terminus is involved in the activation of oncogenic kinases, is localized to the cytoplasmic face of the nuclear pore complex. *J Cell Biol* **127:** 1515-1526, 1994.

58. **Cala, S.E., C. Ulbright, J.S. Kelley, and L.R. Jones.** Purification of a 90-kDa protein (Band VII) from cardiac sarcoplasmic reticulum. Identification as calnexin and localization of casein kinase II phosphorylation sites. *J Biol Chem* **268:** 2969-2975, 1993.

59. **Campbell, K.P., D.H. MacLennan, and A.O. Jorgensen.** Staining of the Ca^{2+}-binding proteins, calsequestrin, calmodulin, troponin C, and S-100, with the cationic carbocyanine dye "Stains-All". *J Biol Chem* **258:** 11267-11273, 1983.

60. **Campbell, K.P., D.H. MacLennan, A.O. Jorgensen, and M.C. Mintzer.** Purification and characterization of calsequestrin from canine cardiac sarcoplasmic reticulum and identification of the 53,000 dalton glycoprotein. *J Biol Chem* **258:** 1197-1204, 1983.

61. **Cantoni, O., D. Boscoboinik, M. Fiorani, B. St„uble, and A. Azzi.** The phosphorylation state of MAP-kinases modulates the cytotoxic response of smooth muscle cells to hydrogen peroxide. *FEBS Lett* **389:** 285-288, 1996.

62. **Cao, H., and R.A. Hegele.** Nuclear lamin A/C R482Q mutation in Canadian kindreds with Dunnigan-type familial partial lipodystrophy. *Hum Mol Genet* **9:** 109-112, 2000.

63. **Century, T.J., I.R. Fenichel, and S.B. Horowitz.** The concentrations of water, sodium and potassium in the nucleus and cytoplasm of amphibian oocytes. *J Cell Sci* **7:** 5-13, 1970.

64. **Chafouleas, J.G., W.E. Bolton, and A.R. Means.** Potentiation of bleomycin lethality by anticalmodulin drugs: a role for calmodulin in DNA repair. *Science* **224:** 1346-1348, 1984.

65. **Chafouleas, J.G., L. Lagace, W.E. Bolton, A.E. Boyd, and A.R. Means.** Changes in calmodulin and its mRNA accompany reentry of quiescent (G0) cells into the cell cycle. *Cell* **36:** 73-81, 1984.

66. **Chaillan-Huntington, C., C.V. Braslavsky, J. Kuhlmann, and M. Stewart.** Dissecting the interactions between NTF2, RanGDP, and the nucleoporin XFXFG repeats. *J Biol Chem* **275:** 5874-5879, 2000.

67. **Charp, P.A.** DNA repair in human cells: methods for the determination of calmodulin involvement. *Meth Enzymol* **139:** 715-730, 1987.

68. **Charuk, J.H.M., C.A. Pirraglia, and R.A.F. Reithmeier.** Interaction of ruthenium red with Ca^{2+}-binding proteins. *Anal Biochem* **188:** 123-131, 1990.

69. **Chi, N.C., E.J.H. Adam, and S.A. Adam.** Different binding domains for Ran-GTP and Ran-GDP/RanBP1 on nuclear import factor p97. *J Biol Chem* **272:** 6818-6822, 1997.

70. **Chi, N.C., E.J.H. Adam, and S.A. Adam.** Sequence and characterization of cytoplasmic nuclear protein import factor p97. *J Cell Biol* **130:** 265-274, 1995.

71. **Chi, N.C., E.J.H. Adam, G.D. Visser, and S.A. Adam.** RanBP1 stabilizes the interaction of Ran with p97 in nuclear protein import. *J Cell Biol* **135:** 559-569, 1996.

72. **Chi, N.C., and S.A. Adam.** Functional domains in nuclear import factor p97 for binding the nuclear localization sequence receptor and the nuclear pore. *Mol Biol Cell* **8:** 945-956, 1997.

73. **Cingolani, G., C. Petosa, K. Weis, and C.W. Müller.** Structure of importin-β bound to the IBB domain of importin-α. *Nature* **399:** 221-229, 1999.

74. **Clarkson, W.D., A.H. Corbett, B.M. Paschal, H.M. Kent, A.J. McCoy, L. Gerace, P.A. Silver, and M. Stewart.** Nuclear protein import is decreased by engineered mutants of nuclear transport factor 2 (NTF2) that do not bind GDP Ran. *J Mol Biol* **272:** 716-730, 1997.

75. **Clarkson, W.D., H.M. Kent, and M. Stewart.** Separate binding sites on nuclear transport factor 2 (NTF2) for GDP-Ran and the phenylalanine-rich repeat regions of nucleoporins p62 and Nsp1p. *J Mol Biol* **263:** 517-524, 1996.

76. **Clawson, G.A., D.S. Friend, and E.A. Smuckler.** Localization of nucleoside triphosphatase activity to the inner nuclear envelope and associated heterochromatin. *Exp Cell Res* **155:** 310-314, 1984.

77. **Clawson, G.A., J. James, C.H. Woo, D.S. Friend, D. Moody, and E.A. Smuckler.** Pertinence of nuclear envelope nucleoside triphosphatase activity to ribonucleic acid transport. *Biochemistry* **19:** 2748-2756, 1980.

78. **Clawson, G.A., M. Koplitz, B. Castler-Schechter, and E.A. Smuckler.** Energy utilization and RNA transport: Their interdependence. *Biochemistry* **17:** 3747-3752, 1978.

79. **Clawson, G.A., A. Lackey, and Z.A. Tokes.** The 46-kDa nucleoside triphosphatase of rat liver nuclear scaffold represents the N-terminal portion of lamins A/C. *Exp Cell Res* **176:** 180-186, 1988.

80. **Clerk, A., A. Michael, and P.H. Sugden.** Stimulation of multiple mitogen-activated protein kinase sub-families by oxidative stress and phosphorylation of the small

heat shock protein, HSP25/27, in neonatal ventricular myocytes. *Biochem J* **333:** 581-589, 1998.

81. **Cockell, M., and S.M. Gasser.** Nuclear compartments and gene regulation. *Curr Opin Genet Dev* **9:** 199-205, 1999.

82. **Conti, E., M. Uy, L. Leighton, G. Blobel, and J. Kuriyan.** Crystallographic analysis of the recognition of a nuclear localization signal by the nuclear import factor karyopherin α. *Cell* **94:** 193-204, 1998.

83. **Corbett, A.H., and P.A. Silver.** The NTF2 gene encodes an essential, highly conserved protein that functions in nuclear transport in vivo. *J Biol Chem* **271:** 18477-18484, 1996.

84. **Cordes, V.C., S. Reidenbach, A. Köhler, N. Struurman, R. Van Driel, and W.W. Franke.** Intranuclear filaments containing a nuclear pore complex protein. *J Cell Biol* **123:** 1333-1344, 1993.

85. **Cowin, P., and B. Burke.** Cytoskeleton-membrane interactions. *Curr Opin Cell Biol* **8:** 56-65, 1996.

86. **Czubryt, M.P., B. Ramjiawan, J.S.C. Gilchrist, H. Massaeli, and G.N. Pierce.** The presence and partitioning of calcium binding proteins in hepatic and cardiac nuclei. *J Mol Cell Cardiol* **28:** 455-465, 1996.

87. **Czubryt, M.P., B. Ramjiawan, and G.N. Pierce.** The nuclear membrane integrity assay. *Mol Cell Biochem* **172:** 97-102, 1997.

88. **Dash, P.K., K.A. Karl, M.A. Colicos, R. Prywes, and E.R. Kandel.** cAMP response element-binding protein is activated by Ca^{2+}/calmodulin- as well as cAMP-dependent protein kinase. *Proc Natl Acad Sci USA* **88:** 5061-5065, 1991.

89. **de la Luna, S., M.J. Burden, C.-W. Lee, and N.B. La Thangue.** Nuclear accumulation of the E2F heterodimer regulated by subunit composition and alternative splicing of a nuclear localization signal. *J Cell Sci* **109:** 2443-2452, 1996.

90. **Dedhar, S., P.S. Rennie, M. Shago, C.Y.L. Hagesteijn, H. Yang, J. Filmus, R.G. Hawley, N. Bruchovsky, H. Cheng, R.J. Matusik, and V. Giguère.** Inhibition of nuclear hormone receptor activity by calreticulin. *Nature* **367:** 480-483, 1994.

91. **Delphin, C., T. Guan, F. Melchior, and L. Gerace.** RanGTP targets p97 to RanBP2, a filamentous protein localized at the cytoplasmic periphery of the nuclear pore complex. *Mol Biol Cell* **8:** 2379-2390, 1997.

92. **Dingwall, C., S.V. Sharnick, and R.A. Laskey.** A polypeptide domain that specifies migration of nucleoplasmin into the nucleus. *Cell* **30:** 449-458, 1982.

93. **Dolphin, P.J., R.M. Amy, and J.C. Russell.** Effect of age on serum lipids and lipoproteins of male and female JCR:LA-corpulent rats. *Biochim Biophys Acta* **1042:** 99-106, 1990.

94. **Dolphin, P.J., B. Stewart, R.M. Amy, and J.C. Russell.** Serum lipids and lipoproteins in the atherosclerosis prone LA/N corpulent rat. *Biochim Biophys Acta* **919:** 140-148, 1987.

95. **Doye, V., and E. Hurt.** From nucleoporins to nuclear pore complexes. *Curr Opin Cell Biol* **9:** 401-411, 1997.

96. **Drivas, G.T., A. Shih, E. Coutavas, M.G. Rush, and P. D'Eustachio.** Characterization of four novel *ras*-like genes expressed in a human teratocarcinoma cell line. *Mol Cell Biol* **10:** 1793-1798, 1990.

97. **Dworetzky, S.I., R.E. Lanford, and C.M. Feldherr.** The effects of variations in the number and sequence of targeting signals on nuclear uptake. *J Cell Biol* **107:** 1279-1287, 1988.

98. **Englmeier, L., J.-C. Olivo, and I.W. Mattaj.** Receptor-mediated substrate translocation through the nuclear pore complex without nucleotide triphosphate hydrolysis. *Curr Biol* **9:** 30-41, 1999.

99. **Fabre, E., N.L. Schlaich, and E.C. Hurt.** Nucleocytoplasmic trafficking: what role for repeated motifs in nucleoporins? *Cold Spring Harb Symp Quant Biol* **LX:** 677-685, 1995.

100. **Feldherr, C.M., and D. Akin.** The location of the transport gate in the nuclear pore complex. *J Cell Sci* **110:** 3065-3070, 1997.

101. **Feldherr, C.M., and D. Akin.** Regulation of nuclear transport in proliferating and quiescent cells. *Exp Cell Res* **205:** 179-186, 1993.

102. **Feldherr, C.M., and D. Akin.** Signal-mediated nuclear transport in proliferating and growth-arrested BALB/c 3T3 cells. *J Cell Biol* **115:** 933-939, 1991.

103. **Ferrier, J., and H. Yu.** Nuclear versus perinuclear and cytoplasmic calcium in osteoclasts. *Cell Calcium* **20:** 381-388, 1996.

104. **Fiorani, M., O. Cantoni, A. Tasinato, D. Boscoboinik, and A. Azzi.** Hydrogen peroxide- and fetal bovine serum-induced DNA synthesis in vascular smooth

muscle cells: positive and negative regulation by protein kinase C isoforms. *Biochim Biophys Acta* **1269:** 98-104, 1995.

105. **Folprecht, G., S. Schneider, and H. Oberleithner.** Aldosterone activates the nuclear pore transporter in cultured kidney cells images with atomic force microscopy. *Pflügers Arch* **432:** 831-838, 1996.

106. **Foo, S.Y., and G.P. Nolan.** NF-κB to the rescue: RELs, apoptosis and cellular transformation. *Trends Genet* **15:** 229-235, 1999.

107. **Fornerod, M., J. van Deursen, S. van Baal, A. Reynolds, D. Davis, K.G. Murti, J. Fransen, and G. Grosveld.** The human homologue of yeast CRM1 is in a dynamic subcomplex with CAN/Nup214 and a novel nuclear pore component Nup88. *EMBO J* **16:** 807-816, 1997.

108. **Franke, W.W.** Structure, biochemistry, and functions of the nuclear envelope. *Int Rev Cytol* **Supplement 4:** 71-236, 1974.

109. **Fujihara, S.M., and S.G. Nadler.** Modulation of nuclear protein import. A novel means of regulating gene expression. *Biochem Pharmacol* **53:** 157-161, 1998.

110. **Fukuda, M., Y. Gotoh, and E. Nishida.** Interaction of MAP kinase with MAP kinase kinase: its possible role in the control of nucleocytoplasmic transport of MAP kinase. *EMBO J* **16:** 1901-1908, 1997.

111. **Georgatos, S.D., J. Meier, and G. Simos.** Lamins and lamin-associated proteins. *Curr Opin Cell Biol* **6:** 347-353, 1994.

112. **Gerasimenko, O.V., J.V. Gerasimenko, A.V. Tepikin, and O.H. Petersen.** ATP-dependent accumulation and inositol trisphosphate- or cyclic ADP-ribose-mediated release of Ca^{2+} from the nuclear envelope. *Cell* **80:** 439-444, 1995.

113. **Gilchrist, J.S., M.P. Czubryt, and G.N. Pierce.** Calcium and calcium-binding proteins in the nucleus. *Mol Cell Biochem* **135:** 79-88, 1994.

114. **Gilchrist, J.S., and G.N. Pierce.** Identification and purification of a calcium-binding protein in hepatic nuclear membranes. *J Biol Chem* **268:** 4291-4299, 1993.

115. **Goldberg, M.W., and T.D. Allen.** The nuclear pore complex: three-dimensional surface structure revealed by field emission, in-lens scanning electron microscopy with underlying structure uncovered by proteolysis. *J Cell Sci* **106:** 261-274, 1993.

116. **Goldberg, M.W., and T.D. Allen.** Structural and functional organization of the nuclear envelope. *Curr Opin Cell Biol* **7:** 301-309, 1995.

117. **Goldfarb, D.S., J. Gariepy, G. Schoolnik, and R.D. Kornberg.** Synthetic peptides as nuclear localization signals. *Nature* **322:** 641-644, 1986.

118. **Görlich, D., M. Dabrowski, J.R. Bischoff, U. Kutay, P. Bork, E. Hartmann, S. Prehn, and E. Izaurralde.** A novel class of RanGTP binding proteins. *J Cell Biol* **138:** 65-80, 1997.

119. **Görlich, D., P. Henklein, R.A. Laskey, and E. Hartmann.** A 41 amino acid motif in importin-α confers binding to importin-β and hence transit into the nucleus. *EMBO J* **15:** 1810-1817, 1996.

120. **Görlich, D., and R.A. Laskey.** Roles of importin in nuclear protein import. *Cold Spring Harb Symp Quant Biol* **LX:** 695-699, 1995.

121. **Görlich, D., and I.W. Mattaj.** Nucleocytoplasmic transport. *Science* **271:** 1513-1518, 1996.

122. **Görlich, D., S. Prehn, R.A. Laskey, and E. Hartmann.** Isolation of a protein that is essential for the first step of nuclear protein import. *Cell* **79:** 767-778, 1994.

123. **Greber, U.F., and L. Gerace.** Depletion of calcium from the lumen of endoplasmic reticulum reversibly inhibits passive diffusion and signal-mediated transport into the nucleus. *J Cell Biol* **128:** 5-14, 1995.

124. **Greco, A., M.A. Pierotti, I. Bongarzone, S. Pagliardini, C. Lanzi, and G. Della Porta.** TRK-T1 is a novel oncogene formed by the fusion of TPR and TRK genes in human papillary thyroid carcinomas. *Oncogene* **7:** 237-242, 1992.

125. **Gregory, P.D., and W. Hörz.** Life with nucleosomes: chromatin remodelling in gene regulation. *Curr Opin Cell Biol* **10:** 339-345, 1998.

126. **Griendling, K.K., and D.G. Harrison.** Dual role of reactive oxygen species in vascular growth. *Circ Res* **85:** 562-563, 1999.

127. **Gueth-Hallonet, C., J. Wang, J. Harborth, K. Weber, and M. Osborn.** Induction of a regular nuclear lattice by overexpression of NuMa. *Exp Cell Res* **243:** 434-452, 1998.

128. **Guyton, K.Z., Y. Liu, M. Gorospe, Q. Xu, and N.J. Holbrook.** Activation of mitogen-activated protein kinase by H_2O_2. *J Biol Chem* **271:** 4138-4142, 1996.

129. **Haas, M., and E. Jost.** Functional analysis of phosphorylation sites in human lamin A controlling lamin disassembly, nuclear transport and assembly. *Eur J Cell Biol* **62:** 237-247, 1993.

130. **Halliwell, B., and J.M.C. Gutteridge.** Role of free radicals and catalytic metal ions in human disease: an overview. *Meth Enzymol* **186:** 1-85, 1990.

131. **Harborth, J., J. Wang, C. Gueth-Hallonet, K. Weber, and M. Osborn.** Self assembly of NuMa: multiarm oligomers as structural units of a nuclear lattice. *EMBO J* **18:** 1689-1700, 1999.

132. **Hardingham, G.E., and H. Bading.** Nuclear calcium: a key regulator of gene expression. *BioMetals* **11:** 345-358, 1998.

133. **Heist, E.K., M. Srinivasan, and H. Schulman.** Phosphorylation at the nuclear localization signal of Ca^{2+}/calmodulin-dependent protein kinase II blocks its nuclear targeting. *J Biol Chem* **273:** 19763-19771, 1998.

134. **Henderson, B.R., and P. Percipalle.** Interactions between HIV Rev and nuclear import and export factors: the Rev nuclear localisation signal mediates specific binding to human importin-beta. *J Mol Biol* **274:** 693-707, 1997.

135. **Hennekes, H., M. Peter, K. Weber, and E.A. Nigg.** Phosphorylation on protein kinase C sites inhibits nuclear import of lamin B_2. *J Cell Biol* **120:** 1293-1304, 1993.

136. **Hernandez-Cruz, A., F. Sala, and P.R. Adams.** Subcellular calcium transients visualized by confocal microscopy in a voltage-clamped vertebrate neuron. *Science* **247:** 858-862, 1990.

137. **Herold, A., R. Truant, H. Wiegand, and B.R. Cullen.** Determination of the functional domain organization of the importin α nuclear import factor. *J Cell Biol* **143:** 309-318, 1998.

138. **Himpens, B., H. de Smedt, and R. Casteels.** Kinetics of nucleocytoplasmic Ca^{2+} transients in DDT_1 MF-2 smooth muscle cells. *Am J Physiol* **263:** C978-C985, 1992.

139. **Himpens, B., H. De Smedt, G. Droogmans, and R. Casteels.** Differences in regulation between nuclear and cytoplasmic Ca^{2+} in cultured smooth muscle cells. *Am J Physiol* **263:** C95-C105, 1992.

140. **Hirai, S., H. Kawasaki, M. Yaniv, and K. Suzuki.** Degradation of transcription factors, c-Jun and c-Fos, by calpain. *FEBS Lett* **287:** 57-61, 1991.

141. **Hocevar, B.A., D.J. Burns, and A.P. Fields.** Identification of protein kinase C (PKC) phosphorylation sites on human lamin B. *J Biol Chem* **268:** 7545-7552, 1993.

142. **Holliday, J., R.J. Adams, T.J. Sejnowski, and N.C. Spitzer.** Calcium-induced release of calcium regulates differentiation of cultured spinal neurons. *Neuron* **7:** 787-796, 1991.

143. **Hozák, P.** The nucleoskeleton and attached activities. *Exp Cell Res* **229:** 267-271, 1996.

144. **Hozák, P., A.M.-J. Sasseville, Y. Raymond, and P.R. Cook.** Lamin proteins form an internal nucleoskeleton as well as a peripheral lamina in human cells. *J Cell Sci* **108:** 635-644, 1995.

145. **Huber, J., U. Cronshagen, M. Kadokura, C. Marshallsay, T. Wada, M. Sekine, and R. Lührmann.** Snurportin1, an m_3G-cap-specific nuclear import receptor with a novel domain structure. *EMBO J* **17:** 4114-4126, 1998.

146. **Hübner, S., H.M.S. Smith, W. Hu, C.K. Chan, H.-P. Rihs, B.M. Paschal, N.V. Raikhel, and D.A. Jans.** Plant importin α binds nuclear localization sequences with high affinity and can mediate nuclear import independent of importin β. *J Biol Chem* **274:** 22610-22617, 1999.

147. **Hübner, S., C.-Y. Xiao, and D.A. Jans.** The protein kinase CK2 site ($Ser^{111/112}$) enhances recognition of the simian virus 40 large T-antigen nuclear localization sequence by importin. *J Biol Chem* **272:** 17191-17195, 1997.

148. **Humbert, J.-P., N. Matter, J.-C. Artault, P. Köppler, and A.N. Malviya.** Inositol 1,4,5-trisphosphate receptor is located to the inner nuclear membrane vindicating regulation of nuclear calcium signaling by inositol 1,4,5-trisphosphate. *J Biol Chem* **271:** 478-485, 1996.

149. **Hyslop, P.A., Z. Zhang, D.V. Pearson, and L.A. Phebus.** Measurement of striatal H_2O_2 by microdialysis following forebrain ischemia and reperfusion in the rat: correlation with the cytotoxic potential of H_2O_2 in vitro. *Brain Res* **671:** 181-186, 1995.

150. **Innocenti, B., and M. Mazzanti.** Identification of a nucleo-cytoplasmic ionic pathway by osmotic shock in isolated mouse liver nuclei. *J Membr Biol* **131:** 137-142, 1993.

151. **Iovine, M.K., and S.R. Wente.** A nuclear export signal in Kap95p is required for both recycling the import factor and interaction with the nucleoporin GLFG repeat regions of Nup116p and Nup100p. *J Cell Biol* **137:** 797-811, 1997.

152. **Irvine, R.F., A.J. Letcher, J.P. Heslop, and M.J. Berridge.** The inositol-tris/tetrakisphosphate pathway - demonstration of Ins(1,4,5)P3 3-kinase activity in animal tissues. *Nature* **320:** 631-634, 1986.

153. **Izaurralde, E., U. Kutay, C. von Kobbe, I.W. Mattaj, and D. Görlich.** The asymmetric distribution of the constituents of the Ran system is essential for transport into and out of the nucleus. *EMBO J* **16:** 6535-6547, 1997.

154. **Jackowski, G., and C.C. Liew.** Fractionation of rat ventricular nuclei. *Biochem J* **188:** 363-373, 1980.

155. **Jackson, M.R., M.F. Cohen-Doyle, P.A. Peterson, and D.B. Williams.** Regulation of MHC class I transport by the molecular chaperone, calnexin (p88, IP90). *Science* **263:** 384-387, 1994.

156. **Jäkel, S., W. Albig, U. Kutay, F.R. Bischoff, K. Schwamborn, D. Doenecke, and D. Görlich.** The importin β/importin 7 heterodimer is a functional nuclear import receptor for histone H1. *EMBO J* **18:** 2411-2423, 1999.

157. **Jäkel, S., and D. Görlich.** Importin β, transportin, RanBP5 and RanBP7 mediate nuclear import of ribosomal proteins in mammalian cells. *EMBO J* **17:** 4491-4502, 1998.

158. **Jans, D.A.** The regulation of protein transport to the nucleus by phosphorylation. *Biochem J* **311:** 705-716, 1995.

159. **Jans, D.A., M.J. Ackermann, J.R. Bischoff, D.H. Beach, and R. Peters.** $p34^{cdc2}$-mediated phosphorylation at T^{124} inhibits nuclear import of SV-40 T antigen proteins. *J Cell Biol* **115:** 1203-1212, 1991.

160. **Jans, D.A., L.J. Briggs, S.E. Gustin, P. Jans, S. Ford, and I.G. Young.** A functional bipartite nuclear localization signal in the cytokine interleukin-5. *FEBS Lett* **406:** 315-320, 1997.

161. **Jans, D.A., and S. H bner.** Regulation of protein transport to the nucleus: Central role of phosphorylation. *Physiol Rev* **76:** 651-685, 1996.

162. **Jans, D.A., T. Moll, K. Nasmyth, and P. Jans.** Cyclin-dependent kinase site-regulated signal-dependent nuclear localization of the SWI5 yeast transcription factor in mammalian cells. *J Biol Chem* **270:** 17064-17067, 1995.

163. **Jiang, C.-J., N. Imamoto, R. Matsuki, Y. Yoneda, and N. Yamamoto.** Functional characterization of a plant importin α homologue. *J Biol Chem* **273:** 24083-24087, 1998.

164. **Jones, D.P., D.J. McConkey, P. Nicotera, and S. Orrenius.** Calcium-activated DNA fragmentation in rat liver nuclei. *J Biol Chem* **264:** 6398-6403, 1989.

165. **Kalderon, D., W.D. Richardson, A.F. Markham, and A.E. Smith.** Sequence requirements for nuclear localisation of SV40 large-T antigen. *Nature* **311:** 33-38, 1984.

166. **Kalderon, D., B.L. Roberts, W.D. Richardson, and A.E. Smith.** A short amino acid sequence able to specify nuclear location. *Cell* **39:** 499-509, 1984.

167. **Kamei, Y., S. Yuba, T. Nakayama, and Y. Yoneda.** Three distinct classes of the α-subunit of the nuclear pore-targeting complex (importin-α) are differentially expressed in adult mouse tissues. *J Histochem Cytochem* **47:** 363-372, 1999.

168. **Kasper, L.H., P.K. Brindle, C.A. Schnabel, C.E.J. Pritchard, M.L. Cleary, and J.M.A. van Deursen.** CREB binding protein interacts with nucleoporin-specific FG repeats that activate transcription and mediate NUP98-HOAX9 oncogenicity. *Mol Cell Biol* **19:** 764-776, 1999.

169. **Katahira, J., K. Straber, A. Podtelejnikov, M. Mann, J.U. Jung, and E. Hurt.** The Mex67p-mediated nuclear mRNA export pathway is conserved from yeast to human. *EMBO J* **18:** 2593-2609, 1999.

170. **Kaufmann, S.H., W. Gibson, and J.H. Shaper.** Characterization of the major polypeptides of the rat liver nuclear envelope. *J Biol Chem* **258:** 2710-2719, 1983.

171. **Kaul, N., N. Siveski-Iliskovic, M. Hill, J. Slezak, and P.K. Singal.** Free radicals and the heart. *J Pharmacol Toxicol Meth* **30:** 55-67, 1993.

172. **Klebe, C., F.R. Bischoff, H. Ponstingl, and A. Wittinghofer.** Interaction of the nuclear GTP-binding protein Ran with its regulatory proteins RCC1 and RanGAP1. *Biochemistry* **34:** 639-647, 1995.

173. **Kloner, R.A., K. Przyklenk, and P. Whittaker.** Deleterious effects of oxygen radicals in ischemia/reperfusion: Resolved and unresolved issues. *Circulation* **80:** 1115-1127, 1989.

174. **Köhler, M., S. Ansieau, S. Prehn, A. Leutz, H. Haller, and E. Hartmann.** Cloning of two novel human importin-alpha subunits and analysis of the expression pattern of the importin-alpha protein family. *FEBS Lett* **417:** 104-108, 1997.

175. **Köhler, M., C. Speck, M. Christiansen, F.R. Bischoff, S. Prehn, H. Haller, D. Görlich, and E. Hartmann.** Evidence for distinct substrate specificities of importin α family members in nuclear protein import. *Mol Cell Biol* **19:** 7782-7791, 1999.

176. **Koletsky, S.** Obese spontaneously hypertensive rats--A model for the study of atherosclerosis. *Exp Mol Pathol* **19:** 53-60, 1973.

177. **Koletsky, S.** Pathological findings and laboratory data in a new strain of obese hypertensive rats. *Am J Pathol* **80:** 129-142, 1975.

178. **Kong, S.K., D. Tsang, K.N. Leung, and C.Y. Lee.** Nuclear envelope acts as a calcium barrier in C6 glioma cells. *Biochem Biophys Res Commun* **218:** 595-600, 1996.

179. **Köppler, P., M. Mersel, J.-P. Humbert, J. Vignon, G. Vincendon, and A.N. Malviya.** High affinity inositol 1,3,4,5-tetrakisphosphate receptor from rat liver nuclei: purification, characterization, and amino-terminal sequence. *Biochemistry* **35:** 5481-5487, 1996.

180. **Kose, S., N. Imamoto, T. Tachibana, T. Shimamoto, and Y. Yoneda.** Ran-unassisted nuclear migration of a 97-kD component of nuclear pore-targeting complex. *J Cell Biol* **139:** 841-849, 1997.

181. **Kutay, U., F.R. Bischoff, S. Kostka, R. Kraft, and D. Görlich.** Export of importin α from the nucleus is mediated by a specific nuclear transport factor. *Cell* **90:** 1061-1071, 1997.

182. **Kutryk, M.J., and G.N. Pierce.** Stimulation of sodium-calcium exchange by cholesterol incorporation into isolated cardiac sarcolemmal vesicles. *J Biol Chem* **263:** 13167-13172, 1988.

183. **Lanford, R.E., and J.S. Butel.** Construction and characterization of an SV40 mutant defective in nuclear transport of T antigen. *Cell* **37:** 801-813, 1984.

184. **Lanford, R.E., P. Kanda, and R.C. Kennedy.** Induction of nuclear transport with a synthetic peptide homologous to the SV40 T antigen transport signal. *Cell* **46:** 575-582, 1986.

185. **Lanini, L., O. Bachs, and E. Carafoli.** The calcium pump of the liver nuclear membrane is identical to that of endoplasmic reticulum. *J Biol Chem* **267:** 11548-11552, 1992.

186. **Laskey, R.A., D. Görlich, M.A. Madine, J.P.S. Makkerh, and P. Romanowski.** Regulatory roles of the nuclear envelope. *Exp Cell Res* **229:** 204-211, 1996.

187. **Lenz-Böhme, B., J. Wismar, S. Fuchs, R. Reifegerste, E. Buchner, H. Betz, and B. Schmitt.** Insertional mutation of the *Drosophila* nuclear lamin Dm_0 gene results in defective nuclear envelopes, clustering of nuclear pore complexes, and accumulation of annulate lamellae. *J Cell Biol* **137:** 1001-1016, 1997.

188. **Li, G., G. Sudlow, and A.S. Belmont.** Interphase cell cycle dynamics of a late-replicating, heterochromatic homogeneously staining region: precise choreography of condensation/decondensation and nuclear positioning. *J Cell Biol* **140:** 975-989, 1998.

189. **Li, P.-F., R. Dietz, and R. von Harsdorf.** Differential effect of hydrogen peroxide and superoxide anion on apoptosis and proliferation of vascular smooth muscle cells. *Circulation* **96:** 3602-3609, 1997.

190. **Liu, K., and G.N. Pierce.** The modulation of membrane ion movements by cholesterol. In: *Membrane Physiopathology*, edited by G. Bkaily. Norwell: Kluwer Academic Publishers, 1994, p. 291-317.

191. **Lo, Y.Y.C., J.M.S. Wong, and T.F. Cruz.** Reactive oxygen species mediate cytokine activation of c-Jun NH_2-terminal kinases. *J Biol Chem* **271:** 15703-15707, 1996.

192. **Loeffler, J.P., N. Kley, J.C. Louis, and B.A. Demeneix.** Ca^{2+} regulates hormone secretion and proopiomelanocortin gene expression in melanotrope cells via the calmodulin and the protein kinase C pathways. *J Neurochem* **52:** 1279-1283, 1989.

193. **Loewenstein, W.R., and Y. Kanno.** Some electrical properties of a nuclear membrane examined with a microelectrode. *J Gen Physiol* **46:** 1123-1140, 1963.

194. **Lowry, O.H., N.J. Rosebrough, A.L. Farr, and A.J. Randall.** Protein measurement with the Folin phenol reagent. *J Biol Chem* **193:** 265-275, 1951.

195. **Lui, P.P.Y., S.K. Kong, K.P. Fung, and C.Y. Lee.** The rise of nuclear and cytosolic Ca^{2+} can be uncoupled in HeLa cells. *Pflügers Arch* **436:** 371-376, 1998.

196. **Macaulay, C., E. Meier, and D.J. Forbes.** Differential mitotic phosphorylation of proteins of the nuclear pore complex. *J Biol Chem* **270:** 254-262, 1995.

197. **MacDonald, J.R.** Nuclear calcium: transfer to and from the cytosol. *Biol Signals Recept* **7:** 137-147, 1998.

198. **MacLennan, D.H., and K.P. Campbell.** Structure, function and biosynthesis of sarcoplasmic reticulum proteins. *Trends Biochem Sci* **4:** 148-151, 1979.

199. **Madden, T.D., D. Chapman, and P.J. Quinn.** Cholesterol modulates activity of calcium-dependent ATPase of the sarcoplasmic reticulum. *Nature* **279:** 538-540, 1979.

200. **Mak, D.-O.D., and J.K. Foskett.** Single-channel inositol 1,4,5-trisphosphate receptor currents revealed by patch clamp of isolated *Xenopus* oocyte nuclei. *J Biol Chem* **269:** 29375-29378, 1994.

201. **Malviya, A.N., P. Rogue, and G. Vincendon.** Stereospecific inositol 1,4,5-[^{32}P]trisphosphate binding to isolated rat liver nuclei: evidence for inositol trisphosphate receptor-mediated calcium release from the nucleus. *Proc Natl Acad Sci USA* **87:** 9270-9274, 1990.

202. **Mancini, M.A., B. Shan, J.A. Nickerson, S. Penman, and W.H. Lee.** The retinoblastoma gene product is a cell cycle-dependent, nuclear matrix-associated protein. *Proc Natl Acad Sci USA* **91:** 418-422, 1994.

203. **Marin, M.C., A. Fernandez, R.J. Bick, S. Brisbay, L.M. Buja, M. Snuggs, D.J. McConkey, A.C. von Eschenbach, M.J. Keating, and T.J. McDonnell.** Apoptosis suppression by bcl-2 is correlated with the regulation of nuclear and cytosolic Ca^{2+}. *Oncogene* **12:** 2259-2266, 1996.

204. **Markovics, J., L. Glass, and G.G. Maul.** Pore patterns on nuclear envelopes. *Exp Cell Res* **85:** 443-451, 1974.

205. **Markwell, M.K., S.M. Haas, N.E. Tolbert, and L.L. Bieber.** Protein determination in membrane and lipoprotein samples: Manual and automated procedures. *Meth Enzymol* **72:** 296-303, 1981.

206. **Marshall, I.C.B., T.M. Gant, and K.L. Wilson.** Ionophore-releasable lumenal Ca^{2+} stores are not required for nuclear envelope assembly or nuclear protein import in *Xenopus* egg extracts. *Cell Calcium* **21:** 151-161, 1997.

207. **Marshall, W.F., J.C. Fung, and J.W. Sedat.** Deconstructing the nucleus: global architecture from local interactions. *Curr Opin Genet Devel* **7:** 259-263, 1997.

208. **Martin, A.F., E.D. Pagani, and R.J. Solaro.** Thyroxine-induced redistribution of isoenzymes of rabbit ventricular myosin. *Circ Res* **50:** 117-24, 1982.

209. **Maruyama, K., T. Mikawa, and S. Ebashi.** Detection of calcium binding proteins by 45Ca autoradiography on nitrocellulose membrane after sodium dodecyl sulfate gel electrophoresis. *J Biochem Tokyo* **95:** 511-9, 1984.

210. **Massaeli, H.** *Role of oxidized low density lipoprotein in calcium homeostasis in vascular smooth muscle cells*. Ph.D. Thesis. Winnipeg: University of Manitoba, 2000.

211. **Mattaj, I.W., and L. Englmeier.** Nucleocytoplasmic transport: the soluble phase. *Annu Rev Biochem* **67:** 265-306, 1998.

212. **Matter, N., M.F. Ritz, S. Freyermuth, P. Rogue, and A.N. Malviya.** Stimulation of nuclear protein kinase C leads to phosphorylation of nuclear inositol 1,4,5-trisphosphate receptor and accelerated calcium release by inositol 1,4,5-trisphosphate from isolated rat liver nuclei. *J Biol Chem* **268:** 732-736, 1993.

213. **Matunis, M.J., E. Coutavas, and G. Blobel.** A novel ubiquitin-like modification modulates the partitioning of the Ran-GTPase-activating protein RanGAP1 between the cytosol and the nuclear pore complex. *J Cell Biol* **135:** 1457-1470, 1996.

214. **Maul, G.G.** The nuclear and the cytoplasmic pore complex: structure, dynamics, distribution and evolution. *Int Rev Cytol* **Supplement 6:** 75-186, 1977.

215. **Maul, G.G., L.L. Deaven, J.J. Freed, G.I.M. Campbell, and W. Beçak.** Investigation of the determinants of nuclear pore number. *Cytogenet Cell Genet* **26:** 175-190, 1980.

216. **Maul, G.G., H.M. Maul, J.E. Scogna, M.W. Lieberman, G.S. Stein, B.Y. Hsu, and T.W. Borun.** Time sequence of nuclear pore formation in

phytohamagglutinin-stimulated lymphocytes and in HeLa cells during the cell cycle. *J Cell Biol* **55:** 433-447, 1972.

217. **Mazzanti, M., L.J. DeFelice, J. Cohn, and H. Malter.** Ion channels in the nuclear envelope. *Nature* **343:** 764-767, 1990.

218. **Mazzanti, M., L.J. DeFelice, and E.F. Smith.** Ion channels in murine nuclei during early development and in fully differentiated adult cells. *J Membr Biol* **121:** 189-198, 1991.

219. **McDonald, J.R., and P.S. Agutter.** The relationship between polyribonucleotide binding and the phosphorylation and dephosphorylation of nuclear envelope protein. *FEBS Lett* **116:** 145-148, 1980.

220. **Mesaeli, N., K. Nakamura, E. Zvaritch, P. Dickie, P. Dziak, K.H. Krause, M. Opas, D.H. MacLennan, and M. Michalak.** Calreticulin is essential for cardiac development. *J Cell Biol* **144:** 857-868, 1999.

221. **Michael, W.M.** Nucleocytoplasmic shuttling signals: two for the price of one. *Trends Cell Biol* **10:** 46-50, 2000.

222. **Michael, W.M., M. Choi, and G. Dreyfuss.** A nuclear export signal in hnRNP A1: a signal-mediated, temperature-dependent nuclea protein export pathway. *Cell* **83:** 415-422, 1995.

223. **Michalak, M., K. Burns, C. Andrin, N. Mesaeli, G.H. Jass, J.L. Busaan, and M. Opas.** Endoplasmic reticulum form of calreticulin modulates glucocorticoid-sensitive gene expression. *J Biol Chem* **271:** 29436-29445, 1996.

224. **Michalak, M., R.E. Milner, K. Burns, and M. Opas.** Calreticulin. *Biochem J* **285:** 681-692, 1992.

225. **Miller, M., M.K. Park, and J.A. Hanover.** Nuclear pore complex: structure, function, and regulation. *Physiol Rev* **71:** 909-949, 1991.

226. **Miller, M.W., and J.A. Hanover.** Functional nuclear pores reconstituted with β1-4 galactose-modified *O*-linked *N*-acetylglucosamine glycoproteins. *J Biol Chem* **269:** 9289-9297, 1994.

227. **Misra, R.P., A. Bonni, C.K. Miranti, V.M. Rivera, M. Sheng, and M.E. Greenberg.** L-type voltage-sensitive calcium channel activation stimulates gene expression by a serum response factor-dependent pathway. *J Biol Chem* **269:** 25483-25493, 1994.

228. **Misteli, T., and D.L. Spector.** The cellular organization of gene expression. *Curr Opin Cell Biol* **10:** 323-331, 1998.

229. **Mizuno, T., T. Okamoto, M. Yokoi, M. Izumi, A. Kobayashi, T. Hachiya, K. Tamai, T. Inoue, and F. Hanaoka.** Identification of the nuclear localization signal of mouse DNA primase: nuclear transport of p46 subunit is facilitated by interaction with p54 subunit. *J Cell Sci* **109:** 2627-2636, 1996.

230. **Moore, M.S., and G. Blobel.** The GTP-binding protein Ran/TC4 is required for protein import into the nucleus. *Nature* **365:** 661-663, 1993.

231. **Moore, M.S., and G. Blobel.** Purification of a Ran-interacting protein that is required for protein import into the nucleus. *Proc Natl Acad Sci USA* **91:** 10212-10216, 1994.

232. **Moore, M.S., and G. Blobel.** Soluble factors required for nuclear protein import. *Cold Spring Harb Symp Quant Biol* **LX:** 701-705, 1995.

233. **Moore, M.S., and G. Blobel.** The two steps of nuclear import, targeting to the nuclear envelope and translocation through the nuclear pore, require different cytosolic factors. *Cell* **69:** 939-950, 1992.

234. **Morel, D.W., P.E. DiCorleto, and G.M. Chisolm.** Endothelial and smooth muscle cells alter low density lipoprotein in vitro by free radical oxidation. *Arteriosclerosis* **4:** 357-364, 1984.

235. **Moroianu, J., and G. Blobel.** Protein export from the nucleus requires the GTPase Ran and GTP hydrolysis. *Proc Natl Acad Sci USA* **92:** 4318-4322, 1995.

236. **Moroianu, J., G. Blobel, and A. Radu.** The binding site of karyopherin α for karyopherin β overlaps with a nuclear localization sequence. *Proc Natl Acad Sci USA* **93:** 6572-6576, 1996.

237. **Moroianu, J., G. Blobel, and A. Radu.** Nuclear protein import: Ran-GTP dissociates the karyopherin αβ heterodimer by displacing α from an overlapping binding site on β. *Proc Natl Acad Sci USA* **93:** 7059-7062, 1996.

238. **Moroianu, J., G. Blobel, and A. Radu.** RanGTP-mediated nuclear export of karyopherin α involves its interaction with the nucleoporin Nup153. *Proc Natl Acad Sci USA* **94:** 9699-9704, 1997.

239. **Murphy, J.R.** Erythrocyte metabolism. III. Relationship of energy metabolism and serum factors to the osmotic fragility following incubation. *J Lab Clin Med* **60:** 86-109, 1962.

240. **Nachury, M.V., U.W. Ryder, A.I. Lamond, and K. Weis.** Cloning and characterization of hSRP1γ, a tissue-specific nuclear transport factor. *Proc Natl Acad Sci USA* **95:** 582-587, 1998.

241. **Nachury, M.V., and K. Weis.** The direction of transport through the nuclear pore can be inverted. *Proc Natl Acad Sci USA* **96:** 9622-9627, 1999.

242. **Nakielny, S., and G. Dreyfuss.** Transport of proteins and RNAs in and out of the nucleus. *Cell* **99:** 677-690, 1999.

243. **Nakielny, S., S. Shaikh, B. Burke, and G. Dreyfuss.** Nup153 is an M9 containing mobile nucleoporin with a novel Ran-binding domain. *EMBO J* **18:** 1982-1995, 1999.

244. **Nicotera, P., D.J. McConkey, D.P. Jones, and S. Orrenius.** ATP stimulates Ca^{2+} uptake and increases the free Ca^{2+} concentration in isolated rat liver nuclei. *Proc Natl Acad Sci USA* **86:** 453-457, 1989.

245. **Nicotera, P., S. Orrenius, T. Nilsson, and P.-O. Berggren.** An inositol 1,4,5-trisphosphate-sensitive Ca^{2+} pool in liver nuclei. *Proc Natl Acad Sci USA* **87:** 6858-6862, 1990.

246. **Ohno, M., A. Segref, A. Bachi, M. Wilm, and I.W. Mattaj.** PHAX, a mediator of U snRNA nuclear export whose activity is regulated by phosphorylation. *Cell* **101:** 187-198, 2000.

247. **Ohno, S., S. Minoshima, J. Kudoh, R. Fukuyama, Y. Shimizu, S. Ohmi-Imajoh, N. Shimizu, and K. Suzuki.** Four genes for the calpain family locate on four distinct human chromosomes. *Cytogenet Cell Genet* **53:** 225-229, 1990.

248. **Omodeo Sale, F., S. Marchesini, P.H. Fishman, and B. Berra.** A sensitive enzymatic assay for determination of cholesterol in lipid extracts. *Anal Biochem* **142:** 347-350, 1984.

249. **Palacios, I., M. Hetzer, S.A. Adam, and I.W. Mattaj.** Nuclear import of U snRNPs requires importin beta. *EMBO J* **16:** 6783-6792, 1997.

250. **Panagia, V., G.N. Pierce, K.S. Dhalla, P.K. Ganguly, R.E. Beamish, and N.S. Dhalla.** Adaptive changes in subcellular calcium transport during catecholamine-induced cardiomyopathy. *J Mol Cell Cardiol* **17:** 411-420, 1985.

251. **Panté, N., and U. Aebi.** Exploring nuclear pore complex structure and function in molecular detail. *J Cell Sci* **Supplement 19:** 1-11, 1995.

252. **Panté, N., and U. Aebi.** Molecular dissection of the nuclear pore complex. *Crit Rev Biochem Mol Biol* **31:** 153-199, 1996.

253. **Panté, N., and U. Aebi.** The nuclear pore complex. *J Cell Biol* **122:** 977-984, 1993.

254. **Parthasarathy, S., D.J. Printz, D. Boyd, L. Joy, and D. Steinberg.** Macrophage oxidation of low density lipoprotein generates a modified form recognized by the scavenger receptor. *Arteriosclerosis* **6:** 505-510, 1986.

255. **Paschal, B.M., C. Delphin, and L. Gerace.** Nucleotide-specific interaction of Ran/TC4 with nuclear transport factors NTF2 and p97. *Proc Natl Acad Sci USA* **93:** 7679-7683, 1996.

256. **Paschal, B.M., and L. Gerace.** Identification of NTF2, a cytosolic factor for nuclear import that interacts with nuclear pore complex protein p62. *J Cell Biol* **129:** 925-937, 1995.

257. **Pemberton, L.F., G. Blobel, and J.S. Rosenblum.** Transport routes through the nuclear pore complex. *Curr Opin Cell Biol* **10:** 392-399, 1998.

258. **Perez-Terzic, C., A. Marquis Gacy, R. Bortolon, P.P. Dzeja, M. Puceat, M. Jaconi, F.G. Prendergast, and A. Terzic.** Structural plasticity of the cardiac

nuclear pore complex in response to regulators of nuclear import. *Circ Res* **84:** 1292-1301, 1999.

259. **Perez-Terzic, C., J. Pyle, M. Jaconi, L. Stehno-Bittel, and D.E. Clapham.** Conformational states of the nuclear pore complex induced by depletion of nuclear Ca^{2+} stores. *Science* **273:** 1875-1877, 1996.

260. **Petersen, O.H., O.V. Gerasimenko, J.V. Gerasimenko, H. Mogami, and A.V. Tepikin.** The calcium store in the nuclear envelope. *Cell Calcium* **23:** 87-90, 1998.

261. **Pierce, G.N., and N.S. Dhalla.** Sarcolemmal Na+-K+-ATPase activity in diabetic rat heart. *Am J Physiol* **245:** C241-C247, 1983.

262. **Pierce, G.N., M.J. Kutryk, and N.S. Dhalla.** Alterations in Ca2+ binding by and composition of the cardiac sarcolemmal membrane in chronic diabetes. *Proc Natl Acad Sci USA* **80:** 5412-5416, 1983.

263. **Pierce, G.N., M.K. Lockwood, and C.D. Eckhert.** Cardiac contracile protein ATPase activity in a diet induced model of noninsulin dependent diabetes mellitus. *Can J Cardiol* **5:** 117-120, 1989.

264. **Pierce, G.N., P.S. Sekhon, H.P. Meng, and T.G. Maddaford.** Effects of chronic swimming training on cardiac sarcolemmal function and composition. *J Appl Physiol* **66:** 1715-1721, 1989.

265. **Poenie, M., J. Alderton, R.Y. Tsien, and R.A. Steinhardt.** Changes of free calcium levels with stages of the cell division cycle. *Nature* **315:** 147-150, 1985.

266. **Post, J.A., A.J. Verkleij, and G.A. Langer.** Organization and function of sarcolemmal phospholipids in control and ischemic/reperfused cardiomyocytes. *J Mol Cell Cardiol* **27:** 749-760, 1995.

267. **Powers, M.A., and D.J. Forbes.** Cytosolic factors in nuclear transport: What's importin? *Cell* **79:** 931-934, 1994.

268. **Powers, M.A., D.J. Forbes, J.E. Dahlberg, and E. Lund.** The vertebrate GLFG nucleoporin, Nup98, is an essential component of multiple RNA export pathways. *J Cell Biol* **136:** 241-250, 1997.

269. **Przywara, D.A., S.V. Bhave, A. Bhave, T.D. Wakade, and A.R. Wakade.** Stimulated rise in neuronal calcium is faster and greater in the nucleus than the cytosol. *FASEB J* **5:** 217-222, 1991.

270. **Pujol, M.J., R. Bosser, M. Vendrell, J. Serratosa, and O. Bachs.** Nuclear calmodulin-binding proteins in rat neurons. *J Neurochem* **60:** 1422-1428, 1993.

271. **Qi, X.-M., M. Simonson, and C.W. Distelhorst.** Bcl-2 inhibits *c-fos* inductin by calcium. *Oncogene* **15:** 2849-2853, 1997.

272. **Radu, A., G. Blobel, and M.S. Moore.** Identification of a protein complex that is required for nuclear protein import and mediates docking of import substrate to distinct nucleoporins. *Proc Natl Acad Sci USA* **92:** 1769-1773, 1995.

273. **Raess, B.U., and F.F. Vincenzi.** A semi-automated method for the determination of multiple membrane ATPase activities. *J Pharmacol Meth* **4:** 273-283, 1980.

274. **Rajagopalan, S., Y. Xu, and M.B. Brenner.** Retention of unassembled components of integral membrane proteins by calnexin. *Science* **263:** 387-390, 1994.

275. **Ramjiawan, B., M.P. Czubryt, J.S.C. Gilchrist, and G.N. Pierce.** Nuclear membrane cholesterol can modulate nuclear nucleoside triphosphatase activity. *J Cell Biochem* **63:** 442-452, 1996.

276. **Ramjiawan, B., M.P. Czubryt, H. Massaeli, J.S.C. Gilchrist, and G.N. Pierce.** Oxidation of nuclear membrane cholesterol inhibits nucleoside triphosphatase activity. *Free Radic Biol Med* **23:** 556-562, 1997.

277. **Rao, G.N.** Hydrogen peroxide induces complex formation of SHC-Grb2-SOS with receptor tyrosine kinase and activates Ras and extracellular signal-regulated protein kinases group of mitogen-activated protein kinases. *Oncogene* **13:** 713-719, 1996.

278. **Rao, L., D. Perez, and E. White.** Lamin proteolysis facilitates nuclear events during apoptosis. *J Cell Biol* **6:** 1441-1455, 1996.

279. **Raza-Egilmez, S.Z., S.N. Jani-Sait, M. Grossi, M.J. Higgins, T.B. Shows, and P.D. Aplan.** NUP98-HOXD13 gene fusion in therapy-related acute myelogenous leukemia. *Cancer Res* **58:** 4269-4273, 1998.

280. **Ren, M., G. Drivas, P. D'Eustachio, and M.G. Rush.** Ran/TC4: a small nuclear GTP-binding protein that regulates DNA synthesis. *J Cell Biol* **120:** 313-323, 1993.

281. **Rexach, M., and G. Blobel.** Protein import into nuclei - association and dissociation reactions involving transport substrate, transport factors, and nucleoporins. *Cell* **83:** 683-692, 1995.

282. **Ribbeck, K., U. Kutay, E. Paraskeva, and D. Görlich.** The translocation of transportin-cargo complexes through nuclear pores is independent of both Ran and energy. *Curr Biol* **9:** 47-50, 1999.

283. **Ribbeck, K., G. Lipowsky, H.M. Kent, M. Stewart, and D. Görlich.** NTF2 mediates nuclear import of Ran. *EMBO J* **17:** 6587-6598, 1998.

284. **Rihs, H.-P., D.A. Jans, H. Fan, and R. Peters.** The rate of nuclear cytoplasmic protein transport is determined by the casein kinase II site flanking the nuclear localization sequence of the SV40 T-antigen. *EMBO J* **10:** 633-639, 1991.

285. **Rihs, H.-P., and R. Peters.** Nuclear transport kinetics depend on phosphorylation-site-containing sequences flanking the karyophilic signal of the Simian virus 40 T-antigen. *EMBO J* **8:** 1479-1484, 1989.

286. **Ris, H.** The 3-D structure of the nuclear pore complex as seen by high voltage electron microscopy and high resolution low voltage scanning electron microscopy. *EMSA Bull* **21:** 54-56, 1991.

287. **Robbins, J., S.M. Dilworth, R.A. Laskey, and C. Dingwall.** Two interdependent basic domains in nucleoplasmin nuclear targeting sequence: Identification of a class of bipartite nuclear targeting sequence. *Cell* **64:** 615-623, 1991.

288. **Roberts, B.L., W.D. Richardson, and A.E. Smith.** The effect of protein context on nuclear location signal function. *Cell* **50:** 465-475, 1987.

289. **Rolls, M.M., P.A. Stein, S.S. Taylor, E. Ha, F. McKeon, and T.A. Rapoport.** A visual screen of a GFP-fusion library identifies a new type of nuclear envelope membrane protein. *J Cell Biol* **146:** 29-43, 1999.

290. **Rout, M.P., J.D. Aitchison, A. Suprapto, K. Hjertaas, Y. Zhao, and B.T. Chait.** The yeast nuclear pore complex: composition, architecture, and transport mechanism. *J Cell Biol* **148:** 635-651, 2000.

291. **Rout, M.P., and S.R. Wente.** Pores for thought: nuclear pore complex proteins. *Trends Cell Biol* **4:** 357-365, 1994.

292. **Russell, J.C., S.K. Ahuja, V. Manickavel, R.V. Rajotte, and R.M. Amy.** Insulin resistance and impaired glucose tolerance in the atherosclerosis-prone LA/N corpulent rat. *Arteriosclerosis* **7:** 620-626, 1987.

293. **Russell, J.C., R.M. Amy, S. Graham, L.M. Wenzel, and P.J. Dolphin.** Effect of castration on hyperlipidemic, insulin resistant JCR:LA- corpulent rats. *Atherosclerosis* **100:** 113-122, 1993.

294. **Russell, J.C., S.E. Graham, and M. Hameed.** Abnormal insulin and glucose metabolism in the JCR:LA-corpulent rat. *Metabolism* **43:** 538-543, 1994.

295. **Russell, J.C., D.G. Koeslag, R.M. Amy, and P.J. Dolphin.** Plasma lipid secretion and clearance in hyperlipidemic JCR:LA- corpulent rats. *Arteriosclerosis* **9:** 869-876, 1989.

296. **Ryan, K.J., and S.R. Wente.** The nuclear pore complex: a protein machine bridging the nucleus and cytoplasm. *Curr Opin Cell Biol* **12:** 361-371, 2000.

297. **Sabri, A., K.L. Byron, A.M. Samarel, J. Bell, and P.A. Lucchesi.** Hydrogen peroxide activates mitogen-activated protein kinases and Na^+-H^+ exchange in neonatal rat cardiac myocytes. *Circ Res* **82:** 1053-1062, 1998.

298. **Sasseville, A.M.-J., and Y. Raymond.** Lamin A precursor is localized to intranuclear foci. *J Cell Sci* **108:** 273-285, 1995.

299. **Saward, L., and P. Zahradka.** Coronary artery smooth muscle in culture: Migration of heterogeneous cell populations from vessel wall. *Mol Cell Biochem* **176:** 53-59, 1997.

300. **Scheidtmann, K.-H., B. Echle, and G. Walter.** Simian virus 40 large T-antigen is phosphorylated at multiple sites clustered in two separate regions. *Virology* **44:** 116-133, 1982.

301. **Schindler, M., and L.W. Jiang.** In: *Biochemical and structural dynamics of the cell nucleus*, edited by E. Wang, J. L. Wang, S. Chien, W. Y. Cheung and C. W. Wu. San Diego: Academic Press, 1990, p. 249-263.

302. **Schlenstedt, G., C. Saavedra, J.D.J. Loeb, C.N. Cole, and P.A. Silver.** The GTP-bound form of the yeast Ran/TC4 homologue blocks nuclear protein import and appearance of poly(A)+ RNA in the cytoplasm. *Proc Natl Acad Sci USA* **92:** 225-229, 1995.

303. **Schroder, H.C., D.E. Nitzgen, A. Bernd, B. Kurelec, R.K. Zahn, M. Gramzow, and W.E.G. Muller.** Inhibition of nuclear envelope nucleoside triphosphatase-regulated nucleocytoplasmic messenger RNA translocation by 9-b-D-Arabinofuranosyladenine 5'-triphosphate in rodent cells. *Cancer Res* **44:** 3812-3819, 1984.

304. **Schroder, H.C., M. Rottmann, M. Bachmann, and W.E. Muller.** Purification and characterization of the major nucleoside triphosphatase from rat liver nuclear envelopes. *J Biol Chem* **261:** 663-668, 1986.

305. **Schroder, H.C., M. Rottmann, R. Wenger, M. Bachmann, A. Dorn, and W.E. Muller.** Studies on protein kinases involved in regulation of nucleocytoplasmic mRNA transport. *Biochem J* **252:** 777-790, 1988.

306. **Schwoebel, E.D., B. Talcott, I. Cushman, and M.S. Moore.** Ran-dependent signal-mediated nuclear import does not require GTP hydrolysis by Ran. *J Biol Chem* **273:** 35170-35175, 1998.

307. **Sekimoto, T., N. Imamoto, K. Nakajima, T. Hirano, and Y. Yoneda.** Extracellular signal-dependent nuclear import of Stat1 is mediated by nuclear pore-targeting complex formation with NPI-1, but not Rch1. *EMBO J* **16:** 7067-7077, 1997.

308. **Seksek, O., and J. Bolard.** Nuclear pH gradient in mammalian cells revealed by laser microspectrofluorimety. *J Cell Sci* **109:** 257-262, 1996.

309. **Sheng, M., S.T. Dougan, G. McFadden, and M.E. Greenberg.** Calcium and growth factor pathways of *c-fos* transcriptional activation require distinct upstream regulatory sequences. *Mol Cell Biol* **8:** 2787-2796, 1988.

310. **Sheng, M., G. McFadden, and M.E. Greenberg.** Membrane depolarization and calcium induce c-fos transcription via phosphorylation of transcription factor CREB. *Neuron* **4:** 571-582, 1990.

311. **Sheng, M., M.A. Thompson, and M.E. Greenberg.** CREB: a Ca^{2+}-regulated transcription factor phosphorylated by calmodulin-dependent kinases. *Science* **252:** 1427-1430, 1991.

312. **Shi, Y., and J.O. Thomas.** The transport of proteins into the nucleus requires the 70-kilodalton heat shock protein or its cytosolic cognate. *Mol Cell Biol* **12:** 2186-2192, 1992.

313. **Shinitzky, M.** Membrane Fluidity and Cellular Functions. In: *Physiology of Membrane Fluidity*, edited by M. Shinitzky. Boca Raton, Florida: CRC Press Inc., 1984, p. 1-51.

314. **Silver, R.B.** Nuclear envelope breakdown and mitosis in sand dollar embryos is inhibited by microinjection of calcium buffers in a calcium-reversible fashion, and by antagonists of intracellular Ca^{2+} channels. *Devel Biol* **131:** 11-26, 1989.

315. **Siniossoglou, S., C. Wimmer, M. Rieger, V. Doye, H. Tekotte, C. Weise, S. Emig, A. Segref, and E.C. Hurt.** A novel complex of nucleoporins, which includes Sec13p and a Sec13p homolog, is essential for normal nuclear pores. *Cell* **84:** 265-275, 1996.

316. **Siomi, H., and G. Dreyfuss.** A nuclear localization domain in the hnRNP A1 protein. *J Cell Biol* **129:** 551-560, 1995.

317. **Siomi, M.C., M. Fromont, J.-C. Rain, L. Wan, F. Wang, P. Legrain, and G. Dreyfuss.** Functional conservation of the transportin nuclear import pathway in divergent organisms. *Mol Cell Biol* **18:** 4141-4148, 1998.

318. **Smith, A., A. Brownawell, and I.G. Macara.** Nuclear import of Ran is mediated by the transport factor NTF2. *Curr Biol* **8:** 1403-1406, 1998.

319. **Smith, C.D., and W.W. Wells.** Solubilization and reconstitution of a nuclear envelope-associated ATPase. Synergistic activation by RNA and polyphosphoinositides. *J Biol Chem* **259:** 11890-11894, 1984.

320. **Smith, S., and G. Blobel.** The first membrane spanning region of the lamin B receptor is sufficient for sorting to the inner nuclear membrane. *J Cell Biol* **120:** 631-637, 1993.

321. **Soullam, B., and H.J. Worman.** The amino-terminal domain of the lamin B receptor is a nuclear envelope targeting signal. *J Cell Biol* **120:** 1093-1100, 1993.

322. **Srinivasan, M., C.F. Edman, and H. Schulman.** Alternative splicing introduces a nuclear localization signal that targets multifunctional CaM kinase to the nucleus. *J Cell Biol* **126:** 839-852, 1994.

323. **Steggerda, S.M., B.E. Black, and B.M. Paschal.** Monoclonal antibodies to NTF2 inhibit nuclear protein import by preventing nuclear translocation of the GTPase Ran. *Mol Biol Cell* **11:** 703-719, 2000.

324. **Stehno-Bittel, L., C. Perez-Terzic, and D.E. Clapham.** Diffusion across the nuclear envelope inhibited by depletion of the nuclear Ca^{2+} store. *Science* **270:** 1835-1838, 1995.

325. **Stewart, M., H.M. Kent, and A.J. McCoy.** Structural basis for molecular recognition between nuclear transport factor 2 (NTF2) and the GDP-bound form of the Ras-family GTPase Ran. *J Mol Biol* **277:** 635-646, 1998.

326. **Stoffler, D., B. Fahrenkrog, and U. Aebi.** The nuclear pore complex: from molecular architecture to functional dynamics. *Curr Opin Cell Biol* **11:** 391-401, 1999.

327. **Stoffler, D., K. Goldie, B. Feja, and U. Aebi.** Calcium-mediated structural changes of native nuclear pore complexes monitored by time-lapse atomic force microscopy. *J Mol Biol* **287:** 741-752, 1999.

328. **Strahm, Y., B. Fahrenkrog, D. Zenklusen, E. Rychner, J. Kantor, M. Rosbash, and F. Stutz.** The RNA export factor Gle1p is located on the cytoplasmic fibrils of the NPC and physically interacts with the FG-nucleoporin Rip1p, the DEAD-box protein Rat8p/Dbp5p and a new protein Ymr255p. *EMBO J* **18:** 5761-5777, 1999.

329. **Strambio-de-Castillia, C., G. Blobel, and M.P. Rout.** Proteins connecting the nuclear pore complex with the nuclear interior. *J Cell Biol* **144:** 839-855, 1999.

330. **Strübing, C., and D.E. Clapham.** Active nuclear import and export is independent of lumenal Ca^{2+} stores in intact mammalian cells. *J Gen Physiol* **113:** 239-248, 1999.

331. **Sundaresan, M., Z.-X. Yu, V.J. Ferrans, K. Irani, and T. Finkel.** Requirement for generation of H_2O_2 for platelet-derived growth factor signal transduction. *Science* **270:** 296-299, 1995.

332. **Sweet, D.J., and L. Gerace.** Taking from the cytoplasm and giving to the pore: soluble transport factors in nuclear protein import. *Trends Cell Biol* **5:** 444-447, 1995.

333. **Tagawa, T., T. Kuroki, P.K. Vogt, and K. Chida.** The cell cycle-dependent nuclear import of v-Jun is regulated by phosphorylation of a serine adjacent to the nuclear localization signal. *J Cell Biol* **130:** 255-263, 1995.

334. **Tang, T.K., C.C. Tang, Y.J. Chao, and C. Wu.** Nuclear mitotic apparatus protein (NuMa): spindle association, nuclear targeting and differential subcellular localization of various NuMa isoforms. *J Cell Sci* **107:** 1389-1402, 1994.

335. **Tokes, Z.A., and G.A. Clawson.** Proteolytic activity associated with the nuclear scaffold. The effect of self-digestion on lamins. *J Biol Chem* **264:** 15059-15065, 1989.

336. **Toledo, A., N. Ramani, and C.V. Rao.** Direct stimulation of nucleoside triphosphatase activity in human ovarian nuclear membranes by human chorionic gonadotropin. *J Clin Endocrinol Metab* **65:** 305-309, 1987.

337. **Tombes, R.M., K.L. Auer, R. Mikkelsen, K. Valerie, M.P. Wymann, C.J. Marshall, M. McMahon, and P. Dent.** The mitogen-activated protein (MAP) kinase cascade can either stimulate or inhibit DNA synthesis in primary cultures of rat hepatocytes depending upon whether its activation is acute/phasic or chronic. *Biochem J* **330:** 1451-1460, 1998.

338. **Towbin, H., T. Staehelin, and J. Gordon.** Electrophoretic transfer of proteins from polyacrylamide gels to nitrocellulose sheets: procedure and some applications. *Proc Natl Acad Sci USA* **76:** 4350-4, 1979.

339. **Truant, R., R.A. Fridell, E.R. Benson, A. Herold, and B.R. Cullen.** Nucleocytoplasmic shuttling by protein nuclear import factors. *Eur J Cell Biol* **77:** 269-275, 1998.

340. **van Deursen, J., J. Boer, L. Kasper, and G. Grosveld.** G_2 arrest and impaired nucleocytoplasmic transport in mouse embryos lacking the proto-oncogene *CAN/Nup214*. *EMBO J* **15:** 5574-5583, 1996.

341. **Van, P.N., F. Peter, and H.D. Söling.** Four intracisternal calcium-binding glycoproteins from rat liver microsomes with high affinity for calcium. *J Biol Chem* **264:** 17494-17501, 1989.

342. **Vanden Hoek, T.L., C. Li, Z. Shao, P.T. Schumacker, and L.B. Becker.** Significant levels of oxidants are generated by isolated cardiomyocytes during ischemia prior to reperfusion. *J Mol Cell Cardiol* **29:** 2571-2583, 1997.

343. **Venkatraman, J.T., and M.T. Clandinin.** Ribonucleic acid efflux from isolated mouse liver nuclei is altered by diet and genotypically determined change in nuclear envelope composition. *Biochim Biophys Acta* **940:** 33-42, 1988.

344. **Venkatraman, J.T., Y.A. Lefebvre, and M.T. Clandinin.** Diet fat alters the structure and function of the nuclear envelope: modulation of membrane fatty acid composition, NTPase activity and binding of triiodothyronine. *Biochem Biophys Res Commun* **135:** 655-661, 1986.

345. **Wada, I., D. Rindress, P.H. Cameron, W.J. Ou, J.J. Doherty, D. Louvard, A.W. Bell, D. Dignard, D.Y. Thomas, and J.J.M. Bergeron.** SSRα and associated calnexin are major calcium binding proteins of the endoplasmic reticulum membrane. *J Biol Chem* **266:** 19599-19610, 1991.

346. **Wang, H., and D.E. Clapham.** Conformational changes of the in situ nuclear pore complex. *Biophys J* **77:** 241-247, 1999.

347. **Watkins, J.L., R. Murphy, J.L.T. Emtage, and S.R. Wente.** The human homologue of Saccharomyces cerevisiae Gle1p is required for poly(A)+ RNA export. *Proc Natl Acad Sci USA* **95:** 6779-6784, 1998.

348. **Weis, K., C. Dingwall, and A.I. Lamond.** Characterization of the nuclear protein import mechanism using Ran mutants with altered nucleotide binding specificities. *EMBO J* **15:** 7120-7128, 1996.

349. **Weis, K., U. Ryder, and A.I. Lamond.** The conserved amino-terminal domain of hSRP1α is essential for nuclear import. *EMBO J* **15:** 1818-1825, 1996.

350. **Wente, S.R., and G. Blobel.** A temperature-sensitive NUP116 mutant forms a nuclear envelope seal over the yeast nuclear pore complex thereby blocking nucleocytoplasmic traffic. *J Cell Biol* **123:** 275-284, 1993.

351. **White, B.A., L.R. Bauerle, and F.C. Bancroft.** Calcium specifically stimulates prolactin synthesis and messenger RNA sequences in GH_3 cells. *J Biol Chem* **256:** 5942-5945, 1981.

352. **Wiese, C., and K.L. Wilson.** Nuclear membrane dynamics. *Curr Opin Cell Biol* **5:** 387-394, 1993.

353. **Wilding, M., E.M. Wright, R. Patel, G. Ellis-Davies, and M. Whitaker.** Local perinuclear calcium signals associated with mitosis-entry in early sea urchin embryos. *J Cell Biol* **135:** 191-199, 1996.

354. **Wilken, N., J.L. Senecal, U. Scheer, and M.C. Dabauvalle.** Localization of the Ran-GTP binding protein RanBP2 at the cytoplasmic side of the nuclear pore complex. *Eur J Cell Biol* **68:** 211-219, 1995.

355. **Williams, D.A., K.E. Fogarty, R.Y. Tsien, and F.S. Fay.** Calcium gradients in single smooth muscle cells revealed by the digital imaging microscope using Fura-2. *Nature* **318:** 558-561, 1985.

356. **Wilson, K.L.** The nuclear envelope, muscular dystrophy and gene expression. *Trends Cell Biol* **10:** 125-129, 2000.

357. **Wozniak, R.W., M.P. Rout, and J.D. Aitchison.** Karyopherins and kissing cousins. *Trends Cell Biol* **8:** 184-188, 1998.

358. **Yamada, M., T. Tachibana, N. Imamoto, and Y. Yoneda.** Nuclear transport factor p10/NTF2 functions as a Ran-GDP dissociation inhibitor (Ran-GDI). *Curr Biol* **8:** 1339-1342, 1998.

359. **Yu, L.-G., D.G. Fernig, M.R.H. White, D.G. Spiller, P. Appleton, R.C. Evans, I. Grierson, J.A. Smith, H. Davies, O.V. Gerasimenko, O.H. Petersen, J.D. Milton, and J.M. Rhodes.** Edible mushroom (*Agaricus bisporus*) lectin, which reversibly inhibits epithelial cell proliferation, blocks nuclear localization sequence-dependent nuclear protein import. *J Biol Chem* **274:** 4890-4899, 1999.

360. **Zafari, A.M., M. Ushio-Fukai, M. Akers, Q. Yin, A. Shah, D.G. Harrison, W.R. Taylor, and K.K. Griendling.** Role of NADH/NADPH oxidase-derived H_2O_2 in angiotensin II-induced vascular hypertrophy. *Hypertension* **32:** 488-495, 1998.

361. **Zbarsky, I.B.** An enzyme profile of the nuclear envelope. *Int Rev Cytol* **54:** 295-360, 1978.

362. **Zhang, J., N. Jin, Y. Liu, and R.A. Rhoades.** Hydrogen peroxide stimulates extracellular signal-regulated protein kinases in pulmonary arterial smooth muscle cells. *Am J Respir Cell Mol Biol* **19:** 324-332, 1998.

363. **Zolotukhin, A.S., and B.K. Felber.** Nucleoporins Nup98 and Nup214 participate in nuclear export of human immunodeficiency virus type 1 Rev. *J Virol* **73:** 120-127, 1999.

H. APPENDIX

Published Manuscripts from this Thesis:

1. **Gilchrist J.S.C., M.P. Czubryt, G.N. Pierce.** Calcium and calcium binding proteins in the nucleus. *Mol Cell Biochem* **135:**79-88, 1994.
2. **Czubryt, M.P., B. Ramjiawan, J.S.C. Gilchrist, H. Massaeli, and G.N. Pierce.** The presence and partitioning of calcium binding proteins in hepatic and cardiac nuclei. *J Mol Cell Cardiol* **28:**455-465, 1996.
3. **Czubryt, M.P., J.C. Russell, J. Sarantopoulos, and G.N. Pierce.** Nuclear cholesterol content and nucleoside triphosphatase activity are altered in the JCR:LA-cp corpulent rat. *J Cell Biochem* **63:**349-357, 1996.
4. **Ramjiawan, B., M.P. Czubryt, J.S.C. Gilchrist, G.N. Pierce.** Nuclear membrane cholesterol can modulate nuclear nucleoside triphosphatase activity. *J Cell Biochem* **63:**442-452, 1996.
5. **Czubryt, M.P., B. Ramjiawan, and G.N. Pierce.** The nuclear membrane integrity assay. *Mol Cell Biochem* **172:**97-102, 1997.
6. **Czubryt, M.P., J.C. Russell, J. Sarantopoulos, and G.N. Pierce.** Age- and sex-related differences in nuclear lipid content and nucleoside triphosphatase activity in the JCR:LA-cp corpulent rat. *Mol Cell Biochem* **176:**327-335, 1997.
7. **Czubryt, M.P., J.A. Austria, and G.N. Pierce.** Hydrogen peroxide inhibition of nuclear protein import is mediated by the mitogen-activated protein kinase, ERK2. *J Cell Biol* **148:**7-15, 2000.